EFFECTS OF CANNABINOIDS AND NOVELTY ON HIPPOCAMPAL ELECTROPHYSIOLOGY

Doran Paul Amos

Thesis submitted to UCL for consideration for the degree of Doctor in Philosophy

Department of Cell and Developmental Biology

UCL

September 2011

Declaration

I, Doran Paul Amos, confirm that the work presented in this thesis is my own. Where information has been derived from other sources, I confirm that this has been indicated in the thesis.

Doran Paul Amos

Acknowledgements

I would like to thank my supervisor, Prof. John O'Keefe, for his support throughout my PhD and for his helpful comments on this thesis. I would also like to thank my secondary supervisor, Prof. Stuart Cull-Candy, for his assistance. I am particularly indebted to Dr Colin Lever, my collaborator and mentor in this work, without whom the studies in this thesis quite literally would not have happened. Colin has always been available to offer advice on the practicalities of running the experiments and the many other questions I had to ask him. I have greatly enjoyed our discussions together. I am also deeply grateful to Dr Francesca Cacucci for her sympathetic support and pragmatic assistance, not least of all in providing the laboratory space in which these experiments were conducted. I thank Dr Tom Wills for teaching me the basics of the surgical and electrophysiological techniques, and for his help with analysis throughout the years. And I acknowledge Steve Burton for keeping the O'Keefe lab running so well and making everyone's lives a lot easier.

I also thank Prof. Kate Jeffery for allowing me to join the ever-burgeoning ranks of the IBN. It has been a wonderful and lively place to work, and has always had a great social atmosphere that I will miss a lot. I have had the privilege to work with many kind and talented people, so I would like to wish all the best (in no particular order) to: Dr Caswell Barry, Dr Robin Hayman, Lin Lin Ginzberg, Lorelei Howard, Aleks Jovalekic, Rebecca Knight, Freyja Olafsdottir, Dr Jonas Hauser, Dr Andrea Alenda-Gonzalez, Dr Hugo Spiers, Elizabeth Marozzi, Madeleine Verriotis, Jonathan Wilson and Martha Gwatkin. And of course last but not least, my lab- and flatmate, Laurenz Muessig.

Thanks to all of you!

Abstract

Exposure to novel environments alters hippocampal cell and theta local field potential activity to support the formation of new or updated spatial representations. It induces remapping of place cell fields, a reduction in CA1 theta frequency and an increase in the spatial scale of entorhinal grid cell fields. A recent model proposes that a reduction in the slope of the theta frequency-running speed relationship (TFRSR) can account for these effects (Burgess, 2008, Hippocampus). In contrast, the model proposes that the Y-axis intercept of the TFRSR is unaffected by novelty but instead correlates with anxiety/arousal. Thus, the theta frequency reduction elicited by a wide range of anxiolytic drugs (Gray & McNaughton, 2000) is suggested to result from a decrease in the intercept. Cannabinoids are anxiolytic at low doses, reduce theta frequency and disrupt the theta-timescale dynamics of place cell firing. In contrast, environmental novelty elicits a coordinated shift in CA1 place cell firing to a later theta-phase.

This thesis examines the electrophysiological effects of environmental familiarity or novelty in combination with a low, intraperitoneal dose of the cannabinoid agonist O-2545, or its vehicle, saline. It was found that exposure to novel environments reduced the slope of the TFRSR whereas the cannabinoid reduced the intercept, in agreement with the model. These effects were not due to decreased body temperature or changes in behaviour. Combining novelty and drug reduced both slope and intercept. Furthermore, the extent of novelty-induced place cell remapping correlated with the reduction in slope. The mean theta-phase of place cell firing shifted later in novelty, but this was disrupted by the cannabinoid. In contrast, the mean theta-phase of the interneuron population was stable across conditions, but novelty increased the dispersion of interneuron theta-phase preferences. These results help to elucidate the mechanisms underlying novelty processing and cannabinoid action in the hippocampus.

Table of Contents

1 Hippocampal anatomy

The brain regions that form part of the hippocampal formation (HF) and the parahippocampal region (PHR) have been classified according to a variety of different systems in the literature. Therefore, in order to make it clear which regions are being referred to in this chapter, I will use the following nomenclature:

> The *hippocampus proper* (HC) contains the *cornu ammonis* fields (CA1-3).
>
> The *hippocampal formation* (HF) is defined as the hippocampus proper, the dentate gyrus (DG) and the subiculum (SUB).
>
> The *parahippocampal region* (PHR) includes the presubiculum (PRE), the parasubiculum (PARA), the entorhinal cortex (EC), the perirhinal cortex (PER) and the postrhinal cortex (POR).

A large part of the anatomical data in this chapter has been summarized from a number of comprehensive reviews in the literature and in print: namely Burwell and Amaral (1998), Furtak et al. (2007), Amaral and Lavenex (2007) and van Strien et al. (2009).

1.1 Morphology and cytoarchitectonics

1.1.1 The hippocampal formation

The hippocampal formation (HF) is a bilaterally symmetric structure that is situated caudally in the rat brain, immediately ventral to the neocortex (Figure 1.1). In each hemisphere of the brain, the HF forms a cashew nut-shaped structure which can be described with reference to two axes (Figure 1.2): the long axis, which is termed the septotemporal (or dorsoventral) axis, curves caudoventrally from the septal pole at the midline towards the temporal lobe; and the transverse (or proximodistal) axis, which is aligned orthogonally to the septotemporal axis and runs parallel to the principal cell layer, proximal-to-distal in the order DG-CA3-CA1-SUB. Along the septotemporal axis, the HF can be also divided into a dorsal, an intermediate and a ventral portion that occupy approximately a third of the

long axis each and can be distinguished on the basis of anatomic and genomic markers (Dong et al., 2009).

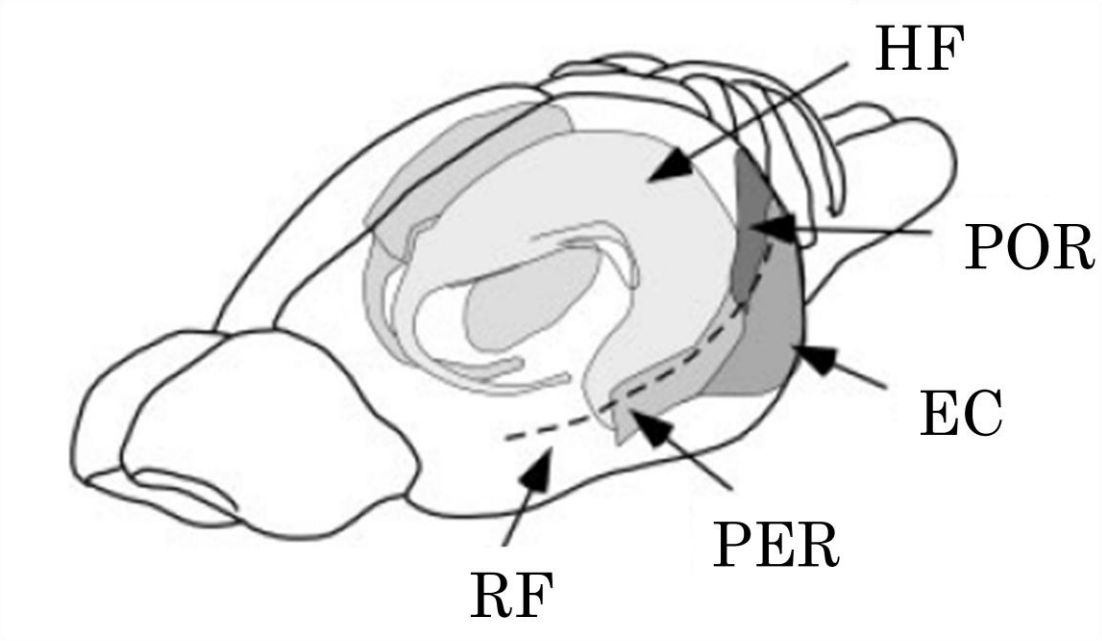

Figure 1.1. Gross morphology of the hippocampal formation and parahippocampal region in the rat brain. Clockwise from top: bilateral halves of the hippocampal formation (HF), postrhinal cortex (POR), entorhinal cortex (EC), perirhinal cortex (PER) and the rhinal fissure (RF). (*Adapted from*: Furtak et al., 2007)

All fields of the HF (CA1-CA3, DG and SUB) possess a trilaminar or allocortical organization (Figure 1.2, B and C). This is in marked contrast to the multilayered neocortical organization of the PHR, which we shall come on to discussing in the following section. Each field of the HF possesses a clearly defined principal cell layer which contains the somas of the principal cells plus some interneurons and stains densely. This is sandwiched between the more diffusely staining superficial and deep layers, which contain the dendrites of the principal cells, afferent and efferent fibres and interneurons. The principal cell layer is tightly-packed in the DG and CA fields, but becomes more diffuse and broader in the SUB (Figure 1.2C). These principal cell layers form a pair of interlocking curves: the first curve is formed by the tooth-shaped DG (hence 'dentate', from the Latin for tooth), which encloses the proximal part of CA3; the second by the CA fields, beginning with CA3 near the DG, which folds back on itself as CA1 emerges, before broadening at the transition to the SUB.

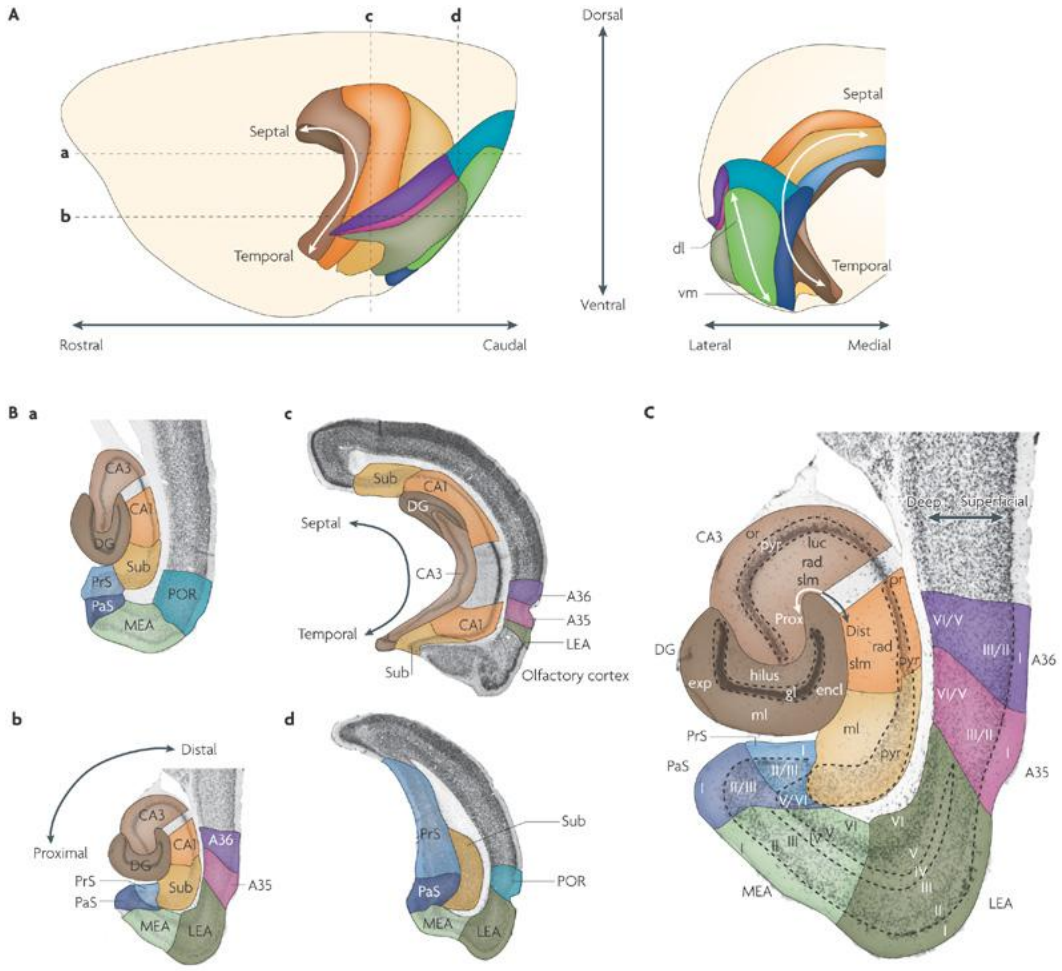

Figure 1.2. Major axes, subdivisions and cytoarchitectonics of the hippocampal formation and the parahippocampal region in the rat brain. Colour-coded areas show the anatomical positions of the dentate gyrus (DG; dark brown), CA3 (light brown), CA1 (mid-orange), subiculum (Sub; light orange), presubiculum (PrS; light blue), parasubiculum (PaS; dark blue), medial entorhinal area (MEA; light green), lateral entrohinal area (LEA; dark green), postrhinal cortex (POR; turquoise) and areas 35 (A35; pink) and 36 (A36; purple) of the perirhinal cortex. **(A)** Left: Schematic lateral view of the left hemisphere, indicating the septo-temporal axis and the anatomical locations of different areas within the hippocampal formation and parahippocampal region (colour-coded, for labels see panel B). Sectioning planes used in panel B are shown with dotted lines (a-d). Right: Posterior view of the left hemisphere, additionally showing the dorsolateral-ventromedial axis of the entorhinal cortex. **(B)** Sections a-d corresponding to those shown in panel A. The septotemporal axis is marked on section c and the proximodistal axis on section b. **(C)** Cytoarchitectonics of the hippocampal formation and parahippocampal region, enlarged from section Bb. The layers labelled are: for the dentate gyrus, the molecular layer (ml), which includes the exposed (exp) and the enclosed (encl) blade, the granule cell layer (gl) and the hilus or polymorph cell layer; for CA3 and CA1, stratum oriens (or), pyramidale (pyr), lucidum (luc), radiatum (rad) and lacunosum-moleculare (slm); for the subiculum, the pyramidal cell (pyr) and molecular layer (ml); and for all subdivisions of the parahippocampal region, the layers are labelled using Roman numerals. The proximodistal and deep-to-superficial axes are also shown. (*Source:* van Strien et al., 2009)

The curvature of the CA and SUB fields means that their deep layers are located towards the ventricular/alvear side of the HF, whilst their superficial layers are adjacent the interior side or hippocampal fissure (Figure 1.2C). The deep layer of the DG, in contrast, curves around and sits next to the proximal portion of CA3, while the superficial layer is the most distant of the layers from CA3. The principal cell layer of the DG forms a 'U' or 'V' shape depending on the septotemporal position at which it is sectioned. This allows three different regions to be distinguished: the enclosed (or suprapyramidal) blade, adjacent to CA1 and the hippocampal fissure; the exposed (or infrapyramidal) blade, adjacent to the ventricle; and the crest region, which falls in between.

The nomenclature for the three layers of the HF varies depending on the field in question (Figure 1.2C). In the DG, the superficial layer is known as the molecular layer (ML), the principal cell layer as the granule cell layer (GCL) and the deep layer as the polymorphic layer (PL). In the CA fields, the principal cell layer is also known as stratum pyramidale (SP) and the deep layer as stratum oriens (SO). The superficial layer can be divided into a number of sub-layers: in CA1 and CA2 these comprise stratum radiatum (SR) and stratum lacunosum-moleculare (SLM). CA3 is identical in its laminar structure to CA1/CA2, except that a narrow cell-free zone can also be distinguished in between SP and SR, known as stratum lucidum (SL). This nomenclature in the SUB is identical to the DG, with the exception that the principle cell layer is known as the pyramidal cell layer (PCL), and that the molecular layer can be divided into a deep and a superficial portion on the basis of afferent connectivity.

1.1.2 The parahippocampal region

The HF and the parahippocampal region (PHR) can be easily distinguished by examining their laminar structures. The allocortical organization of the HF abruptly changes to a six-layered organization that is more similar to the neocortex at the border of the SUB and PRE. This marks the boundary between the HF and the PHR. In this section, I shall describe the basic anatomy and cytoarchitectonics of the areas that comprise the PHR: the PRE, PARA, EC, POR and PER.

The pyramidal layer of the SUB is continued in the PRE as the deep cell layers (V-VI), but additional superficial cell layers (II-III) also emerge at the SUB-PRE boundary, separated from the deep layers by a cell-free layer (IV), the lamina dessicans (LD). This laminar structure is continued in the PARA and the EC and

so all these structures (PRE, PARA and EC) can be considered as extending the proximodistal axis of the HF, with the DG at the proximal end and the EC at the distal end. The PRE and PARA can also be referenced along the septotemporal axis used for the HF, although the PARA occupies only the temporal half of this axis.

The EC covers a large area of the caudoventral cortical surface and from a rostroventral location adjacent to the temporal pole of the HF, extends caudally in a predominantly dorsolateral direction. This defines the two major axes of the EC, known as the rostrocaudal and ventromedial-dorsolateral axes.

The EC is divided into two areas on the basis of cytoarchitectonics and connectivity. The lateral entorhinal area (LEA) occupies a relatively rostrolateral position in the EC and the medial entorhinal area (MEA) is located more medially and extends dorsocaudally. The LEA has a clearly defined layer II which contains densely-packed cells which are clustered into islands; in contrast, layer II is less well-defined in MEA and its layer II cells are slightly larger and are not clustered (Amaral and Lavenex, 2007). Additionally, the EC can be divided into three bands: a medial band, which includes the most rostral and ventromedial part of the EC; a lateral band, that forms a long strip extending along the dorsolateral and caudal edges of the EC; and an intermediate band, which covers the area in between (Figure 1.4). The significance of the division of the EC into different areas and bands will become clearer once the connectivity of the HF and the PHR are discussed in the following section.

The disappearance of the LD marks the boundary of the EC with the PER or POR, which possess a more typically neocortical six-layered structure, with the exception that they lack a well-defined granular layer (IV). The PER and POR form thin strips on the cortical surface located immediately dorsal to the EC, with the border between the EC and PER/POR roughly aligned with the rhinal fissure (Figure 1.1). The POR can be distinguished from the PER by its connectivity and by the presence of ectopic layer II cells that give layer II of the PER an irregular appearance (Burwell et al., 1995). Anatomically, the PER is positioned more rostrolaterally, adjacent to the LEA, whilst the POR extends caudomedially from the border with the PER. The PER can be divided into an agranular area 35 (A35) and a dysgranular area 36 (A36). The PER and POR share the rostrocaudal axis with the EC and are additionally mapped according to the major dorsolateral axis of the brain.

1.2 Connectivity

1.2.1 Major fibre bundles

Afferent and efferent connections link the HF both commissurally and with other brain regions, including a number of subcortical regions and most prominently with the PHR, particularly the EC. These connections are organized into distinct fibre bundles that occupy a significant volume of the rat brain surrounding the HF (Figure 1.3). The broad connectivity and morphology of the major fibre systems will be outlined in this section, prior to a more detailed discussion of the specific patterns of hippocampal and entorhinal connectivity in the subsequent sections.

1.2.1.1 Alveus

The alveus is a thin sheet of myelinated afferent and efferent fibres that cover the deep layers of the HF, carrying both extrinsic and intrinsic HF connections. It is the main pathway for connections between the EC and the septal HF, from CA1 to SUB and between the HF and its subcortical targets. Alvear fibres arising from the HF targeting subcortical regions collect in a band along the rostrolateral edge of the HF, known as the fimbria (Latin for 'fringe'). Moving temporal-to-septal towards the midline, the fimbria grows progressively broader as it collects more afferent fibres. These fibres are topographically organized, with temporal and septal afferents positioned laterally and medially, respectively.

1.2.1.2 Fimbria-fornix

Fibres of the bilateral fimbria heading medially converge with subcortical afferents arising from the septal third of the HF near the midline to form a flattened bundle, known as the fornix (Latin for 'arch'). These two fibre systems form part of a shared pathway and are therefore often referred to collectively as the fimbria-fornix.

The fimbria-fornix extends rostroventrally from the point of convergence and then descends towards its subcortical targets along a number of pathways, referred to as the columns of the fornix. The fornix splits close to the anterior commissure into a rostrally-directed precommissural fornix, which innervates the septal nuclei and nucleus accumbens, and a caudally-directed postcommissural fornix, which innervates the diencephalon. The fimbria-fornix contains both afferent and efferent connections between the HF and subcortical regions, the importance of which are discussed further below.

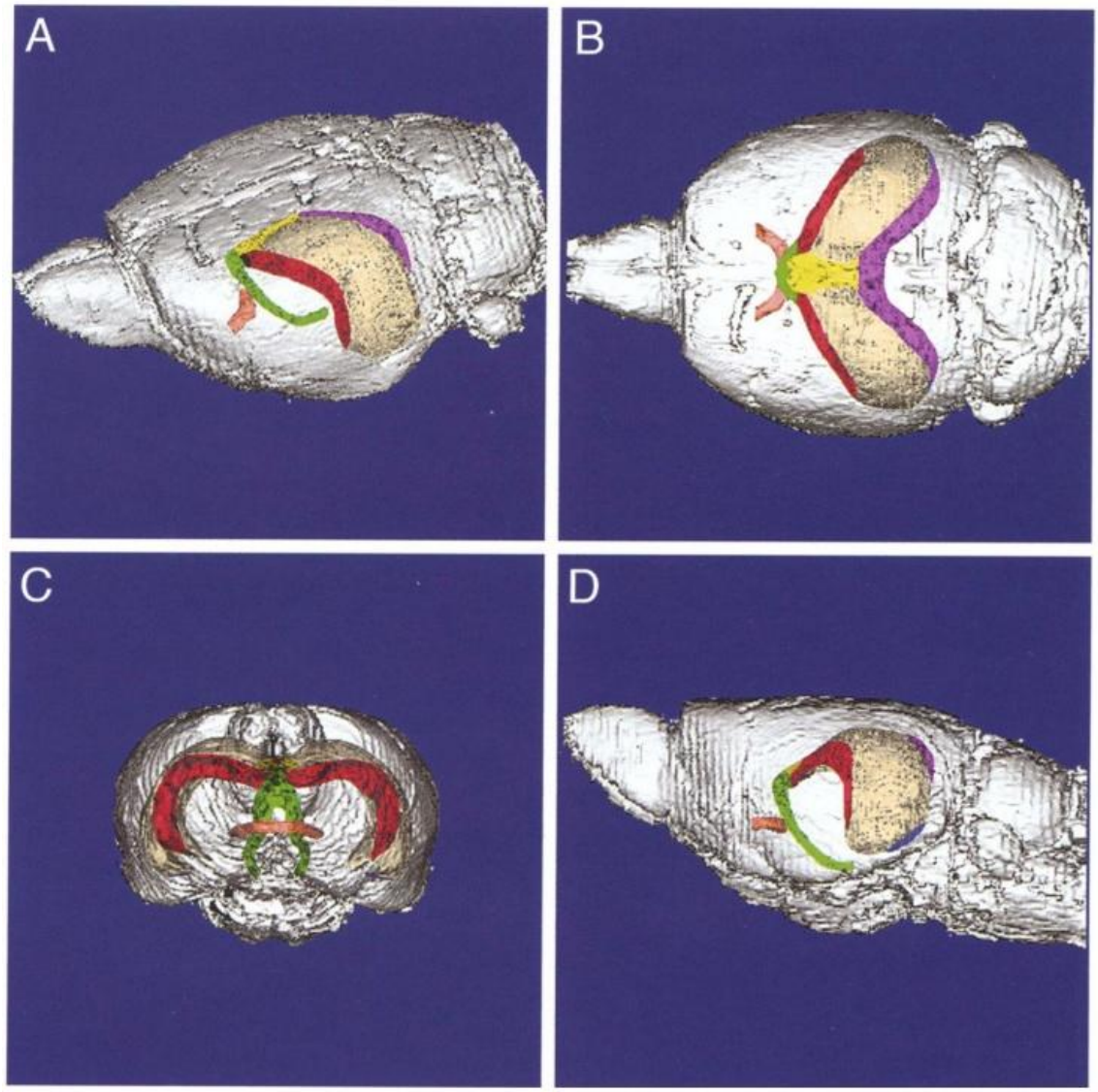

Figure 1.3. Major fibre systems of the rat hippocampal formation. (A) View from a rostrodorsal position, (B) from above, (C) from the front and (D) from the left. The fibre systems shown are the fimbria (red), dorsal fornix (yellow), ventral hippocampal commissure and postcommissural fornix (green), dorsal hippocampal commissure (purple) and the precommissural fornix (tan). (*Source:* Amaral and Lavenex, 2007)

1.2.1.3 Angular bundle

As mentioned previously, the alveus is the major route for connections between the EC and septal HF. Moving septal-to-temporal along the HF, the proportion of EC efferents taking this route decreases and instead they arrive in the HF via a fibre pathway interposed between the EC and the PRE and PARA, the angular bundle. The fibres of the angular bundle perforate the SUB en route to the DG and CA

fields of the HF and so this pathway is known as the perforant path. In addition, the angular bundle carries fibres between the EC and its cortical and subcortical targets, as well as commissural connections between the EC and PRE.

1.2.1.4 Dorsal and ventral hippocampal commissures

Commissural fibres of the HF and PHR are also carried via the dorsal and ventral hippocampal commissures. The ventral hippocampal commissure is located caudally to the septal nuclei at the rostromedial tip of the HF. It contains a large number of intrinsic commissural connections targeting both homotopic and heterotopic fields in the contralateral HF. Additionally, there are a smaller number of fibres which project to contralateral subcortical targets via the fornix. The fibres of the dorsal hippocampal commissure lie bilaterally along the dorsocaudal edge of the HF and meet at the midline just rostral to the splenium of the corpus callosum. They carry afferent and efferent connections to and from the contralateral EC and the PRE.

1.2.2 Intrinsic connections of the hippocampal formation

The most striking feature of the intrinsic connectivity of the HF is the almost exclusively unidirectional pattern of connections that link each field in the order DG-CA3-CA1-SUB. The projections from the SUB and CA1 to the deep layers of the EC, along with those returned from the superficial layers of the EC to all fields of the HF, complete the "polysynaptic loop". This predominantly unidirectional flow of information is in stark contrast to the reciprocal connectivity typically observed within neocortical regions. Another distinctive feature of the intrinsic connectivity of the HF is the extensive bilateral recurrent connectivity of CA3, which suggests that autoassociational or reverbatory activity are also important in hippocampal processing. Together, these unique features constitute what has been termed the "standard view" of hippocampal intrinsic connectivity (van Strien et al., 2009).

However, it must be noted that the full picture is not so simple, since infrequently acknowledged back-projections and recurrent connections also exist within the HF (van Strien et al., 2009). Therefore in order to present a balanced view, I shall describe the instrinsic connectivity of the HF using the "standard view" as an explanatory framework, but will make reference to the evidence for recurrent and back-projections where necessary. The DG is the "first" step in the polysynaptic loop to receive input from the EC, so I shall begin with this structure and follow the loop step-by-step until the SUB.

1.2.2.1 DG to CA3 (mossy fibres)

The unmyelinated axons of DG granule cells project exclusively to CA3/CA2 and are known as mossy fibres due to the varicosities that occur along their lengths. These fibres terminate in the stratum lucidum of CA3, with granule cells from all transverse positions projecting to the full proximodistal extent of CA3 (Amaral and Lavenex, 2007). Although the forward DG-to-CA3 is dominant, there is also evidence of a weak back-projection from CA3 to DG (van Strien et al., 2009).

1.2.2.2 CA3/CA2 recurrent collaterals

CA3/CA2 pyramidal cells send divergent projections along the entire septotemporal extent of the HF to both the ipsi- and contralateral CA3/CA2 fields. This means that any two pyramidal cells within the bilateral CA3/CA2 fields are linked to one another by at most a few synapses. The potential implications of this are discussed in more detail in a later section. Although often only the recurrent connectivity of the CA3/CA2 is highlighted, weaker and more restricted recurrent projections are also observed in DG, CA1 and SUB (Witter, 2006; van Strien et al., 2009).

1.2.2.3 CA3/CA2 to CA1 (Schaffer collaterals)

Projections from CA3/CA2 to CA1 are known as Schaffer collaterals and spread divergently to targets in both ipsi- and contralateral CA1. Individual CA3/CA2 pyramidal cell axon collaterals can extend along as much as two-thirds of the septotemporal extent of CA1 (Li et al., 1994). However, there is a gradient to these projections, with those arising more proximally in CA3 terminating in more septal and superficial levels of CA1 and those from more distal locations terminating in the deeper layers of temporal CA1 (Amaral and Lavenex, 2007). Back-projections also exist from CA1 to CA3, though these may be inhibitory in nature (van Strien et al., 2009).

1.2.2.4 CA1 to SUB

There is a strong forward projection from CA1 to SUB that is topographically mapped along the proximodistal axis. The proximal third of CA1 projects to the distal third of the SUB, the distal third of CA1 to the proximal third of the SUB and the middle third of CA1 to the middle third of the SUB (Amaral and Lavenex, 2007). The importance of this topography will be discussed later in reference to the projections of the EC to CA1 and SUB. In addition to the forward projection, there is a weak back-projection from SUB to CA1 (Witter, 2006)

1.2.3 Extrinsic connections of the hippocampal formation

The extrinsic connections of the HF can broadly be divided into those connecting to subcortical regions and those connecting to cortical regions. The PHR is of central significance in cortical communication with the HF, being the 'gateway' through which nearly all cortical inputs or outputs pass. Therefore, I will return to discussing the role of the PHR later and will focus in this section on the subcortical and non-parahippocampal cortical connections with the HF.

1.2.3.1 Subcortical connections

Basal forebrain

The most significant projections between the HF and the subcortical regions are those linking the HF and the septal nuclei. The medial septum and diagonal band of Broca (MS/DBB) are the major source of subcortical input to the HF, sending strong projections of a predominantly cholinergic and GABAergic nature to DG and CA3, and weaker projections to CA1 and SUB. In turn, CA1, CA3 and SUB project strongly to the lateral septal nucleus (LS). This strong reciprocal connectivity reflects the central role that the septal nuclei play in generating theta activity in the HF. This is a substantial topic of great relevance to this thesis, so I shall return to discussing it further at the end of the chapter.

Other nuclei of the basal forebrain lack this strong reciprocal connectivity. The nucleus accumbens (NAcc) and adjacent regions of the olfactory tubercle receive a prominent but unidirectional innervation from the SUB.

Amygdaloid complex

Input to the HF from the amygdala mainly comes from the basal nucleus and terminates predominantly in the temporal portions of CA1, CA3 and SUB (Pikkarainen et al., 1999; Pitkänen et al., 2000). The temporal two-thirds of CA1 and the temporal one-third of SUB send reciprocal projections to the amygdala. Ventral SUB also strongly innervates the bed nucleus of the stria terminalis. Since the amygdala is implicated in regulating emotional reactivity, these anatomical connections suggest that the ventral portion of the HF is involved in processing affective stimuli (Fanselow and Dong, 2010).

Hypothalamus

The supramammilary nucleus (SuM) is the major source of hypothalamic input to the HF, sending strong and specifically targeted innervation to the DG, CA2 and SUB. This structure is also part of the network involved in generating theta activity in the HF and PHR (discussed at the end of the chapter). Projections from the septal two-thirds of the SUB constitute the main output of the HF to the hypothalamus, terminating in the mammillary nuclei. The ventromedial nucleus of the hypothalamus also receives a prominent innervation arising from the temporal third of the SUB.

Thalamus

Distinct but intermingled cell populations in the nucleus reuniens (RE) give rise to separate projections to CA1 and SUB. Recently it has been shown that lesions of the RE lead to abnormalities in goal-seeking behaviour in a spatial memory task (Dolleman-van der Weel et al., 2009). This may be related to the specific targeting of RE input to the intermediate septotemporal portion of the HF, which is implicated in translating rapid place learning into navigational performance (Bast et al., 2009). The paraventricular (PVN) and parataenial (PT) nuclei are the other main sources of thalamic innervation to the SUB. The SUB sends reciprocal connections to several thalamic targets, including RE and the PVN.

Brainstem

Brainstem input is likely to be related to arousal levels and originates mainly from the nucleus locus coeruleus (LC), which sends a noradrenergic innervation to all fields of the HF, with particularly dense projections to DG and CA3. Serotonergic innervation of the HF from the brainstem is generally much sparser. However, a dense projection innervating all fields arises from the median raphe nucleus (MR), which is involved in regulating theta activity (discussed further at the end of the chapter). Dopaminergic afferents from the ventral tegmental area (VTA) terminate mainly in the SUB (Amaral and Lavenex, 2007).

1.2.3.2 Non-parahippocampal cortical connections

As explained above, the major conduit for neocortical communication with the HF is the PHR. The DG and CA3/CA2 have no known connections with the neocortex, but CA1 and the SUB do project directly to some areas.

The major neocortical target for CA1 afferents, excluding the PHR, is the medial frontal lobe, which may support route planning and encode goal locations (Poucet et al., 2004). The retrosplenial cortex also receives projections from the septal portions of both CA1 and the SUB. As I shall describe in the next section, this region also has strong reciprocal connections with several areas of the PHR. A number of other neocortical regions are targets for subicular afferents, the most significant of which are the medial and ventral orbitofrontal cortices, and the prelimbic and infralimbic cortices.

There is no convincing evidence that any of these regions reciprocate these projections directly (Amaral and Lavenex, 2007). This therefore highlights the central role of the PHR as the 'gateway' for neocortical communication with the HF.

1.2.4 The parahippocampal region

An understanding of the anatomy of the PHR is critical to understanding the functioning of the HF. The PHR is both the route through which nearly all cortical information flows and an integral part of the hippocampal polysynaptic loop. In this section, I shall discuss the intrinsic, cortical and subcortical connections of the PHR and its connectivity with the HF in terms of the evidence that parallel "streams" of information processing may exist in the entorhino-hippocampal system.

1.2.4.1 The pre- and parasubiculum

It makes sense to begin the discussion of parahippocampal connectivity with the PRE and PARA, since these regions sit at the border of the HF and the PHR. These structures are reciprocally and bilaterally connected and share many of the same afferent connections. Both PRE and PARA are strongly reciprocally connected to the anterior thalamic nuclei (ATN), a connection not seen anywhere else in the PHR or HF. This is an important connection in terms of hippocampal functioning, since the anterior thalamic nuclei contain cells signalling the head direction of the animal (Taube, 1995). Cortical projections to both structures arise almost exclusively from visual and visuospatial areas, including RSP and occipital visual cortex (Amaral and Lavenex, 2007).

Both cortical and thalamic information is relayed to the HF primarily via the robust projection from the PARA to the DG and also from the PRE to the SUB. Since the SUB itself sends a projection to both PRE and PARA, this allows

hippocampal output to be fed directly back into the hippocampal loop via the PARA. Thus, the connections of the PARA in particular suggest that it is involved in conveying visual, visuospatial and head direction information to the HF, as well as facilitating re-entrant processing within the hippocampal loop. The PARA also projects strongly to layer II of the EC, terminating preferentially but not exclusively in the MEA. In contrast, the major target of output from the PRE is layer III of the EC, specifically the MEA.

1.2.4.2 Entorhino-hippocampal projections

The significance of such EC layer and area specificity can be understood better by considering the connections of the EC and HF. Layer II afferents from EC terminate almost exclusively in DG and CA3/CA2, targeting the most superficial layer in both cases (the ML and SLM, respectively). Those arising from the LEA terminate predominantly in the superficial half of the layer, whilst those from the MEA terminate predominantly in the deeper half of the layer (Amaral and Lavenex, 2007).

In contrast, layer III afferents from the MEA and LEA are organised topographically along the proximodistal axis and project predominantly to CA1 and SUB. As with the layer II projection, the SLM layer is targeted, although in this case axon terminals are found throughout the whole extent of SLM. The topographic projection from LEA innervates distal CA1 and proximal SUB, whereas that from the MEA innervates proximal CA1 and distal SUB. Not only are these topographic segregations maintained in the return projections to the EC, but they are also preserved in the connectivity of the proximal and distal regions of CA1 and SUB, as described previously.

Additionally, the organisation of the SUB is columnar and output from each proximodistal third projects to different targets in the brain (Witter, 2006). Projections from the proximal third of the SUB innervate the infralimbic and prelimbic cortices, the NAcc and the LS; those from the distal third project to the RSP and the PRE; and those from the intermediate third reach the midline thalamic nuclei (Witter, 2006). Thus, throughout the entorhino-hippocampal circuit, there is consistent anatomical evidence for the presence of parallel processing streams.

1.2.4.3 The perirhinal and postrhinal cortices

Such parallel processing is also suggested by the subcortical and cortical afferent connectivity of the PER and the POR, the major inputs to the LEA and MEA, respectively. The PER is a convergence point for polymodal sensory information arriving from cortical and subcortical regions. A35 of the PER receives robust projections from both cortical (piriform) and subcortical olfactory areas, as well as insular cortex. A36 is strongly innervated by auditory-related thalamic nuclei and the ventral temporal association cortex, which conveys polymodal information (Furtak et al., 2007). In conjunction with the affective information arriving to both A35 and A36 via their strong reciprocal connections to the amygdala, this diverse polymodal input suggests that the PER processes contextual information. A35 has strong reciprocal connections with the LEA, whereas those between the LEA and A36 are much weaker. The intrinsic connections of the PER suggest that information from A36 is funnelled to A35, en route to the LEA (Amaral and Lavenex, 2007).

In contrast to the PER, the major projections to the POR arrive primarily from visual and visuospatial areas. Robust and reciprocal projections exist with the dorsal RSP, visual association areas, posterior parietal cortex and the caudal portion of the ventral temporal association areas. All of these regions have been implicated in visual and visuospatial processing (Furtak et al., 2007). Visual-related subcortical input also reaches the POR from the lateral posterior nucleus of the dorsal thalamus, whose homolog in primates supports visual attention (Posner and Petersen, 1990). Visual and visuospatial information from the POR is then relayed predominantly, although not exclusively, to the MEA.

There is also a remarkable similarity between the inputs the LEA and PER, and the MEA and POR. Thus, the LEA receives stronger projections from the insular cortex, whereas the MEA is more robustly innervated by the cingulate, parietal and occiptal cortices (Burwell and Amaral, 1998). These anatomical connections suggest that two parallel streams exist, one carrying contextual information via the PER and LEA and the other carrying visual and visuospatial information via the POR and MEA.

However, these conclusions must be tempered by a few observations. Firstly, it must be remembered that the PER and the POR are robustly and reciprocally connected (Burwell and Amaral, 1998). Secondly, there are also reciprocal, albeit

relatively weaker, connections which "mix" the two streams in the PHR, connecting the LEA to the POR and the MEA to the PER (detailed in van Strien et al., 2009). Finally, there are extensive associational connections between the MEA and LEA, which are discussed below (Burwell and Amaral, 1998). Overall, the existence of such connections suggest that although processing may occur preferentially in two parallel streams, it would be overly simplistic to consider them as being completely segregated from one another.

1.2.4.4 Projections of the entorhinal cortex along the hippocampal septotemporal axis

The patterns of associational connectivity within the EC suggest that it can be divided into three bands along the rostromedial-caudolateral axis: a medial, an intermediate and a lateral band (Figure 1.4). Associational projections arising from the rostromedial EC terminate predominantly in rostromedial EC, forming the medial band. Caudoventral associational projections are likewise mostly restricted within a caudoventral region, the lateral band, and those distributed between these bands form the intermediate band. Interestingly, these bands cross the border of the MEA and LEA and so must 'mix' the two streams discussed above.

The difference in anatomical positioning of the bands means that they receive differential cortical and subcortical innervation. The lateral portion of the EC receives the majority of the cortical input, carrying exteroceptive sensory information. In contrast, cortical innervation of the medial portion is much sparser and instead it is innervated by structures such as the amygaloid complex, which convey interoceptive or affective information.

This separation of the EC into three bands is preserved in the projection of the EC to the HF, with the lateral band projecting to the septal half of the HF, the medial band to the temporal quarter and the intermediate band to the remaining quarter of the septotemporal axis. In agreement with this, there is some evidence of restriction in the septotemporal extent of projections from field-to-field in the HF. The axonal plexus of septally-located CA3 pyramidal cells innervate roughly two-thirds of the septotemporal extent of CA1, whereas those located temporally innervate one-third (Li et al., 1994). Similarly, the axon plexus of a CA1 pyramidal cells innervate roughly a third of the septotemporal extent of the SUB (Tamamaki et al., 1987).

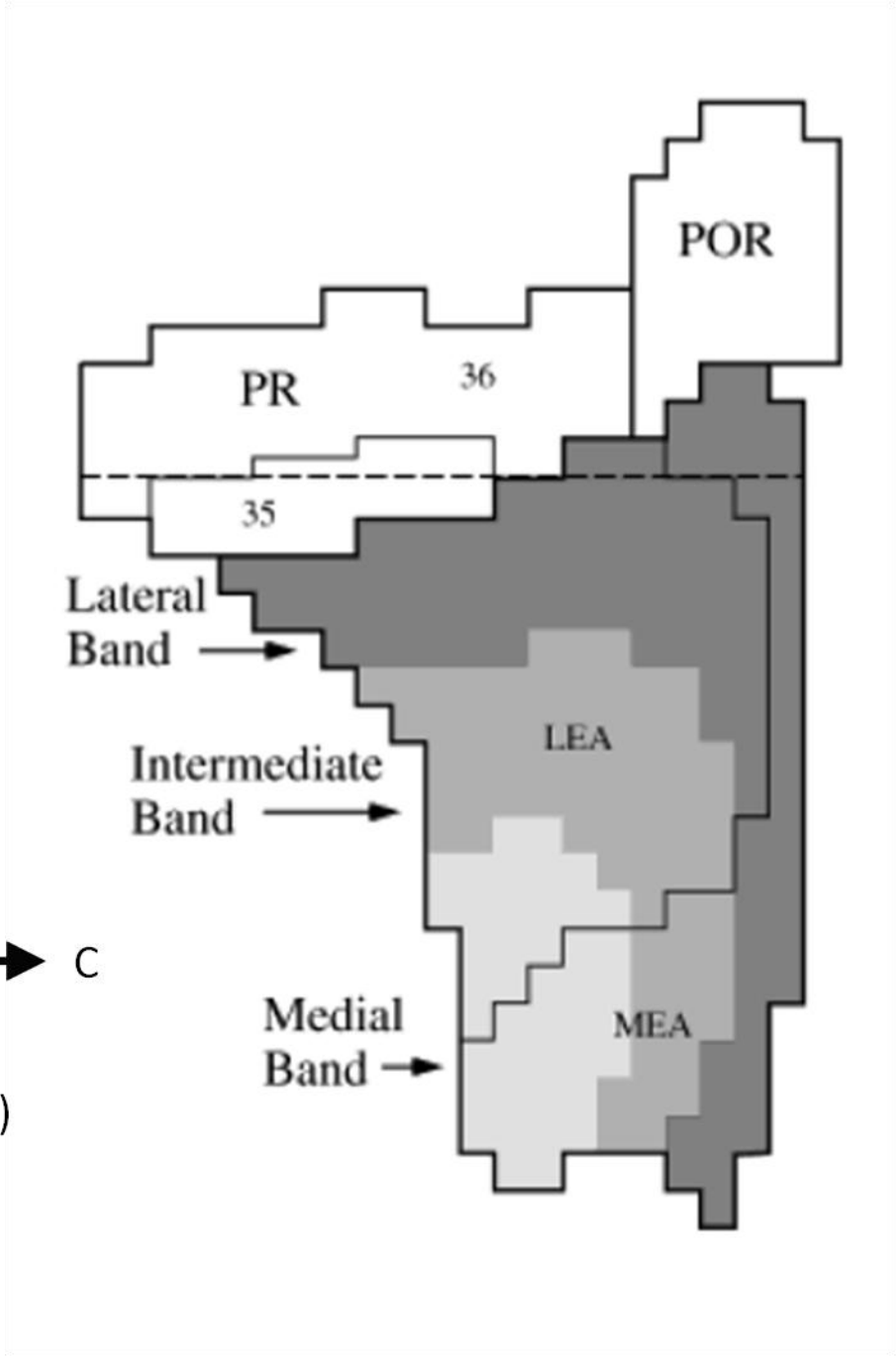

Figure 1.4. A flattened map of the entorhinal, perirhinal (PR; including areas 35 and 36) and postrhinal (POR) cortices showing bands of preferential associational connectivity within the entorhinal cortex. These occupy distinct areas that cross the border of the medial and lateral entorhinal areas: the medial band is restricted to a rostromedial patch, the lateral band covers the lateral and caudal edge, and the intermediate band covers the area in between. The major axes are shown on the left. (*Adapted from:* Burwell and Amaral, 1998)

Therefore, although there is some divergent spread of information along the septotemporal axis, there is still a possibility of some septotemporally restricted processing. In agreement with this, behavioural and electrophysiological studies support the idea of functional dissociations between the ventral and dorsal HF (Moser and Moser, 1998; Fanselow and Dong, 2010).

1.3 Cell types of the hippocampal formation

In this section, I will give a brief overview of the different cell types found in the HF, particularly in relation to their morphology and laminar organisation. A discussion of the glial cells of the HF, or any cell type of the PHR is beyond the scope of this thesis. Therefore, I will begin by discussing the principal cells of the HF and then move on to a more detailed description of the interneurons, in particular the basket cell class due to its relevance to cannabinoid action in the HF.

1.3.1 Principal cells

The principal cell type of the CA1-3 fields and the SUB is the pyramidal cell, whilst that of the DG is the granule cell. The morphology of these two cell types is quite distinct. The granule cell exhibits a unipolar cone-shaped dendritic tree that extends superficially into the ML of the DG. In contrast, pyramidal cells have a bipolar dendritic arbour: their apical dendrites project superficially (towards the hippocampal fissure), whilst their basal dendrites extend to deeper layers (SO in the CA fields, PL in the SUB). Granule cells far outnumber the other principal cells of the HF: there are around 1,200,000 granule cells in the DG of the adult rat, compared to approximately 8-10 times fewer principal cells in every other field of the HF (West et al., 1991).

1.3.2 Interneurons

In addition to the excitatory principal cells, a wide diversity of inhibitory GABAergic interneuron types are found throughout the HF. Far from simply being involved in supporting the activity of the principal cells, the interneurons are now understood to be critical to hippocampal functioning (Klausberger and Somogyi, 2008). Although a complete description of the full diversity of such interneurons is beyond the scope of this thesis, it is necessary to give a brief overview of the main categories and laminar organisation of these cells. In this section, I shall describe

the morphology of the relevant interneuron types and will return to discussing the electrophysiology of these cells in the following chapter.

1.3.2.1 Dendritic-targeting interneurons

Hippocampal interneurons can be categorised according to a number of different criteria, but it is most useful to begin with a division according to whether the interneuron targets the dendritic or perisomatic region of the principal cell. The majority of interneuron classes in the HF target the dendrites; indeed such dendritic innervation accounts for 92% of GABAergic input to the pyramidal cells of CA1 (Megías et al., 2001). There are at least 12 different types of dendritic-targeting interneuron that together can be found in every layer of CA1. These interneuron types are reviewed in detail in (Klausberger, 2009).

1.3.2.2 Perisomatic-targeting interneurons

In addition to the dendritic-targeting interneurons, there are two types of interneuron that target the perisomatic region: the basket cell and the axo-axonic cell.

Axo-axonic cells

Axo-axonic cell somata are found in or adjacent to the principal cell layer and their axonal projections innervate the axon initial segment of the principal cells. Since the axon initial segment is crucial to the initiation of action potentials (Clark et al., 2009), it was long supposed that the axo-axonic cell was involved in inhibiting pyramidal cell activity. However, recent findings have shown that due to a depolarised reversal potential in the axon initial segment relative to the somatodendritic compartment, these cells may actively discharge instead of inhibit pyramidal cells (Szabadics et al., 2006).

Basket cells

A description of the basket cell type is particularly important to understanding cannabinoid action in the hippocampus, so I shall describe it in greater detail. The "basket cell" is in fact not a homogenous cell type, but is a category that encompasses a population of interneurons possessing somewhat heterogenous afferent connections, axonal arborisation and neurochemical markers (Freund and Buzsáki, 1996). However, the common feature of these cells is their targeting of the somata and proximal dendritic regions of the principal cells.

At least 2 morphologically distinct types of basket cell in the DG: the pyramidal and the hilar basket cells (Freund and Buzsáki, 1996). Pyramidal basket cells are located in the deep portion of the GCL and their dendrites extend both superficially to the pial surface or hippocampal fissure and deep to the PL. As such, they are likely to be activated by feedforward excitation from the EC, CA3 and intrinsic commissural/associational connections, as well as feedback mossy fibre inputs. In contrast, the hilar basket cell has a dendritic tree that is largely restricted to the PL (hilus) and therefore is unlikely to receive any input from EC afferents.

In the CA fields of the HF, basket cells can be distinguished by the laminar position of their somata, which are either in SP (or occasionally the adjacent portion of SO) or in SR (Pawelzik et al., 2002). Both types of basket cell have dendritic trees that extend throughout all layers of the HF. As such, they may receive input from a wide range of afferent, efferent and intrinsic sources, such as entorhinal and subcortical afferents mossy fibres (in CA3) (Freund and Buzsáki, 1996).

The neurochemical expression pattern of the basket cell population also facilitates a division into two types. Importantly, expression of the cannabinoid-1 receptor (CB1R) is specific to a subset of basket cells that express cholecystokinin (CCK) (Katona et al., 1999). A mutually exclusive subset of basket cells is CB1R-negative and expresses parvalbumin (PV) (Kosaka et al., 1987). Microscopic examination of CCK-expressing basket cells has shown that they are predominantly bitufted and therefore are likely to correspond to the pyramidal basket cells of the DG and to both SR and SP basket cell types of the HPC (Freund and Buzsáki, 1996).

The PV- and CCK-expressing subtypes of basket cell have distinct connectivity, receptor expression and electrophysiological properties that suggest they play different roles in hippocampal functioning (Freund and Katona, 2007). This is topic is discussed in greater detail in the following chapter.

1.4 Anatomy of the hippocampal theta rhythm

1.4.1 The two components of theta

The theta rhythm, also termed rhythmical slow activity (RSA), is a high amplitude electrical oscillation of 6-12 Hz which occurs in the local field potential (LFP) of the

HF in rats during wakeful activity and rapid eye movement (REM) sleep (Whishaw and Vanderwolf, 1973). An understanding of the mechanisms by which the theta rhythm is generated is central to this thesis. Therefore, in this section I shall describe the anatomical and neurochemical bases of theta, before coming on to discuss the electrophysiological basis of theta in the following chapter.

Theta can be classified into two types on the basis of pharmacology and behavioural correlates. One type of theta has a frequency of 7-12 Hz and is resistant to the cholinergic antagonist atropine. It occurs during "voluntary" movements involving translation through space and has therefore been termed translation- or t-theta (Vanderwolf, 1969). The other type of theta has a frequency of 4-6 Hz and is observed during "automatic" behaviours such as chewing, scratching or sneezing, as well as during periods of alert immobility. This theta is known as arousal-, attentional- or a-theta. It co-occurs with t-theta during movement and, unlike t-theta, is sensitive to atropine (Kramis et al., 1975). During periods of quiescence in the rat, an asynchronous LFP activity known as large irregular activity (LIA) is observed. Theta activity may therefore represent the "on-line" state of the hippocampus (Buzsáki, 2002)

1.4.2 Pharmacological bases of theta

1.4.2.1 Cholinergic projections from the medial septum/diagonal band of Broca

This pharmacological dissociation of theta into two types implies that there are distinct neurotransmitter pathways in the brain contributing to the generation of the theta rhythm. Since atropine and other anticholinergic drugs block a-theta, this type of theta must depend on the cholinergic system. Localised injection studies have confirmed that the MS/DBB is a critical node in this network. Intraseptal administration of atropine is sufficient to abolish a-theta, but spares t-theta. Conversely, the intraseptal infusion of the cholinergic agonist carbachol induces persistent theta activity in the HF (Monmaur and Breton, 1991). This theta persists in all behavioural conditions, even during quiet immobility. These results demonstrate that the generation of a-theta depends on a cholinergic pathway passing through the MS/DBB.

Nonetheless, the question of whether a-theta requires the MS/DBB itself or simply a cholinergic stimulation of the HF is not fully answered by such studies.

Microinfusion of carbachol to the HF of urethane-anaesthetised rats elicits theta, suggesting that hippocampal stimulation alone may be sufficient (Rowntree and Bland, 1986). However, it is unclear from these results whether the theta elicited depends on activity induced in the MS/DBB via reciprocal septohippocampal projections. Intrahippocampal carbachol administration following inactivation of the MS/DBB with procaine, a local anaesthetic, fails to induce theta (Colom et al., 1991), apparently suggesting that the MS/DBB is required for hippocampal theta.

1.4.2.2 Roles of septohippocampal cholinergic, GABAergic and glutamatergic projections

An alternative explanation is that this failure results from a "hyperinhibition" of the HF, following the inactivation of GABAergic projections from the MS/DBB. When both carbachol and bicuculline, a GABA-A antagonist, are infused to the HF following procaine inactivation of the MS/DBB, short trains of theta-like activity are observed in the HF (Colom et al., 1991). These results lead to two conclusions: firstly, that the HF possesses an intrinsic network capable of generating brief trains of theta-like oscillations without the MS/DBB; and secondly, that such intrinsic networks are normally entrained to a theta rhythm by synergistic cholinergic and GABAergic inputs from the MS/DBB (Colom et al., 1991; Smythe et al., 1992).

Recent evidence suggests that glutamatergic projections may also play a role in theta generation. These account for approximately a quarter of the septohippocampal projection and arise predominantly from the medial septal region (Colom et al., 2005). Infusion of NMDA to the MS/DBB or HF induces theta activity in the HF, whilst infusion of the NMDA antagonist AP5 to either region reduces theta power (Bland et al., 2007). Therefore, contributions from cholinergic, GABAergic and glutamatergic septohippocampal projections are all significant in generating theta in the HF.

1.4.2.3 Cytoarchitectonic distribution of septohippocampal projections

Immunocytochemical studies reveal that the septohippocampal cholinergic projection innervates both pyramidal cells and interneurons in all fields of the HF (Léránth and Frotscher, 1987). In contrast, the GABAergic projection predominantly targets interneurons, with no discrimination between subtypes (Freund, 1992). The densest septal GABAergic input is to CA3, particularly in SO and SP, and also to the PL of the DG. In these fields, each interneuron receives

multiple synapses. In contrast, in CA1 innervation is much sparser and there are fewer synapses per interneuron (Freund and Buzsáki, 1996). Glutamatergic septohippocampal projections innervate the DG and CA1-3, but their laminar and synaptic targets are not known (Colom et al., 2005).

1.4.2.4 Cortical pathways of atropine-resistant theta

Whilst a-theta depends on a direct projection from the MS/DBB to the HF, the generation of the atropine-resistant t-theta relies on a network involving both the MS/DBB and the EC. Lesions or inactivation of the MS/DBB eliminate all theta activity in the HF, demonstrating that both a- and t-theta depend on the MS/DBB. Similarly, lesion of the fornix carrying subcortical afferents (including those from the MS/DBB) also abolishes both thetas (Green and Arduini, 1954). In contrast, lesions of the EC abolish t-theta but preserve a-theta (Vanderwolf et al., 1985). This suggests that the EC is part of a pathway that conveys the atropine-resistant t-theta to the HF.

Vanderwolf and colleagues (Vanderwolf et al., 1985) dissected the contribution of different cortical regions to the atropine-resistant t-theta using selective lesions. After isolation of the EC from its cortical inputs, normal a-theta and t-theta activity were observed in the HF, but this theta was rendered sensitive to atropine. Seeking to discover which cortical pathways were important to atropine-resistant theta, they found the greatest suppression of t-theta when the cingulate cortex was lesioned. In contrast, lesions of the entire neocortex that spared the cingulate cortex had much smaller effects, whilst control lesions to areas such as the amygdala, olfactory bulb or cerebellum had little or no effect.

These results suggest that a large proportion of the fibres conveying t-theta pass through the cingulate cortex en route to the EC. However, since cingulate cortex lesions only partially diminish atropine-resistant theta, whilst complete cortical isolation of the EC abolishes it, other cortical routes must also be involved in conveying t-theta to the EC. Therefore, the most congruent explanation for the source of atropine-resistant theta is that it depends on a non-cholinergic system comprising both septal afferents reaching the HF through the fornix and cortical afferents arriving via a distributed neocortical network that includes the cingulate and entorhinal cortices (Vanderwolf et al., 1985).

1.4.2.5 Roles of glutamatergic, GABAergic and serotonergic systems in atropine-resistant theta

A precise pharmacological definition of these pathways has proved elusive, but several neurotransmitter systems have been implicated. As described previously, glutamatergic and GABAergic projections from the MS/DBB are a significant source of non-cholinergic subcortical theta input to the HF. Glutamatergic entorhino-hippocampal neurotransmission via the NMDA receptor is critical, as ketamine and other NMDA blockers abolish the atropine-resistant component of theta (Horvath et al., 1988). This pathway is conveyed via layer II and III afferents from the EC to the distal dendrites of CA1 and CA3 pyramidal cells (Buzsáki, 2002).

The serotonergic system has also been implicated in atropine-sensitive theta. Preventing the synthesis of serotonin by chronic administration of *p*-chlorophenylalanine (PCPA), a tryptophan hydroxylase inhibitor, renders the remaining theta sensitive to atropine (Vanderwolf and Baker, 1986). Conversely, increasing the level of serotonin pharmacologically or by stimulation of brainstem serotonergic nuclei leads to an increase in atropine-resistant theta and type I behaviours (Peck and Vanderwolf, 1991; Robertson et al., 1991). Hippocampal levels of the serotonergic metabolite 5-HIAA have also been found to correlate positively with t-theta activity in the HF (Gemma et al., 1999). Thus, the generation of atropine-resistant theta involves the combined activity of the serotonergic, glutamatergic and GABAergic pathways.

1.4.3 Ascending brainstem theta-generating pathways

1.4.3.1 Regions involved in theta generation

As described in the previous section, both a- and t-theta depend critically on the activity of the MS/DBB. The MS/DBB is a critical node in a larger ascending brain network responsible for generating the theta rhythm (Figure 1.5). This network originates in the nucleus reticularis pontis oralis (RPO) of the rostral pons, which is modulated by cholinergic input from another brainstem structure, the pedunculopontine nucleus (PPN). Depolarisation of the RPO is sufficient to cause an increase in theta frequency in the HF, but notably, neurons of the RPO exhibit tonic, not rhythmic activity (Vertes and Kocsis, 1997).

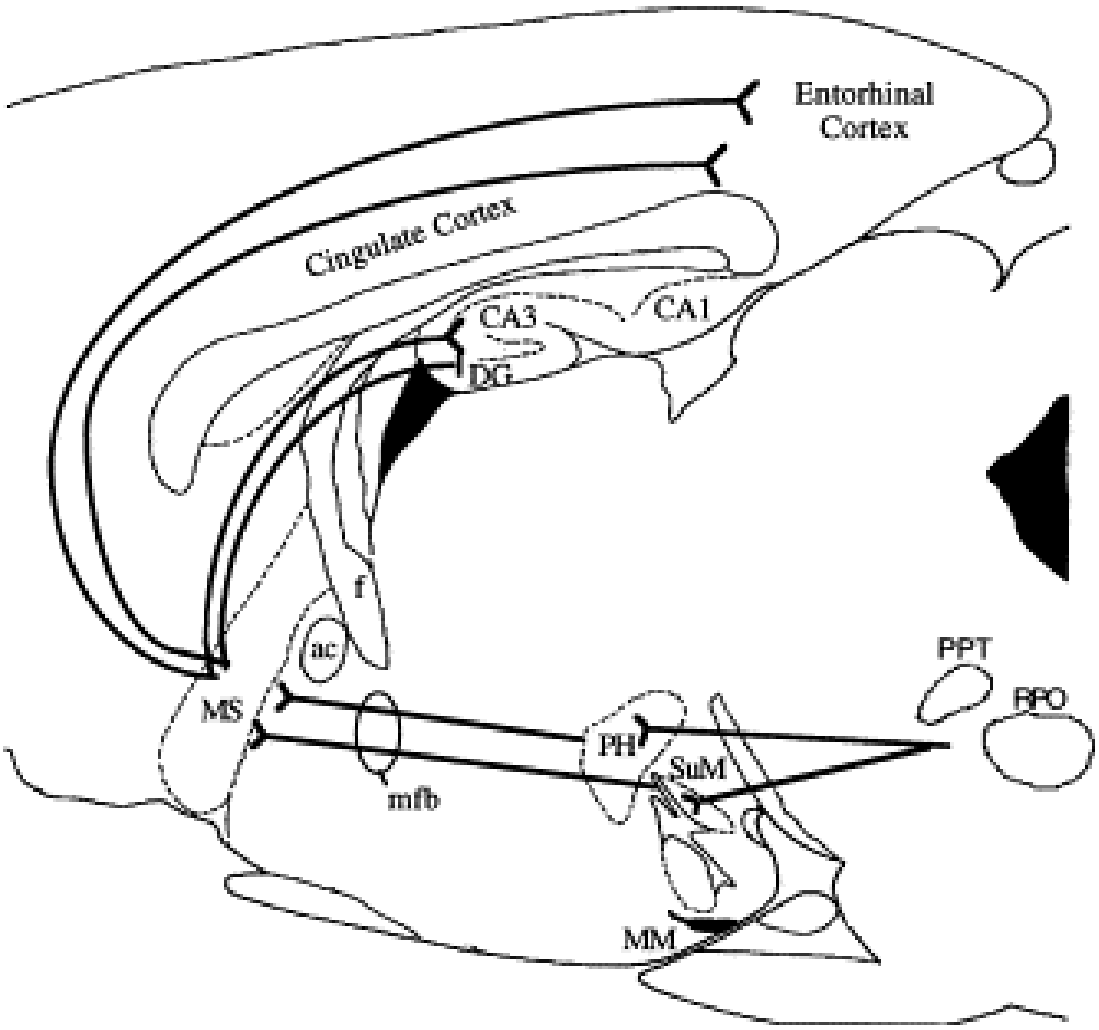

Figure 1.5. Sagittal view of the rat brain showing the anatomical regions in the ascending brainstem theta-generating pathways. The pathway originates in the brainstem reticular formation (bottom right), where the nucleus reticularis pontis oralis (RPO) is modulated by input from the pedunculopontine nucleus (PPT). The RPO projects to the posterior hypothalamus (PH) and supramamillary nucleus (SuM), which in turn project to the medial septum/diagonal band of Broca (MS). The MS gives rise to a direct projection to the hippocampal formation (DG, CA3 and CA1 are labelled) and an indirect projection that is conveyed to the hippocampus via the cingulate and entorhinal cortices. (*Source:* Bland and Oddie, 1998)

In contrast, cells within the supramammillary nucleus (SuM) of the hypothalamus, which receives tonic input from the RPO, display such rhythmic theta activity

(Kirk and McNaughton, 1991). However, since lesion of the SuM does not disrupt theta activity in the HF (Thinschmidt et al., 1995), this rhythmicity likely depends on reciprocal connections with the MS/DBB (Swanson and Cowan, 1979). In the freely moving animal, the SuM is thought to act in synergy with other brain areas in the ascending theta-generating pathways to modulate theta frequency (Vertes and Kocsis, 1997; Kirk, 1998). The SuM also projects strongly to regions with substantial connections to the HF, including the RE, EC and LS, as well as to the DG and CA3/CA2 fields of the HF.

Activity from the RPO is also conveyed via the posterior nucleus of the hypothalamus (PH), which is connected with the MS/DBB, but not to the HF itself. In contrast to the cells of the SuM, only tonic firing is observed in the PH and so it has been suggested that this region is involved in setting the general level of activity during theta behaviours (Vertes et al., 1995). Another pathway through which RPO activity reaches the forebrain is via the nucleus incertus (NI) (Teruel-Martí et al., 2008). This region is also connected to several of the subcortical areas involved in theta generation which have already been discussed, including the SuM, PH and MS/DBB.

Whilst these regions are associated with generating and synchronising the theta rhythm in the HF, serotonergic inputs originating in the median raphe nucleus (MR) of the brainstem exert a desynchronising influence on theta. The MR sends dense projections to both the MS/DBB and to all fields of the HF (Vertes et al., 1999). Lesions of the MR result in a continuous theta activity in the HF, regardless of behaviour (Maru et al., 1979). These results suggest that the MR plays an important role in regulating theta activity in the HF under different behavioural conditions.

1.4.3.2 Contributions of the different regions to the theta generation

So what are the relative contributions of the MS/DBB and the regions of the ascending brainstem pathway to theta generation? Jackson and Bland (2006) used independent and paired stimulations of the MS/DBB, PH and RPO combined with theta recording from the HF to investigate this. They applied a stimulation known to elicit a low frequency hippocampal theta to one region and a high frequency theta to the other. They found that if the MS/DBB was paired with either the PH or the RPO, the MS/DBB determined the hippocampal theta frequency. This

demonstrates that the MS/DBB has the dominant influence in setting the frequency of hippocampal theta.

These results emphasise the importance of the MS/DBB in theta generation and in combination with other findings, have led to the suggestion that it acts as a "pacemaker" for theta in the HF (Petsche et al., 1962; Stewart and Fox, 1990). It is still an open question as to whether the MS/DBB actively "drives" hippocampal theta or if it simply "facilitates" the emergence of intrinsic oscillatory networks within the HF. These are issues which will be discussed further in the following chapter.

1.5 Summary

Both the intrinsic and extrinsic connectivity of the hippocampal formation are distinctive and suggest that it processes information in a different way to the neocortex. Intrinsically, a unidirectional pattern of connectivity predominates, suggesting a sequential processing of information through the "polysynaptic loop". The extensive connectivity between the DG and CA3, as well as that of the CA3 auto-associational network indicate the importance of integration of information, especially in the early stages of the hippocampal loop.

In contrast, by examining the interconnections of the HF and PHR, the 'gateway' for cortical input to the HF, two orthogonal systems of parallel processing become apparent. One emerges from distinct bands along the rostromedial-dorsolateral axis of the EC and divides the HF septotemporally. The other carries two streams of information passing through the MEA and LEA that are separated along the proximodistal axis of the HF. These connections suggest that segregation of information is also important in hippocampal functioning.

In addition to being one of the few brains regions to receive highly processed, multimodal cortical input (via the EC), the HF receives several subcortical inputs, of which the most prominent is that arising from the MS/DBB. This MS/DBB is critical for hippocampal theta, which depends on an ascending network that originates in the brainstem. Afferent pathways carrying theta rhythmic input from the MS/DBB reach the HF both directly and indirectly via the cortex, and rely on the synergistic contributions of a number of different neurotransmitter systems. These inputs give rise to two components of theta which can be distinguished pharmacologically or behaviourally.

The anatomy and pharmacology covered in this chapter provide the necessary groundwork for understanding the electrophysiological functioning of the HF, as well as the possible mechanisms by which cannabinoids and novelty influence hippocampal activity.

2 Hippocampal electrophysiology

All principal cells and interneurons of the HF exhibit electrophysiological activity which can be measured in the freely moving animal by chronically implanting electrodes into the HF. This allows the recording of the activity of individual cells (termed "single units"), as well as the local field potential (LFP), an extracellular current which arises from the concerted activity of hippocampal cell ensembles (Buzsáki, 2002). Modern recording technologies allow the isolation and electrophysiological characterisation of many single units simultaneously, using "tetrodes" that consist of four electrodes coiled tightly together (Recce and O'Keefe, 1989; Szabó et al., 2001). Combined with behavioural analyses, these are powerful tools for elucidating the mechanisms of hippocampal function.

Many of the results presented in this thesis have been collected using such extracellular recording techniques, so in this chapter I have summarised the relevant literature on the electrophysiology of the HF. The chapter is divided into four sections which deal with different aspects of hippocampal electrophysiology:

2.1 The local field potential

The characteristics, mechanisms and functions of the LFP, focusing on theta, gamma and ripple oscillations.

2.2 Interneurons

The activity and function of interneurons in the HF, in particular those expressing cannabinoid receptors.

2.3 Place cells

The spatial firing properties of the pyramidal cells of the HF, known as place cells.

2.4 Grid and head direction cells

The spatial and directional firing properties of two types of cell found outside of the HF (the grid cell and the head direction cell), which are important to place cell activity and spatial cognition.

2.1 The local field potential

The local field potential (LFP) recorded from the hippocampus of the rat occurs in both rhythmical and non-rhythmical varieties. Rhythmical activity can be divided into delta (1-4 Hz), theta (5-12 Hz), beta (12-30 Hz), gamma (30-100 Hz) and ripple (100-200 Hz) frequency bands. Such rhythmical activity arises from the synchronised periodic activity of neuronal populations and afferent inputs to the HF (Buzsáki et al., 1983). In contrast, non-rhythmical activity is produced by the aperiodic activity of hippocampal neurons and is divided into two types, termed small and large amplitude irregular activity (SIA and LIA, respectively). Non-rhythmical activity is generally associated with quiescent or consummatory behavioural states, as are delta and ripple activity. In contrast, theta, beta and gamma activities are associated with movement and active behaviours.

A discussion of all the elements of the hippocampal LFP is beyond the scope of this thesis. Therefore, I shall focus on three types of LFP activity that are particularly relevant to understanding the literature and data subsequently presented: namely, theta, gamma and ripple oscillations.

2.1.1 Theta

Understanding the electrophysiological basis and functions of the theta oscillation is central to this thesis. Therefore, I shall describe in detail the literature concerning these topics, in order to complement the anatomical and pharmacological findings presented in the previous chapter.

2.1.1.1 Amplitude

The currents responsible for the extracellularly recorded theta oscillation (typically 0.5-2 mV in the rat in SP of CA1) arise from the combination of intrinsic and extrinsic current sources. The cytoarchitectonic arrangement of the CA1 layer into a large cellular sheet in which the dendrites and axons of the pyramidal cells are aligned likely contributes to the large extracellular field potential, as only small amplitude LFP signals are found in the non-laminar subcortical nuclei (Buzsáki, 2002). Theta is at its highest amplitude in SLM of CA1, but can also be recorded in CA3, DG and SUB, as well as extrahippocampal regions including EC, PER, cingulate cortex and amygdala (Buzsáki, 2002). In addition to interlaminar variations, theta amplitude is also dependent on the running speed (McFarland et al., 1975) and age of the animal (Wills et al., 2010).

The theta-wave current generated in CA1 arises mainly from a combination of perforant path input from EC, Schaffer collateral input from CA3, local interneuron activity and voltage-dependent currents in pyramidal cells (Buzsáki, 2002). Current source density (CSD) analysis indicates a number of current dipoles across the layers of CA1, with a prominent sink and source in SLM and SP, respectively, during the peak of SP theta (Mitzdorf 1985; G Buzsáki 1986; Brankack et al. 1993). Pyramidal cell dendrites in SLM receive EC input along the perforant path, suggesting that EC input drives the current sink. This is confirmed by lesion of the EC which abolishes the sink in SLM (Ylinen et al., 1995). The source in SP arises from rhythmic inhibitory postsynaptic potentials (IPSPs) from local perisomatic-targeting interneurons (axo-axonic and basket cell types) (Buzsáki, 2002). Additionally, there is a smaller sink in SR corresponding to Schaffer collateral input from CA3 (Buzsáki, 2002). Finally, voltage-dependent oscillations have been observed in the somata (Leung and Yim, 1991; Strata, 1998) and dendrites (Kamondi et al., 1998) of pyramidal cells and these also contribute to theta-associated currents.

2.1.1.2 Frequency

In the awake rat, the frequency of theta typically varies from 7-10 Hz, increasing linearly with the animal's running speed (Slawinska and Kasicki, 1998; Jeewajee et al., 2008a). Additionally, theta frequency is dependent on the age (Wills et al., 2010) and body temperature (Whishaw and Vanderwolf, 1971; Deboer, 2002) of the animal. In anaesthetised preparations, theta frequency is typically much lower (around 4-5 Hz), making comparisons of theta activity in awake and anaesthetised states difficult.

The pacing of the theta frequency is thought to arise from interactions between the HF and the MS/DBB via their reciprocal connections, but there is disagreement in the field about which region is dominant. The studies discussed in the previous chapter suggest a pivotal role for the medial septum/diagonal band of Broca (MS/DBB) in determining the frequency of the hippocampal theta rhythm, leading to its hypothesised role as the theta "pacemaker" (Petsche et al., 1962). However, there is also evidence that circuits intrinsic to the HF also have the potential to generate theta activity (reviewed in Buzsáki, 2002), suggesting that the theta rhythm could originate within the HF.

Evidence for an intrinsic hippocampal theta oscillator comes from the observation that application of the cholinergic agonist carbachol to hippocampal slices *in vitro* induces short bursts of theta-like activity (Konopacki et al., 1987; Bland et al., 1988; Fellous and Sejnowski, 2000). Furthermore, recordings from a complete septohippocampal preparation *in vitro* suggest that during carbachol-induced theta activity, hippocamposeptal inhibitory projections are dominant in setting the rhythmic activity of septal interneurons (Manseau et al., 2008). This rhythmic activity is proposed to emerge from the recurrent CA3 network (Kocsis et al., 1999), which is supported by the observation that hippocampal pyramidal cells show intrinsic theta-band oscillations *in vitro* (Leung and Yim, 1991; Strata, 1998). These findings suggest that the theta oscillation originates in CA3, which then synchronises septal rhythmicity.

In contrast, the septal "pacemaker" theory first put forward by Petsche and colleagues (1962) argues that the MS/DBB drives the hippocampal theta rhythm. Strikingly, lesion of the MS/DBB abolishes hippocampal theta, whilst rhythmic electrical stimulation leads to a matching theta frequency in the HF (Green and Arduini, 1954; Jackson and Bland, 2006). Electrode recordings in the MS/DBB of freely moving animals show cells with both bursting and non-bursting theta-modulated activity (Petsche et al., 1962; Gaztelu and Buño, 1982; King et al., 1998). Furthermore, information analyses of the firing activity of simultaneously recorded septal and hippocampal GABAergic interneurons during theta imply that septal interneurons drive hippocampal theta activity (Hangya et al., 2009).

Taken together and in light of the strong reciprocal connections between the septal nuclei and the HF, these findings suggest that interactions between the two regions are likely to determine the frequency of theta.

2.1.1.3 Phase

The phase of theta reverses across SP, such that theta recorded from SO and the hippocampal fissure are completely out-of-phase (Winson, 1974). This phase shift can be understood with reference to the out-of-phase current sources and sinks affecting the somata and dendrites of pyramidal cells, as described above. The prevalent view has been that theta oscillations are in-phase within a given layer throughout the whole HF (Buzsáki et al., 1983), but a recent study suggests that theta acts a travelling wave that moves roughly along the septotemporal axis of the

HF (Lubenov and Siapas, 2009). The speed of motion of the theta wave corresponds to a 4-8°/mm difference in phase in the CA1 region (Czurkó et al., 2011).

2.1.1.4 Functions

Theta activity is critical to hippocampal function in a number of ways. Firstly, the strength of potentiation or depotentiation of pyramidal cell synapses varies with the phase of theta. Long-term potentiation (LTP) (Bliss and Lomo, 1973), a long-lasting increase in synaptic efficacy elicited by a brief stimulation, is potently induced by theta-frequency stimulation *in vitro* (Rose and Dunwiddie, 1986) and this occurs optimally at the peak of the theta oscillation (Pavlides et al., 1988; Huerta and Lisman, 1993; Hölscher et al., 1997). The significance of this to the encoding of novel information is discussed in the Novelty chapter.

Secondly, the phase of theta is important in the temporal coding of information. It has been shown that the phase of pyramidal cell firing encodes information about an animal's spatial position, a phenomenon known as phase precession (O'Keefe and Recce, 1993) which is discussed in more detail in the section on place cells below.

Thirdly, there is now evidence that a reduction in the frequency of theta signals novelty (at least in the case of novel environments) (Jeewajee et al., 2008b). The influence of novelty on theta are discussed at greater length in the Novelty chapter.

Finally, according to the oscillatory interference model, the interference of theta-band oscillations is the underlying mechanism by which grid and place fields are generated depending on the animal's motion through space (Burgess, 2008). This model is described in more detail in the Models chapter.

2.1.2 Gamma

Gamma oscillations are higher frequency (30-100 Hz) rhythms found in all subfields of the HF and also in other cortical sites, including the EC (Bragin et al., 1995; Chrobak and Buzsáki, 1998). Within the HF, they are at their highest amplitude in the dentate hilar region (Buzsáki et al., 1983). Gamma activity occurs most prominently during exploratory behaviours including sniffing, as well as during REM sleep. It is typically modulated in synchrony with theta, such that gamma oscillations define short time windows "nested" within each theta cycle to which interneurons and principal cells phase-lock their firing (Bragin et al., 1995; Klausberger et al., 2003, 2005; Senior et al., 2008). This temporal structuring of

cell activity by gamma is thought to be important in the formation of cell assemblies, the dynamic routing of information flow and the encoding and retrieval of memories (Lisman, 2005; Colgin et al., 2009; Colgin and Moser, 2010).

Unlike theta, hippocampal gamma oscillations remain after lesion of all subcortical afferents to the HF (Buzsáki et al., 1987), implying that gamma is generated within the HF. Multisite recording studies have identified the source of the intrahippocampal generators as DG and CA3 (Bragin et al., 1995; Csicsvari et al., 2003). However, it is clear that the EC also contributes to hippocampal gamma, since bilateral lesion of this structure significantly diminishes the power and frequency of DG gamma (Bragin et al., 1995). Interestingly, this lesion eliminates high frequency gamma in the HF (50-100 Hz), whilst sparing a slower frequency gamma oscillation (25-50 Hz) that originates in CA3. A recent study suggests that these two gamma bands, termed "slow" gamma (25-50 Hz) and "fast" gamma (65-140 Hz), may be important for routing information between CA1-CA3 and CA1-EC, respectively (Colgin et al., 2009).

2.1.3 Ripples and large amplitude irregular activity

Large amplitude irregular activity (LIA) occurs during periods of quiescence in the awake rat and in the deep layers of EC and SR of CA1 consists of large amplitude aperiodic sharp waves, which are generated by bursts of activity in CA3 (Buzsáki et al., 1983). These sharp waves are often accompanied by high frequency oscillations (100-200 Hz) in CA1, known as ripples (O'Keefe and Nadel, 1978), which can be divided into slow (100-130 Hz) and fast (140-200 Hz) types. Parallel CA1-CA3 recordings show that fast ripples emerge in CA1, whereas slow ripples are generated in CA3 and conveyed to CA1 via SC inputs (Csicsvari et al., 1999a).

Pyramidal cell activity in CA1 is phase-locked to ripple events, whereas different classes of interneurons show different patterns of ripple-associated activity (Klausberger et al., 2003, 2005). The firing patterns of different interneuron classes are discussed in more detail in the following section.

Ripples are thought to be important in the consolidation of memory traces, possibly participating in the transfer of information from the hippocampus to neocortex during sleep or periods of quiescence (Sirota et al., 2003; Diekelmann and Born, 2010). Recently it was shown that blocking sharp wave-ripple activity after learning of a spatial task was sufficient to impair subsequent performance, supporting these conclusions (Girardeau et al., 2009).

2.2 Interneurons

The neurons of the HF can be divided broadly into two types: excitatory principal cells and inhibitory interneurons. In contrast to the relatively homogenous principal cells, the interneurons constitute a large diversity of cell types (Freund and Buzsáki, 1996; Klausberger and Somogyi, 2008). Within the CA1 subfield alone, at least 21 classes of interneuron have been identified which differ in their morphology, laminar distribution, molecular expression profiles and afferent and efferent connectivity (Klausberger and Somogyi, 2008). To describe all these interneuron types in detail would require a thesis by itself, so I shall restrict myself to discussing the most prominent delineations of hippocampal interneuron function, before focusing on the cannabinoid-sensitive interneuron types which are particularly relevant to understanding the data presented in the later chapters.

2.2.1 Complementarity in interneuron electrophysiology

Electrophysiological studies have revealed that different interneuron classes play distinct and complementary roles in hippocampal network activity during theta, gamma and ripple activity (Klausberger et al., 2003, 2005; Klausberger and Somogyi, 2008). In particular, a functional dichotomy has been observed between the mutually exclusive interneuron populations expressing the Ca^{2+}-binding protein parvalbumin (PV) or the neuropeptide cholecystokinin (CCK).

2.2.1.1 Parvalbumin-expressing interneurons

The temporal firing patterns of PV-expressing interneurons are distinct for each class during theta, gamma and ripple oscillations, providing a reliable "fingerprint" of activity across all such events (Figure 2.1; (Klausberger et al., 2003; Tukker et al., 2007). They also respond faithfully to artificial trains of repeated stimulation, showing no diminution in their firing frequency over time (a non-accommodating firing pattern) (Glickfeld and Scanziani, 2006). It has therefore been suggested that they provide a reliable "spatiotemporal structuring" of pyramidal cell activity, providing inhibition at specific times to precise locations on the somatodendritic tree (Klausberger and Somogyi, 2008).

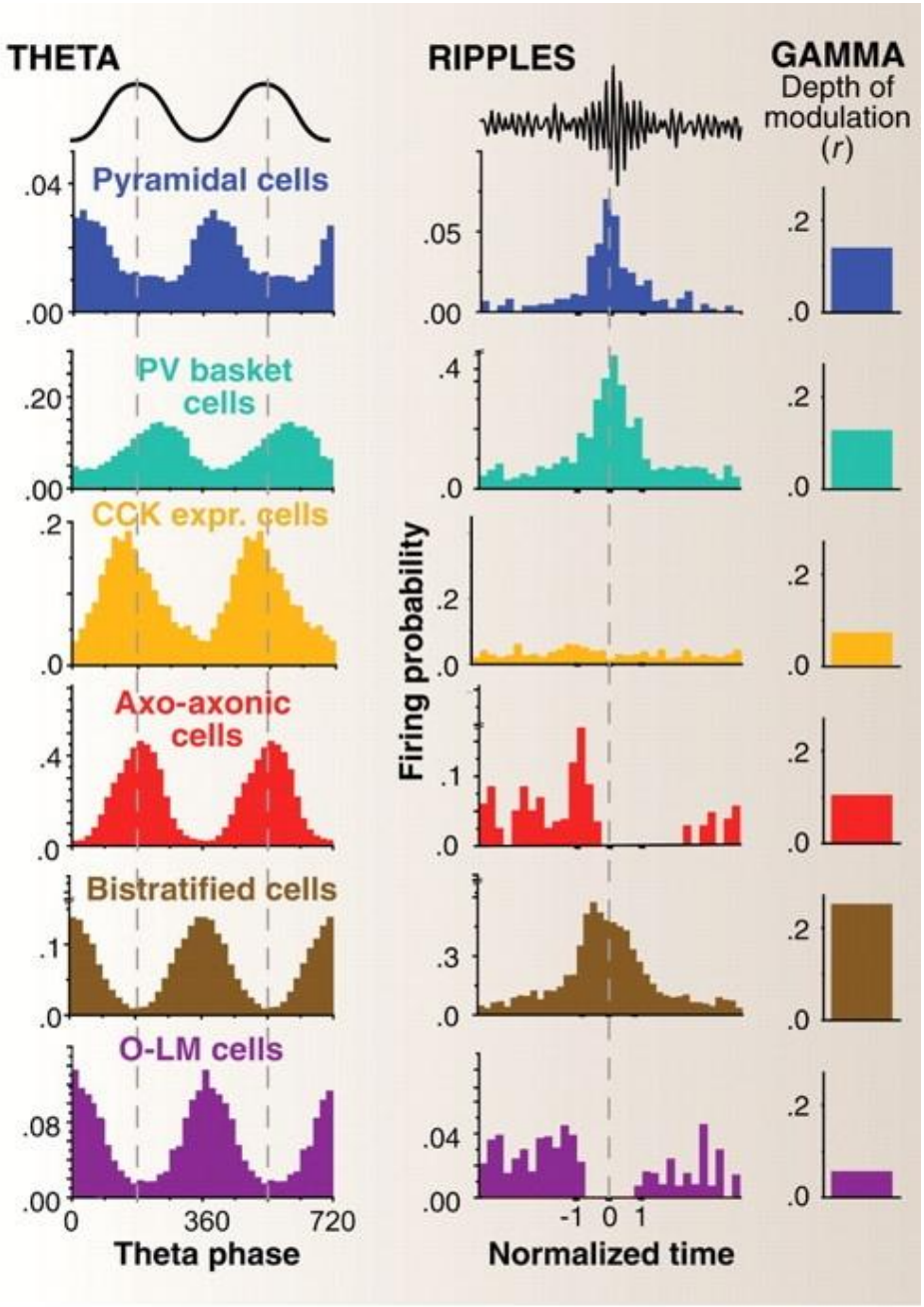

Figure 2.1. The firing patterns of CA1 pyramidal cells (dark blue) and defined classes of interneuron are distinct during different network states in anaesthetised rats. Parvalbumin- (PV) expressing interneurons include PV basket (blue-green), axo-axonic (red), bistratified (brown) and O-LM (purple) cells, whilst CCK-expressing cells (yellow) form a separate class. The *left* and *middle* columns show the temporal spiking probability of each class relative to theta and to the peak amplitude of ripple events, respectively. The *right* column shows the depth of gamma modulation for each class, determined by spike phase analysis. All local field potential activity relates to recordings from stratum pyramidale of CA1. (*Adapted from*: Klausberger and Somogyi, 2008)

2.2.1.2 Cholecystokinin-expressing interneurons

In contrast, CCK interneurons only transiently follow an input spike train and quickly accommodate their firing (Glickfeld and Scanziani, 2006). CCK interneuron activity is likely to be less temporally precise as they release GABA asynchronously, in contrast to the highly synchronous release from PV cells (Hefft and Jonas, 2005; Daw et al., 2009). However they still show moderate gamma modulation in anaesthetised recordings, firing at a gamma phase immediately before CA1 pyramidal cells discharge (Tukker et al., 2007). They also show a clear phase preference during the slower theta oscillation, discharging on average just before the peak in stratum pyramidale theta (Figure 2.1; Klausberger et al., 2005), which corresponds to the time at which pyramidal cells start firing as the rat enters the cell's place field (see section 2.3.3 for an explanation of place fields) (Figure 2.3c; O'Keefe and Recce, 1993; Huxter et al., 2003). During ripples, they fire in an episode-dependent manner with each CCK cell showing a unique pattern of activation, unlike the stereotyped firing activity of PV-expressing cells (Klausberger et al., 2005). These findings suggest that CCK interneurons are involved in controlling the precise phase of place cell firing during theta and gamma oscillations. Furthermore, the episode-specific modulation of CCK cell activity during ripples suggests that their activity may be influenced by contextual or interoceptive information.

2.2.2 Cannabinoid-sensitive interneurons

The cannabinoid 1 (CB1) receptor is the major cannabinoid-sensitive receptor in the brain and is found at high concentrations in all subfields of the HF (Herkenham et al., 1991). CB1 receptors are located presynaptically on interneurons and mediate a short-term depression of GABA release in response to a retrograde release of endogenous cannabinoids (endocannabinoids) from active pyramidal cells, a phenomenon known as depolarisation-induced suppression of inhibition (DSI) (Katona et al., 1999; Tsou et al., 1999; Freund et al., 2003). The mechanisms of cannabinoid signalling and DSI are discussed in greater detail in the following chapter.

CCK-expressing basket cells (CCK-BCs) constitute the vast majority of hippocampal CB1-expressing cells, accounting for 80-96% of the CB1-positive cell population (Katona et al., 1999; Tsou et al., 1999). CB1 receptor expression has also been reported on other interneuron types targeting the dendrites of pyramidal

cells, namely the Schaffer collateral-associated, apical dendrite innervating and perforant path-associated interneurons, but in far lower levels (Marsicano and Lutz, 1999; Klausberger et al., 2005; Ali, 2007). Furthermore, recent findings indicate that cannabinoid control of GABA release is much weaker at dendritic compared to perisomatic CB1-positive pyramidal cell synapses (Lee et al., 2010), implying that the predominant effect of cannabinoids in the HF is on CCK-BCs. Therefore, I shall focus on this interneuron type and contrast it to the mutually exclusive (CB1-negative) PV-expressing basket cell (PV-BC) type in order to draw out the functional implications of cannabinoid action on the HF.

2.2.3 Basket cells

Basket cells constitute the major perisomatic interneuron type of the cerebral cortex and target the perisomatic region of principal cells in the HF, which includes the soma, axon initial segment and the proximal dendritic membrane up to 100μm from the soma (Megías et al., 2001; Papp et al., 2001). Their perisomatic targeting means that they are ideally positioned to control principal cell oscillations, synchrony and synaptic integration (Cobb et al., 1995; Fricker and Miles, 2000). The majority of basket cells express PV (Kosaka et al., 1987), whilst a mutually exclusive subset express the CCK (Nunzi et al., 1985). The CCK- and PV-expressing types differ markedly in their afferent connectivity, electrophysiological properties and expression of transmitters, modulators and receptors (Freund, 2003).

2.2.3.1 Functions

These differences have led to the suggestion that the two types of basket cell perform distinct functions (Freund, 2003; Freund and Katona, 2007). CCK-BCs are proposed to integrate anxiety- and arousal-related inputs to selectively modulate the firing of target pyramidal cells and undergo fine-tuning of their activity in response to differing levels of input and output activity. In contrast, PV-BC firing is argued to be more “hard-wired” and primarily involved in coordinating precisely-timed oscillatory activity in the hippocampal network. In the subsequent sections, I shall outline the findings which support such a dichotomy in PV- and CCK-BC function.

2.2.3.2 Dendritic inputs and receptors

The two basket cell types differ in their subcortical and local inputs and in the receptors associated with each.

CCK-BCs are the predominant recipients of subcortical inputs, including a prominent serotonergic innervation arising from the brainstem median raphe nuclei. They selectively express 5-hydroxytryptamine type 3 ($5HT_3$) receptors (Freund et al., 1990; Morales and Bloom, 1997; Férézou et al., 2002), antagonists of which are known to be anxiolytic (Jones et al., 1988; Costall et al., 1990).

In contrast, both types of basket cell receive cholinergic septo-hippocampal innervation, but CCK-BCs are more sensitive to cholinergic modulation, which may relate to the different nicotinic and muscarinic receptor expression profiles of each type (Cea-del Rio et al., 2010). Nicotinic receptors (specifically, the α7 subtype in the HF) are found only on CCK-BCs (Freedman et al., 1993; Frazier et al., 1998; Morales et al., 2008). Both types express the excitatory muscarinic receptor M1 post-synaptically, but only CCK-BCs express M3 receptors (Cea-del Rio et al., 2010; Chiang et al., 2010). In contrast, pre-synaptic M2 receptor expression is higher in PV-BCs (Hájos et al., 1998), which when activated likely lead to a suppression of GABA release (Fukudome et al., 2004). *In vitro* hippocampal slice recordings suggest that these differences in muscarinic receptor expression are significant, since coincident glutamatergic Schaffer collateral input and muscarinic activation increases the excitability of CCK-BCs but not PV-BCs (Cea-del Rio et al., 2010).

The two basket cell types differ also in their local afferent inputs. PV-BCs receive fewer GABAergic inhibitory inputs than CCK-BCs but three times as many GABA-negative asymmetrical, presumed excitatory glutamatergic Schaffer collateral inputs (Gulyás et al., 1999; Mátyás et al., 2004). This suggests that inputs from CA3 play a much more substantial role in PV-BC activity, whereas CCK-BC activity depends on the interplay between local GABAergic inhibition and their subcortical inputs. In line with this Glickfeld and Scanziani (2006) found that the peak amplitude of excitatory post-synaptic currents (EPSCs) elicited by Schaffer collateral stimulation is more than seven times higher in CB1-negative (presumed PV-positive) than CB1-positive (presumed CCK-positive) BCs in CA1 (ref).

NMDA receptor expression is also much sparser at PV-BC glutamatergic terminals than in CCK-BCs (Nyíri et al., 2003). This suggests that the glutamatergic drive to

PV-BCs is mediated primarily by AMPA receptors and is non-plastic, whereas that to CCK-BCs is modifiable depending on the afferent pyramidal cell activity.

CCK-BCs are also selectively innervated by calretinin-positive interneuron-selective (CR-IS) interneurons, which may provide an additional source of temporal synchrony to the CCK-BCs (Gulyás et al., 1996).

2.2.3.3 Axonal outputs and receptors

PV- and CCK-BCs are indistinguishable anatomically in terms of the terminals they form on the perisomatic compartments of pyramidal cells. However, there are important differences in the expression of receptors on both the presynaptic and postsynaptic membranes.

$GABA_A$ receptors at postsynaptic sites on pyramidal cells receiving CCK-BC innervation are selectively enriched in α2 subunits (Nyíri et al., 2001), whereas those receiving PV-BC innervation are composed mainly of α1 subunits (Thomson et al., 2000; Klausberger et al., 2002). Interestingly, the anxiolytic benzodiazepine drugs are known to mediate their effects via α2-enriched $GABA_A$ receptors (Löw et al., 2000), providing a further link between anxiety and CCK-BCs.

Of course, CCK itself plays an important role in anxiety regulation (Ravard and Dourish, 1990; Harro et al., 1993). The predominant receptor for CCK in the brain (which is found at CCK-BC terminals) is the CCK_B receptor, with agonists and antagonists exerting anxiogenic and anxiolytic actions respectively. CCK-positive interneurons release CCK in a Ca^{2+}-dependent manner and represent the major source of this cortical neuropeptide (Vallebuona et al., 1993). Interestingly, it now appears that CCK functions as a "molecular switch" in the hippocampal network, increasing the inhibitory input on to pyramidal cells by directly depolarising PV-BCs and down-regulating CCK-BC activity via retrograde CB1 signalling (Földy et al., 2007). Presynaptic cannabinoid signalling is a major topic of this thesis and will be discussed in detail in the following chapter.

However, it is important to note that presynaptic inhibition can also be mediated by $GABA_B$ receptors, which are found in large numbers in CCK-BCs but not PV-BCs (Sloviter et al., 1999). Activation of $GABA_B$ receptors on CCK-BCs directly blocks GABA release, but tonic inhibition of release is controlled by CB1, not $GABA_B$ receptors (Neu et al., 2007). This suggests that $GABA_B$ receptors are involved in phasic autocrine inhibition of CCK-BCs. Importantly, $GABA_B$ and CB1

receptors share the same G-protein signalling pathway and both inhibit CCK-BC activity by modulating N-type Ca^{2+} channels (Neu et al., 2007).

In contrast, presynaptic modulation of PV-BC activity is controlled by muscarinic M2 receptors. As described above, these are found in higher concentrations in PV-BCs. Recent findings suggest that cholinergic activation of these receptors reduces inhibitory currents in postsynaptic pyramidal cell boutons (Szabó et al., 2010).

2.2.3.4 Electrophysiology

As the data in this thesis are collected using extracellular recordings in awake, freely moving rats, I will focus on the implications of findings in the literature regarding the expected firing activity of PV- and CCK-BCs in the awake animal.

On the basis of studies in anaesthetised animals, both BC types are expected to be both theta- and gamma-modulated. These studies suggest that CCK-BCs will fire just before CA1 pyramidal cells on gamma cycles (Tukker et al., 2007). Likewise, CCK-BCs would be expected to fire just before place cells fire on the theta cycle as the rat enters the cell's place field (see following section on place cells; Figure 2.1 and Figure 2.3c; O'Keefe and Recce, 1993; Huxter et al., 2003; Klausberger et al., 2005). In comparison, PV-BCs are predicted to fire later on both theta and gamma cycles (Klausberger et al., 2003).

A major difference in the two types is in their activity during sharp-wave ripple (SWR) events, when recorded in an anaesthetised preparation (Figure 2.1; Klausberger et al., 2003, 2005). PV-BC firing is reliably increased in synchrony with ripple events, whereas CCK-BC firing on average shows no change, but individual cells show firing rate modulation in an episode-dependent manner.

In terms of their firing activity, *in vitro* recordings suggest that the majority of PV-BCs are fast-spiking, whereas most CCK-BCs are regular-spiking (Kawaguchi et al., 1987; Pawelzik et al., 2002). Due to the technical difficulties of recording identified interneurons *in vivo*, there are only sparse data concerning the firing rates of the two types in anaesthetised animals (Klausberger et al., 2003, 2005) and these find no difference in the firing rates of the two BC types.

The majority of studies examining hippocampal interneuron firing in freely moving animals have only distinguished interneurons *en masse* from principal cells (e.g. Ranck, 1973; Nitz and McNaughton, 2004; Hangya et al., 2010), however some have distinguished more classes on the basis of firing activity (e.g. Anderson and

O'Mara, 2003). Czurko and colleagues (2011) attempted to identify putative PV- and CCK-BC classes in awake, freely moving rats on the basis of their theta phase preferences (Klausberger et al., 2003, 2005). They found no differences in firing rates between the two classes (or indeed between any of the theta-modulated interneuron classes they identified). Therefore, it is unclear if the firing rates of the two basket cell types are similar *in vivo* to *in vitro*.

As well as suggesting that the two basket cell types can be distinguished by their firing rates, *in vitro* studies indicate that there is a significant difference in the response of the two types to repeated afferent stimulation. Glickfeld & Scanziani (2006) found that EPSC amplitude was maintained in CB1-negative (putative PV-) BCs under repeated stimulation, but in CB1-positive (putative CCK-) BCs there was a short-term depression in EPSC amplitude with successive stimulations. This contributes to the non-accommodating and accommodating firing patterns shown by PV- and CCK-BCs, as described previously.

The exact firing patterns of PV- and CCK-BCs critically depends on the excitatory input to each. Whilst PV-BCs can respond to a single source of feed-forward excitatory input, the stronger inhibition to CCK-BCs, coupled with their longer membrane time constants, means that they are most likely to be activated by multiple inputs integrated over larger time windows. The spiking pattern of each BC type *in vivo* is not known, but these findings suggest PV-BCs may show more sustained firing during each theta cycle, whereas CCK-BC firing could be more transient.

2.3 Place cells

In 1971, O'Keefe and Dostrovsky first described the spatially-related activity of neurons in the rat hippocampus. These cells were termed "place cells" as each cell fired only in a particular location of the environment, known as its "place field" (Figure 2.2, bottom right). This led O'Keefe and Nadel (1978) to propose that the hippocampus is the neural substrate of an allocentric "cognitive map" of space. Studies in the 40 years since the discovery of place cells have reported place-related firing in all areas of the HF (Moser et al., 2008), with the most distinct spatial firing found in the CA1 and CA3 regions (Barnes et al., 1990).

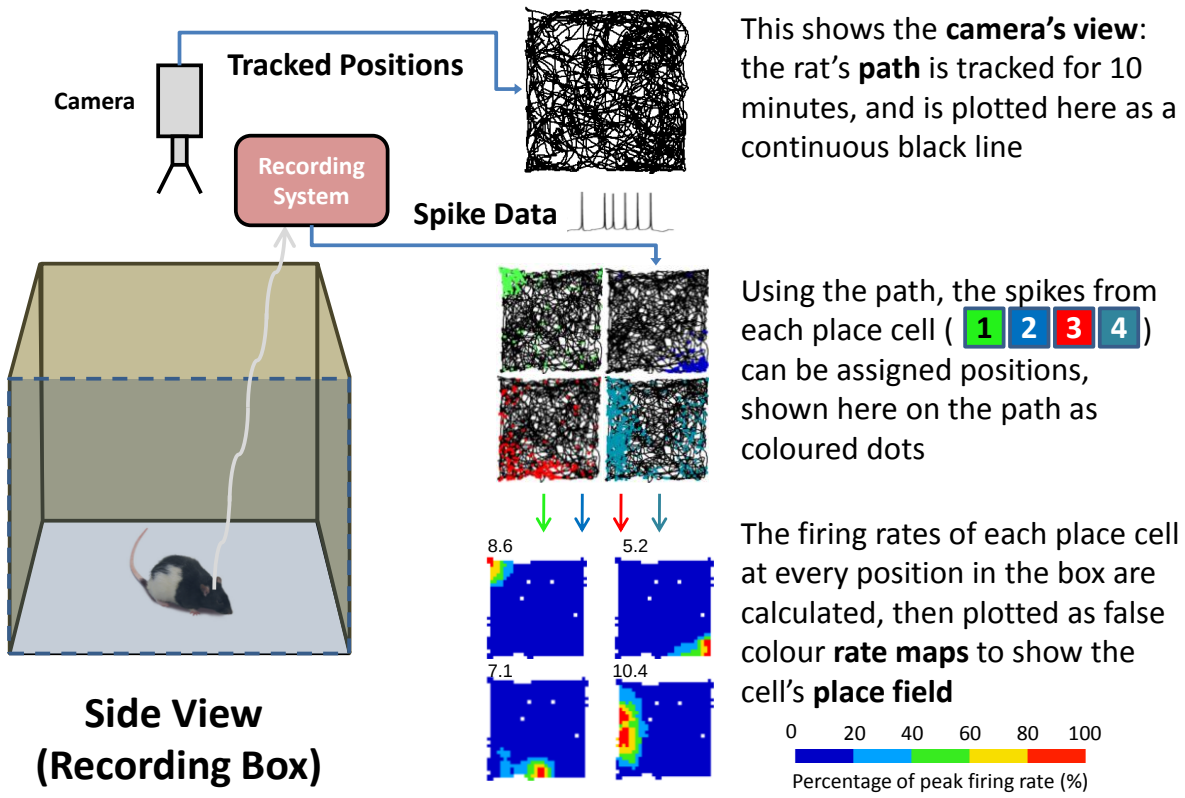

Figure 2.2. Summary of the basic steps involved in the recording and subsequent processing of the animal's spatial trajectory and hippocampal place cell activity. The trajectory alone can be plotted as a path plot (top right); the activity of individual place cells can be plotted as a spike plot (middle right) or as a rate map (bottom right). The rate map plots the spatial firing of the place cell using a false colour gradient scaled to the peak firing rate of the cell. The peak firing rate in Hz is then typically displayed to the top left of the rate map, as shown.

2.3.1 Basic properties

2.3.1.1 Firing characteristics

Place cells fire with characteristic bursts of 2-6 action potentials of progressively diminishing amplitude separated by up to 6ms each, known as "complex spikes" (Ranck, 1973; Harris et al., 2001). The time interval of action potentials fired within a complex spike implies that the firing rate of the cell can approach 200 Hz for brief periods. However, the peak rate is normally estimated by collecting all the spikes fired in a small region of space (a "spatial bin", typically around 2.4 × 2.4 cm) during a trial and smoothing this with neighbouring bins, yielding a peak rate

that varies from 1 – 30 Hz. In contrast, the mean rate of the place cell across the trial is very low, typically below 1 Hz. This is a reflection of the high degree of spatial selectivity of place cells, with out-of-field firing rates approaching 0 Hz.

2.3.1.2 Anatomical identity

Anatomically, the place cells are likely to correspond to the pyramidal cells of the HF, since these cells exhibit complex-spiking behaviour in *in vitro* hippocampal slice recordings and in combined intracellular and extracellular recordings *in vivo* (Henze et al., 2000). If place cells are recorded from CA1 in freely moving animals, their spiking activity is found to excite hippocampal interneurons on a timescale that implies monosynaptic transmission (Csicsvari et al., 1998). The pyramidal cells are the only excitatory cells of this field and indeed make such monosynaptic connections onto local interneurons, providing strong evidence that they are the place cells.

2.3.1.3 Active and silent cells

If place cells are recorded from two or more environments, it quickly becomes apparent that cells which are active in one environment may be silent in some or all of the other environments (O'Keefe and Conway, 1978). Additionally, a proportion of pyramidal cells display no spontaneous activity in the freely moving animal and therefore are "invisible" under normal recording conditions. Thompson and Best (1989) estimated the proportion of active pyramidal cells by comparing the numbers recorded in three environments to an estimate of the "total population" numbers counted during slow-wave sleep or during anaesthesia (when much larger numbers of cells become active). They reported that just over a third of pyramidal cells were active in at least one of the three environments. Wilson and McNaughton (1993) recorded large place cell ensembles in different environments and estimated the proportion that have a field in each environment is 30-70%. Thus it is clear that a significant proportion of putative place cells are silent in any given environment. The balance between active and silent cells in the hippocampus may be important for the efficient "sparse coding" of information, maximising the number of environments that the place cell population can represent (Barnes et al., 1990; Muller, 1996).

2.3.2 Encoding of information

2.3.2.1 Rate coding

The spatial position of the animal is thought to be conveyed via two coding mechanisms. The first is the variation of firing rate within the place field. In an open field environment, the firing rate within a field approximately follows a 2-dimensional Gaussian distribution, such that there is a single peak at the centre and a gradual decrease of firing rate towards the edge of the field (Figure 2.2, bottom right and Figure 2.3b; O'Keefe and Burgess, 1996). Towards the walls or corners of a walled environment the field often becomes flattened against the boundaries, but normally retains a single peak. Within the field, the firing rate varies from 0 Hz at the edge up to as much as 30 Hz at the peak. Hence, the firing rate conveys information about the animal's proximity to the centre of the place field.

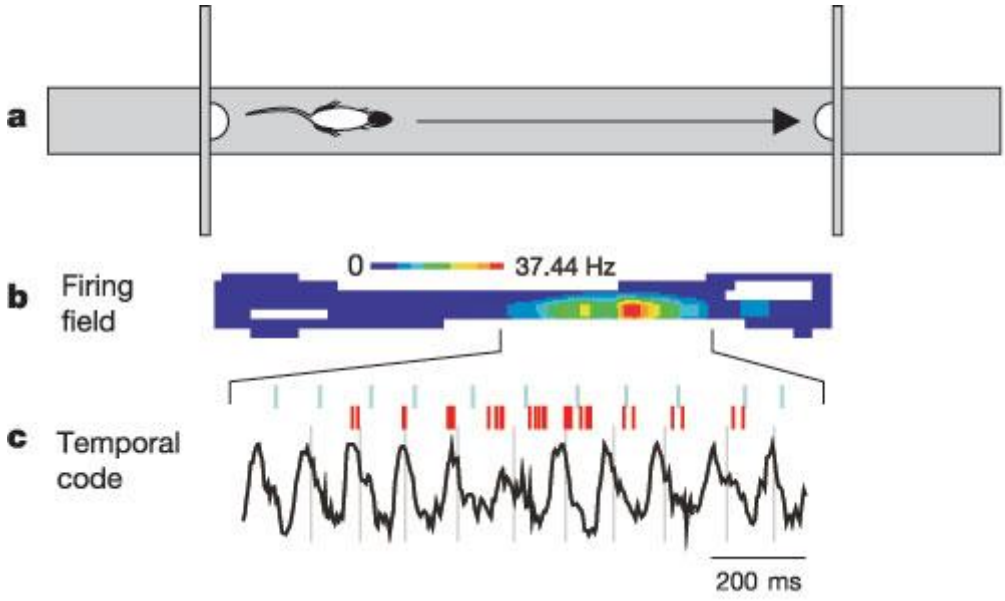

Figure 2.3. Rate and temporal coding by a place cell during runs on a linear track. (a) Overhead view showing eastward run of rat on linear track between two feeding points at either end of the track. (b) False-colour firing rate map of a single place cell during all eastward runs recorded during a trial, showing rate coding of spatial position. (c) The temporal firing of the place cell (raster spike plot in red) relative to the concurrently recorded theta oscillation (black trace, below) shows a gradual precession in theta firing phase across the field. Light blue bars mark the times at which the voltage of the theta oscillation changes from positive to negative, whilst the longer grey bars mark the times when theta phase is estimated to be 270°. (*Adapted from*: Huxter et al., 2003)

There is also evidence of an excess variance or "overdispersion" in place cell activity, which may indicate rate coding of variables other than position (Fenton and Muller, 1998; Olypher et al., 2002). There are many suggestions as to what variables might be encoded in this way, including speed (Huxter et al., 2003; Geisler et al., 2007), time (Wiener et al., 1989), odour (Wiebe and Stäubli, 1999; Wood et al., 1999) and goal-related information (Hok et al., 2007).

2.3.2.2 Phase coding

The second way in which spatial position is encoded in place cell firing is via the phase of the spikes relative to the ongoing LFP theta oscillation. O'Keefe and Recce (1993) discovered that as the animal runs through a place field, the spikes of the place cell precess (that is, fire at progressively earlier phases) by up to 360° on subsequent cycles of theta (Figure 2.3c). This "phase precession" correlates better with the animal's position in the field than other variables such as the time spent in the field or the instantaneous firing rate of the cell (Huxter et al., 2003). Using such information in combination with the rate can improve the estimation of the animal's position by more than 40% (Jensen and Lisman, 2000).

It has also been reported that in rats running on a wheel, the phase can vary depending on the orientation of the apparatus in the room (Hirase et al., 1999; Harris et al., 2002). However, phase precession in open field environments does not display such directional modulation (Huxter et al., 2008). Importantly, it has also been confirmed that rate and phase can vary independently and therefore comprise complementary systems for encoding position (Huxter et al., 2003). Hence, the rate and phase codes work together to accurately specify the animal's position in an environment.

2.3.2.3 Ensemble coding

The accuracy of the spatial signal may also depend on combining the activity of more than one place cell. It is common to find place cells with overlapping fields in the small (less than $1m^2$) environments typically used in experimental studies. Given that multiple place cells will therefore be active at any given location, collectively they may provide a more accurate "ensemble code" of space (Muller, 1996; Fenton et al., 2008).

The importance of ensemble coding becomes more apparent if one considers that place cells may have multiple spatial fields, especially as the size of the recording

environment grows. Place cells recorded from the dorsal pole of the HF in small environments (less than $1m^2$) usually have a single firing field, with multiple fields observed in as little as 5-10% of the population (O'Keefe, 2007). However, higher numbers of fields are observed in larger environments. Fenton and colleagues (2008) found that CA1 place cells with single fields in a 68 cm diameter cylinder had an average of four fields in a larger 150 × 140 cm enclosure. This suggests that individual place cells may not provide unambiguous information about the animal's location and that the ensemble activity of place cells could be important in conveying the spatial signal.

2.3.3 Place field properties

2.3.3.1 Anatomical gradients

Field number and dispersion increases proximal-to-distal in CA1

The proximodistal location in the HF from which place cells are recorded also affects the numbers of fields observed and other field characteristics. Henriksen et al. (2010) found that place cells recorded from distal CA1 have higher numbers of fields and less spatial selectivity than those recorded from more proximal locations. In a large 2m diameter cylinder, approximately 45% of place cells had multiple fields in proximal CA1, whereas in distal CA1 this rose to around 70%. As discussed in the previous chapter, this may be due to different "streams" of information reaching distal and proximal CA1: whereas proximal CA1 receives projections from the MEA which are likely to convey more spatial information, distal CA1 is innervated by the LEA which may carry more contextual, non-spatial information.

Field size increases dorsal-to-ventral

The size of the place fields observed also depend on an anatomical gradient of field size in the HF. As place cells are recorded from progressively more ventral locations of the HF, the size of their fields gradually increase. The sizes of place fields in CA3 vary from less than a metre at the dorsal pole to approximately 10 metres at the ventral pole (Kjelstrup et al., 2008). As noted in the previous chapter, three distinct bands along the rostromedial-caudolateral axis of the EC (which also runs broadly ventral-to-dorsal) project to different portions along the dorsoventral axis of the HF. Hence, place cells in the dorsal HF receive input from the dorsal- or lateral-most band of the EC that carries more exteroceptive spatial information,

whereas those in the ventral HF receive input from the most ventral or medial band carrying more interoceptive non-spatial information. The increase in place field sizes from the dorsal to the ventral HF are mirrored by a similar gradient in the scale of spatially-selective cells located along the dorsoventral axis of the EC, known as grid cells, which are discussed at the end of this chapter.

2.3.3.2 Distribution of fields

In contrast, the location in the environment represented by each place cell has no relationship to its anatomical location (Redish et al., 2001). In fact, often even small numbers of anatomically neighbouring cells have such a diversity in their field locations that they represent all the different areas of an environment. If a rat forages in a small enclosed environment, the fields are generally distributed evenly over the entire floor surface (Muller et al., 1987), with a slight tendency to cluster close to the walls (Hetherington and Shapiro, 1997). On an small open platform, it is common to find a concentration of fields at or even over the edge of the platform (O'Keefe, 2007). Some authors have also reported greater numbers of fields at the goal location or other important decision points in navigational maze tasks (Hollup et al., 2001; Ainge et al., 2007). However, the general finding with such tasks has been that there is no tendency for place cells to cluster at decision points or around goal locations (O'Keefe, 1976; Olton et al., 1978; McNaughton et al., 1983; O'Keefe and Speakman, 1987). In fact, the construction of the cognitive map appears to occur spontaneously without requiring a goal or navigational task; curiosity alone is sufficient.

2.3.3.3 Directionality of fields

An allocentric map-like representation also implies that place is represented in a way that is independent of the egocentric orientation of the animal. Indeed in open field environments, place cells possess omnidirectional firing fields that represent a particular place regardless of the direction from which the animal enters the field (Muller et al., 1994). However if the animal is trained to run in both directions along a narrow linear track, the fields that emerge are directional (McNaughton et al., 1983). Thus, a place cell may fire only when the animal runs in one direction or even in a different location in each direction. Such directionality could be caused by the constrained shape of the environment itself, by the restriction of sensory information or by the stereotyped patterns of behaviour in which the animal engages.

Markus et al. (1995) investigated the importance of these factors by examining place field characteristics in an open circular platform and a narrow-laned plus-maze environment. As expected, in the plus-maze the place fields were more directional than on the platform and this remained true regardless of the abundance or scarcity of sensory cues. However, they found that fields on the platform became more directional if the rat was trained to collect food using stereotyped paths, as opposed to foraging freely. This suggests that the behaviour of the animal is the most important factor in determining the directionality of place fields, above sensory or environmental influences.

2.3.3.4 Stability of fields

Place fields in a familiar environment reliably demonstrate the same locational firing on repeated trials, regardless of whether the animal experiences other environments or not in the interim. Fields can remain stable for periods at least as long as several months (Thompson and Best, 1990; Lever et al., 2002). These estimates may be limited more by the difficulty of recording an individual cell for such a prolonged period than by the stability of the cell's field.

2.3.4 Determinants of place cell firing

2.3.4.1 Sensory cues

An allocentric spatial representation system of the sort proposed by O'Keefe and Nadel (1978) should be able flexibly integrate multiple sources of information to determine the animal's position. In agreement with this, O'Keefe and Conway (1978) observed that place cell activity could persist after the removal of one or more sensory cues and could combine information from several modalities. Even when all visual cues were removed by turning the lights in the room off, the place cells retained their firing fields (O'Keefe, 1976). This suggested that these cells were genuinely responding to place and not some simple combination of sensory stimuli.

Subsequent experimental investigations have confirmed this conclusion and provided a more detailed understanding of the influence that different cues have on place cell firing. The location of the cue relative to the environment is important, since place cells typically respond to distal cues instead of proximal ones. Cressant et al. (1997) found that if the distal cues in an environment were rotated but the

proximal cues were fixed, the place fields rotated in tandem. In contrast, place fields stayed in the same position if only the proximal cues were rotated.

However, the relative influence of proximal or distal cues depends on the exact environmental configuration used. When multiple salient proximal and distal cues are provided, removing or interchanging one or more cues reveals that individual place cells may respond either to individual proximal or distal cues, or to the relationships between them (Shapiro et al., 1997). Hence, this suggests that the determinants of place cell fields are varied and can involve complex influences from one or more spatially-relevant cues.

An important determinant of the location of a place field may be the boundaries of the environment. O'Keefe and Burgess (1996) recorded cells with well-defined fields in a small square environment and examined what happened when either or both the dimensions of the environment were enlarged. They found that the fields appeared to "decompose" into two subfields as the walls were extended. Furthermore, they suggested that this decomposition could be accounted for if the firing in the field depended on a combination of Gaussian-tuned distance inputs from one or more of the boundaries (walls). The boundary vector cells of the SUB (Lever et al., 2009) and border cells of the MEA (Solstad et al., 2008) may be the neural bases of these inputs.

2.3.4.2 Path integration

The stability of place fields in the dark (O'Keefe, 1976) suggests that place cell firing can persist when there is little or no sensory input. As well as exteroceptive cues, place cell fields are also responsive to interoceptive information that depends on the motion of the animal's head and body through space. There are several sources for this information: proprioceptive signals arrive from the head, body and limbs; vestibular signals convey linear and angular rotation and acceleration; and motor reafferents feed a 'copy' of intended motions back to the brain (Etienne and Jeffery, 2004). In addition, self-motion judgements can be informed by optic flow and whisker-detected airflow during movement. All these forms of information can be combined to give a continuous estimate of motion through space, a process known as "path integration".

Even when sensory cues are available, path integrative inputs can have a dominant influence on place cell firing under certain conditions. During the first few runs out of a moveable start box along a linear track, the locations of fields

closest to the start box are determined by the distance from the start box and not by external cues (Gothard et al., 1996; Redish et al., 2000). These effects are only transient, but nonetheless demonstrate that the animal can derive its position through the integration of self-motion information and that this is sufficient to (at least temporarily) drive place cell firing.

2.4 Grid and head direction cells

In order to move within a cognitive map, an animal must be able to track its motion through space and update its position on the map accordingly. In this section, I describe how information about the direction and speed in which the animal is moving are combined to produce a spatially stable distance-dependent firing activity in cells of the EC. As discussed in the previous chapter, the EC is the "gateway" to the HF, so place cell activity in the HF depends critically on this process.

2.4.1 Head direction cells

"Head direction cells" display firing activity that is tuned to the allocentric direction in which the rat's head is pointing (Muller et al., 1996). Head direction cells are found throughout a widespread network that includes both subcortical (lateral mammillary and dorsal and ventral thalamic nuclei) and cortical regions (RSC, MEA, PRE and PARA) (Blair et al., 1998; Stackman and Taube, 1998; Sargolini et al., 2006; Boccara et al., 2010). Some head direction information is relayed to the HF directly through the PRE and PARA, but the major recipient of such information is the MEA.

2.4.2 Speed inputs to the hippocampal formation

The origins of the speed-related inputs are less clear, but it is likely that given the multiple kinds of interoceptive information available (proprioceptive, vestibular, motor reafference, and optic or whisker-detected flow) that this input arrives from several hippocampally-projecting brain regions. Linear velocity-related firing has been reported in the neurons of the interpenduncular nucleus (IPN) and also the lateral habenula, which additionally conveys angular velocity information that may support head direction firing in the VTN (Sharp et al., 2006). Optokinetic information from the retina are combined with proprioceptive and somatosensory inputs from the spinal cord in the vestibular nuclei (Smith, 1997; Smith et al.,

2010). This information is relayed to thalamic nuclei en route to the HF (Shiroyama et al., 1999; Krout et al., 2002). Lastly, the RSC is thought to be important in translating egocentric to allocentric reference frames and contains cells signalling angular and linear velocity (Cho and Sharp, 2001).

There is ample evidence that speed information reaches the HF and PHR, as speed-modulation is observed in both the local field potential and single unit activity. The frequency and amplitude of the theta oscillation have been shown to correlate positively with the running speed of the animal (Whishaw and Vanderwolf, 1973; McFarland et al., 1975; McNaughton et al., 1983; Rivas et al., 1996; Slawinska and Kasicki, 1998; Maurer et al., 2005; Terrazas et al., 2005; Jeewajee et al., 2008a). Likewise, interneurons, place and grid cells in the HF and MEA show a linear increase in their intrinsic firing frequency with speed (McNaughton et al., 1983; Wiener et al., 1989; Czurkó et al., 1999; Hirase et al., 1999; Geisler et al., 2007; Jeewajee et al., 2008a). Finally, speed-modulated head direction cells have also been found in the PRE (Burgess, 2008) and the MEA (Sargolini et al., 2006). This suggests that these regions of the PHR are particularly important in combining speed and directional inputs to facilitate path integration.

2.4.3 Grid cells

2.4.3.1 Spatial firing properties

The PRE, PARA and MEA contain cells exhibiting a remarkable spatial firing pattern that indicates an integration of speed and directional inputs (Hafting et al., 2005; Boccara et al., 2010). These cells are spatially-modulated like place cells but instead of firing in a single location, they fire at the nodes of a triangular grid that cover the whole environment, and so are known as "grid cells" (Figure 2.4; Fyhn et al., 2004; Hafting et al., 2005). Like the place cells (in open field environments), grid cell fields are omnidirectional. The equally-spaced firing peaks suggest that grid cells signal the distance the animal has travelled, which lead to them being termed the "metric for space" (Moser and Moser, 2008). However, recent evidence shows that environmental novelty expands the spatial scale of grid cells, suggesting that the grid cell metric may become plastic under some circumstances (Fyhn et al., 2007; Barry et al., 2009, SFN Abstract 101.24).

The grids formed are characterized by three measures: the scale (size of and distance between fields), the orientation (rotation in the horizontal plane relative

to an external reference) and the offset (displacement in the horizontal plane relative to an external reference). Although the grid cells were originally found in the MEA, they have subsequently also been reported as being abundant in the PRE and PARA (Boccara et al., 2010).

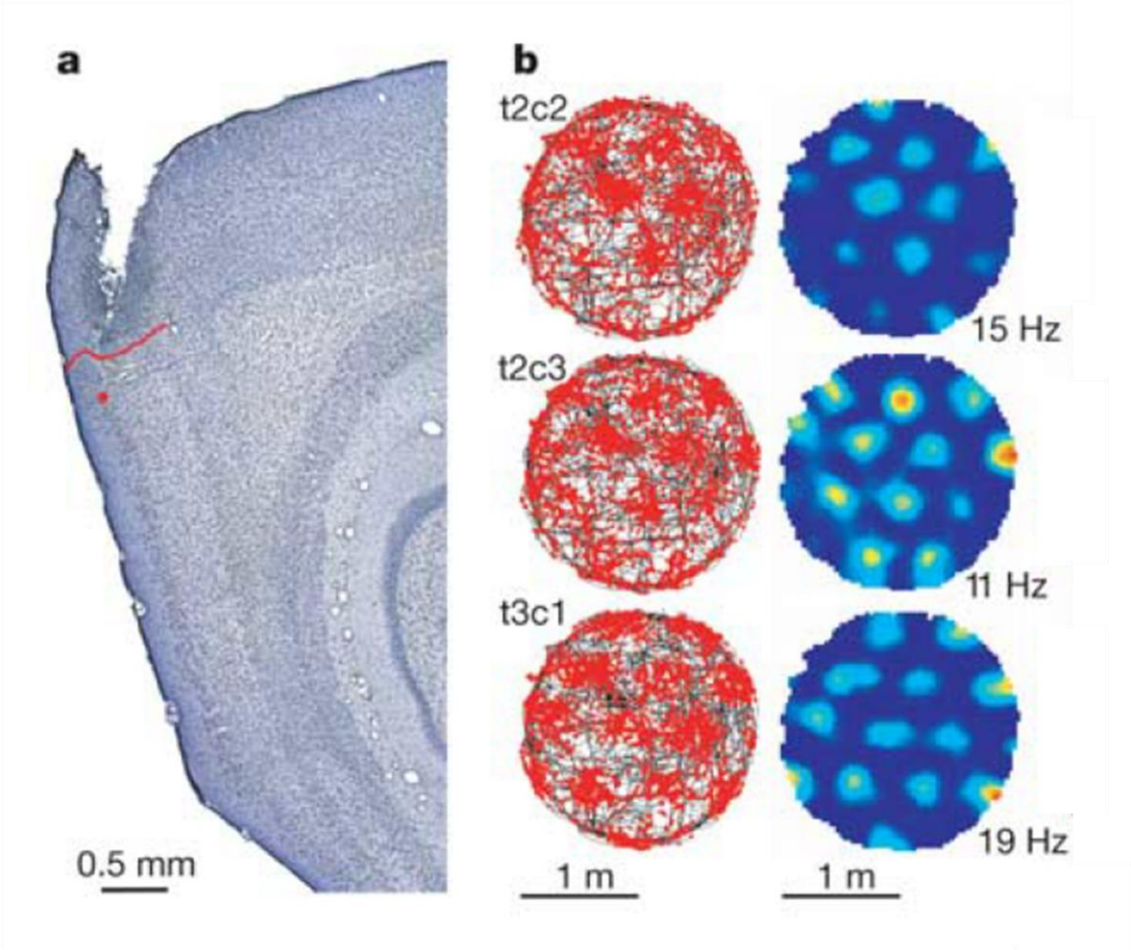

Figure 2.4. Anatomical location and spatial firing fields of grid cells recorded in the medial entorhinal area (MEA). (a) Sagittal Nissl-stained section showing the recording location (red dot) in layer II of dorsal MEA and the border of the entorhinal and postrhinal cortices (red line). (b) Three simultaneously recorded grid cells (labelled t2c2, t2c3 and t3c1) show spatial firing fields arranged in a triangular grid across the circular environment. The *left* column shows the spikes of each cell (red) overlaid on the rat's path (black line) during a single trial, whilst the *right* column shows the same data as a false-colour rate map, with the peak rate of each cell in the bottom right. (*Adapted from*: Hafting et al., 2005)

2.4.3.2 Relationship of anatomical location to spatial firing

A couple of interesting parallels can be drawn between the relationships of anatomical location and firing activity in grid cells and place cells. Recording grid cells from a single location in the MEA, one finds that they all share the same orientation and scale but they differ non-systematically in their offsets. This is reminiscent of the variation in locations represented by neighbouring place cells, which likewise display no topographic relationship of anatomy to space. The variation in offsets among neighbouring grid cells means that together even a small number can 'carpet' the entire surface of the environment, just as a small number of neighbouring place cells can represent all the places within an environment. The second parallel is the increased scale of both grid cells and place cells when one records from progressively more anatomically ventral locations (equivalent to the septotemporal axis in the HF and the dorsolateral-ventromedial axis in the EC). The scale of grids increases linearly from approximately 50cm at the dorsal-most part of the MEA to roughly 3m at around three-quarters of the dorsoventral extent of the MEA (Brun et al., 2008b). Combined with the anatomical data discussed in the previous chapter, these findings suggest an intimate relationship between place cells and grid cells both anatomically and functionally.

The anatomical distribution of grid orientations within the EC still remains to be established definitively, although it is clear that there is variation across the region (Hafting et al., 2005). However, architectonic features of the EC such as the periodic bundling of pyramidal cell dendrites and axons, cyclic variations in cytochemical markers and the clustering of stellate cells into small patches suggest that it possesses a modular architecture (Witter and Moser, 2006; Burgalossi et al., 2011). Anecdotal electrophysiological reports argue that neighbouring grid cells recorded on a single tetrode share the same grid orientation, whereas distant ones recorded from different tetrodes do not (Hafting et al., 2005). Preliminary experimental evidence using multi-site recording from the MEC supports the idea that grid cells are clustered into discrete patches sharing a common orientation (Stensland et al., 2010).

2.4.3.3 Determinants of grid cell firing

Hafting and colleagues (2005) studied the basic cue-related properties of grid cells and found them to be similar to those of the place cells. As with place cells, grid cell firing responds to changes in the positions of salient landmarks but persists in

their absence. Hence, rotation of a cue card attached to the wall of an environment will cause an equivalent and coherent rotation in all the grid cells recorded. When all visual cues are removed by recording in the dark, grid cell fields become more dispersed but continue to fire in the same location. Thus, like place cells, grid cells provide a robust spatial signal that is not depend on individual sensory cues.

Grid cells are also influenced by the positions of environmental boundaries. In a complementary study to that conducted by O'Keefe and Burgess (1996), Barry and colleagues (2007) asked how extending or shortening the walls of a square-shaped recording environment in either or both dimensions would affect grid cell fields. They found that the grid fields rescaled in correspondence with the change in the size of the environment, but the magnitude of the grid rescaling was below that of the environmental change. This likely reflects a compromise between path integrative and sensory-derived inputs to grid cells. The rescaling of the grids may arise from the interaction of grid cells with place cells, which could serve to 'anchor' the grid map at specific locations (O'Keefe and Burgess, 2005; Barry et al., 2007), and may also involve boundary-sensitive cells such as boundary vector cells (Lever et al., 2009) or border cells (Solstad et al., 2008).

2.5 Summary

In this chapter, I have described in detail the LFP and single unit activities in the HF that contribute towards the electrophysiological signals which can be recorded extracellularly in freely moving rats. I have focused on the roles of LFP gamma, ripple and especially theta oscillations in hippocampal function. Gamma is thought to be important in the formation of cell assemblies and the dynamic routing of information within the entorhino-hippocampal network. In contrast, ripples represent the synchronised activity of large hippocampal ensembles and are thought to relate to memory consolidation. Finally, theta arises from the periodic activity of cells within the HF and is important in synaptic potentiation/depotentiation, temporal coding of information by place cells and novelty signalling. Furthermore, it is proposed to be involved in the formation of place cell and grid cell spatial fields (discussed further in Chapter 5). As an understanding of the theta oscillation is particularly central to this thesis, I have explained the factors that influence the amplitude, frequency and phase of the recorded theta signal. The variation in these variables depends on the anatomical

recording location (septotemporal and laminar position within the HF), as well as other factors including the animal's running speed, age and body temperature. An appreciation of the influence of these factors will be important in comprehending and analysing the data presented in this thesis.

Secondly, I have described the significance of hippocampal interneuron activity to hippocampal function and their relationship to the theta oscillation. The mutually exclusive CCK- and PV-expressing interneuron classes of the HF differ in their activities during theta, gamma and ripple oscillations and in their electrophysiological properties, suggesting they support complementary roles in the spatiotemporal control of hippocampal activity. CCK-BCs constitute the vast majority of CB1-expressing interneurons in the HF, whereas PV-BCs do not express CB1. Consideration of the inputs, outputs and receptor expression of these two BC types suggests that CCK-BCs are involved in integrating anxiety- and arousal-related inputs to modulate the activity of place cells, whereas PV-BCs provide a high fidelity temporal regulation of hippocampal oscillatory activity. Therefore, this distinction suggests that the cannabinoid agonists used experimentally in this thesis will selectively affect CCK-BCs and influence anxiety- and arousal-related processes in the HF.

Thirdly, I have described the electrophysiological and spatial firing properties of place cells. A subset of these cells is active in each environment and signals the animal's position in space by a combination of rate, phase and ensemble coding. In a small open field recording environment, place cells normally possess a single omnidirectional field that is stable over prolonged periods. The properties of the place fields recorded varies depending on anatomical recording location, with field size increasing dorsoventrally and field number increasing proximodistally in the HF. However, there is no topographic mapping of field location to anatomy, with even a small number of place cells recorded from a single location showing disparate field locations. Place cell firing is strongly controlled by sensory cues, particularly by distal cues and by the locations and distances to environmental boundaries. Path integrative inputs also reach the place cells and can drive place cell firing under certain conditions, such as in the dark or transiently during runs on a linear track. These findings will be important for interpreting and understanding the place cell data described in this thesis.

Finally, I have described the other elements of the "cognitive map", namely the grid cells and head direction cells that are proposed to provide distance and directional

information, respectively. Additionally, I have highlighted the sources of speed-related inputs to the PHR and HF, as data concerning the running speed of the rat are central to this thesis. Head direction cells show no spatial firing correlate, but instead are active when the rat points his head in a specific direction. In contrast, grid cells recorded from the MEA exhibit a striking pattern of multiple spatial fields arranged in a triangular grid across the surface of the environment. This grid is characterised according to its offset and orientation relative to environment features, in addition to its scale, corresponding to the size and spacing of the spatial fields. The anatomical variation in grid cell fields shows a clear parallel to place cells, with an increase in field size along the dorsoventral axis and a wide variation in offsets among local populations of grid cells. Furthermore, grid cells behave similarly to place cells after manipulation of the cues or boundaries of an environment. These findings support the anatomical data presented in the previous chapter in pointing to a close functional relationship between the HF and EC. The specific relationship between place cells, grid cells and head direction cells is modelled in greater detail in Chapter 5, in which I introduce the oscillatory interference model of Burgess & O'Keefe (O'Keefe and Recce, 1993; O'Keefe and Burgess, 2005; Burgess et al., 2007; Burgess, 2008) that forms a substantial part of the theoretical basis of this thesis.

3 Cannabinoids

Use of the psychoactive plant *Cannabis sativa* by humans dates back to at least the 3rd millennium B.C., according to archaeological evidence (Mechoulam, 1986). Preparations of the plant are ingested or smoked and induce effects including altered mood and emotional responses, sedation, memory dysfunction, deficits in motor coordination and impairment of executive function (Pertwee, 2000; Howlett et al., 2004). These effects reflect the widespread expression of cannabinoid-specific receptors throughout the brain, which mediate a direct influence on electrophysiological activity (Herkenham et al., 1991). Cannabinoid injections are employed in the experimental work presented in this thesis, so in this chapter I describe the relevant findings in the literature.

This chapter is divided into the following sections:

3.1 Pharmacology

Overview of the endogenous and exogenous cannabinoid ligands, their receptors and mechanisms of cannabinoid signalling at the synapse.

3.2 Behavioural and cognitive effects

The nature and aetiology of cannabinoid-mediated behavioural and cognitive effects, focusing on those especially relevant for this thesis.

3.3 Electrophysiological effects

Influence of cannabinoids on single unit and LFP activity, focusing on the hippocampus, septum and entorhinal cortex.

3.1 Pharmacology

3.1.1 Endogenous and exogenous ligands

The modern era of scientific research on cannabis began with the successful isolation and synthesis of the main psychoactive component of cannabis, (−)-*trans*-Δ^9-tetrahydrocannabinol (Δ^9-THC), by Mechoulam's laboratory in the 1960s (Mechoulam and Gaoni, 1967; Mechoulam et al., 1967). This critical work opened the door for the subsequent discovery of the neuronal receptors responsible for mediating the effects of cannabis on the brain, and their corresponding endogenous ligands, known as endocannabinoids. The chemical structures of three common endocannabinoids are shown on the left in Figure 3.1 and their cannabinoid receptor binding properties in Table 3.1. These compounds share two structural motifs: a polyunsaturated fatty acid moiety and a polar head group consisting of ethanolamine or glycerol.

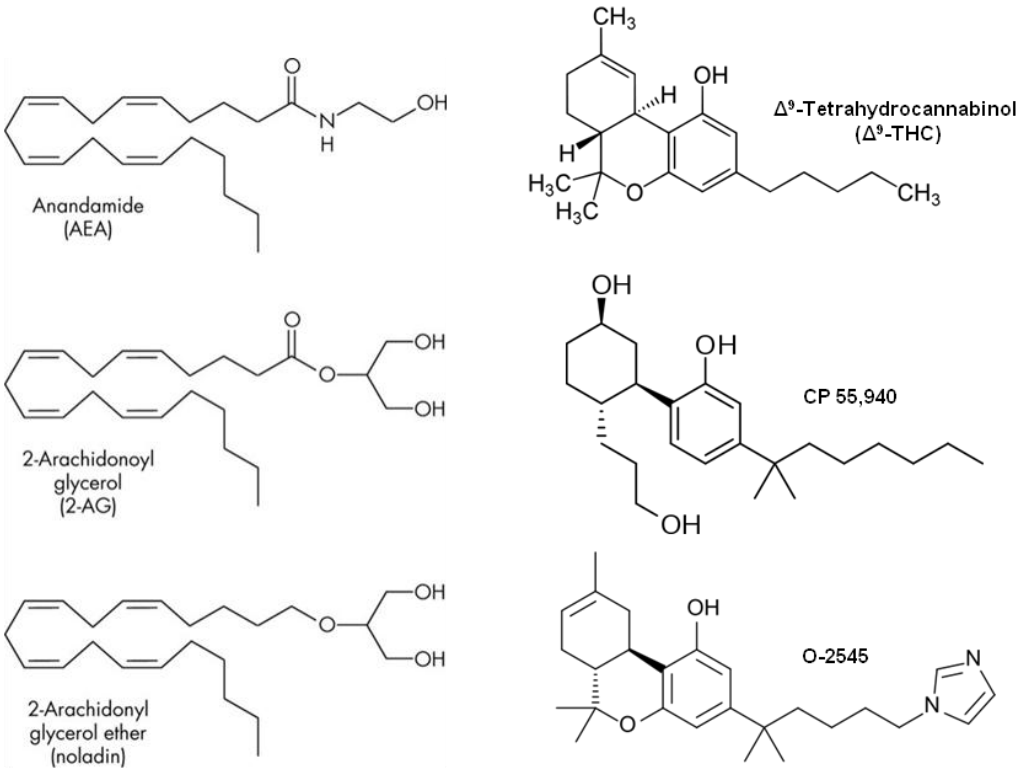

Figure 3.1. Chemical structures of three endogenous (left column) and three exogenous cannabinoids (right column). Synthetic chemical modification of the plant-derived Δ^9-tetrahydrocannabinol (top right) has lead to the development of potent cannabinoid receptor agonists such as CP 55,940 and O-2545 (middle and bottom right, respectively). AEA: Arachidonoylethanolamide. (*Adapted from:* Tomida et al., 2004).

In addition to the endogenously synthesised and plant-derived cannabinoids, synthetic chemistry has produced many highly potent, specific agonists and antagonists of the cannabinoid receptors (three shown in Figure 3.1, with receptor binding properties in Table 3.1; reviewed in Pop, 1999). *In vivo* research with these drugs has been complicated by the need to dissolve them in toxic or psychoactive solvents, as they are generally hydrophobic like their endogenous and plant-derived analogues. However, the recent discovery of highly potent water-soluble cannabinoids (Martin et al., 2006) greatly facilitates the study of the encocannabinoid system in animal models of cognition and indeed, such a water-soluble synthetic cannabinoid, O-2545, has been used for the experimental work in this thesis.

Table 3.1. Pharmacological properties of commonly-studied endogenous and exogenous agonists of the CB1 and CB2 receptors. (*Sources*: Martin et al., 2006; Pertwee, 2006, 2008)

Name	**Source**	**K_i (nM) at CB_1R**	**K_i (nM) at CB_2R**
Arachidonoylethanolamide (anandamide)	Endogenous	89	371
2-Arachidonylglycerol (2-AG)	Endogenous	519	618
2-Arachidonyl glycerol ether (noladin)	Endogenous	21.2	> 3000
Δ^9-Tetrahydrocannabinol (Δ^9-THC)	Plant-derived	5.05	3.13
CP 55,940	Synthetic	0.58	0.68
O-2545	Synthetic	1.5	0.32

3.1.2 Receptors

3.1.2.1 Types

For many years, the corresponding receptors for these ligands were believed to comprise solely of two G-protein-coupled receptors, the CB_1 and CB_2 receptors (Howlett, 2002). However, more recently with accruing evidence, the list has been expanded to include the transient receptor potential vanilloid type 1 receptor ($TRPV_1$) ion channel and an additional G-protein-coupled receptor, known as GPR55 (Ross, 2003; Ryberg et al., 2007). CB_2 receptors are found predominantly in microglia, at peripheral sites and in the immune system and are not believed to be involved in cognitive functioning (Cabral et al., 2008). $TRPV_1$ receptors, which form part of the related endovanniloid system, are also activated by some endogenous endocannabinoids, including anandamide and *N*-arachidonoyldopamine (De Petrocellis and Di Marzo, 2009). Recent evidence suggests that $TRPV_1$ receptors may be cognitively relevant, as they can affect synaptic plasticity in hippocampal slices *in vitro* (Gibson et al., 2008; Chávez et al., 2010), but there is little supporting behavioural data so far. The physiological roles and pharmacological mechanisms of GPR55 receptor functioning are not currently well understood (Moriconi et al., 2010).

Of all the receptor types in the endocannabinoid system, the CB_1 receptor is by far the best characterised. Numerous *in vitro* slice recording and *in vivo* behavioural experiments, along with psychometric studies in humans, have demonstrated the potent effects of CB_1 receptor agonists and antagonists on diverse systems involved in emotion, memory, addiction, movement and appetite (Black, 2004; Moreira and Lutz, 2008; Fernández-Ruiz, 2009). Therefore, in this chapter I shall focus on the pharmacological, behavioural, cognitive and electrophysiological effects mediated via the CB1 receptor.

3.1.2.2 Neuroanatomical distribution

Neuroanatomical studies have revealed a widespread and heterogenous pattern of CB_1 receptor expression in the brain, with the highest densities being found in the cerebral cortex, substantia nigra pars reticulata, globus pallidus, lateral caudate-putamen, entopenduncular nucleus, molecular layer of the cerebellum and parts of the olfactory bulb (Herkenham et al., 1991). Notably, expression is low in most parts of the brainstem, which may explain why cannabinoids exhibit no toxicity even at high doses.

Hippocampus

Expression of CB_1 receptors is also high within all subfields of the hippocampus proper, and at moderate levels in its major afferents, including the amygdala, entorhinal cortex and medial and lateral septum (Herkenham et al., 1991; Marsicano and Lutz, 1999; Nyíri et al., 2005). As described in Chapter 2, expression in the hippocampal subfields is predominantly localised to the presynaptic GABAergic terminals of cholecystokinin-expressing basket cells (Katona et al., 1999). In contrast, whilst CB_1 receptors are also found on the glutamergic terminals of pyramidal and granule cells, their expression levels are between 10-20 times lower (Kawamura et al., 2006).

Septum

Both receptor labelling and mRNA expression studies reveal a moderate level of expression in the medial and lateral septum (Herkenham et al., 1991; Mailleux and Vanderhaeghen, 1992; Matsuda et al., 1993). Interestingly, CB1 is selectively expressed on a subset of cholinergic neurons in the medial septum (Nyíri et al., 2005). This therefore suggests that cannabinoids are important in modulating cholinergic inputs from the MS/DBB to the HF which mediate the atropine-sensitive a-theta.

Entorhinal cortex

The entorhinal cortex shows a moderate density of CB1 receptor staining (Herkenham et al., 1991). As in other cortical areas, expression of CB1 receptors in the EC is highly colocalised with CCK on GABAergic interneurons (Marsicano and Lutz, 1999). However, a unique characteristic of the EC is the presence of a population of low CB1-expressing non-GABAergic cells that express CCK. These low CB1-expressing cells are found in high numbers in layers II-III and V-VI, along with many scattered high CB1-expressing cells. This suggests that cannabinoids have a role in regulating principal cell, as well as interneuron, activity in the EC.

3.1.3 Synthesis and synaptic activity

Detailed research over many years has showed that cannabinoids act as retrograde messengers, acting on the pre-synaptic terminal to inhibit the release of classical neurotransmitters. Two related phenomena of depolarisation-induced suppression of inhibition or excitation (DSI or DSE) have been described, referring to inhibition of neurotransmission at inhibitory or excitatory terminals, respectively (Diana and

Marty, 2004). Following post-synaptic depolarisation, endogenous cannabinoids are rapidly synthesised "on-demand" from precursor fatty acid molecules in the post-synaptic membrane (Di Marzo et al., 1994). After diffusing across the synaptic cleft, the cannabinoids activate CB_1 receptors embedded in the pre-synaptic membrane and cause a short-lasting (~10 second) attenuation of pre-synaptic neurotransmitter release. Although DSI was first characterised in the early 1990s (Llano et al., 1991), it was Wilson and Nicoll (2001) who first demonstrated using hippocampal *in vitro* slice recording techniques that cannabinoids are the signalling molecules responsible for this phenomenon.

A large post-synaptic depolarisation and influx of Ca^{2+} is required to elicit cannabinoid release and DSI (Freund et al., 2003). In terms of hippocampal activity *in vivo*, the precise conditions required to elicit DSI are not known. A sufficient depolarisation might occur during place cell complex spike bursts as the animal enters the place field (Klausberger et al., 2005). Back-propagating dendritic action potentials could combine with activated post-synaptic metabotropic glutamate or muscarinic acetylcholine receptors to drive cannabinoid release, leading to DSI in CCK-positive basket cells (Martin and Alger, 1999; Nakamura et al., 1999; Maejima et al., 2001). Endocannabinoids may also be important in regulating memory consolidation during slow-wave sleep, when ripple activity, and therefore levels of place cell depolarisation, are greatly enhanced (Howlett et al., 2004).

3.2 Behavioural and cognitive effects

Systemically injected cannabinoids induce observable behavioural effects so readily that the pharmaceutical industry uses these as indicators of cannabinoid efficacy; the so-called "tetrad assay" assesses the fourfold measures of catalepsy, antinociception, hypothermia, and hypolocomotion (Fride et al., 2006). In line with their diverse neuroanatomical targets, cannabinoids have a wide range of cognitive and behavioural effects relating to appetite, motivation, addiction, emotion and memory (Black, 2004; Moreira and Lutz, 2008; Fernández-Ruiz, 2009). In this section, I focus on the behavioural effects which are particularly relevant to understanding the data in this thesis and link these to the specific brain regions thought to mediate the effects.

3.2.1 Hypolocomotion and catalepsy

Cannabinoid agonists or agents that otherwise elevate cannabinoid levels have been widely demonstrated to inhibit motor activity (Järbe and Hiltunen, 1987; Crawley et al., 1993; Fride and Mechoulam, 1993; Wickens and Pertwee, 1993; Järbe et al., 1998). These effects depend on the CB1 receptor, as locomotion is found to return to normal after subsequent administration of a CB1-selective antagonist (Souilhac et al., 1995; Di Marzo et al., 2001). Motor inhibition by cannabinoids is mediated via the structures of the basal ganglia, which all contain high levels of the endogenous cannabinoids, as well as their receptors, and synthetic and degradative enzymes (Fernández-Ruiz, 2009). Cannabinoid signalling in these regions is important in modulating glutamatergic, GABAergic and dopaminergic transmission that regulate the control of movement (Sañudo-Peña et al., 1999; Fernández-Ruiz and Gonzáles, 2005).

3.2.2 Anxiogenesis and anxiolysis

The evidence in the literature suggests that the effects of cannabinoid agonists on anxiety are biphasic, with low doses exerting anxiolytic effects and high doses exerting anxiogenic effects (Haller et al., 2004; Rubino et al., 2007, 2008; Moreira and Wotjak, 2010). Thus, studies have found both anxiolytic and anxiogenic effects of cannabinoids on standard tests of anxiety in rodents such as the elevated plus-maze (Onaivi et al., 1990; Roohbakhsh et al., 2007; Rubino et al., 2007). As anxiety responses rely on a carefully regulated network of brain regions, the precise outcome in each case depends on the contributing influences of dose, environmental conditions and the strain of animal used (reviewed in (Viveros et al., 2005).

There are two networks which are central to the anxiety-modulating effects of cannabinoids. The first is the neuroendocrine hypothalamic-adrenal-pituitary (HPA) axis, activation of which leads to elevated production of anxiogenic glucocorticoids. Regulation of the HPA axis depends on negative feedback of glucocorticoids on the hypothalamus, a process which is mediated by synthesis and release of endocannabinoids in the paraventricular nucleus (Cota, 2008). Therefore, endocannabinoids are involved in returning the HPA axis to baseline after a stressful stimulus.

The second is a cortical emotion-regulating network that links the amygdala, HF and prefrontal cortex (PFC). Studies indicate that endocannabinoids are important in regulating the extinction of conditioned fear responses in the amygdala (Viveros

et al., 2007). After presentation of the conditioned stimulus, endocannabinoid synthesis is increased in the amygdala (Bisogno and Di Marzo, 2007). Pharmacological blockade or genetic inactivation of the CB1 receptor impairs fear extinction, suggesting cannabinoids are important in controlling the retention of anxiety-related behaviours (Lafenêtre et al., 2007). The HF and PFC also play an important role in anxiety regulation, with local injection of Δ^9-THC into either structure mediating an anxiolytic effect at low doses and an anxiogenic effect at high doses (Rubino et al., 2008).

3.2.3 Novelty-related exploration

A related issue to the regulation of locomotion and anxiety is the control of novelty-related exploratory behaviours. As discussed above, cannabinoid agonists reduce locomotion and affect anxiety levels, but there may be an independent contribution from a modulation of novelty-seeking behaviour.

Fox et al. (2009) studied novelty investigation on a hole-board test with systemic administration of the CB1-selective agonist WIN 55,212-2. They found that the drug decreased the number of visits to novel holes but not the overall number of holes visited, suggesting that ambulatory deficits were not responsible for the decreased novelty exploration. However, this does not rule out the potential role of an impairment of spatial memory (discussed below) in explaining these results.

The study of Hernández-Tristán et al. (2000) also used a hole-board test to probe exploratory behaviour and found marked thigmotaxic (wall-hugging) behaviour after injection of Δ^9-THC. They claim that the impaired exploration of the centrally-located holes cannot be explained by a decrease in locomotor activity alone, since other locomotion-impairing agents tend to slow but not completely abolish hole exploration. However, it seems likely that the avoidance of the central area can be accounted for by an anxiogenic effect alone.

Novelty-related behaviours depend on a complex interaction of different brain regions and neurotransmitter systems (Oades et al., 2005; Hasselmo and Stern, 2006; Düzel et al., 2010), which incorporate those controlling memory, movement and anxiety (discussed in the relevant sub-sections). Noradrenergic (NA) signalling dependent on the locus coeruleus (LC) may also be important as it has been particularly linked to regulating novelty-seeking behaviour (Sara et al., 1995; Mansour et al., 2003). Administration of cannabinoid agonists increases LC neuron burst firing (Mendiguren and Pineda, 2006) suggesting NA levels will be elevated

in afferent regions. Whilst NA efflux has indeed been found to be increased in frontal cortex, decreased NA levels are reported in the HF (Hernández-Tristán et al., 2000; Oropeza et al., 2005; Page et al., 2008). Therefore, there appear to be distinct effects on NA signalling in different brain regions. Additional behavioural and pharmacological data are required to understand exactly if and how these influence novelty-related behaviours.

3.2.4 Hypothermia

The induction of hypothermia is a consistent and widely reported effect of systemic cannabinoid administration (Chaperon and Thiébot, 1999; Fride et al., 2006; Smirnov and Kiyatkin, 2008). A consideration of body temperature is essential for a proper understanding of the theta LFP data presented in this thesis, since temperature and theta frequency are linearly correlated (Whishaw and Vanderwolf, 1971; Deboer, 2002).

Research into the brain regions responsible for mediating cannabinoid-induced hypothermia has identified the preoptic anterior hypothalamus (POAH) as a key central target. Rawls et al. (2002) found that a dose-dependent hypothermia could be elicited by systemic injection of the CB1-selective agonist WIN 55212-2 into the POAH. This temperature reduction was blocked by a CB1, but not a CB2, antagonist, demonstrating that activation of CB1 receptors alone is sufficient to induce the effect. The cannabinoid system is thought to interact closely with endogenous opioid and vanniloid systems to regulate temperature (Rawls et al., 2006a, 2006b, 2007).

3.2.5 Spatial memory impairment

The cognitive effects of cannabinoid administration have been studied extensively using a number of different spatial memory paradigms which are known to be hippocampus-dependent. The majority of the published literature is based on data from systemic injections, using a wide variety of spatial tasks including the 8-arm radial maze, the water maze and T-maze alternation (Molina-Holgado et al., 1995; Jentsch et al., 1997; Ferrari et al., 1999). These studies have indicated that cannabinoids strongly impair short-term and working memory, but the extent to which the deficits in task performance are due to a hippocampal effect alone are not always clearly distinguished with systemic injections. Effects on extra-hippocampal brain regions involved in processes such as motivation and reward may also play a role in these results (Gardner, 2005; Moreira and Lutz, 2008).

One way to avoid these complications is to deliver cannabinoids directly to the hippocampus via local microinjection. Using bilateral infusion of the cannabinoid agonist CP 55,940 to the dorsal hippocampi, (Lichtman et al., 1995) were able to demonstrate that spatial memory could be impaired in rats whilst sparing any effects in the tetrad assay. More recently, the same group showed convincingly that only intrahippocampal infusion of a CB_1 antagonist to sites inside the hippocampus, not immediately dorsal or ventral to it, could reverse the spatial memory impairment of systemically administered Δ^9-THC (Wise et al., 2009). These results imply that spatial memory impairments can be elicited by the action of cannabinoids on the hippocampus alone, and more specifically via the CB_1 receptor. These impairments correlate with a decrease in the power of hippocampal theta oscillations in both humans and rats, as discussed below (Robbe et al., 2006; Böcker et al., 2010).

3.3 Electrophysiological effects

3.3.1 Hippocampus

The effects of cannabinoids on hippocampal electrophysiology in anaesthetised and *in vitro* preparations have already been discussed in Chapter 2. Therefore, I shall focus on *in vivo* electrophysiological studies of freely moving animals in this section.

The work of Hampson and Deadwyler has focused on combining hippocampal cell recording with the delayed non-match to sample task (DNMS), a spatial memory paradigm in which the animal must alternate the location it visits after a delay period in order to receive a reward. By recording pyramidal cells from the CA1 and CA3 subfields during this task, they determined that the effects of cannabinoids on the memory encoding phase, rather than on retrieval, were particularly crucial (Hampson and Deadwyler, 2000). Their results suggest that cannabinoids detrimentally affect spike timing and the ability of hippocampal cell ensembles to maintain distinct task-specific firing patterns relevant for memory and behaviour (Heyser et al., 1993).

Robbe and colleagues have examined the effects of cannabinoids on hippocampal place cells and network oscillations in two studies (Robbe et al., 2006; Robbe and Buzsaki, 2009). They found that even though the performance of rats administered

systemically with CP 55,940 or Δ^9-THC was reduced to chance on a spatial alternation task, place cell fields and firing rates were only slightly altered. The only consistent effect across both studies on place field properties was a small reduction in field size. This implies that although the rats possessed an intact spatial representation, their ability to navigate successfully was still otherwise impaired. They found instead that the memory impairment correlated directly to a reduction in theta power induced by the cannabinoid (Buonamici et al., 1982; Hajós et al., 2008; Böcker et al., 2010). They proposed that both the theta power reduction and the observed memory deficit were due to a disruption of place cell spike timing that impaired the coordination and communication of hippocampal cell assemblies. In the later of the two studies they showed that cannabinoids disrupt the precise spike timing required for phase precession, breaking the tight relationship between place cell firing phase and distance travelled (O'Keefe and Recce, 1993; Huxter et al., 2003; Robbe and Buzsaki, 2009). They also reported a speed-independent reduction in theta frequency, although the contribution of a cannabinoid-mediated body temperature decrease to this result was not determined.

3.3.2 Septum

Hajós et al. (2008) studied the theta-band oscillatory firing of MS/DBB neurons in anaesthetised rats after systemic injection of the CB1 agonist CP 55,940. They found that theta rhythmic activity was abolished in these cells, but that their overall firing rate was unchanged. Thus, cannabinoids also disrupt spike timing in the MS/DBB and this likely contributes to the decreased theta power observed in the HF.

The effects of cannabinoids on hippocampal theta frequency might arise from their influence on septal cholinergic activity. Cholinergic signalling is important in setting the hippocampal theta frequency via the cholinergic a-theta pathway, with inhibition of the pathway leading to an increased frequency and stimulation to a decreased frequency (Givens and Olton, 1995). Tzavara et al. (2003) showed that cannabinoid modulation of cholinergic signalling from the MS/DBB is biphasic, with a low systemic dose inducing a transient increase in hippocampal acetylcholine release and a high dose leading to a prolonged decrease. Local infusion of a CB1 antagonist showed that the former effect depends on CB1 receptors in the MS/DBB, whereas the latter depends on CB1 receptors in the HF. The relatively low dose used in the Robbe study (Robbe and Buzsaki, 2009) may therefore have reduced theta frequency by transiently increasing the cholinergic

drive from the MS/DBB. Tzavara et al. also showed that the increase and decrease of cholinergic signalling were mediated by dopaminergic D1 and D2 receptors, respectively. Since a prominent dopaminergic projection to the MS/DBB arises from regions of the basal ganglia (Lindvall and Stenevi, 1978), cannabinoid binding in these areas is also important in regulating acetylcholine release to the HF (Day and Fibiger, 1994; Nava et al., 2000).

3.3.3 Entorhinal cortex

In the study of Hajós et al. (2008) discussed previously, systemic injection of the cannabinoid agonist CP 55,940 reduced both theta and gamma power in the EC of freely moving rats. In contrast, an *in vitro* study of MEA found that whilst a CB1 agonist inhibited GABAergic synaptic transmission in both superficial and deep layers, there was no effect on beta or gamma oscillations (Morgan et al., 2008). However, application of a CB1 antagonist/inverse agonist lead to a suppression of beta and gamma in superficial MEA, accompanied by an enhancement of these frequency bands in deep layers. Thus, the precise effects of cannabinoids on entorhinal activity are not clear, but there is some evidence that they can directly influence cell firing and network oscillations.

A recent study by Varga et al. (2010) demonstrated that CB1-expressing basket cells in the MEA selectively innervate principal cells in layer II that project outside the hippocampus, avoiding neighbouring cells that give rise to the perforant pathway input to the DG and CA3. This suggests that the entorhinal afferents to the HF may not be a major target of cannabinoid action. In agreement with this, studies of DSE on both DG granule cells and CA1 pyramidal cells have found that cannabinoid modulation of intrinsic inputs (mossy cell and SC, respectively) is much stronger compared to the effect on PP inputs (Chiu and Castillo, 2008; Xu et al., 2010). However, modulation of PP inputs may be enhanced by septal cholinergic drive, which stimulates DG granule cells to decrease PP inputs via cannabinoid signalling (Colgin et al., 2003). In general, these studies suggest that cannabinoids have a more significant role in regulating activity within the hippocampal circuit than in controlling input via the EC. However, an increase in septal cholinergic inputs can enhance cannabinoid inhibition of entorhinal inputs, which may occur *in vivo* during exposure to novelty when hippocampal levels of acetylcholine are elevated (Givens and Olton, 1995; Thiel et al., 1998; Giovannini et al., 2001).

3.4 Summary

Studies on the plant-derived cannabinoid Δ^9-THC lead to the discovery of the endogenous cannabinoid system, with subsequent research in synthetic chemistry making it possible to probe the functioning of this system with highly potent artificial agonists and antagonists. The psychoactive effects of cannabinoids are mediated almost exclusively via CB1 receptors, which are widely expressed throughout the brain, with especially high levels in the cerebral cortex, basal ganglia, hippocampus, cerebellum and olfactory bulb. CB1 receptors are expressed pre-synaptically and mediate inhibition of neurotransmitter release in response to retrograde cannabinoid signalling. This signalling requires a strong post-synaptic depolarisation leading to elevated Ca^{2+} levels. The precise conditions under which cannabinoids are released in the hippocampus *in vivo* is not known, but this may occur during place cell complex spike bursts as the rat enters a cell's place field, and/or during synchronised ripple events in slow-wave sleep.

In line with their widespread expression in the brain, cannabinoids exert diverse effects on cognition and behaviour. They have been consistently shown to reduce locomotion, an effect which is mediated via binding of cannabinoids to receptors in the basal ganglia. Cannabinoids modulate anxiety in a biphasic manner, as low doses are anxiolytic, but high doses are anxiogenic. These effects are due to cannabinoid action on HPA axis and on a cortical emotion-regulating network including the amygdala, HF and PFC. Cannabinoids have been show to decrease exploratory behaviour in novel environments, but it is not clear if there is an independent effect on novelty-seeking behaviour or if this can be explained by effects on anxiety and locomotion alone. Cannabinoids also reduce body temperature by binding to receptors in the preoptic anterior hypothalamus. Finally, they impair spatial memory, which has been convincingly shown to depend on hippocampal CB1 receptors.

Recordings from place cells during spatial memory tasks indicate that this memory impairment does not depend on a degradation of place cell field properties, but rather a disruption of spike timing. This may prevent the coordination and communication of hippocampal cell assemblies and therefore impair memory retention. Spike timing is also disrupted in the MS/DBB, which may contribute to, or perhaps cause, the reduction in theta power observed in the HF. The concurrent reduction in theta frequency may result from a modulation of the septal cholinergic a-theta pathway by cannabinoids. The electrophysiological effects of cannabinoids

on the EC are less clear, but the evidence suggests they have less of a role in regulating the intrinsic or afferent activity of the EC than in the HF. However, cholinergic stimulation from the MS/DBB may increase cannabinoid release in the DG during exposure to novelty. The findings summarised here lay the groundwork for understanding the effects of cannabinoids on hippocampal single unit and LFP activity, independently or in combination with environmental novelty.

4 Novelty

A substantial body of evidence points to the central role of the HF in the detection, assimilation and encoding of novel stimuli (Sokolov, 1963; Nyberg, 2005; Kumaran and Maguire, 2006). Of particular importance is the updating of "cognitive map" representations in the HF associated with the exploration of altered or previously unvisited environmental contexts (O'Keefe and Nadel, 1978; Lee et al., 2005; Lenck-Santini et al., 2005). The data in this thesis have been collected using an "environmental novelty" paradigm in which the animal is familiarised to a single environment in a particular location that is subsequently replaced unexpectedly by a novel environment and set of cues in the same location. This paradigm has previously been demonstrated to induce reliable changes in hippocampal theta and single unit activity (Jeewajee et al., 2008b; Lever et al., 2010).

In this chapter, I describe these findings and other relevant results from the literature regarding the effects of environmental novelty in two sections:

4.1 Theta

Effects of environmental novelty on the frequency of theta and the phase of single unit activity relative to theta.

4.2 Single units

Place cell remapping, its environmental and experiential determinants, and the role of extrinsic and intrinsic inputs and inhibitory control by interneurons.

4.1 Theta

Recordings of the LFP theta oscillation constitute a large part of the data presented in this thesis, so it is important to describe the current understanding of the influence of environmental novelty on theta. Therefore below, I summarise relevant findings in the literature.

4.1.1 Frequency

A recent study by Jeewajee et al. (2008b) suggests that environmental novelty is signalled by a decrease of the theta frequency in the HF. Rats were first run repeatedly in a single environment for five days, leading to a gradual increase in theta frequency as the environment became more familiar. On the subsequent three days, trials in two novel environments were interspersed with the familiar environment trials. For both novel environments, a large decrease in the theta frequency was observed during the first exposure (relative to the familiar environment). The magnitude of the frequency decrease lessened with subsequent exposures, mirroring what was seen with the "familiar" environment during the first five days. The theta frequency decrease could not be accounted for by differences in behaviour or running speed. Therefore the authors proposed that it may be driven by an increase in cholinergic input to the HF from the MS/DBB, which is known to be elevated during the first exposure to a novel environment (Givens and Olton, 1995; Thiel et al., 1998; Giovannini et al., 2001).

4.1.2 Phase

4.1.2.1 Place cell firing

The relationship between the firing phase of CA1 pyramidal cells and the theta rhythm has been investigated in a couple of studies. Manns et al. (2007) used two tasks to compare the mean theta phase of pyramidal spiking in familiar and novel contexts. The first task using object novelty paradigm and found a consistently later phase of firing when rats inspected a novel object compared to a familiar one. In contrast, the phase was equally likely to shift later or earlier in the second odour-cued delayed non-match-to-sample task.

The findings of Lever et al. (2010) were in line with the first experiment, showing a later phase of pyramidal cell firing in response to environmental novelty in CA1 (15-50° later) but not in SUB. This phase shift correlated with the degree of CA1 place cell remapping and therefore may reflect a change from a retrieval- to an

encoding-associated theta phase required to stabilise the new representation (Hasselmo et al., 2002). Although the authors were not able to determine the absolute theta phase due to the variation across the layers of CA1 (Winson, 1974), other studies have suggested that pyramidal cells fire just after the trough of SP theta (~45° later) in familiar environments (Csicsvari et al., 1999b; Mizuseki et al., 2009, 2011). The 15-50° phase shift would therefore shift pyramidal cell firing towards the peak of theta. As I shall discuss in the next section, this is consistent with the phase of theta where synaptic potentiation and therefore the storage of novel environmental information are expected to be most effective (Huerta and Lisman, 1993; Hasselmo et al., 2002).

4.1.2.2 Relationship to synaptic plasticity and cholinergic modulation

Numerous studies indicate that the theta phase at which hippocampal cells are stimulated has important implications for the modification of synaptic connections. A consistent finding is that stimulation synchronised to the peak of theta potently enhances synaptic efficacy (via LTP induction), whereas stimulation delivered during the theta trough either has no effect or may even decrease synaptic efficacy (Pavlides et al., 1988; Huerta and Lisman, 1993; Hölscher et al., 1997). Interestingly, theta phase-dependent synaptic plasticity is enhanced by cholinergic activation, suggesting that novelty-induced elevations in acetylcholine may help to facilitate the encoding of new information (Huerta and Lisman, 1993; Hölscher et al., 1997; Hasselmo, 2006).

In line with this, Villarreal et al. (2007) found that application of the cholinergic blocker atropine during the initial exposure to a novel environment attenuated the theta phase modulation of CA3 intrinsic (recurrent) and extrinsic entorhinal (perforant path) inputs normally induced by environmental novelty alone. Specifically, such novelty alone was associated with an increase of entorhinal input on the peak of theta accompanied by an attenuation of intrinsic CA3 inputs. Conversely, on the trough of theta there was an attenuation of entorhinal inputs and an enhancement of intrinsic inputs.

Models of memory encoding and retrieval, particularly those advanced by Hasselmo and colleagues, have emphasised the role of the cholinergic system in facilitating the encoding of new information (Hasselmo et al., 2002; Hasselmo and Stern, 2006; Hasselmo and Sarter, 2011). In particular, they have noted that cholinergic stimulation is associated with enhanced inputs from cortical regions to

the HF and accompanied by attenuated intrinsic activity within the HF (Hounsgaard, 1978; Hasselmo and Schnell, 1994; Fernández de Sevilla et al., 2002; Villarreal et al., 2007). During novelty, enhanced acetylcholine levels cause entorhinal inputs to the HF to dominate over intrinsic inputs. These inputs arrive during the peak of SP theta and therefore drive the encoding of new cortically-derived sensory information. They further propose that in the absence of cholinergic stimulation, the hippocampus enters a complementary "retrieval mode" in which intrinsic inputs dominate. Schaffer collateral (CA3-CA1) inputs carrying previously stored representations are then synchronised to the trough of SP theta, preventing synaptic potentiation and the aberrant re-encoding of old information. Therefore, there is an interplay of cholinergic modulation and theta phase that functions to switch the HF between complementary encoding and retrieval modes.

The experimental and modelling work described above indicates that the theta phase of cell firing is crucial determining whether it is likely to lead to long-lasting changes in synaptic efficacy and therefore putatively the encoding of novel information.

4.2 Single units

In addition to effects on the theta phase of firing, introduction of a rat to a novel environment can often induce dramatic changes in the spatial field properties of place cells. Below I describe the nature of such effects and the current understanding of the environmental and anatomical determinants governing place cell activity in novel environments. At the end of the section, I discuss the role of interneurons in supporting place cell activity under novel conditions.

4.2.1 Place cell remapping

4.2.1.1 The discovery of remapping

In a seminal study, (Muller and Kubie, 1987) explored the effects of environmental modifications on place cell activity. They familiarised rats to a small cylinder until they had established a stable spatial representation and then replaced the environment with one double the size. They observed two distinct effects on the place cells. In roughly a third of the cells, there was a corresponding scaling of field locations: the fields maintained the same angular and radial position as in the original cylinder (although their field sizes did not scale). However in

approximately half of the cells, the place cell activity changed dramatically from that in the smaller cylinder. Some of these cells fired in one of the cylinders but not the other, whilst others had fields in completely unrelated positions. Thus even though the environment was in the same position in the room and had only been scaled in size, there was a sudden shift in place cell field locations. This "remapping" effect could be replicated by introducing the rat to a rectangular-shaped environment after training in the cylinder, causing the firing activity of all the cells recorded to change unpredictably.

4.2.1.2 Complete, partial and rate remapping

Thus, it was clear that the remapping could differ in extent: in the case of the larger cylinder, there was a "partial remapping" of the place cell population, whereas in the rectangle there was a "complete remapping". Complete remapping (also sometimes termed "global remapping") involves an abrupt shift in the locations of all place fields combined with the silencing of a subset of place cells in one or other of the environments (Muller and Kubie, 1987; Leutgeb et al., 2004). This implies that non-overlapping or orthogonalised patterns of activity are formed for each of the two environments, also known as "pattern separation" (Leutgeb et al., 2004, 2005a). This may facilitate subsequent unambiguous recall of one or other of the representations in the presence of small differences in sensory input (Wills et al., 2005).

In contrast during partial remapping, some place cells keep the same fields as they expressed in the original environment, whereas others change their field locations unpredictably or may become silent (Muller and Kubie, 1987). Partial remapping may reflect the anchoring of different subsets of place cells to different "reference frames". Zinyuk et al. (2000) placed the rat on a rotating platform in a cue-rich room and found a dissociation of the place cell representation into "platform-bound" and "room-bound" subsets. Skaggs and McNaughton (1998) connected two visually identical boxes with a corridor and found that some cells had the same fields in both boxes whereas others differed, possibly suggesting the presence of separate "box" and "room" representations. However, it has not been resolved whether the two representations can be simultaneously active or whether only one can be active at a time (Gothard et al., 1996; Jezek et al., 2010, FENS Abstract 087.29).

Finally, the firing rate of place cells can also change in response to an environmental modification without any change in their field locations; this is

termed “rate remapping” (Leutgeb et al., 2005b). Rate changes in CA1 can be rather moderate, but in CA3 and DG rates may vary over an order of magnitude (Leutgeb et al., 2005a, 2007). Rate remapping can be induced by small environmental modifications, such as changing the colours of the walls of an environment whilst keeping the distal cues constant (Leutgeb et al., 2005b). In contrast, simultaneous changes of colour, odour, wall texture and shape which often employed to elicit complete remapping (Wills et al., 2005; Fyhn et al., 2007). This implies a crucial determinant of the type and extent of remapping observed is the extent of the environmental novelty.

4.2.1.3 Importance of experience

Numerous studies have also demonstrated the importance of the animal’s experience, as well as inter-animal differences, in determining the form and degree of remapping observed (Quirk et al., 1990; Bostock et al., 1991; Lever et al., 2002; Wills et al., 2005). With inexperienced animals and small environmental differences, remapping usually take time to emerge. Bostock et al. (1991) familiarised rats to a cylindrical environment with a white card and then substituted this for a black cue card. In the initial exposures to the black card, the representation was similar to that with the white card. However after a number of repeated exposures, in half of the rats the field locations of all the place cells shifted in an abrupt and coherent fashion with the precise timecourse varying between subjects. In the other half no remapping was observed (sometimes termed “null remapping”). Therefore both the experience of the animal and inter-animal differences contributed to the remapping observed.

Lever et al. (2002) likewise found that in inexperienced animals the representation of two environments, in this case differing only in shape, diverged over time. In contrast to the former study however, the fields of individual place cells changed at different rates and developed incrementally over the course of weeks or months. Instead of abrupt and coherent shifts in field locations, the majority of new fields emerged as place cells gradually diminished their firing in one location and increased it in the new (remapped) location. Nevertheless both studies found that the silencing of cells in one or other of the environments was a prominent feature of remapping, although the speed of this effect varied in line with the different timecourses of remapping observed in the two studies.

The critical influence of experience on the dynamics of remapping has been further clarified by two studies using "morph box" environments. The morph box consists of 32 vertical wall segments which can be rearranged to form a square, a circle or a number of intermediate octagon shapes. In a seminal study, Wills et al. (2005) initially trained rats to discriminate between square and circle environments that differed in colour, odour and the texture of their walls. They found that the animals formed distinct remapped representations in CA1 for each of these shapes within a few trials, which could then be "transferred" to a morph box configured as a square or circle. The dynamics of these representations were studied using a scrambled probe sequence of square, circle and intermediate octagon environments. The authors found an abrupt and coherent shift in the location of all the place fields which occurred midway between the square and circle shapes. This suggested that "all-or-none" or "attractor" dynamics determined the selection of one or other of the representations.

In contrast, Leutgeb and colleagues (2005) found a predominantly progressive transformation between place fields in CA1 and CA3 with either an ordered or scrambled probe sequence of square, circle and intermediate morph box shapes. These contradictory results can be understood as arising from the differences in the training and experience of the animals in the two studies. Leutgeb and colleagues initially trained animals on a single morph box arranged in square and circle configurations. These environments therefore differed only in shape and not odour, colour or wall texture as in the Wills study. After training only partial remapping was observed in CA1 and there was a high degree of similarity in the spatial firing in CA3 in the square and circle, suggesting poor discrimination between the shapes. All rats then experienced a series of probe trials with a progressive transformation from the square to the circle, which in combination with the poor discrimination may have biased the remapping towards the progressive transformation reported. The lack of an abrupt transition during the subsequent scrambled probe sequence may therefore be due to this prior probe experience or the lack of distinctly remapped square and circle representations. The differences in the results obtained by these studies thus demonstrate the important link between the animal's experience and the remapping dynamics which are observed.

4.2.1.4 Grid cell behaviour during remapping

Fyhn and colleagues (2007) conducted a highly informative study to investigate whether complete (global) and rate remapping correspond to different responses in

the activity of MEA grid cells. They found that rate remapping was associated with a stable firing pattern of the grid cells, which maintained a constant rate, offset, orientation and scale in the familiar and novel environments. In contrast, complete remapping was associated with a 'realignment' of the grid cell firing patterns, involving a coherent rotation and shift in offset of all grid cells recorded. Interestingly, in about half of the animals the complete remapping was also associated with an increase in the scale of the grid of approximately 2-5%.

This phenomenon was studied in greater detail by Barry and colleagues (2009, SFN Abstract 101.24), who found that after the initial expansion of the grid during the first exposure to a novel environment, it gradually diminishes in scale with each successive exposure. This suggests a novelty habituation effect, whereby the amount of grid expansion may correlate with the animal's familiarity with an environment. This change in grid scale has been proposed to drive remapping, according to the oscillatory interference model (Burgess, 2008). Several predictions made by this model are tested in this thesis and therefore it is discussed in greater detail in a following chapter.

4.2.1.5 Anatomical basis of remapping

Entorhinal cortex

It has been suggested that complete and rate remapping arise from the differential contributions of the MEA and the LEA to place cell firing (Leutgeb et al., 2005b; Fyhn et al., 2007). As discussed in the Anatomy chapter, the MEA is the route for "more spatial" cortical input and this is reflected in the spatial activity of the grid cells recorded there. When these grid cells shift or realign under complete remapping, the spatial firing locations of place cells are likewise shifted (Fyhn et al., 2007). In contrast during rate remapping, there is no change in either the positions or the rates of MEA grid cells. This suggests that the changes in rate observed are a result of firing rate modulations of the "less spatial", contextual inputs from the LEA (Leutgeb et al., 2007; Rennó-Costa et al., 2010).

CA3

Complete remapping involves the representation of environments with statistically independent or "orthogonalised" patterns of activity in the HF, but there is evidence that the degree of orthogonalisation differs between the subfields. Leutgeb et al. (2004) recorded CA1 and CA3 place cell ensembles in two rooms with

three environments which varied in the similarity of their sizes and geometries. Changing the room elicited only partial remapping (and therefore partial orthogonalisation) in CA1, but complete orthogonalisation in CA3. When the similarity of the environment within the room was varied, the degree of orthogonalisation likewise varied in CA1 but remained constant in CA3. A similar finding was reported by Lee et al. (2004), who also found that CA3 ensembles displayed greater coherence in the face of changing environmental input than CA1 ensembles. This suggests the recurrent network of place cell connectivity in CA3 may support "pattern completion" processes, in which differing inputs are reconciled into a stable "attractor" state (Marr, 1971; Wills et al., 2005; Leutgeb et al., 2007).

Dentate gyrus

The DG, on the other hand, has been suggested to be the locus of the complementary process of "pattern separation" (Marr, 1971; Leutgeb and Moser, 2007). This would imply that cell populations in the DG support unique spatial representations that allow discrimination even between very similar environments. Leutgeb et al. (2007) recorded DG granule cells and CA3 place cells whilst rats experienced a series of morph box trials in which the shape of the environment gradually transformed from a square to a circle (or the reverse). They found only a progressive change in rate across all CA3 cells, whereas each DG cell expressed multiple firing fields that varied independently in rate across the course of the transformation. These findings suggest that even small changes to the environment can cause distinct patterns of firing in DG granule cells, supporting the idea that the DG is involved in pattern separation.

CA1

The complementary processes of pattern separation and completion, in the DG and CA3 respectively, ultimately determine the Schaffer collateral input which contributes to the activity of CA1 place cells. Each CA3 cell contributing to this pathway sends divergent projections to many CA1 cells, which also receive strong input from layer III of the EC (see Anatomy chapter). Hence, CA1 place cells combine the coherent and orthogonalised CA3 input with entorhinal inputs that may carry more variable sensory- and contextual-related information. This may account for the fact that the CA1 population can sometimes behave incoherently in the face of conflicting environmental inputs (Shapiro et al., 1997; Lee et al., 2004).

4.2.2 Place cell-interneuron interactions in novel environments

A number of studies have examined the interactions between interneurons and principle cells of the entorhino-hippocampal system during exposure to a novel environment.

Nitz and McNaughton (2004) used a novelty paradigm where the rat was familiarised to one part of an environment and subsequently allowed to explore the novel part that was made available by removing a barrier or connecting the two parts. This allowed them to examine the moment-to-moment changes in firing activity of interneurons and principal cells recorded from CA1 and the DG as the rat ran back and forth between the novel and familiar areas. They found that whereas the firing rate of interneurons in CA1 decreased in the novel portion, the interneurons of the DG increased their firing. The principal cells of each region showed the opposite effect, with the rates of CA1 place cells increasing and those of DG granule cells decreasing. These findings suggest that during exposure to a novel environment, disinhibition of place cells in CA1 may help to facilitate remapping (Wilson and McNaughton, 1993; Frank et al., 2004). At the same time, an increase in the level of inhibition to the DG may help to prevent interference from retrieved representations .

Frank and colleagues (2004) used an 8-arm radial maze task where the rat was first familiarised to 3 arms in a 'T' configuration and then one of the remaining 5 novel arms was opened on each probe trial to allow the rat to explore it. Recordings were made from place cells and interneurons over several days of exposure to the novel arm. They found that place cells could develop a field after a single pass through a novel arm and that the stabilisation of the fields required approximately 5-6 minutes experience across the days. Interneurons recorded on the first day showed a decreased firing rate during the first minute of novel experience that subsequently reached similar levels to those observed in the familiar arm. Additionally during the first day, interneuron firing increased in the novel arm over the course of the trial; on the second day, it remained steady; and on the third, it resembled that of the familiar arms, showing a gradual decrease over the period of the trial. As with the findings of Nitz and McNaughton (2004) outlined above, these results support the notion that an initial disinhibition of place cells facilitates rapid remapping on exposure to novelty, which is then attenuated by an increasing interneuron firing rate with time.

4.3 Summary

Environmental novelty induces substantial changes in both the LFP and single unit activity of the HF. Theta frequency is reduced during the initial exposure to an environment and gradually increases with subsequent exposures, showing a habituation effect that suggests it is involved in signalling novelty. This process may depend on cholinergic stimulation of the HF, which is known to be elevated in novel environments. Cholinergic modulation is also important in facilitating the encoding of novel stimuli by strengthening entorhinal inputs carrying sensory information from the cortex and enhancing synaptic potentiation in the HF. The theta phase of cell activity is crucial to determining whether information is retrieved or stored, with environmental novelty putatively shifting CA1 place cell firing phases toward the peak of theta when encoding is optimal.

The locations of the firing fields of CA1 place cells also change in response to environmental novelty, with the extent of the change being determined by a combination of environmental and experiential factors. This remapping is termed complete (global) or partial, depending on if it involves an abrupt shift across the whole place cell population or more gradual and incoherent changes in discrete sub-populations. Additionally, small modifications to the environment can elicit rate remapping, whereby place cell firing rates change but their fields do not shift. Place cell remapping may be facilitated by disinhibition of place cells, with studies indicating that interneuron firing rates in CA1 are decreased during the first minutes of exploration in a novel environment. The contributions of DG and CA3 inputs are also important to determining remapping in CA1, as they are thought to play an important role in pattern completion and separation processes that depend on sensory information arriving via the entorhinal “gateway”.

Studies of entorhinal grid cell activity during exposure to novel environments indicate that whilst complete remapping is accompanied by a coherent realignment of grid fields, rate remapping does not change the spatial firing patterns of grid cells. In tandem with grid cell realignment, there is an expansion of grid fields that habituates over time with subsequent exposures to an originally novel environment. This parallels the habituation seen with the theta frequency reduction in novelty and indeed these effects are mechanistically linked in the oscillatory interference model of place and grid cell firing. This model provides much of the theoretical framework on which the experiments in this thesis are based and is the topic of the following chapter.

5 Models of spatial firing

Together, the place, grid and head direction cells respectively encode the position, distance and directional information required for spatial navigation. However, the precise ways in which these different signals are integrated in spatial cognition are not well understood. Several models have been proposed to explain how the different cell types are interrelated and in particular how the spatial firing of grid (and subsequently, place) cells arises. These models can be divided into two types: the "continuous attractor" and the "oscillatory interference" models. I shall briefly discuss the former, but since the experiments in this thesis are based on the latter type, I shall cover these in greater detail.

This chapter is therefore separated into two sections:

5.1 Continuous attractor models

Models that propose that grid cells form part of a recurrently-connected "attractor network", which possesses the intrinsic connectivity necessary to produce grid-like firing patterns.

5.2 Oscillatory interference models

Models that propose that the grid firing pattern can be produced by the interference of two theta-band oscillations. The theoretical basis and experimental predictions of the oscillatory interference model of Burgess (2008) are laid out in detail.

5.1 Continuous attractor models

An "attractor network" is a recurrently-connected neuronal network capable of maintaining a stable activity state in the face of perturbations such as noise (Hopfield, 1982; Amit, 1989; Rolls et al., 1998). Some authors have proposed that the grid cells of the MEA form such a network and that the rat's current position is represented by a peak of activity stabilised as an attractor (Fuhs and Touretzky, 2006; McNaughton et al., 2006a). A large number of neighbouring positions are represented in the network and movement of the rat causes the activity peak or "attractor bump" of the network to shift smoothly (continuously) in the appropriate direction.

Such a model requires a strict topography of connectivity between grid cells to maintain the attractor state. In the model of Fuhs & Touretzky (2006), this topography was suggested to correspond to the anatomy of the MEA, such that neighbouring grid cells would exhibit highly similar spatial firing fields. However, electrophysiological recordings show that neighbouring grid cells have a variety of different offsets (Hafting et al., 2005). Therefore, McNaughton and colleagues (2006a) proposed an updated model in which this topography arises from a cortical tutor network which trains the MEA grid cell network during development with an anatomically scrambled pattern of projections. This implies that the necessary topography is maintained in the connections of grid cells and not in their anatomical locations. In addition to the grid cell network, the model posits another network or "layer" of cells which are responsible for moving the grid cell attractor bump in line with the rat's current direction and speed. The speed- and direction-modulated grid cells which have been reported in layers III and V of the MEA may support such a function (Sargolini et al., 2006).

5.2 Oscillatory interference models

In contrast to the network-level mechanisms described by the continuous attractor model, the oscillatory interference model proposes that the spatial firing properties of grid cells arise from the interference of theta-band oscillatory inputs within individual cells. Several variants of this model exist (Blair et al., 2007, 2008; Hasselmo, 2008), but I shall focus on the original model proposed by Burgess and colleagues (O'Keefe and Burgess, 2005; Burgess et al., 2007; Burgess, 2008) as the

predictions of this model are tested in the experimental data presented in this thesis.

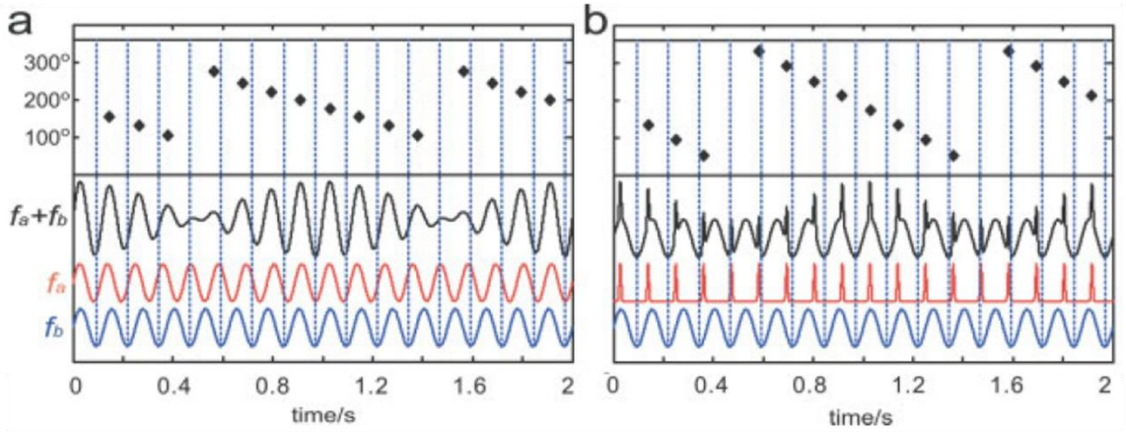

Figure 5.1. Oscillatory interference of a sinusoidal baseline oscillation f_b (blue lines) with an active oscillation f_a (red lines) models phase precession. (a) Interference (i.e. summation) of two sinusoidal oscillations (bottom panel) produces a resultant oscillation (f_a+f_b; black line) of intermediate carrier frequency ½(f_a+f_b) that is amplitude modulated at a beat frequency f_a-f_b. Spikes fired at the peaks of the resultant oscillation (black dots, top panel) show phase precession relative to the baseline oscillation f_b (troughs of the baseline oscillation are marked with vertical dotted lines). (b) Same as a, except active oscillation f_a is modelled as punctate input to the cell, representing synaptic input from an oscillating neuron. (*Adapted from*: Burgess, 2008).

5.2.1 Place cell phase precession

The oscillatory interference model was first proposed to explain the phase precession phenomenon described previously, whereby a place cell fires a progressively earlier phases on each successive theta cycle during a field traversal (O'Keefe and Recce, 1993). This phase precession was modelled by O'Keefe and Recce (1993) as the interference (i.e. summation) of two theta-band oscillations, one at the frequency of the LFP theta rhythm and the other higher in frequency by an amount proportional to the rat's running speed (baseline oscillation f_b (blue) and active oscillation f_a (red), respectively, on Figure 5.1a). The interference of two such oscillations produces a resultant oscillation with a "carrier frequency" that is an

average of the two, amplitude modulated by a lower "beat frequency" (resultant oscillation f_a+f_b (black) on Figure 5.1a; carrier frequency $(f_a+f_b)/2$, modulated by beat frequency f_a-f_b).

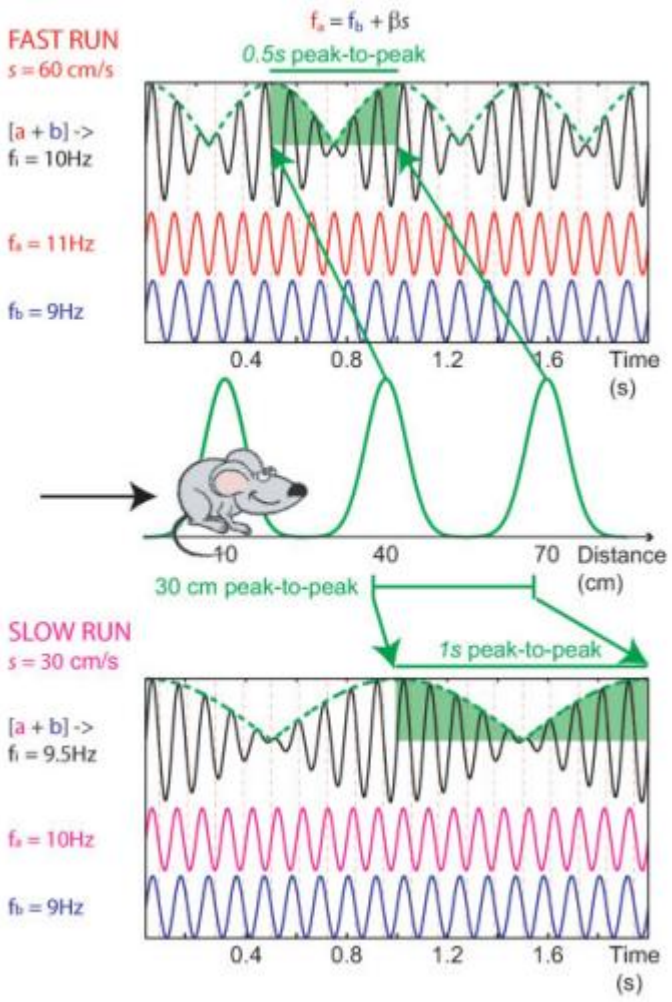

Figure 5.2. The oscillatory interference model generates fields of a constant spatial scale, regardless of whether the rat runs fast (60 cm/s, top) or slow (30 cm/s, bottom). In both cases, the frequency of the active oscillation fa is calculated from that of the baseline oscillation f_b according to the equation $f_a=f_b+\beta s$, where β=1/30 and s is the running speed in cm/s. Middle panel: The rat (shown as cartoon figure) runs eastward through regularly spaced grid fields on a linear track (green lines show the firing rate of the grid cell at each position). Top panel (fast run) shows how these fields are generated by the interference of the baseline oscillation f_b (blue trace, 9 Hz) with the active oscillation f_a (red trace, 11 Hz) to give a resultant oscillation f_a+f_b (black trace) of carrier frequency f_i (10 Hz), amplitude modulated by a beat frequency of f_a-f_b (2 Hz i.e. 0.5s peak-to-peak). Therefore the peak-to-peak timing of the amplitude modulation (0.5s) corresponds to the 30cm peak-to-peak distance of the grid cell as the rat runs at 60 cm/s. Bottom panel (slow run) shows the same as the top panel except the rat's speed is now 30cm/s, leading to an appropriate doubling of the peak-to-peak timing (1s). (*Adapted from*: Jeewajee et al., 2008a)

This resultant oscillation is identified with the membrane potential oscillation (MPO) of the place cell itself. The model predicts that spikes will be fired by the place cell on the peaks of the MPO (above a certain firing threshold); a prediction that was recently confirmed by intracellular place cell recording in mice navigating a virtual environment (Tank ref). The cell therefore fires at a slightly higher frequency than the LFP theta oscillation (f_b), leading to a progressive phase precession over time (top panel on Figure 5.1a).

The precise rate of phase precession is determined by the frequency difference between the baseline and the active oscillation, which is the beat frequency. As this frequency difference is proposed to vary with running speed, the beat frequency modulation maintains a constant spatial size regardless of the speed of the rat (Figure 5.2). This amplitude modulation is identified with the place field itself: when the active and baseline oscillations are in-phase the rat is at the centre of the place field; conversely, when they are out of phase the rat is outside the field. However, the MPO generated by the model has multiple spatial peaks, not the single peak expected for a place cell. In the original model, it was proposed that the two oscillations are out of phase except when the rat is in the place field and speed-related inputs increase the cell's MPO to drive spiking and phase precession.

5.2.2 Grid cell firing

In contrast to the single spatial fields of place cells, grid cells possess multiple fields arranged in a triangular grid across the surface of the environment (Hafting et al., 2005). Grid cells also phase precess and furthermore can do so independently of place cells (Hafting et al., 2008). Therefore, their discovery 12 years after the original oscillatory interference model lead to an immediate recognition of the resemblance between the multi-peaked interference pattern generated by the model and the multiple fields of grid cells (Figure 5.2; Hafting et al., 2005; O'Keefe and Burgess, 2005). However, the model only accounted for movement along one dimension and could not account for the triangular grid field pattern observed in a two dimensional space.

5.2.2.1 Velocity-controlled oscillators

Burgess and colleagues therefore extended the model into two dimensions, by suggesting that multiple active oscillations tuned to different heading directions might drive the firing of a grid cell. Head direction input reaches the MEA via the anatomical connections described previously and indeed, conjunctive grid x head-

direction cells have been recorded in the deeper layers of MEA (Sargolini et al., 2006). These directional inputs are proposed to modulate the frequency of a set of "velocity-controlled oscillators" (VCOs) in a preferred heading direction . The active frequency of the VCO at time t ($f_a(t)$) deviates from a baseline frequency ($f_b(t)$) by an amount proportional to the rat's speed and direction of movement (velocity vector $\underline{v}(t)$) relative to the preferred direction of the VCO (unit vector $\underline{d}$)

$$f_a(t) = f_b(t) + ß\underline{v}(t).\underline{d} \quad (1)$$

where ß is the frequency-speed gain or spatial scale factor (described in more detail below), and "." indicates the vector dot product. Substituting the vector notation, this equation can also be written

$$f_a(t) = f_b(t) + ßs(t)\cos(\varphi(t) - \varphi_d) \quad (2)$$

where $s(t)$ is the rat's running speed, $\varphi(t)$ is the running direction and φ_d is the VCO's preferred direction.

5.2.2.2 Source of velocity-controlled oscillatory input

The VCOs may correspond to individual dendrites of the grid cell itself (Figure 5.3a) or to other neurons innervating the grid cell (Figure 5.3b). In the former case, the active oscillatory input would be sinusoidal, whereas in the latter case it would be punctate, corresponding to excitatory postsynaptic potentials (EPSPs) induced by synaptic excitation. In both of these cases, the effects of summing the active and baseline oscillations is similar (compare Figure 5.1, a and b). In support of the former, intracellular slice recordings from the MEA show a gradient in the frequency of subthreshold MPOs of layer II stellate cells (putative grid cells), decreasing from dorsal to ventral MEA (Giocomo et al., 2007). Interference of these different frequencies with the baseline frequency could produce the dorsal-to-ventral gradient of grid scales observed in the MEA (Hafting et al., 2005).

However, it might not be biophysically feasible for multiple oscillations to co-exist in a grid cell (Hasselmo, 2008), suggesting that there is a population of neuronal VCOs. The anatomical identity of these cells is still unknown, but they may correspond to the persistent spiking cells found in the MEA (Hasselmo, 2008). An alternative proposal is that subcortical central pattern generator (CPG) circuits provide this functionality. In support of this, recent findings show that cells in neurons in the rostral anteroventral thalamus display cosine-modulated directional

firing frequencies, as predicted by the model (Welday et al., 2010, SFN Abstract 203.20). The VCOs themselves may be driven by head direction cells that modulate their firing frequency with running speed; these have been reported in the PRE (Burgess, 2008) and the MEA (Sargolini et al., 2006).

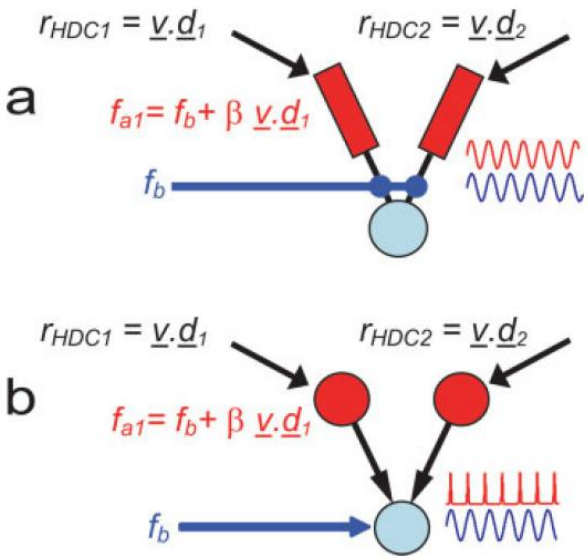

Figure 5.3. Velocity-controlled oscillators (VCOs; red shapes) driving grid cell firing (light blue circle) may be implemented as (a) dendritic subunits or (b) separate neurons. (a) Speed-modulated head direction cell inputs (r_{HDC1} and r_{HDC2}) drive the active oscillation f_{a1} (red sinusoid) in dendritic VCO subunits of the grid cell (red rectangles) relative to the somatic oscillation fb (blue sinusoid). (b) Same as a, except the VCOs are neurons which drive excitatory postsynaptic potentials (EPSPs; red punctate oscillation) in the grid cell relative to the baseline oscillation f_b (blue sinusoid). In both cases, the equations describing the activity of the VCOs are identical. (*Source*: Burgess, 2008)

5.2.2.3 Grid field generation

Crucially, the phase VCO firing relative to the baseline oscillation is the time integral of its frequency, just as the spatial position of the rat is the time integral of its velocity. Therefore, the phase of firing of individual VCOs accurately reflects the movement of the animal in the preferred direction (Figure 5.4, top two panels).

Grid firing patterns are produced if multiple inputs from VCOs with preferred directions differing by multiples of 60° are combined (Figure 5.4). The wiring of each grid cell with the appropriately oriented VCO inputs is proposed to occur during development. Importantly, firing of the grid cell only occurs when the VCO phases are aligned in both space and time; in other words, the grid cell acts as a VCO spike coincidence detector. This phase alignment is facilitated by feedback from place cells, as discussed in a following section.

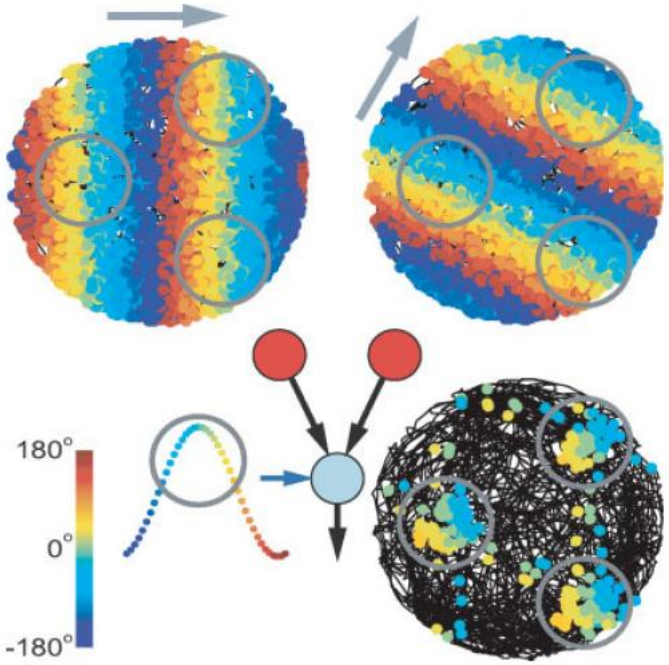

Figure 5.4. Simulation demonstrating how multiple velocity-controlled oscillator (VCO) inputs can be summated to produce grid cell firing in two dimensions. Top: Spikes fired by two VCOs with eastward and northeasterly preferred directions (differing by 60°) during a trial in a circular environment are colour-coded by their phase of firing relative to the baseline oscillation f_b (bottom left). Note that the VCOs fire at all locations in the environment, but that the phase of spiking varies along the preferred direction. Bottom middle and left: The two neuronal VCOs (red circles) provide input to a single grid cell (light blue circle) that also receives the baseline oscillation fb (blue arrow). When the spikes of the two VCOs are in-phase at the peak of the baseline oscillation, the grid cell fires. Bottom right: Spikes fired by the grid cell during the trial (colour-coded by phase) are at the apices of a triangular grid. Grey rings show identical locations on each of the spike plots for clarity. (*Source*: Burgess, 2008)

The phase of each VCO determines the offset of the grid relative to the environmental boundaries, whilst their preferred directions determine the grid orientation. What about the grid scale? The parameter ß in equation (2) can be thought of in temporal terms as the frequency gain per unit speed. However, due to the grid cell's "transformation" of VCO phases into spatially stable firing fields, this parameter also determines the spatial scale of the grid cell. Holding all other parameters constant, an increase of ß will increase the frequency-speed gain of the VCOs and likewise the spatial frequency of the grid cell's firing fields. In terms of spatial scale, this corresponds to a decrease in the size of the grid. Conversely, a decrease in ß will decrease the spatial frequency of the grid cell, thereby increasing its grid scale. Grid scale is known to increase along the dorsoventral axis of the MEA and so in the model this corresponds to an increase in the ß of the VCOs. The relevance of the spatial scale parameter ß to predictions tested in this thesis are discussed below.

5.2.3 Theta frequency-speed relationship

5.2.3.1 Derivation

An important prediction of the model tested in this thesis relates to the relationship between the LFP theta frequency and the running speed of the rat. Theta frequency is known to increase linearly with the running speed of the animal (Slawinska and Kasicki, 1998; Jeewajee et al., 2008a). In this section, I will therefore describe the derivation of the equation for this relationship.

Equation (2) implies that the firing frequency of the VCO (f_a) can vary both above and below the baseline frequency (f_b). This implies that the synaptic input to the VCO from speed-modulated head direction cells is both inhibitory and excitatory. This problem can be resolved by assuming that these cells provide only excitatory inputs ($V(t)$) to the VCO, raising its firing frequency above the "resting", zero speed frequency (f_0) according to

$$f_a(V(t)) = f_0 + ßV(t), \tag{3}$$

where

$$V(t) = s(t)(1 + \cos\{\varphi(t) - \varphi_d\}). \tag{4}$$

We can now rewrite equation (2), combining equations (3) and (4) and including all parameters that can influence the VCO's active frequency (f_a) as

$$f_a(s(t), \varphi(t), ß, \varphi_d) = f_0 + ßs(t)(1 + \cos\{\varphi(t) - \varphi_d\}). \quad (5)$$

The implicit assumption of equations (1) and (2) is that the baseline frequency (f_b) is constant throughout the MEA. In the original oscillatory interference model (O'Keefe and Recce, 1993), this was identified with the LFP theta oscillation which has been shown to have a constant frequency throughout the HF and MS/DBB (Bullock et al., 1990; Maurer et al., 2005). However alongside this "global" constant theta frequency, differences exist in the intrinsic oscillatory frequencies of local cell populations, both in the HF and the MEA (Maurer et al., 2005; Jeewajee et al., 2008a). Therefore, it is more congruent with these data to model the baseline frequency as the average of all local VCO active frequencies, assuming VCOs with preferred directions evenly spaced around 360°. On this basis, the baseline frequency can be calculated using equation (5), by averaging over all preferred directions φ_d

$$\begin{aligned} f_b(s(t), ß) &= \langle f_a(s(t), \varphi(t), ß, \varphi_d)\rangle_{\varphi d} \\ &= \langle f_0 + ßs(t)(1 + \cos\{\varphi(t) - \varphi_d\})\rangle_{\varphi d} \\ &= f_0 + ßs(t) \end{aligned} \quad (6)$$

The theta frequency (f_θ) is then modelled simply as the global average of all VCOs, using equation (6) and averaging over all spatial scale factors (ß), reflecting the variation in grid scale along the dorsoventral axis of the MEA and giving

$$f_\theta\big(s(t)\big) = \langle f_b(s(t), \beta)\rangle_\beta = \langle f_a(s(t), \varphi(t), \beta, \varphi_d)\rangle_{\varphi_d \beta} = f_0 + \langle\beta\rangle s(t) \quad (7)$$

5.2.3.2 Intercept and slope

Equation (7) models the relationship between theta frequency and running speed, suggesting it is composed of two components: a zero speed (movement-independent) component f_0 and a speed-related (movement-dependent) component that increases the theta frequency according to the global spatial scale factor $\langle\beta\rangle$. Represented

graphically, these correspond to the intercept and slope of the linear regression of theta frequency against running speed.

Importantly, changes to the theta frequency necessarily imply changes to the frequencies of the VCOs (see equation (7) above) and therefore also the grid cells. As discussed previously, the spatial scale of grid cells depends on the beat frequency of the interference between baseline and active VCO frequencies (given by f_a-f_b), so combining equations (5) and (6)

$$f_a(s(t), \varphi(t), ß, \varphi_d) - f_b(s(t), ß) = f_0 + ßs(t)(1 + \cos\{\varphi(t) - \varphi_d\}) - f_0 - ßs(t)$$

$$= ßs(t)\cos(\varphi(t) - \varphi_d) \quad (8)$$

Thus, the grid scale depends on ß but not on f_0. Therefore a prediction of the model is that a change in the global spatial scale factor $\langle\beta\rangle$ (the slope) will imply a change in the local VCO ß throughout the dorsoventral extent of the MEA and a concomitant change in grid scale. Conversely, a change in f_0 (the intercept) will not affect grid scale. As described in the previous chapter, environmental novelty increases grid scale (Barry et al., 2009, SFN Abstract 101.24) and therefore the model predicts that this is due to reduction in $\langle\beta\rangle$ (the slope).

The model identifies the intercept and slope with the two types of theta previously described, namely the anxiety/arousal-related theta (a-theta) and the translation-related theta (t-theta), respectively (Kramis et al., 1975). When recorded in isolation, the frequency of t-theta is higher than that of a-theta (typically 8-9 Hz and 6-7 Hz, respectively), with the former recorded during movement and the latter during alert immobility. The cholinergic a-theta and non-cholinergic t-theta pathways converge on the HF, but the relative contributions of each during motion are not clear. Both t-theta and $\langle\beta\rangle$ depend on the activity of the EC, since lesions abolish the former (Buzsáki et al., 1983) whilst the latter is derived from the spatial scale of entorhinal grid cells. In contrast, grid cell firing is unaffected by changes to f_0 that will nonetheless influence theta frequency even during immobility, when t-theta is not present (equation (7), when $s(t) = 0$). Therefore, this suggests a link between f_0 and the immobility-related a-theta, which depends on the integrity of the MS/DBB but not the EC (Vanderwolf et al., 1985).

5.2.4 Place cell firing

The mechanisms by which place cell firing are produced are similar in both types of models (O'Keefe and Burgess, 2005; McNaughton et al., 2006a; Solstad et al., 2006; Burgess et al., 2007), so I shall describe them briefly here. The firing fields of the grid cell population differ in scale and offset (and orientation across hemispheres) and by summing inputs from a subset of these grid cells, localised firing fields resembling those of place cells can be generated (O'Keefe and Burgess, 2005; Solstad et al., 2006). All that is required is that the firing fields of the grid cells overlap, therefore allowing their coincident firing to bring the place cell over its firing threshold. Computational modelling suggests that combining a modest number of grid fields (10-50) is sufficient to reproduce the single place fields observed in the small-sized recording environments which are typically used experimentally (Solstad et al., 2006).

5.2.4.1 Phase resetting

Place cells fire in specific locations in an environment and so their activity is associated with particular combinations of sensory cues, unlike the multi-field grid cells. Therefore, the firing of place cells offers a way to correct path integrative error that may have accumulated in the grid cell system by reference to the external environment.

In the model, this is proposed to occur by the phase resetting of grid cells and their afferent VCO inputs by place cells (O'Keefe and Burgess, 2005; Burgess et al., 2007; Burgess, 2008). As discussed previously, the phase of VCO inputs to a grid cell determine the spatial offset of the grid. If the connections from grid cells that generate specific place cells are reciprocated, then this provides a "feedback" mechanism for place cell resetting of grid cell (and subsequently VCO) phase. Anatomical evidence suggests that similar regions of MEA and CA1 are indeed mutually connected in this way (Kloosterman et al., 2004). This is proposed to occur by resetting the phase of the grid cell and VCOs to the peak of the LFP theta oscillation, when place cells are most active. Phase resetting of theta has been observed relative to the timing of sensory stimuli (e.g. Buzsáki et al., 1979; Williams and Givens, 2003), but its role in grid cell activity remains to be demonstrated.

5.2.4.2 Remapping

As described in the previous chapter, place cell remapping is associated with an expansion in the scale of the grid during global remapping, whereas there is no change in grid scale during rate remapping (Fyhn et al., 2007). Global remapping involves a dramatic shift in place cell firing locations and activity, whereas rate remapping is associated with stable place fields but a change in firing rate. This suggests a global remapping mechanism whereby grid cells expand their fields in response to novelty (Fyhn et al., 2007; Barry et al., 2009, SFN Abstract 101.24), therefore misaligning the grids relative to one another and disrupting the overlap in grid cell inputs that normally drive the place cells. In the model, the degree of grid expansion and misalignment will depend on the size of the reduction in the global spatial scale factor $\langle\beta\rangle$ (the slope of the theta frequency-speed relationship). Therefore, a prediction of the model is that there will be a correlation between the reduction in slope elicited by novelty and the degree of place cell remapping.

5.3 Summary

In this chapter, I have described the models which have been proposed to account for the spatial firing activity of place cells and grid cells. In particular, I have laid out in detail the theoretical basis of the oscillatory interference model of Burgess & O'Keefe (O'Keefe and Recce, 1993; O'Keefe and Burgess, 2005; Burgess et al., 2007; Burgess, 2008). In doing so, I have explained the origins of the predictions which are tested experimentally in this thesis and therefore the rationale for the experimental designs I have employed.

In summary, the model proposes the following predictions:

1. There are two dissociable components of the theta frequency-speed relationship, corresponding to the intercept and slope
2. The intercept is determined by a-theta and is associated with anxiety- and arousal-related processes
3. The slope is determined by t-theta and corresponds to the spatial scale of grid cells
4. The grid scale increase associated with environmental novelty implies a reduction of the slope
5. The degree of reduction in slope correlates with the extent of place cell remapping

6 Methods

6.1 General methods

6.1.1 Housing

All rats were individually housed under a 12-h light:12-h dark cycle (lights on at 08:00 h). Rats were given water *ab libitum* throughout, and food *ab libitum* up until the time of the surgery, after which the experimental protocol dictated the feeding regimen. All experiments were carried out in accordance with the UK Animals (Scientific Procedures) Act 1986.

6.1.2 Surgery and electrophysiological recording

Rats were anaesthetized with isoflurane/O_2 and given injections of an antibiotic (2.5% solution of enrofloxacin, 0.25 ml, subcutaneous) and an analgesic (0.3 mg/ml, buprenorphine hydrochloride, 0.01 ml, intramuscular). Microdrives were chronically implanted into the hippocampus (at 4.0mm posterior, -2.5mm lateral relative to Bregma, unless otherwise stated) and rats were given 1 week for postoperative recovery, after which tetrodes were lowered over several days. EEG and single unit data was recorded from tetrodes in dorsal CA1. All electrode wire was HM-L-coated, 90% platinum-10% iridium (17µm-diameter; California Fine Wire, Grover Beach, CA).

Trial data was recorded using an Axona data acquisition system (Axona, St. Albans, UK). Single unit signals were amplified (15-50K) and band-pass filtered (500 Hz-7kHz). Each channel was continuously monitored at a sampling rate of 50 kHz and action potentials were stored as 50 points per channel (1ms, with 200µs pre-threshold and 800µs post-threshold) whenever the signal from any of the 4 channels of a tetrode exceeded a given threshold. EEG signals were amplified 2000-8000 times, band pass filtered at 0.34-125Hz and sampled at 4800Hz. Two arrays of small LEDs were attached to the headstage to track head position and orientation at 50Hz.

6.1.3 Drugs

CP55940 (Tocris Bioscience, Bristol, UK) was dissolved at a concentration of 100µg/ml in a vehicle of 5% ethanol, 5% cremophor in saline (0.9%). The water-soluble cannabinoid O-2545 (Tocris Bioscience, Bristol, UK) was dissolved at

100μg/ml in a vehicle of physiological (0.9%) saline. All solutions were stored in the freezer at -20°C until use and diluted to a lower concentration in the vehicle, if necessary, for each experiment. Intraperitoneal (i.p.) injections were administered at a volume of 0.5ml/kg. All other reagents were purchased from Sigma-Aldrich (St. Louis, MO, USA).

6.1.4 Apparatus

All screening and trials, unless otherwise specified, were carried out in a square walled open-field environment (dimensions 62x62x50cm), in which the rat foraged for sweetened rice.

6.1.5 Analysis

6.1.5.1 Selection of EEG channel

The peak theta frequency was estimated for every recorded EEG channel by calculating the power spectrum using a fast Fourier transform and finding the frequency with maximal power in the range 7-10 Hz. The theta power index was calculated for each EEG channel in each trial by dividing the power in a 2 Hz band centred on the peak theta frequency by the total power in the whole spectrum. The EEG channel on each day with the maximum mean theta power index across the baseline and probe trials was used for all subsequent analyses for that day.

6.1.5.2 Relationship between EEG theta frequency and running speed

To characterize the dynamic relationship between theta frequency and running speed, a cycle-by-cycle approach was used to estimate momentary EEG frequencies. The recorded EEG signal was filtered using a 6–12 Hz, 251-tap, Blackman windowed, band-pass sinc (sine cardinal) filter. Windowing the filter achieves good stop-band attenuation and small pass-band ripple. An analytic signal was then constructed using the Hilbert transform and takes the form $S_a(t_k) = S(t_k) + i\boldsymbol{H}[S(t_k)]$ where $\boldsymbol{H}$ specifies the Hilbert transform, $S(t_k)$ is the filtered EEG signal, $t_k = k\Delta$, where $k = 1,\ldots,K$ indexes the time-step, and Δ is the inverse of the sampling rate. The phase of the analytic signal $\varphi(t_k)$ gives the phase of the EEG at t_k and the difference in phase between each time point defines the frequency. Since the EEG sampling rate was five times that of position, instantaneous frequency was averaged over every five consecutive values corresponding to each position sample. Thus, concurrent measurements of speed and EEG theta frequency were produced every 20 ms.

To quantify the linear relationship between theta frequency and speed in a given trial, a regression line was fitted to the frequency-speed data points for speeds between 5 and 30 cm/s. Speeds below 5 cm/s were excluded to avoid non-theta epochs during quiescence or immobility. Speeds above 30 cm/s were excluded to avoid too few samples in some trials, and erratic head movement at high speeds. The intercept, measured in Hz, was defined as the intercept of the regression line with the y-axis at zero speed (0 cm/s).

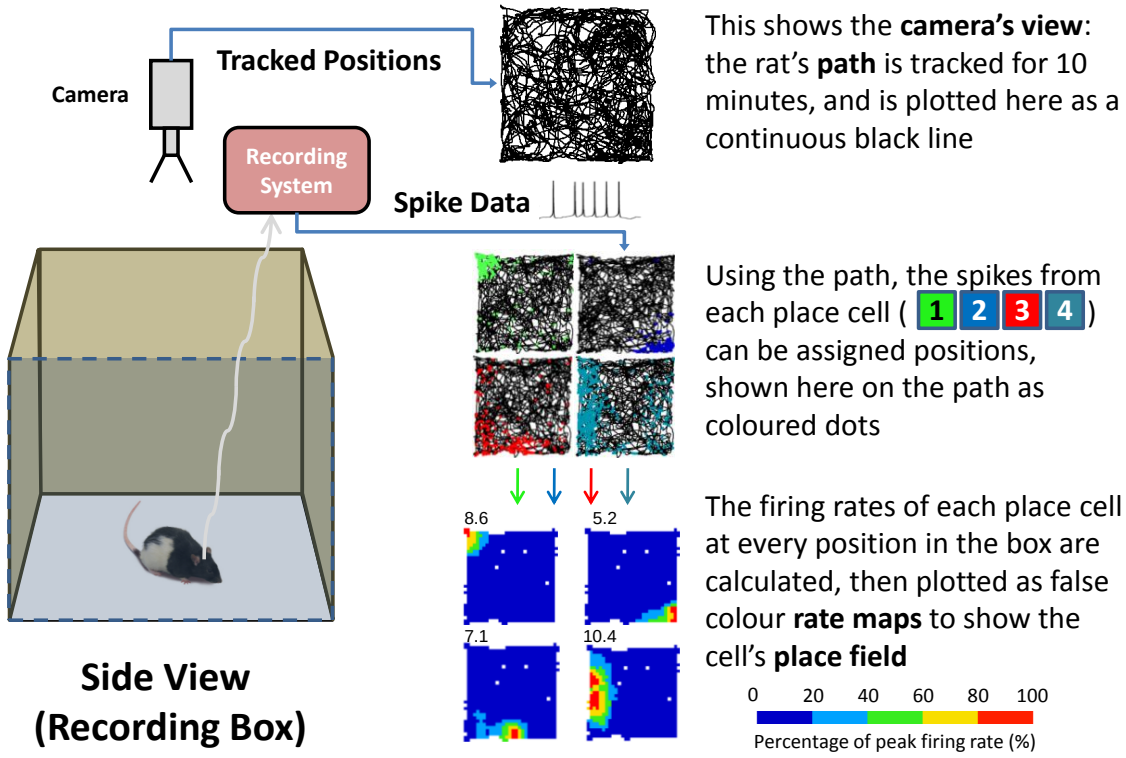

Figure 6.1. Summary of the basic steps involved in the recording and subsequent processing of the animal's spatial trajectory and hippocampal place cell activity. The trajectory alone can be plotted as a path plot (top right); the activity of individual place cells can be plotted as a spike plot (middle right) or as a rate map (bottom right). The rate map plots the spatial firing of the place cell using a false colour gradient scaled to the peak firing rate of the cell. The peak firing rate in Hz is then typically displayed to the top left of the rate map, as shown.

6.1.5.3 Cluster cutting and spatial firing analyses

Cluster cutting of spike data was performed manually using custom-made software (TINT, Axona, St. Albans, UK). Locational firing rate maps were constructed from

2.1 x 2.1 cm binned data, smoothed using a 5 x 5 bin boxcar filter. Spike count divided by dwell time gave firing rate per bin. Firing rate maps are auto-scaled false colour maps, each colour representing a 20% band of peak firing rate, from dark blue (0-20%) to red (80-100%). Peak rate (after smoothing) is the maximal firing rate in any bin and is shown to the top left of the firing rate maps (examples in Figure 2.2, bottom right). Mean rate is the total number of spikes fired by the cell during the trial, divided by the trial duration.

6.2 Pilot intraperitoneal cannabinoid injection study

6.2.1 Methods

6.2.1.1 Subjects and housing

Subjects were 2 male Lister-Hooded rats, which were individually housed under a 12-h light:12-h dark cycle (lights on at 08:00 h). Both rats were implanted with microdrives under deep anaesthesia, as described in the General Methods. One was implanted with a standard microdrive and the other implanted with a modified microdrive containing a intrahippocampal cannula (microinfusion drive). The electrodes in both cases were implanted at the standard coordinates in the left hippocampus described in the General Methods, whilst the cannula in the latter rat was implanted at approximately -1.8ML, -3.2AP and 1.1mm below the dura, and blocked with a stylet which protruded a further 1.0mm.

6.2.2 Results

6.2.2.1 Previous studies and pharmacology of selected cannabinoids

The behavioural effects of intraperitoneal injections of cannabinoids have been studied in rats in a number of spatial memory tasks, including T-maze alternation (Robbe et al., 2006; Robbe and Buzsaki, 2009), the 8-arm radial maze (Molina-Holgado et al., 1995) and the water-maze (Ferrari et al., 1999). However, I wished to optimize the dose of cannabinoid for use in an open field apparatus, which is well-suited to studying the spatial firing characteristics of place cells. Therefore, pilot studies were performed with two rats to study the effects of two synthetic cannabinoids, CP55940 and O-2545, on behaviour in the open field.

In Table 6.1, the pharmacological properties of these two compounds are compared to those of Δ^9-tetrahydrocannabinol (Δ^9-THC), the principal psychoactive compound of

Cannabis sativa, and the endogenous cannabinoids arachidonoylethanolamide (anandamide), 2-arachidonoylglycerol (2-AG) and 2-archidonoyl glycerol ether (noladin).

Table 6.1. Pharmacological properties of commonly-studied endogenous and exogenous ligands of the CB1 and CB2 receptors, including the compounds used for pilot studies (last two rows). (*Sources*: Martin et al., 2006; Pertwee, 2006, 2008)

Name	Source	K_i (nM) at CB_1R	K_i (nM) at CB_2R
Arachidonoylethanolamide (anandamide)	Endogenous	89	371
2-Arachidonoylglycerol (2-AG)	Endogenous	519	618
2-Arachidonoyl glycerol ether (noladin)	Endogenous	21.2	> 3000
Δ^9-Tetrahydrocannabinol (Δ^9-THC)	Plant-derived	5.05	3.13
CP 55,940	Synthetic	0.58	0.68
O-2545	Synthetic	1.5	0.32

6.2.2.2 Behavioural and electrophysiological effects

First, the behavioural effects of different doses of the cannabinoid receptor agonist CP55940 were examined. Published experimental studies have typically employed intraperitoneal (i.p.) doses of 100µg/kg CP55940 (1.0ml/kg of a 100µg/ml solution) (Robbe et al., 2006; Robbe and Buzsaki, 2009). Two rats were chronically implanted with left hippocampal microdrives and familiarized to a small walled box, measuring 62x62x50cm. Once electrodes had been lowered to the pyramidal layer

of CA1, injections were administered at a range of doses across non-consecutive recording days and the effects of the drug on behaviour and hippocampal electrophysiology were monitored. In contrast to the relatively mild behavioural effects reported for this dose in a previous study (Robbe and Buzsaki, 2009), I found that it had severe sedative effects on the rats (Figure 6.2, A1 and A2). Even after halving the dose (50μg/kg), strong behavioural effects were observed that lasted for over 3 hours after the injection (Figure 6.2, A1 and A2).

However, by halving the dose again to 25μg/kg, it was possible minimise the effects on the rat's behaviour and locomotory activity. Nevertheless, a sedative effect was still noticeable 30 minutes after the injection and the rat's pathlength did not approach baseline values until approximately 90 minutes after the injection (Figure 6.2, B1). Additionally, across different recording days the effect on the theta frequency-speed relationship was found to be quite variable, reducing on some days and increasing on others (Figure 6.2, B2). Although the three days shown indicate an upward trend with successive injections, this was not a consistent effect across the pilot study. As described in the introduction, it is well-known that the theta frequency is dependent on the rat's state of arousal and is highly influenced by novelty (Jeewajee et al., 2008b). The variability could therefore have been due to small differences in the experimental protocol day-to-day and so it was decided that a more controlled experimental protocol would be necessary to achieve consistent results (described in the following section).

Although the initial pilot studies had been conducted with CP55940, it was not possible to use this in the experimental study as the drug was upgraded to Schedule I classification shortly before, meaning that it could not be used without a specific licence. Therefore, the final optimisation of dose (data not shown) was completed with the novel synthetic cannabinoid agonist O-2545 (Martin et al., 2006), which possesses similar binding kinetics at cannabinoid receptors to CP55940 (see Table 3.1). This compound also had the advantage of being soluble in saline, eliminating the need to use a vehicle containing toxic solvents as had been the case with CP55940.

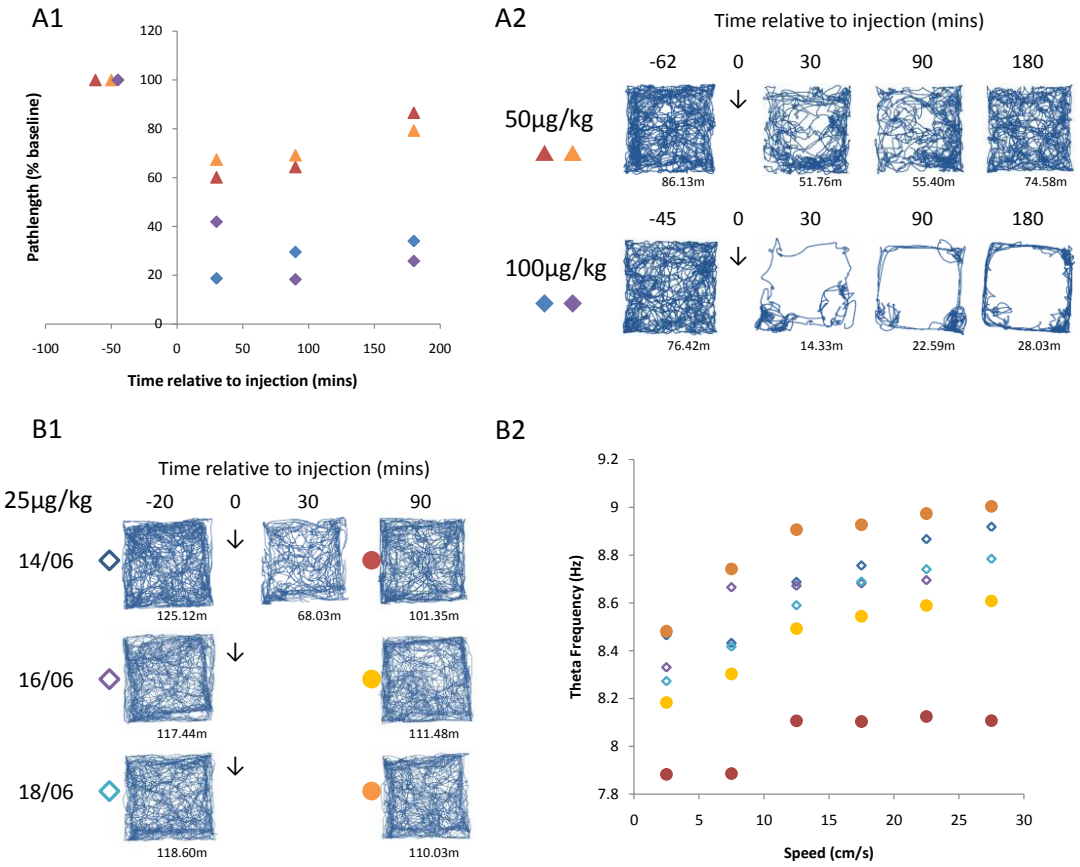

Figure 6.2. Pilot studies into the effects of intraperitoneal injection of CP55940 at doses of 25, 50 and 100 µg/kg on locomotor activity and the theta frequency-speed relationship. (A1) Injection timecourse showing the large and long-lasting reductions in pathlength of injections of 50 µg/kg on 2 days (red and orange triangles) and 100 µg/kg on 2 days (blue and purple diamonds). (A2) Corresponding path plots for the data shown in A1 comparing baseline (left-most plot) and drug trials (3 plots to the right); at 100 µg/kg the drug effects are especially pronounced, with evidence of a strong sedative and anxiogenic influence. (B1) Path plots from 3 days of the 25 µg/kg dose. Effects on pathlength are still noticeable at 30 minutes after i.p. injection of a 25 µg/kg dose, but by 90 minutes the locomotory behaviour begins to resemble that of the baseline. (B2) Theta frequency-speed plot of the trials shown in A1 (open diamonds are data from the corresponding baseline trials, and filled circles are from the corresponding 90 minute trials). However, effects on the theta frequency were variable across days, possibly reflecting the sensitivity of the theta frequency to differing experimental schedules day-to-day (note that although these 3 days shown a steady upward trend in the theta frequency of the 90 minute trials, this was not a consistent finding on other pilot days). Error bars are not shown for clarity.

6.3 Experimental study of the effects of cannabinoids and novelty on hippocampal electrophysiology

6.3.1 Subjects and housing

Subjects were 6 individually housed male Lister-Hooded rats weighing 363-445g at time of surgery. They were housed under a 12-h light:12-h dark cycle (lights on at 08:00 h) and were food restricted from 1 week after surgery (c. 85% bodyweight).

6.3.2 Surgery and electrophysiological recording

Rats were chronically implanted with microdrives in either the left (4 rats; 4.0mm posterior and -2.5mm lateral to Bregma) or both the left and right hippocampi (2 rats; left drive 4.5mm posterior and -3.0mm lateral to Bregma, right drive 3.2mm posterior and +2.0mm lateral to Bregma) under deep anaesthesia, as described in the General Methods. They were given 1 week for postoperative recovery after which tetrodes were lowered over several days.

6.3.3 Apparatus

The test environments were a square walled open-field environment (dimensions 62x62x50cm) with polypropylene walls and floor, referred to as Fam; a circular walled open-field environment (80 cm diameter, 51 cm walls) with grey-painted wooden walls and a black ribbed rubber floor, referred to as NovA; and a wall-less open-field environment (100x100cm) with a unpainted wooden floor, referred to as NovB.

The distal cues were also changed and were as follows for each environment: for the Fam environment, a large filebox was positioned on the ceiling and other prominent cues such as the door to the west and a shelf to the east were visible from the floor of the box; for the NovA environment, a large black sheet was hung to the east and a black-and-white cue card was suspended close to the south; for the NovB environment, distal cues were identical to the Fam environment, but many objects in the room that had previously been hidden by the walls of the Fam environment were now visible.

Each test environment was centred at the same location in the recording room and was swapped according to the experimental schedule. In between trials, subjects were placed on a holding platform (43x32x9cm) located in the same room, next to the test environments.

6.3.4 Drugs

The water-soluble cannabinoid O-2545 (Tocris Bioscience, Bristol, UK) was dissolved at 100μg/ml in a vehicle of physiological (0.9%) saline. Intraperitoneal (i.p.) injections were administered at a volume of 0.5ml/kg. This dose, based on pilot data, was chosen to avoid locomotion-reducing effects in the open field (see Pilot Study section above).

6.3.5 Procedure and task design

Prior to beginning the experiment, each rat received at least 15 exposures to the Fam environment over a period of at least a week. The experimental schedule consisted of two blocks of 5 days each, A (Days A1-A5) and B (B1-B5), separated by one rest day on which no experiment was run (Figure 6.3). On each experimental day, the rat foraged for sweetened rice in four 10 min trials with an i.p. injection of O-2545 or its vehicle, saline, in between the 3rd and 4th trial. In between each trial, the rat was placed on the holding platform. The trials were carried out at approximately the same time every day, with the 1st-3rd trials 90, 60 and 30 mins before the injection, respectively, and the 4th trial 30 mins after the injection. On the first 4 days of each block, all trials were in the Fam environment. On the 5th day, the rat was introduced to either the NovA (A block) or NovB (B block) environment on the 4th (post-injection) trial, which was placed in position along with any new cues 20 minutes after the injection. In 4 rats, the Fam environment was also removed and replaced 20 mins after the injection (Days A1-4 and B1-4) to mimic the novel environment change. On the first 2 days of each block, vehicle was injected, and on the final 3 days injections alternated between drug and vehicle in a counterbalanced way across blocks and rats.

6.3.6 Temperature recording

Rats were habituated to aural temperature measurement using a Thermoscan IRT4520 (Braun, Kronberg im Taunus, Germany) before the beginning of the experimental protocol. During days A1-5 and B1-5, three temperature recordings were taken in 4 rats before and after each trial. The highest readings from before and after each trial were selected, and the average of these used as the temperature value for the trial.

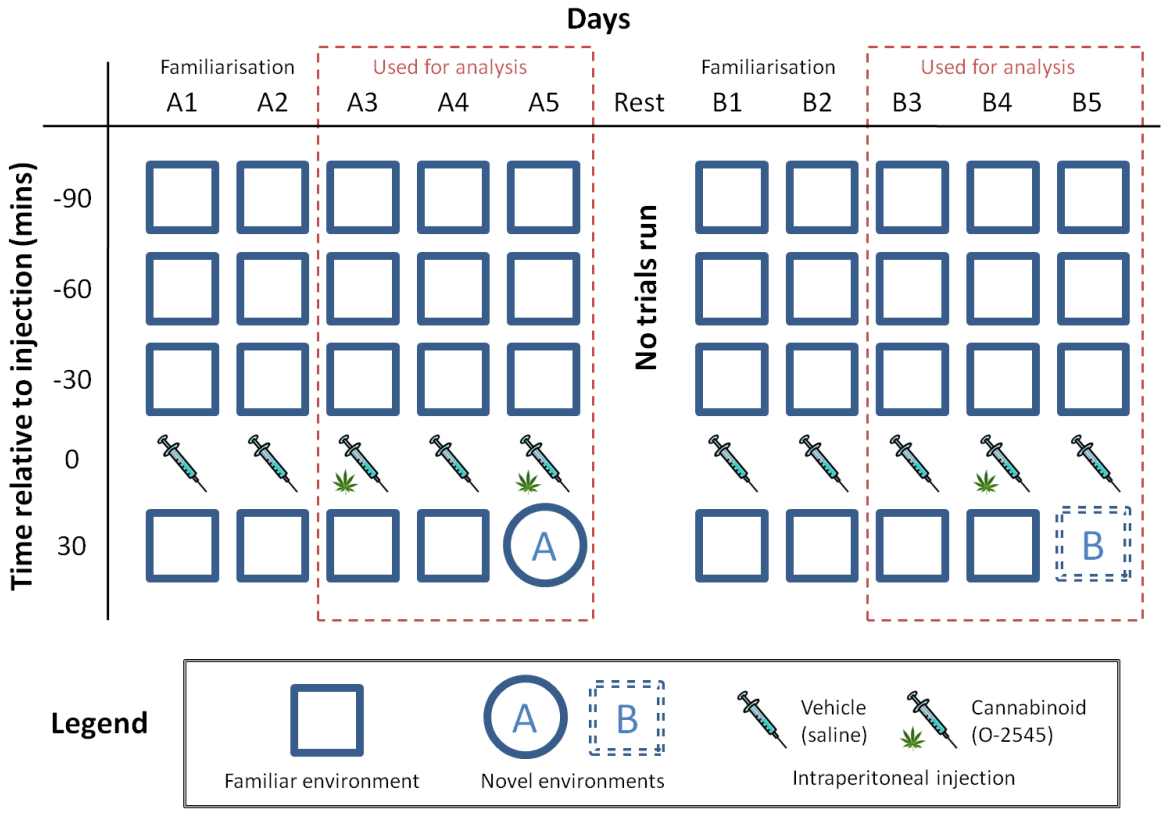

Figure 6.3. Summary of the experimental protocol. Each day is one column and each row represents the specific timepoint on each day when a trial (either in familiar or novel environments, shown in legend on left) or injection (either vehicle or cannabinoid, shown in legend on right) was carried out. Three rats experienced the protocol shown, whilst the other three experienced a counterbalanced protocol that was identical, except that the drug was administered on days A4, B3 and B5 instead. Analysis was conducted on data from days A3-A5 and B3-B5, whilst days A1-A2 and B1-B2 were used to familiarize the rat to the experimental procedure and ensure that the novelty on days A5 and B5 was "unexpected".

6.3.7 Analysis

6.3.7.1 Experimental days analysed

All analysis was conducted on data from days A3-A5 and B3-B5, as indicated in Figure 6.3. This was to ensure the rat was sufficiently familiarized with the experimental protocol and that the environmental novelty delivered on days A5 and B5 was "unexpected" (Jeewajee et al., 2008b).

6.3.7.2 Plots of grouped theta frequency-speed data

In order to plot theta frequency-speed graphs of all rats grouped by condition, theta frequency data from each day (in each rat) were normalized to the mean theta frequency across all baseline trials on that day (all 3 pre-injection trials). This allowed changes in theta frequency to be assessed independently of variation between rats or days. Data were then plotted by multiplying the normalized values by the mean theta frequency value across all baseline trials for all rats within each condition.

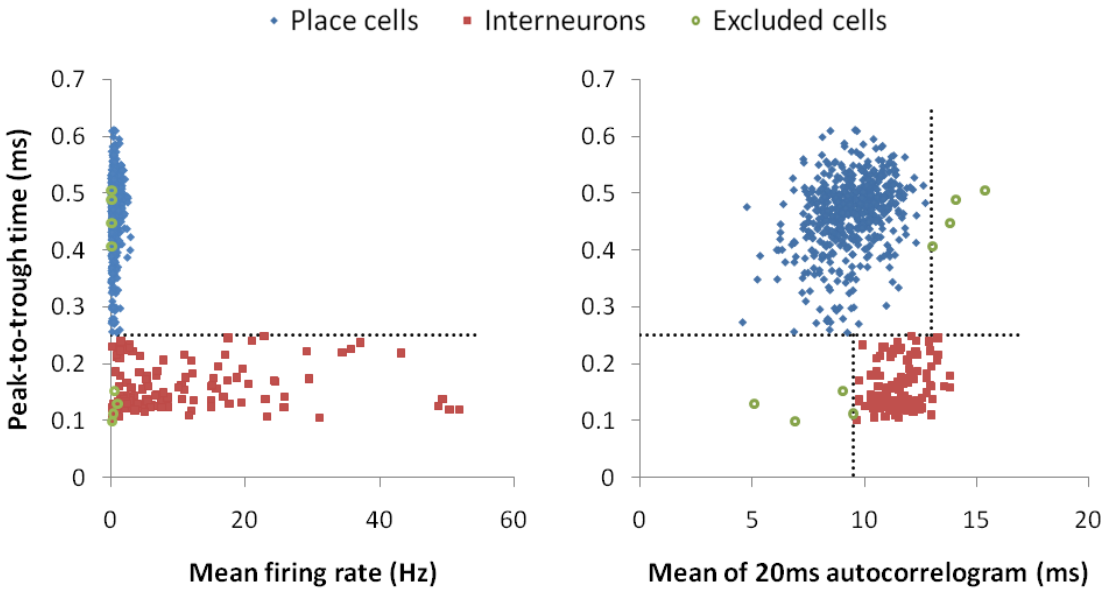

Figure 6.4. Classification of single units into place cells and interneurons was accomplished by plotting the peak-to-trough time against the mean firing rate (left) and the mean of the 20ms autocorrelogram (right). The latter plot (right) shows a clear separation between place cells (blue diamonds) and interneurons (red squares). A small number of outliers was removed from each group (green circles, n=4 per group) on the basis of the autocorrelogram mean.

6.3.7.3 Single unit classification

Single units were classified into place cells and interneurons on the basis of mean firing rate, the peak-to-trough time of the mean waveform and the mean of the 20ms autocorrelogram (Csicsvari et al., 1999b; Cacucci et al., 2004; Le Van Quyen et al., 2008). A plot of the peak-to-trough time against mean rate revealed that

many cells with a peak-to-trough time below 0.25ms had substantially elevated firing rates, in line with the expected characteristics of fast-spiking interneurons (Figure 6.4, left). Separation of the single units by their peak-to-trough time and autocorrelogram mean showed two distinct clusters (Figure 6.4, right). An equal number of outliers was removed from each cluster (n=4 cells). The final inclusion criteria for place cells were: peak-to-trough time at least 0.25ms, autocorrelogram mean less than 13ms. For interneurons, they were: peak-to-trough time less than 0.25ms, autocorrelogram mean greater than 9.5ms.

6.3.7.4 Field size

The field size was calculated as a proportion of the total area of the environment. For each cell in each trial, this was calculated by dividing the number of bins in the smoothed ratemap with a rate at least 20% of the peak rate by the total number of bins visited during the trial.

6.3.7.5 Spatial information

Spatial information is a measure of how accurately the firing of a cell predicts the current position of the animal (Skaggs et al., 1993). The mutual information between firing rate R and location X in bits/second was calculated as:

$$I(R \mid X) \approx \sum_i p(\vec{x}_i) f(\vec{x}_i) \log_2 \left(\frac{f(\vec{x}_i)}{F} \right)$$

where $p(\vec{x}_i)$ is the probability of the animal being at location X, $f(\vec{x}_i)$ is the firing rate at location X and F is the mean firing rate of the cell. The spatial information in bits/spike was then calculated by dividing the mutual information, $I(R \mid X)$, by the mean rate, F.

6.3.7.6 Remapping analyses

The extent of remapping between the baseline and probe trials was estimated using two measures of spatial firing similarity. As the novel environments were a different size and shape to the familiar environment, ratemaps were first transformed to the familiar shape using a transformation that preserves the similarity of un-remapped fields (Lever et al., 2002; Wills et al., 2005). This transformation finds corresponding bins across environments that share the same angle and proportional distance from the centre of the environment, using nearest neighbour interpolation.

The population ratemap correlation measures how similar the firing activity of the place cell population is within each spatial bin across two trials, including cells that are silent in either trial. For each spatial bin of the ratemap, the rates of all place cells in that bin were correlated across the two trials to give a Pearson's correlation coefficient *r*. The mean of the correlation coefficients across all bins was taken as the estimate of the degree of remapping between the trials.

The spatial correlation measures the firing similarity of each cell across two trials, excluding cells that are silent in either trial. It was calculated as the 2-dimensional Pearson's correlation coefficient of the ratemaps from the two trials (`corr2` in Matlab).

6.3.7.7 Theta phase

A theta phase was assigned to each spike occurring at time t using a linear interpolation of the phase of the analytic signal $\varphi(t)$, given by the Hilbert transform of the concurrently recorded EEG (as described in the General Methods). The relative phase shift from baseline to probe trials was calculated as the circular mean of the phases of all spikes (or cells) in the probe trial minus the equivalent mean from the baseline trial. The mean phase of the baseline trial was arbitrarily assigned to 0°. Phase histograms were plotted by binning spikes or cells into 10° bins.

6.3.7.8 Statistics

The experiment was designed as a two-way factorial investigation of the effects of cannabinoids and novelty on hippocampal electrophysiology, so two-way repeated measures ANOVAs were used to quantify within-subject effects. Subjects with missing data in any of the four conditions were excluded from the relevant analyses. Individual conditions were compared using post-hoc paired t-tests. Phase analyses were conducted using linear statistics as the vast majority of phase values fell in the range ±90°, the maximal value across all analyses being a single outlier at 138.8° (discussed in the Single Units results chapter).

7 Dissociation of two components of the theta frequency-speed relationship by cannabinoids and novelty

7.1 Introduction

The theta rhythm (6-12Hz) is the predominant local field potential (LFP) oscillation found throughout the entorhino-hippocampal system during waking activity in the rat. Theta activity depends anatomically on the contributions of two distinct pathways: a type I 'translational' theta (t-theta) that is movement-dependent and depends on the entorhinal cortex , and a type II 'arousal/anxiety' theta (a-theta) that is commonly observed during immobility and depends on a direct projection from the MS/DBB (Kramis et al., 1975). The precise behavioural correlates and functional roles of theta are still not fully understood, but they are thought to include anxiety processing (Gray and McNaughton, 2000; Seidenbecher et al., 2003; Gordon et al., 2005; Adhikari et al., 2010), novelty detection/encoding (Hasselmo et al., 2002; Jeewajee et al., 2008b) and spatial navigation (Winson, 1978; McNaughton et al., 2006b; Geisler et al., 2007; Burgess, 2008). Accordingly, theta frequency has been shown to increase with the rat's running speed (Slawinska and Kasicki, 1998; Jeewajee et al., 2008a) and is reduced by a wide range of anxiolytic drugs (Gray and McNaughton, 2000; McNaughton et al., 2007) and by environmental novelty (Jeewajee et al., 2008b). However, the interdependence of these effects and pathways through which they exert their influence on theta frequency are not currently known.

A recent model (Burgess, 2008) attempts to reconcile the apparently disparate roles of theta in spatial cognition, anxiety and novelty in terms of the relationship between theta frequency and running speed. The model proposes that the linear relationship of frequency to running speed can be written as:

$$f_\theta(t) = f_0 + <\beta> s(t),$$

where t is the time; $f_\theta(t)$ is the theta frequency at time t; $s(t)$ is the speed at time t; f_0 is the theta frequency at zero speed; and $<\beta>$ is the global average of the increase in the intrinsic oscillatory frequency of velocity-controlled oscillators (VCOs) with running speed (see Models chapter for more details). Velocity-dependent increases in firing frequency have been reported for both place (Geisler et al., 2007) and grid (Jeewajee et al., 2008a) cells of the entorhino-hippocampal system and recently in

hippocampally-projecting thalamic neurons (Welday et al., 2010, SFN Abstract 203.20). The zero-speed frequency, f_0, reflects the baseline (minimum) intrinsic oscillation frequency of the VCOs. If the linear relationship described by this equation is represented graphically, then f_0 corresponds to the Y-axis intercept and $<\beta>$ to the slope of the line. In the model, the intercept and slope are identified with the two types of theta: the speed-independent component (f_0 or intercept) with the 'immobility-related' anxiety/arousal- or a-theta (type II); and the speed-dependent component ($<\beta>$ or slope) with the 'movement-related' translational- or t-theta (type I).

7.2 Experimental rationale

In this experiment, I aimed to manipulate the intercept (f_0) and the slope ($<\beta>$) of this relationship both independently and in combination. As well as reducing the theta frequency, environmental novelty is known to cause an expansion of grid cell firing fields (Fyhn et al., 2007; Barry et al., 2009, SFN Abstract 101.24). The model predicts that this increase in grid scale depends on a reduction in the slope ($<\beta>$) and therefore I aimed to use environmental novelty to affect t-theta and selectively reduce the slope. In contrast, the theta frequency reduction caused by a wide range of anxiolytic drugs is predicted by the model to affect a-theta and therefore be linked to a reduction in the intercept (f_0). As intraperitoneal injection of cannabinoids reduces theta frequency (Robbe and Buzsaki, 2009) and cannabinoids are anxiolytic at low doses (Haller et al., 2004; Rubino et al., 2007, 2008; Moreira and Wotjak, 2010), I aimed to use this drug to selectively reduce the intercept. This study therefore aimed to test the predictions of the model by examining the independent and combined effects of cannabinoids and novelty on the slope and intercept of the theta frequency-speed relationship.

7.3 Results

Six rats were implanted with microdrives in the left hippocampus (n=4) or both the left and right hippocampi (n=2) and habituated over a prolonged period to a small square box (62×62×50cm), the familiar environment (Fam), and to intraperitoneal (i.p.) injections of the vehicle (0.5 ml/kg saline).

7.3.1 Histology

Histological examination of all six rats confirmed that tetrodes were implanted into the CA1 subfield of the hippocampus in all cases (Table 7.1 and Figure 7.1).

Table 7.1. Recording locations for the six rats in the experiment.

Rat	Hemisphere	Estimated final recording layer	Estimated recording location behind bregma (mm)
1	Left	CA1 stratum radiatum	4.0 AP
2	Left	CA1 stratum oriens	4.6 AP
2	Right	CA1 pyramidal layer/stratum radiatum	3.5 AP
3	Left	CA1 stratum radiatum	3.7 AP
4	Left	CA1 stratum radiatum	4.1 AP
5	Left	CA1 pyramidal layer/stratum oriens	4.4 AP
6	Left	CA1 pyramidal layer/stratum radiatum	4.4 AP
6	Right	CA1 stratum radiatum	3.5 AP

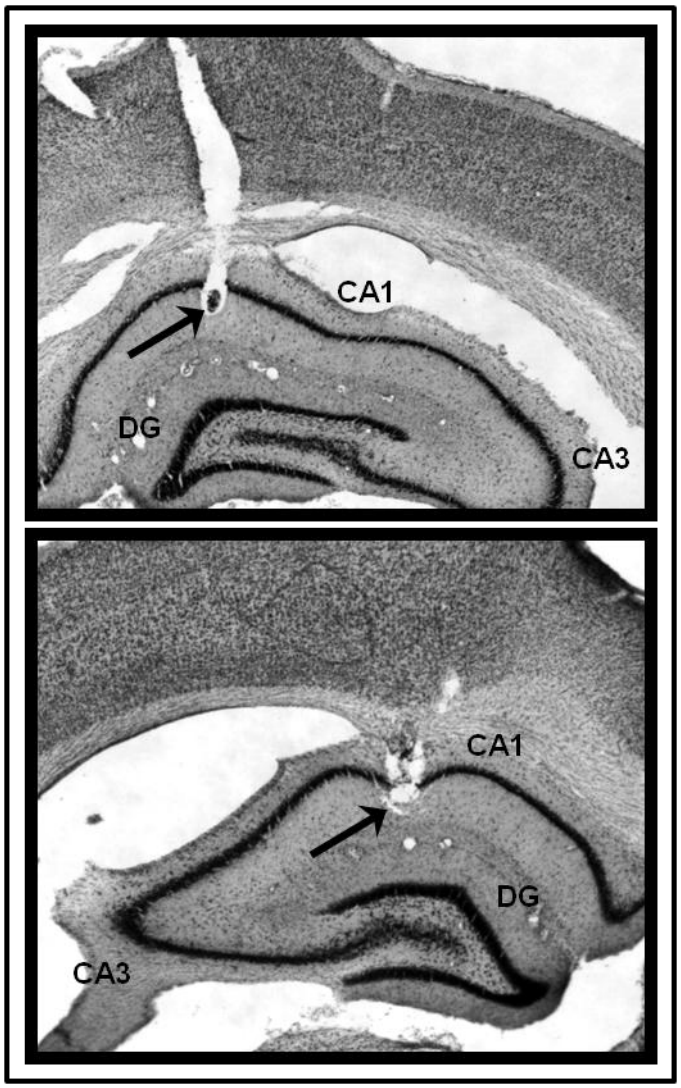

Figure 7.1. Location of recording electrodes. Cresyl-violet stained sections of the dorsal hippocampus are shown for two rats. Arrows indicate the deepest point reached by the tetrode. (Top panel) The electrode track in CA1 stratum radiatum of Rat 4. (Bottom panel) The end of the electrode track in CA1 stratum radiatum in the right hemisphere of Rat 6.

7.3.2 Summary of the experimental procedure

Electrophysiological data were collected in two blocks, A and B, each consisting of five days (A1-5 and B1-5) separated by one rest day (see Methods, Figure 3). Each block began with two familiarisation days (A1-2 and B1-2) that were used to habituate the rat to the full experimental procedure, followed by three experimental days (A3-5 and B3-5). On each day, the rat experienced three baseline trials in Fam, followed by an i.p. injection of drug or vehicle (according to the schedule) and a probe trial in Fam 30 minutes later. On familiarisation days,

vehicle (0.5ml/kg saline) was always injected after the third baseline trial. On experimental days, injections of vehicle and cannabinoid (0.5ml/kg 100μg/ml O-2545) were alternated on consecutive days, with the order counter-balanced across blocks and rats. On the final day of each block, the environment was changed prior to the probe trial for one of two novel environments: NovA, a circular enclosure, on day A5; or B, an unenclosed square, on day B5. The basic experimental design allowed all the combinations of the vehicle/drug (Veh/Drug) and familiar/novel (Fam/Nov) conditions to be studied, resulting in four crossover conditions (Veh × Fam, Veh × Nov, Drug × Fam and Drug × Nov). Only data from the experimental days were used for the subsequent analyses.

Sample raw LFP epochs from probe trials of Rat 4 on three consecutive days (days A3-A5) are shown in Figure 7.2 (top panel). The mean data from these epochs are plotted on a theta frequency-speed graph (Figure 7.2, bottom panel) to show the basic effects of cannabinoid injection and environmental novelty on the theta frequency-speed relationship. In this simplified example, it can be seen that Drug reduces the intercept relative to Veh × Fam and Novelty reduces the slope (the slope effect shown is mild, compare to group results in Figure 7.3). Although mean data from the whole epoch are plotted in Figure 7.2 for illustrative purposes, the full analysis used estimates of frequency and speed taken throughout each 10 minute trial at 50 Hz (see Methods for more details).

7.3.3 Effects on intercept and slope

First, the relationship between theta frequency and the rat's running speed was examined in each of the four conditions (Veh × Fam, Veh × Nov, Drug × Fam and Drug × Nov). According to previous observations from our group, the differences in both behaviour and theta frequency are most likely to be minimal between the last two trials of a day consisting of repeated exposures to the same environment (Lever et al., 2006; Jeewajee et al., 2008b). Therefore, analyses were conducted by comparing data from the baseline trial immediately prior to injection (henceforth, referred to as "baseline") and the probe trial 30 minutes after injection of vehicle or drug. Theta frequency data from each day and rat were binned into 2.5 cm/s wide bins in the range 5-30 cm/s. A linear regression analysis of speeds between 5 and 30 cm/s was chosen to provide a good estimate of the theta frequency-speed relationship (Jeewajee et al., 2008a), since this excludes non-theta behaviours below 5 cm/s and artefacts or sparse data above 30 cm/s.

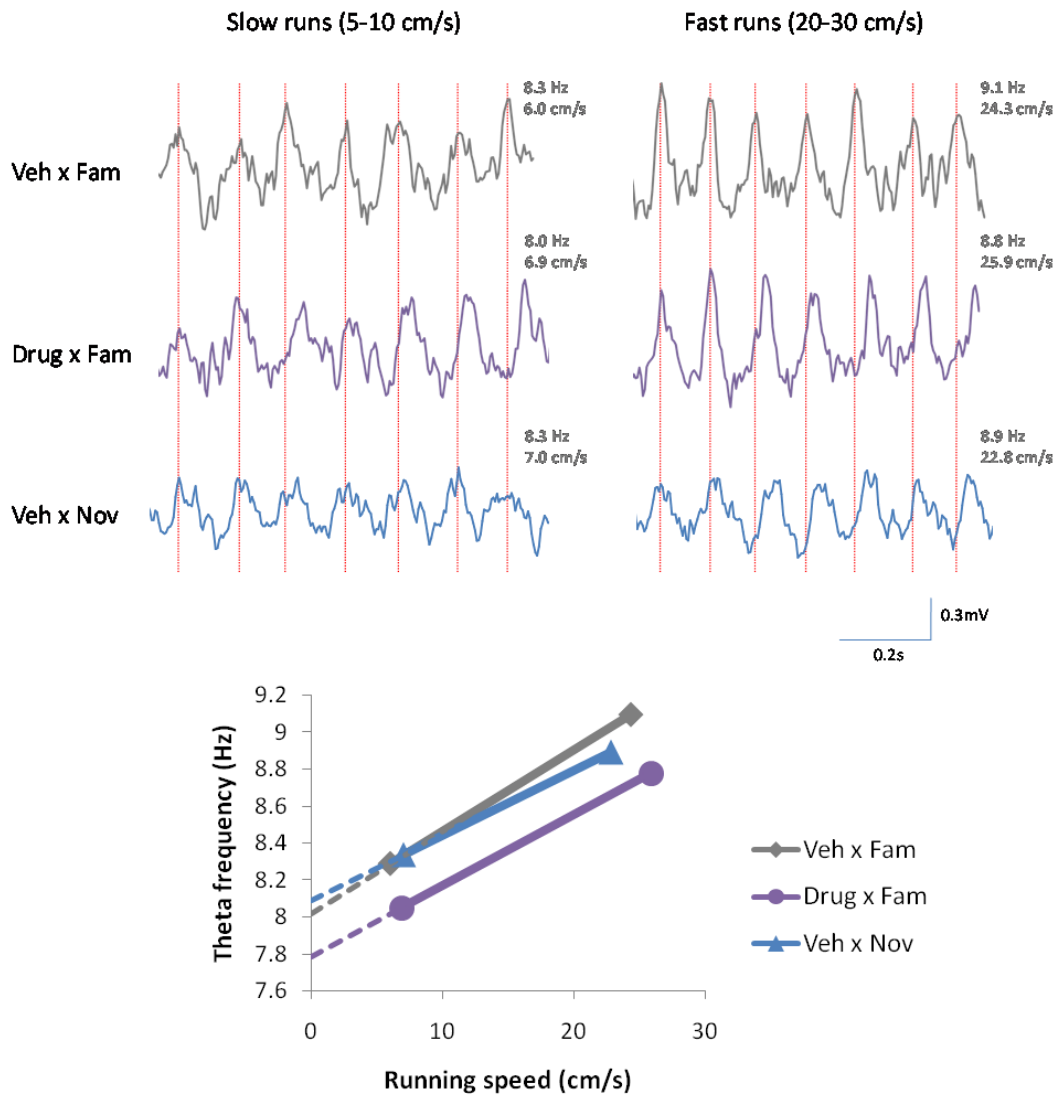

Figure 7.2. LFP theta data collection and plotting on theta frequency-speed graph. (Top panel) Example raw LFP epochs from probe trials of Rat 4 on three consecutive days after either vehicle (top row) or cannabinoid injection (middle row) in the familiar environment, or following vehicle injection in a novel environment (bottom row). Slow runs (left column, 5-10 cm/s) exhibit a lower theta frequency than fast runs (right column, 20-30 cm/s). Red vertical lines are aligned with the peaks of the LFP theta wave in Veh × Fam to allow relative frequencies to be compared across conditions. Mean theta frequencies (calculated by the Hilbert transform) and running speeds for each epoch are given at the top right of each trace. Scale bar shown at bottom right. (Bottom panel) Mean data from LFP epochs shown above, plotted on a theta frequency-speed graph. Solid lines indicate the regression line fit to the data which gives the *slope* and, by extrapolation to the y-axis (dotted lines), the *intercept*. Compared to Veh × Fam (grey), in Drug × Fam (purple) the intercept is reduced, whereas in Veh × Nov (blue) the slope is reduced (note on this day the slope reduction was fairly mild, see Figure 7.3 for overall group results).

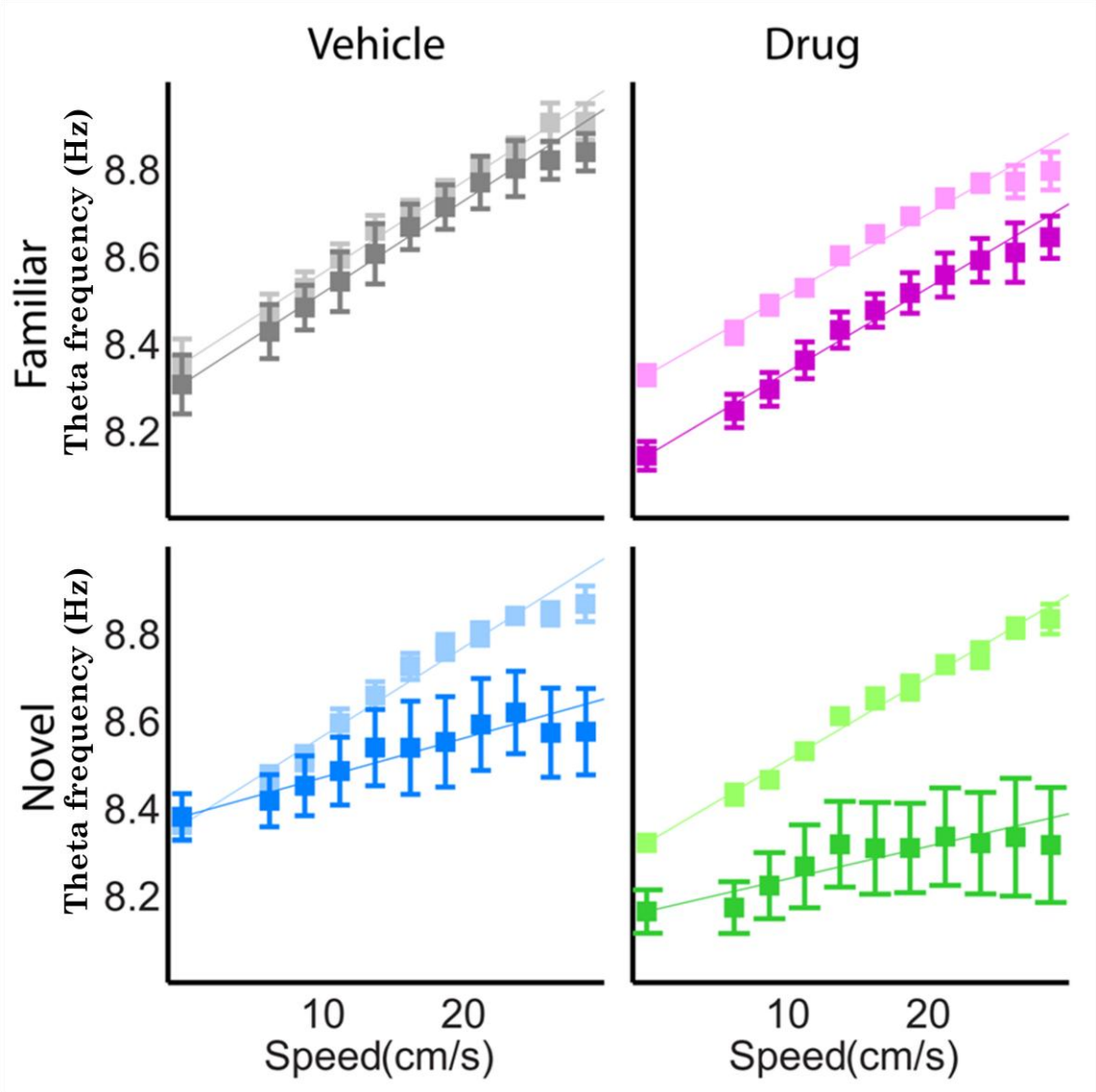

Figure 7.3. Theta frequency plotted against running speed in each of the four conditions from grouped data across all rats (top left: Veh × Fam; top right: Drug × Fam; bottom left: Veh × Nov; bottom right: Drug × Nov). Darker colours indicate the probe trial and lighter colours the baseline trial. Data points from 5-30 cm/s show the experimentally measured theta frequency values ± SEM, normalized across rats. Linear regression of these data was used to calculate the slope and intercept of the relationship (Y-axis data points indicate intercept estimates ± SEM).

I then compared the intercept and slope of the linear regression in each of the four conditions to look for independent and combinatorial effects of the experimental manipulations (Figure 7.3). In the control condition, Veh injection coupled with the Fam environment had no effect on either intercept or slope (Figure 7.3, top left

plot; intercept: paired t_5=0.7, p=0.53, 0.02 Hz mean decrease; slope: paired t_5=0.6, p=0.57, 0.08 Hz/m/s mean reduction). However when cannabinoid was injected before the Fam trial, I found a specific reduction in the intercept but no change in the slope, in line with the predictions of the model (Figure 7.3, top right plot; intercept, paired t_5=4.8, p=0.002, one-tailed, 0.21 Hz mean reduction; slope t_5=0.2, p=0.87, 0.026 Hz/m/s mean reduction). In contrast, environmental novelty alone specifically reduced the slope and did not affect the intercept (Figure 7.3, bottom left plot; slope, paired t_5=7.0, p=0.0005, one-tailed, 1.1 Hz/m/s mean reduction; intercept t_5 =0.1, p=0.93, 0.008 Hz mean reduction).

A two-way repeated measures ANOVA on the data from all six rats confirmed the main effects of Drug on intercept and Novelty on slope (Drug: intercept $F_{1,5}$=6.85, p=0.047, slope $F_{1,5}$=0.54, p=0.83; Novelty: slope $F_{1,5}$=449, p = 4 x10^{-6}, intercept $F_{1,5}$=0.99, p=0.77). Finally, there was no interaction between Drug and Novelty (two-way repeated measures ANOVA; Drug × Novelty: intercept $F_{1,5}$=0.31, p=0.60, slope $F_{1,5}$=0.54, p=0.83), suggesting a linear summation of the effects of Drug and Novelty on intercept and slope, respectively. Indeed, when both manipulations were used together (Drug × Nov; Figure 7.3, bottom right plot), the effects on the intercept and slope were commensurate with an additive combination of the Drug and Novelty effects (mean intercept and slope reductions of Drug or Nov alone: 1.1 Hz/m/s and 0.20 Hz, respectively; mean intercept and slope reductions of Drug and Nov in combination: 1.2 Hz/m/s and 0.15 Hz, respectively).

7.3.4 Behavioural and physiological effects

7.3.4.1 Locomotor activity

The reduction elicited in the intercept and slope (by Drug and Novelty, respectively) could arise due to gross differences in behaviour caused either by the cannabinoid injection or by environmental novelty. Cannabinoids exert potent inhibitory effects on locomotor activity (Fernández-Ruiz, 2009) which could account for the intercept reduction by Drug. On the other hand, exploratory behaviour induced by environmental novelty and an associated increase in locomotor activity might be driving the reduction in slope.

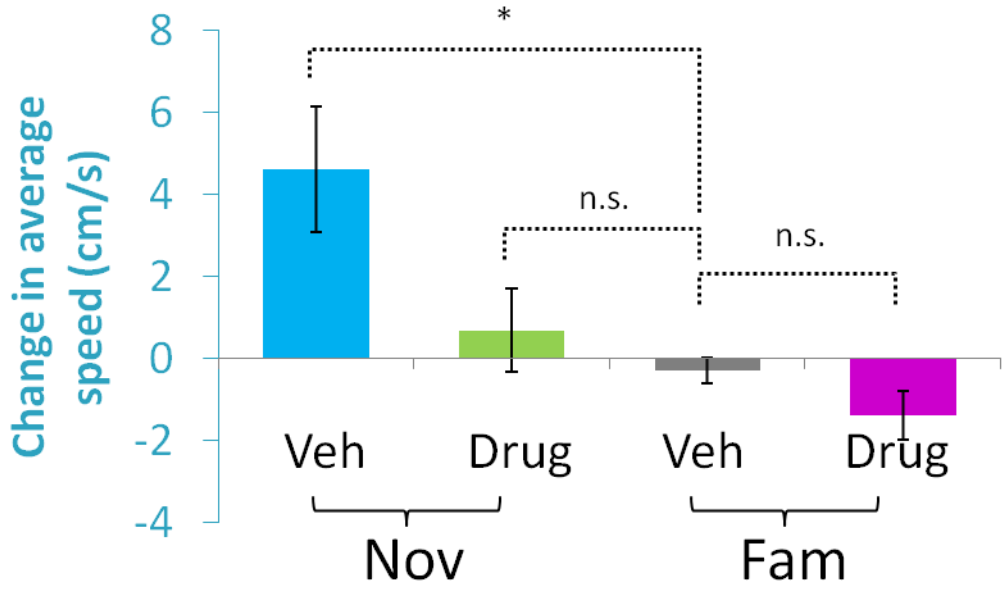

Figure 7.4. Changes in average speed from the baseline to probe trial in the four experimental conditions. There were no significant changes in any of the conditions with the exception of Veh × Nov, in which there was a marked increase.

Change in average speed

In order to test for such effects, the change in average speed from the baseline to probe trials was calculated for each rat on each experimental day (Figure 7.4). The Drug caused only a minor and non-significant reduction in average speed in the Fam environment compared to Veh (paired t_5=1.6, p=0.17, 2.4% vs. 11.0% mean reductions after Veh and Drug, respectively), suggesting that a change in locomotor activity could not account for the intercept reduction by cannabinoid. In contrast, Novelty alone significantly increased average speed (paired t_5=2.8, p=0.04, 39.7% mean increase) but when combined with Drug, this increase was greatly attenuated (paired t_5=1.8, p=0.13, mean increase 5.4%). However, the attenuation of the Novelty-induced speed increase by Drug did not reach significance (paired t_5=1.7, p=0.14, mean attenuation of 85.1%). A two-way repeated measures ANOVA confirmed the main effect of Novelty on average speed ($F_{1,5}$=17.7, p=0.008) and showed no effect of the cannabinoid and no interaction of the two factors (Drug: $F_{1,5}$=4.8, p=0.08; Drug × Novelty: $F_{1,5}$=1.4, p=0.29).

Despite the large differences in average speed following Veh or Drug injection in Novelty, the slope reduction was similar in both conditions (mean reduction in Veh

× Nov: 1.09 Hz/m/s, in Drug × Nov: 1.19 Hz/m/s; paired t_5=0.25, p=0.81). This suggests that there is no relationship between the change in average speed and the slope reduction in novelty. In order to confirm this, I performed a linear regression analysis on these two variables for all Nov days in all rats. The regression confirmed the lack of a correlation between changes in average speed and slope (Figure 7.5; Pearson's r=+0.393, p=0.21), demonstrating that the slope reduction did not arise from gross differences in behaviour. Therefore, there is no evidence that changes in average speed can account for either the intercept or slope reduction.

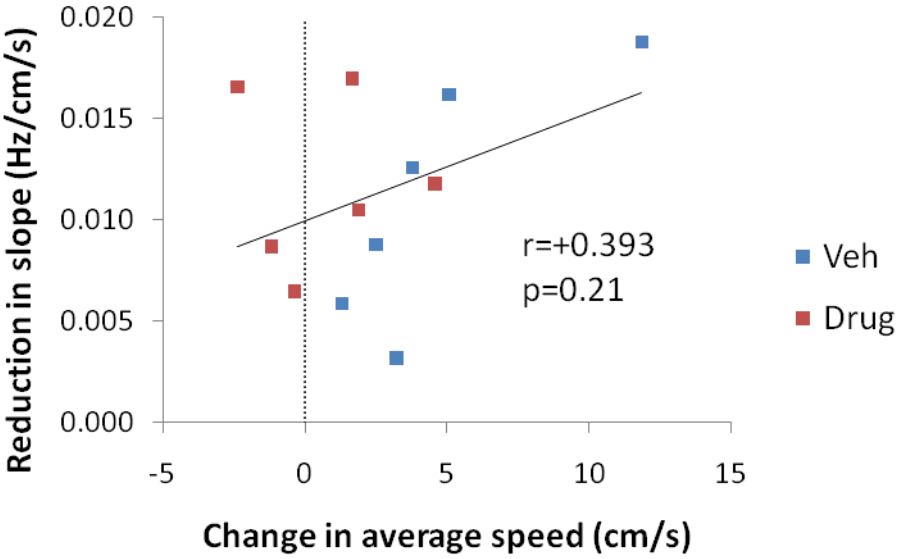

Figure 7.5. Lack of a correlation between the reduction in slope and change in average speed from the baseline to probe trials on Nov days. Each of the six rats contributes one Drug data point (red) and one Veh data point (blue).

7.3.4.2 Anxiolytic action of cannabinoid

Consistent with an anxiolytic action of the Drug, I found that anxiety-related thigmotaxic (wall-hugging) behavior was reduced by cannabinoid injection. The Drug increased the amount of time spent in the centre half-radius of the enclosed novel environment (NovA; 225.8 ± 23.8 seconds vs. 177.2 ± 13.3 seconds after Drug or Veh injection, respectively; n=3 rats in each group). However, there were insufficient data to confirm this effect statistically (unpaired t_2=2.3, p=0.15). Nevertheless, these findings suggest that the cannabinoid tended to increase

exploration of the centre of the walled novel environment. Therefore, the attenuation of average speed by Drug in novelty (Figure 7.4, compare left two bars) is unlikely to arise from anxiety-related behavioural inhibition, but might reflect a more generalised impairment of novelty-elicited locomotor activity.

7.3.4.3 Body temperature

Another factor which could affect the intercept or slope reductions is the body temperature of the rat, which has previously been reported to correlate linearly with theta frequency (Whishaw and Vanderwolf, 1971; Deboer, 2002). Therefore, I asked if changes in body temperature (n=4 rats, aural temperature) could account for the differences in intercept and slope observed. Consistent with reports in the literature (Smirnov and Kiyatkin, 2008), I found that Drug reduced body temperature (Figure 7.6; two-way repeated measures ANOVA; Drug: $F_{1,3}$=18.1, p=0.024, 0.40°C mean reduction), whereas there was no effect of Novelty or any interaction of the two manipulations (Figure 7.6; two-way repeated measures ANOVA; Novelty: $F_{1,3}$=0.76, p=0.45, 0.10°C mean increase; Drug × Novelty: $F_{1,3}$=0.26, p=0.64). These results suggested that it was unlikely that body temperature could explain the slope reductions, but they might account for the intercept reduction elicited by the cannabinoid.

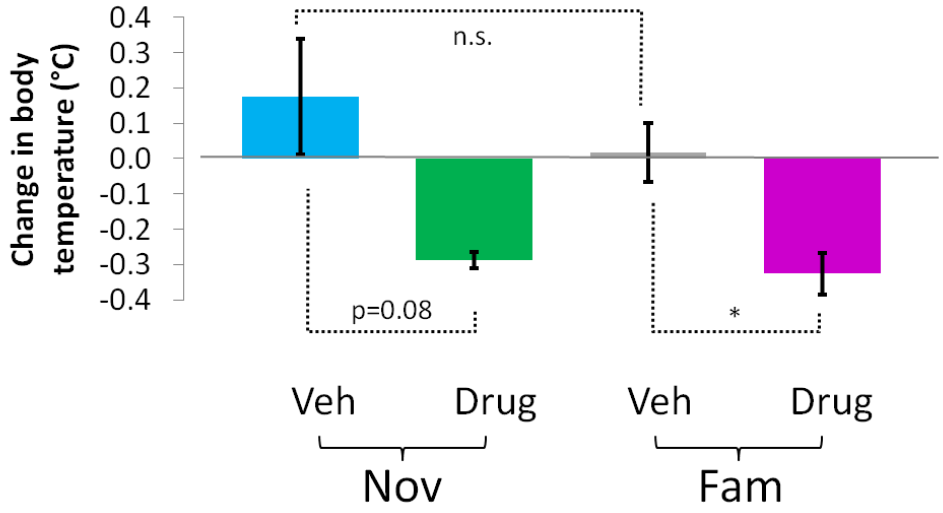

Figure 7.6. Changes in body temperature from the baseline to probe trial in each of the four conditions. There was no change in the Veh × Fam condition and a small but non-significant increase in the Veh × Nov condition. Drug injection was associated with a decreased body temperature in both Fam and Nov environments, although the effect only reached the level of significance in the Fam environment.

Correlations of intercept and slope with temperature

Since the Drug reduces both body temperature and intercept, a direct regression analysis of the change from baseline and probe trials (as Figure 7.5) could not be used. Instead, I used data from all pre-injection baseline trials on both experimental and familiarisation days to determine the effect of body temperature on the intercept (Figure 7.7; n=105; 12 trials excluded due to poor LFP data; 3 trials excluded due to missing temperature data). I found no significant correlation between temperature and intercept on baseline trials in any rat (n=105, range: Pearson's r=-0.16 to +0.36, p=0.054 to 0.47), suggesting a lack of a relationship between intercept and temperature. In order to verify that the accuracy of the body temperature readings was not influencing the results, I additionally correlated body temperature against slope (Figure 7.8). In contrast to the intercept, there was a significant positive correlation of temperature and slope from baseline trials in 3 out of 4 rats (Figure 7.8; n=105, range: Pearson's r=+0.23 to +0.50, p = 0.005 to 0.28). This indicates that changes in body temperature are likely to primarily affect the slope of the theta frequency-speed relationship, rather than the intercept.

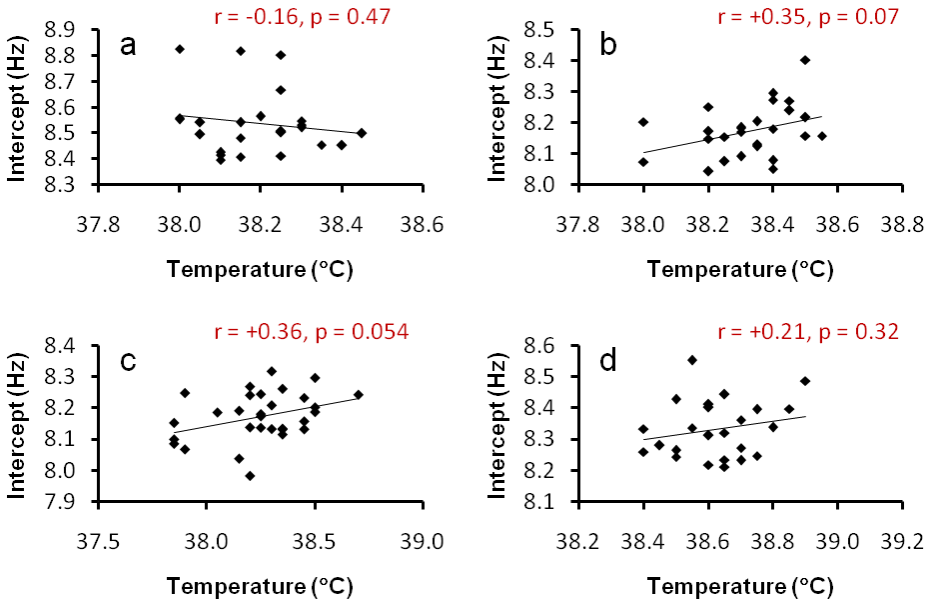

Figure 7.7. Intercept and body temperature were not significantly correlated in any of the four rats, but approached significance in 2 rats (Rats 3 and 5). Plots show (a) Rat 2, (b) Rat 3, (c) Rat 5 and (d) Rat 6.

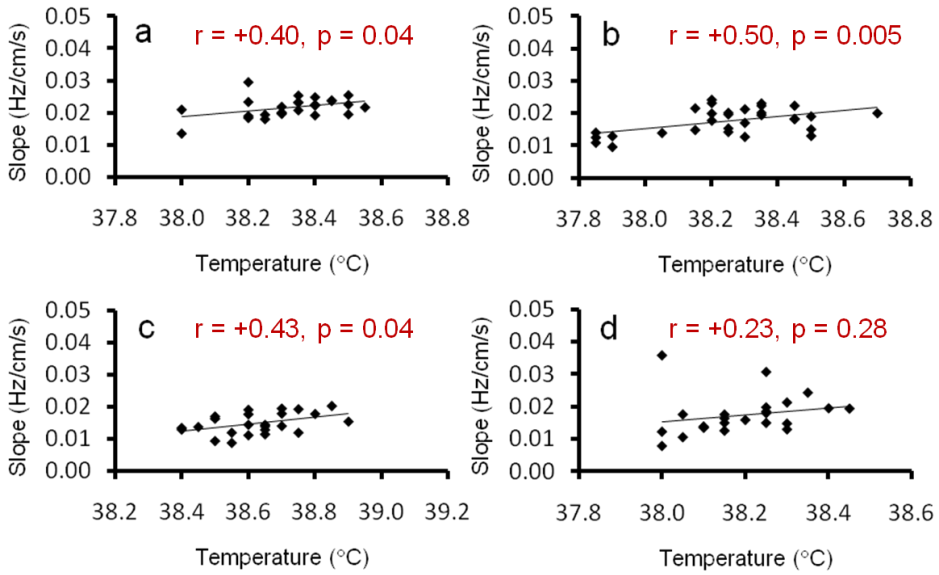

Figure 7.8. Slope and body temperature were positively correlated in baseline trials, with the correlation reaching the level of significance in 3 out of 4 rats. Plots show data for (a) Rat 3, (b) Rat 5, (c) Rat 6 and (d) Rat 2.

Temperature-correction of intercept reduction

Although none of the rats showed a significant correlation between intercept and body temperature, two were close to significance ($p < 0.08$). I therefore further investigated the contribution of body temperature to intercept by partialling out its effects (n=4 rats). After such "temperature-correction", the reduction of intercept by Drug remained significant in the Fam condition (paired $t_3=2.4$, $p=0.048$, one-tailed; 0.16 Hz mean reduction), but this was no longer the case in the Nov condition (paired $t_3=0.9$, $p=0.21$, one-tailed; 0.12 Hz mean reduction).

However, a comparison of the mean intercept reduction across the Veh and Nov conditions before (n=6 rats) and after (n=4 rats) temperature-correction indicated that body temperature accounted for only 24.1% of the intercept reduction (Figure 7.9). Furthermore, the magnitude of the Drug effect on intercept remained similar before and after temperature-correction (Figure 7.9; Drug: mean intercept reduction of 0.17 Hz and 0.16 Hz, before and after correction, respectively; Veh: 0.01 Hz increase and 0.02 Hz decrease), suggesting that the lack of statistical significance arose from a reduced number of samples in the latter case (n=6 rats and n=4 rats before and after temperature-correction, respectively).

To test if this was the case, I "temperature-corrected" the intercept data from the 2 rats without temperature readings using the mean temperature-intercept relationships from the 4 temperature-measured rats in each of the four conditions. When these data were combined (n=6 rats), the predicted reduction of intercept by cannabinoid was significant (two-way repeated measures ANOVA; $F_{1,5}$=9.13, p=0.043), whereas there was no effect of novelty or any interaction effects (Novelty: $F_{1,5}$=0.3, p=0.63; Drug × Novelty: $F_{1,5}$=0.1, p=0.76). These results therefore indicate that the influence of body temperature on intercept was minor and is unlikely to account for the intercept reduction observed.

Temperature-correction of slope reduction

Finally, in order to confirm that changes in temperature did not account for the slope reduction, I performed an identical "temperature-correction" on these data. I found no evidence of an effect of temperature on the magnitude or significance of the novelty-induced slope reduction in either the Veh or Drug conditions (Veh × Nov: paired t_3=8.2, p=0.002, one-tailed, 1.2 Hz/m/s mean reduction; Drug × Nov: paired t_3=5.8, p=0.005, one-tailed, 1.2 Hz/m/s mean reduction). Therefore, the slope change was likewise not accounted for by changes in body temperature.

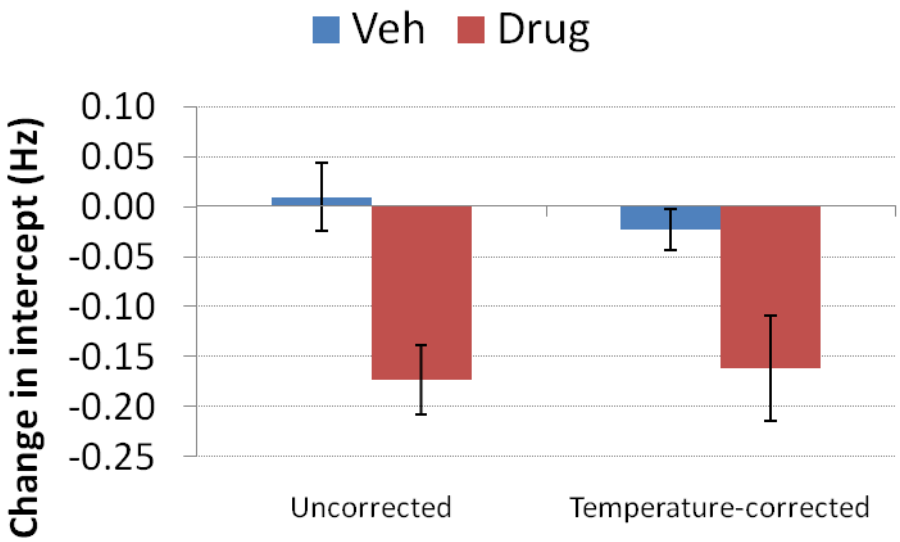

Figure 7.9. Effect of partialling out the influence of temperature on the intercept reduction elicited by Drug. The magnitude of the reduction is similar when original data from six rats (uncorrected, left) is compared to the "temperature-corrected" data from the four rats with temperature readings. Note that the magnitude of the effect does not change greatly (24.1% decrease) but the SEM increases due to the smaller sample size.

7.4 Summary

In line with the predictions the model, I found that the intercept of the theta frequency-speed relationship is selectively reduced by cannabinoid injection, whilst the slope is selectively reduced by environmental novelty. In combination the two effects are additive, providing evidence that two dissociable components contribute to the theta frequency-speed relationship (Burgess, 2008). By demonstrating a link between novelty and slope, these results also provide indirect evidence that grid cell expansion in novelty (Fyhn et al., 2007; Barry et al., 2009, SFN Abstract 101.24) is associated with a reduction in slope. They also show that the reduction of the intercept or the slope cannot be accounted for by changes in locomotor activity or body temperature. Further experimental studies will be required to determine whether the two components dissociated in this experiment, namely the intercept and slope, can be identified with the "immobility-related" a-theta and "movement-related" t-theta, respectively.

8 Effects of cannabinoids and novelty on hippocampal place cell and interneuron activity

8.1 Introduction

In addition to recording the LFP data presented in the previous chapter, single unit data were concurrently recorded from all six rats. In this chapter, I describe the independent and combined effects of intraperitoneal O-2545 injection (Drug) and environmental novelty (Nov) relative to their controls (Veh: saline, and Fam: environmental familiarity, respectively) on the activity of hippocampal place cells and interneurons. As with the LFP data, all single unit analyses have been performed by comparing data from the trials immediately before and after injection of Veh or Drug (termed the "baseline" and "probe" trials, respectively).

8.2 Single unit classification

Spike data were first assigned to single units using conventional cluster cutting techniques on the basis of their spike amplitude, waveform and the presence of a clear refractory period on the autocorrelogram. I then sought to classify each single unit as a place cell or interneuron, or otherwise to exclude cells that did not fall into either of these classes (Figure 8.1). Previous studies have used parameters such as the mean firing rate, spike width and peak-to-trough time to classify cells in the HF (Csicsvari et al., 1999b; Cacucci et al., 2004; Le Van Quyen et al., 2008; Czurkó et al., 2011). Plotting the peak-to-trough time against the mean firing rate of the cells (Figure 8.1, left) revealed that many cells with a peak-to-trough time less than 0.25ms had much higher mean firing rates, in line with the expected waveform and firing characteristics of fast-spiking interneurons. Although it is common to only include interneurons with a mean firing rate above a certain threshold, for example 5 Hz (Czurkó et al., 2011), cannabinoid-expressing interneurons are regular-spiking *in vitro* (Kawaguchi et al., 1987; Pawelzik et al., 2002) and so may display low firing rates *in vivo*. Therefore, I chose not to exclude any cells on the basis of mean firing rate and instead looked for an alternative separation criterion.

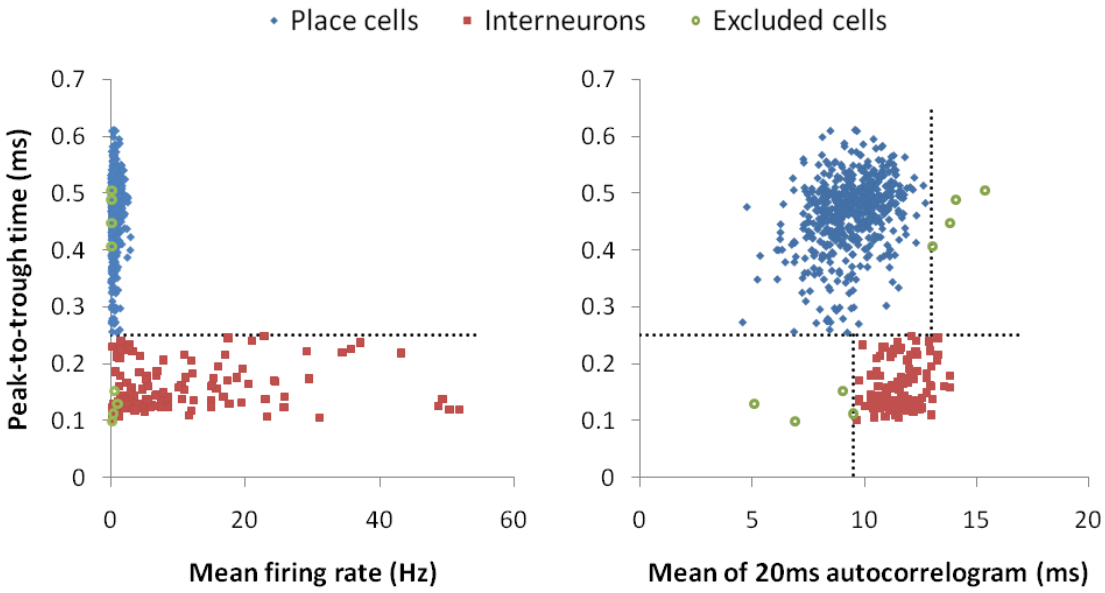

Figure 8.1. Classification of single units into place cells and interneurons was accomplished by plotting the peak-to-trough time against the mean firing rate (left) and the mean of the 20ms autocorrelogram (right). The latter plot (right) shows a clear separation between place cells (blue diamonds) and interneurons (red squares). A small number of outliers was removed from each group (green circles, n=4 per group) on the basis of the autocorrelogram mean.

Another parameter which has been used successfully to separate pyramidal cells and interneurons is the first moment (mean) of the autocorrelogram (Csicsvari et al., 1999b; Le Van Quyen et al., 2008). The autocorrelogram mean is expected to be lower for place cells as they exhibit complex-spiking activity in which they fire brief trains of action potentials separated by up to 6ms each and then quickly fall silent (Ranck, 1973; Harris et al., 2001). In contrast, interneurons typically fire with a less stereotyped but more sustained spiking activity, leading to a higher autocorrelogram mean. I found a clear separation of the cells when their peak-to-trough times were plotted against the means of their 20ms autocorrelograms (Figure 8.1, right). Therefore, the cells were divided into place cells and interneurons according to the 0.25ms peak-to-trough time criterion established previously and an equal number of outliers was removed from each group on the basis of the 20ms autocorrelogram mean (n=4 per group, cells excluded with mean

< 9.5ms for interneurons, > 13ms for place cells). All subsequent analyses were performed separately on the identified place cell and interneuron populations.

8.3 Place cell ratemaps

Spatial firing maps (ratemaps) were generated for all the place cells recorded to allow quantification of peak firing rates and place field properties (see Methods chapter for details and an explanation of ratemaps). The following pages show representative place cell ratemaps recorded before and after injection of vehicle (Veh) or cannabinoid (Drug). The pre-injection baseline trial is always recorded in Fam, whilst the post-injection probe trial is in either the familiar environment (Fam), the novel walled circle (NovA) or the novel unenclosed square (NovB).

8.3.1 Familiar environment (Fam)

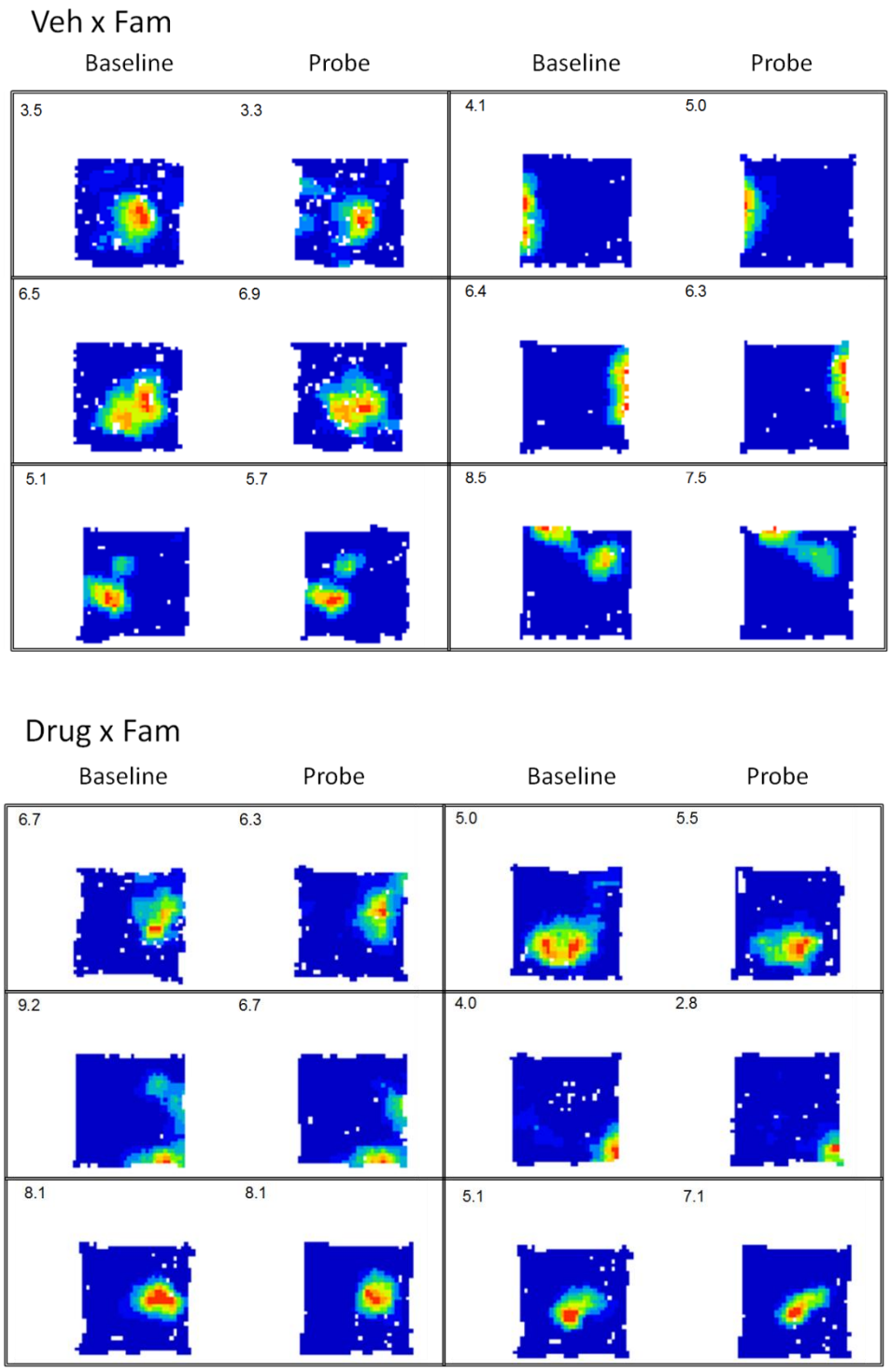

Figure 8.2. Spatial firing activity of six example place cells recorded in the familiar environment before and after vehicle (Veh × Fam) or cannabinoid injection (Drug × Fam). The cannabinoid had little effect on the spatial firing of place cells in the Fam environment. Each box of the figure shows the ratemap of a single place cell recorded in the pre-injection baseline trial (left) and the subsequent post-injection probe trial (right). The number to the top left of each ratemap indicates the peak firing rate of the cell during the 10 min trial in Hz.

8.3.2 Novel walled circle (NovA)

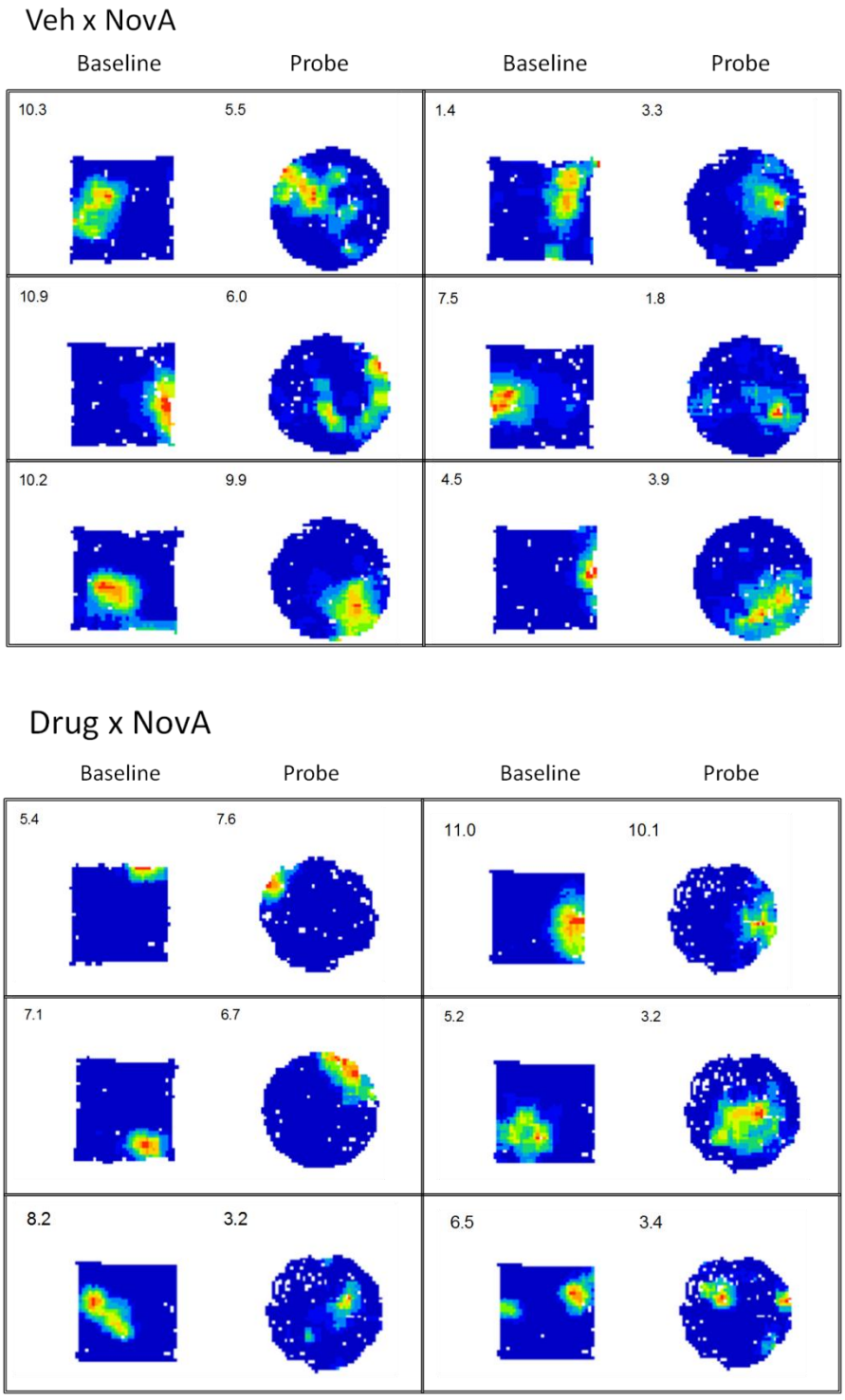

Figure 8.3. Ratemaps of six example place cells recorded first in the familiar environment (baseline trial, left ratemap in each box) and then in the novel walled circle (NovA probe trial, right in box) after vehicle (Veh × NovA) or cannabinoid injection (Drug × NovA). Peak firing rates tended to decrease in the novel probe trial relative to baseline. Peak firing rate (Hz) is shown to the top left of each ratemap. Note, only "active" cells firing at least 120 spikes with a peak rate above 1 Hz in both trials are shown.

8.3.3 Novel unenclosed square (NovB)

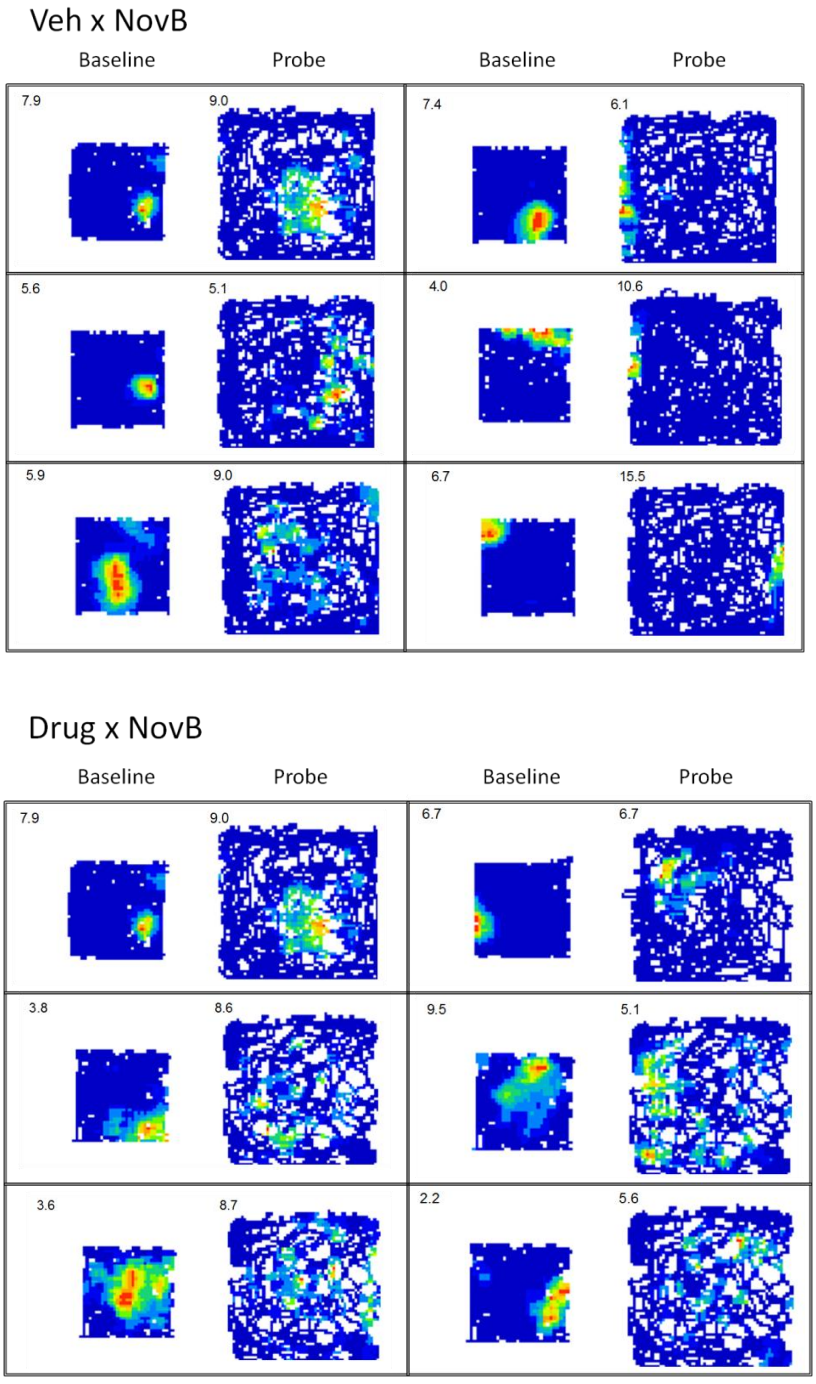

Figure 8.4. Spatial firing activity of six example place cells recorded in the familiar environment before injection (baseline trial, left ratemap in each box) and novel unenclosed square (NovB probe trial, right in box) after vehicle (Veh × NovB) or cannabinoid injection (Drug × NovB). Peak firing rates tended to increase in the novel probe trial relative to baseline. Due to the larger size of NovB, the overall coverage was lower in some cases, especially after cannabinoid injection. Peak firing rate (Hz) is shown to the top left of each ratemap. Note, only "active" cells firing at least 120 spikes with a peak rate above 1 Hz in both trials are shown.

8.4 Firing rate of single units

8.4.1 Place cells

8.4.1.1 Mean rate

First, I assessed the effects of Veh or Drug injection on the mean firing rates of the place cells (n=556), including cells that were silent in either the baseline or probe trials (Figure 8.5). In the Fam environment, there was no change in mean rate after either Veh or Drug injection (Veh: paired t_{169}=0.8, p=0.43, mean rate 0.63 Hz vs. 0.61 Hz in baseline vs. probe respectively; Drug: paired t_{162}=0.3, p=0.97, mean rate 0.67 Hz vs. 0.67 Hz in baseline vs. probe respectively), suggesting that Drug alone does not alter the overall firing rate of the place cells under familiar conditions. In contrast, there was a significant reduction in mean firing rate of the place cells in the Nov environment after either injection (Veh: paired t_{119}=2.0, p=0.04, mean rate 0.51 Hz vs. 0.40 Hz in baseline vs. probe respectively; Drug: paired t_{103}=3.2, p=0.002, mean rate 0.62 Hz vs. 0.40 Hz in baseline vs. probe respectively). A repeated measures ANOVA confirmed that the mean rate reduction by novelty was a consistent effect across rats ($F_{1,4}$=16.3, p=0.02), whilst there was no effect of the cannabinoid or any interaction between the two (Drug: $F_{1,4}$=2.9, p=0.17; Drug × Novelty: $F_{1,4}$=3.0, p=0.16). The reduction after Drug in Nov was approximately twice that after Veh (0.22 Hz vs. 0.11 Hz), but this appeared to be due to a difference in baseline values as the mean firing rates in the probe trial were identical (0.40 Hz in both cases).

Next I asked if the specific reduction of mean rate in the Nov environments was a result of place cells silencing their activity in the Nov probe trial (Figure 8.6). I therefore included only "active" place cells that fired with a mean rate of at least 0.2 Hz and a peak rate of at least 1.0 Hz during both baseline and probe trials (49 of 120 cells included from Veh × Nov, 45 of 104 from Drug × Nov). The magnitude of the change in mean rate was similar for both Veh and Drug conditions when compared with the results from the whole place cell population (compare Figure 8.5 and Figure 8.6; Veh: mean rate reduction of 0.11 Hz in both cases; Drug: mean rate reduction 0.22 Hz vs. 0.28 Hz in the whole population vs. active cells, respectively). However, a repeated measures ANOVA showed that the main effects of cannabinoid or novelty, and their interaction were outside the range of significance (Drug: $F_{1,4}$=3.3, p=0.15; Novelty: $F_{1,4}$=1.8, p=0.25; Drug × Novelty: $F_{1,4}$=3.6, p=0.13).

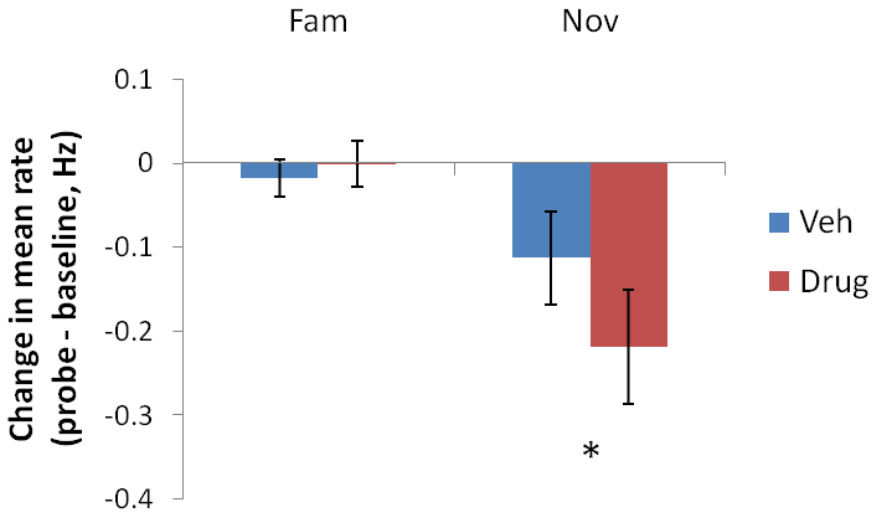

Figure 8.5. Mean rates of the entire place cell population (including cells that are silent in either baseline or probe trials) are stable in the Fam environment (left) after either Veh or Drug, but reduce in the Nov environments (right). The magnitude of the reduction in Nov is approximately twice as large with the Drug compared to Veh, but this reflects differences in the baseline trial rates, rather than probe trial rates.

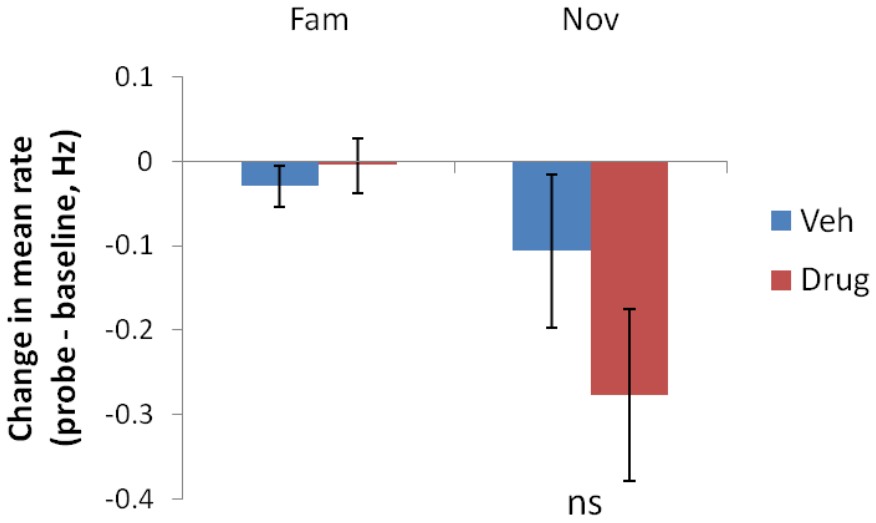

Figure 8.6. The magnitude and direction of changes of active place cells (peak rate at least 1.0 Hz, mean rate at least 0.2 Hz during both trials) is similar to that of the entire place cell population. This suggests that the mean rate reduction in novelty is not due to cells completely silencing their activity in the probe trial. However, these results were not significant.

Although the possibility that the mean rate reduction arose from the silencing of cells cannot be excluded, the similarity of the mean rate changes in the smaller subset of active cells and the whole population suggests that there were not major differences in their physiological responses to novelty. Overall these results are consistent with a tendency towards reduced rates in the active place cells that mirrors the novelty-induced reduction in mean rate seen in the whole place cell population. Furthermore, in both cases novelty was associated with a larger mean rate reduction after Drug injection than Veh injection.

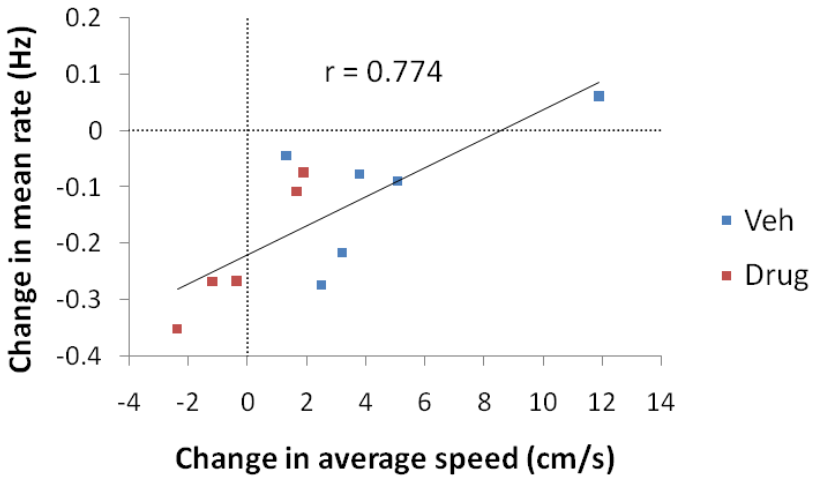

Figure 8.7. The difference in magnitude of place cell mean rate reductions after Veh (blue) and Drug (red) injection is accounted for by changes in average running speed. The correlation indicates that environmental novelty is associated with a 0.22 Hz reduction in mean rate if average speed is unchanged (y-axis intercept of regression line).

As described in the previous chapter, Drug injection was associated with lower average running speeds in the Nov environments than Veh injection (Figure 4 in the previous chapter). Previous studies indicate that speed is correlated with the mean firing rate of place cells (Huxter et al., 2003; Geisler et al., 2007), so this might account for the difference in magnitude of mean rate reductions in Nov by Veh and Drug. In agreement with this, I found a significant positive correlation when the change in average speed from the Fam baseline to Nov probe trial after either Veh or Drug injection was regressed against the overall change in mean rate for each of the six rats (Figure 8.7; Pearson's r=+0.774, p=0.005; note that n=6 for Veh × Nov and n=5 for Drug × Nov, because one rat had no cells on a Drug × Nov

day). The linear regression of these data suggests that in the absence of any change in average speed, Nov is associated with a 0.22 Hz reduction in the mean rate of place cells (y-intercept of regression line in Figure 8.7). Therefore, environmental novelty is associated with a reduction in place cell firing rates, even if only place cells that maintain their activity in both trials are considered.

8.4.1.2 Peak rate

Peak firing rates were compared across the four conditions using only the subset of active place cells (firing with at least a 0.2 Hz mean rate and 1.0 Hz peak rate) to ensure there were adequate data in each case for a good peak rate estimate. Peak firing rates were similar in the Fam environment after either Veh or Drug injection, with a small reduction in both cases (Figure 8.8; Veh: peak rate 7.2 Hz vs. 6.9 Hz in baseline vs. probe respectively; Drug: peak rate 7.4 Hz vs. 7.2 Hz in baseline vs. probe respectively). The reductions in peak rate observed in the Nov environments were comparatively larger than in Fam, particularly after the Drug (Figure 8.8; Veh: peak rate 6.6 Hz vs. 6.2 Hz in baseline vs. probe respectively; Drug: peak rate 7.5 Hz vs. 6.5 Hz in baseline vs. probe respectively). However, none of these effects reached a level of statistical significance, and nor did their interaction (Drug: $F_{1,4}$=0.2, p=0.71; Novelty: $F_{1,4}$=0.004, p=0.95; Drug × Novelty: $F_{1,4}$=0.2, p=0.67).

However, when the data were examined by separating out trials in each of the Nov environments, it was clear that peak rates decreased in NovA but increased in NovB (Figure 8.9). Furthermore, the changes were of comparable magnitude after either Veh or Drug injection (NovA: peak rate reductions of 2.6 Hz and 2.9 Hz after Veh and Drug, respectively; NovB: peak rate increases of 1.6 Hz and 2.3 Hz after Veh and Drug, respectively). Therefore, data were pooled within each novel environment across Veh and Drug conditions. Paired t-tests on these data confirmed that peak rates decreased in NovA, but increased in NovB (NovA: paired t_{51}=3.8, p=0.0003, peak rate 8.2 Hz vs. 5.4 Hz in baseline vs. probe, respectively; NovB: paired t_{42}=2.4, p=0.02, peak rate 5.7 Hz vs. 7.6 Hz in baseline vs. probe, respectively).

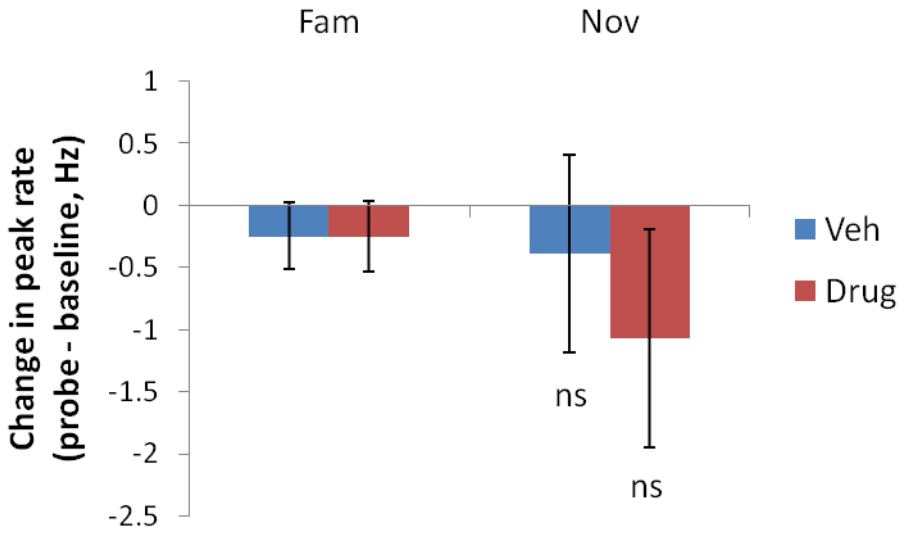

Figure 8.8. The peak rate of place cells remained stable in the Fam environment after either Veh or Drug injection (left), but there was a trend towards a reduction in Nov with the Drug (right).

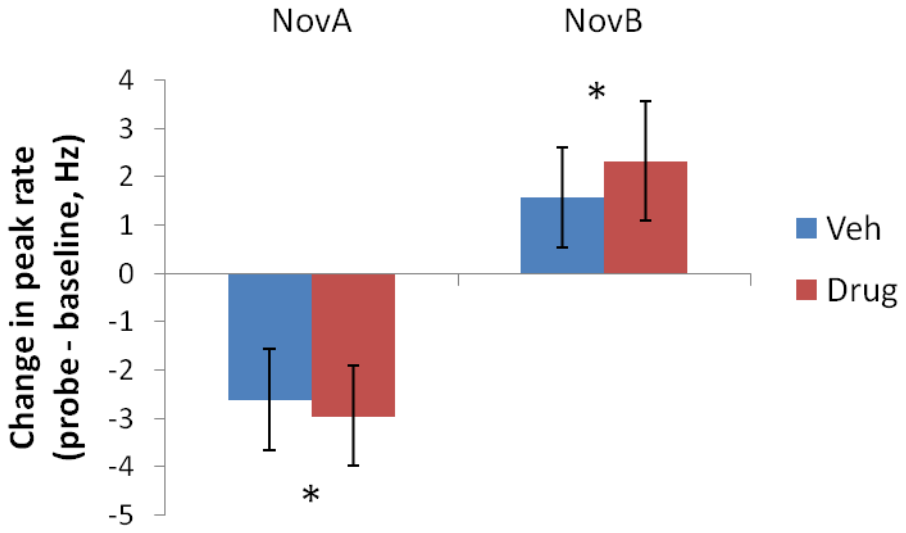

Figure 8.9. Dividing the Nov data recorded in the two novel environments (NovA and NovB) revealed that NovA was associated with a decrease in peak rates (left), whereas NovB was associated with an increase. The magnitude of peak rate changes was comparable for both Veh and Drug in both novel environments.

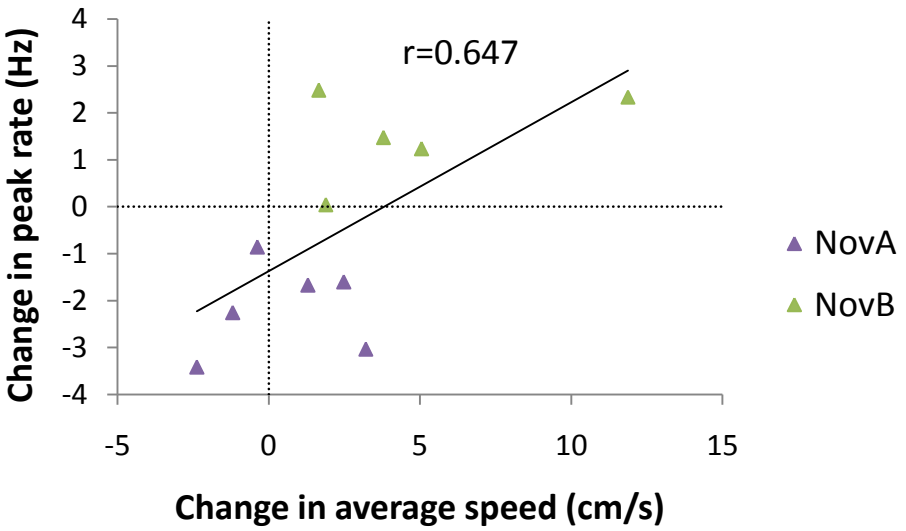

Figure 8.10. The difference of peak rate changes in NovA and NovB results from a change in average speed, in line with the relationship observed between mean rate and average speed. The linear regression suggests that novelty induces a 1.4 Hz reduction in peak rate on average (y-axis intercept of regression line), if average speed is constant across the baseline and probe trials. Thus, both mean and peak rate analyses suggest that place cell firing is reduced by environmental novelty.

In agreement with the relationship observed between changes in mean rate and average speed in Nov (Figure 8.7), a regression of changes in place cell peak rates against running speed for the six rats also showed a significant positive correlation (Figure 8.10; Pearson's r=0.647, p=0.03). The regression suggests that on average, peak rates are reduced by 1.4 Hz in the novel environments if average running speed is unchanged (y-axis intercept of regression line on Figure 8.10). Therefore, the results of both the mean and peak rate data indicate that novelty reduces place cell firing rates. In contrast, Drug-related changes can be accounted for by differences in average speed, suggesting that the low dose of cannabinoid employed did not alter the mean or peak firing rate of place cells. These results are in agreement with a previous study that also found no influence of cannabinoids on place cell firing rates (Robbe and Buzsaki, 2009).

8.4.2 Interneurons

8.4.2.1 Mean rate

Next I analysed the mean firing rate of interneurons recorded across all rats and days (n=115). In agreement with the stable mean rates of place cells in Fam (Figure 8.5), the mean rate of interneurons in Fam was likewise unaltered after either Veh or Drug injection (Figure 8.11; Veh: mean rate 10.6 Hz vs. 10.5 Hz in baseline vs. probe, respectively; Drug: mean rate 10.9 Hz vs. 10.8 Hz in baseline vs. probe, respectively). In contrast, interneuron mean rates were increased in Nov after either Veh or Drug injection (Veh: mean rate 10.1 Hz vs. 12.1 Hz in baseline vs. probe, respectively; Drug: 11.7 Hz vs. 12.8 Hz in baseline vs. probe, respectively). However, the effects of novelty did not reach the level of significance (Novelty: $F_{1,4}=3.6$, $p=0.13$), and there was no effect of the cannabinoid or any interaction of the two factors (Drug: $F_{1,4}=0.2$, $p=0.67$; Drug × Novelty: $F_{1,4}=0.7$, $p=0.45$). The trend towards increased interneuron rates in novelty is congruent with the concurrent decrease in place cell rates observed (Figure 8.5).

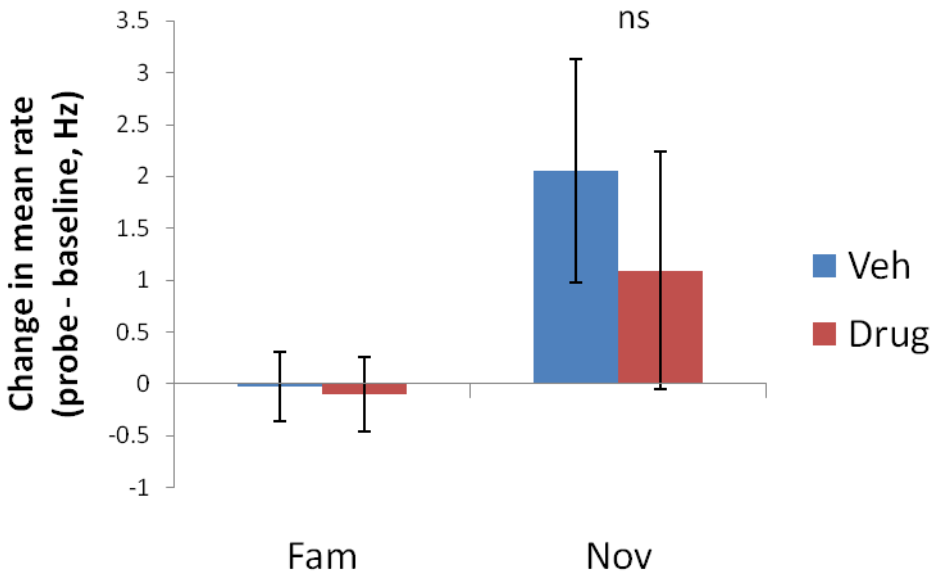

Figure 8.11. Mean rates of interneurons were not affected by Veh or Drug injection in Fam (left). There was a non-significant trend toward an increase in Nov (right, p=0.13), which is congruent with the simultaneous decrease in place cell mean firing rates.

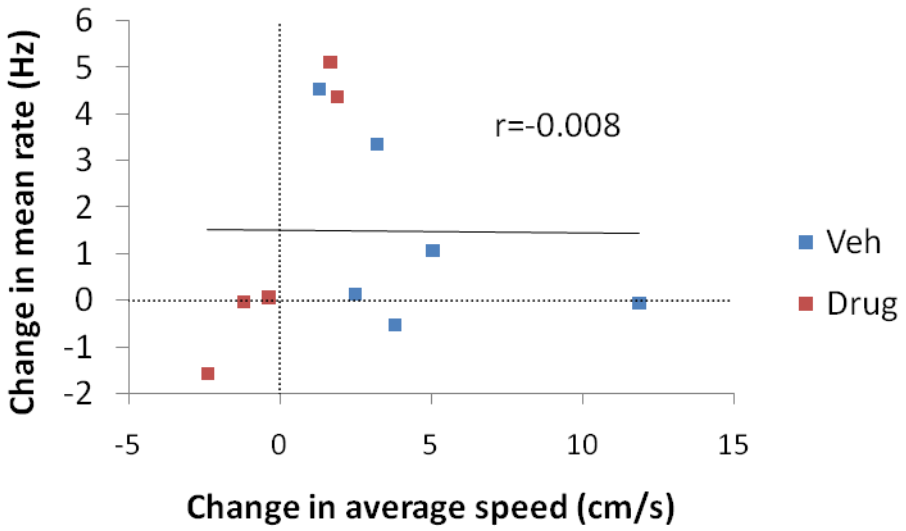

Figure 8.12. The change in mean rates of interneurons in Nov was not a result of changes in average speed, unlike the place cells. Therefore the trend towards an increased inhibitory drive in Nov is not induced by a greater degree of locomotor activity. The distribution of the data suggests that interneuron firing is up-regulated on some days (> 3.0 Hz increase). The cause is unknown, but it may reflect sampling of different interneuron classes (in different layers) across days.

This difference in magnitude could result from differences in average speed between baseline and probe trials in the Nov condition, as was observed with place cells. However, a linear regression of the change in interneuron mean rate against the change in average speed for the six rats showed that there was no correlation between these variables (Figure 8.12; Pearson's r=-0.008, p=0.98). Examining the data from individual days (Figure 8.12), it was clear there were four days on which the mean rate was greatly elevated (> 3.0 Hz increase) whilst the remaining days showed smaller changes (within ± 2.0 Hz). The reason for this variation is not known, but they may reflect the differential responses of distinct interneuron classes (perhaps from different layers). With further analysis, it may be possible to classify these interneurons on the basis of their firing characteristics or theta phase preferences (Klausberger et al., 2003, 2005; Czurkó et al., 2011).

8.5 Theta phase of spike ensembles

8.5.1 Place cells

The theta-band activity of every place cell recorded across all six rats (n=556) was first characterised by analysing the phase of each spike with reference to the concurrently recorded LFP theta oscillation. A previous study from our group indicates that environmental novelty induces a later phase of place cell ensemble spiking in CA1 relative to a familiar environment (Lever et al., 2010). Therefore in order to assess the relative change in phase, spike data were first pooled within the baseline and probe trials on each day for each rat. The mean phase of the spike ensemble on the baseline trial of each day was used as a reference for that day (phase 0°), against which all spikes in both trials were assigned phases. Data were then pooled across all rats and days for the baseline and probe trials in each of the four conditions to examine the effects of each manipulation on the phase of place cell firing (Figure 8.13 and Figure 8.14).

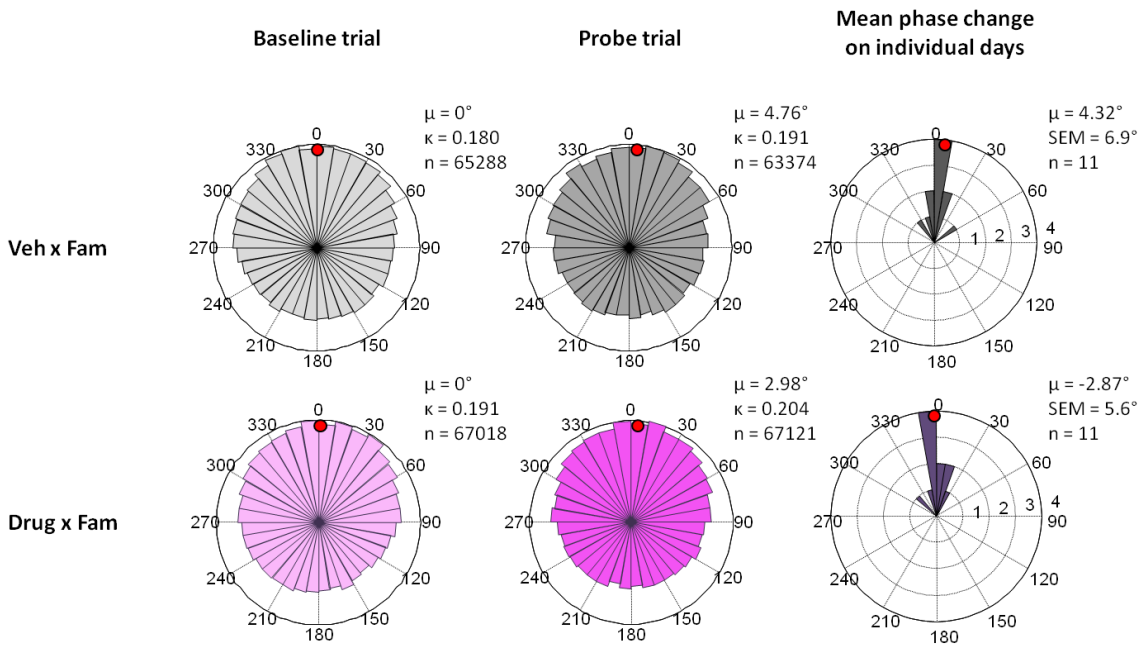

Figure 8.13. Overall mean place cell spike ensemble phases (μ) and the Von Mises' phase concentration (κ) were unchanged from the baseline (left column) to probe (middle column) trials in the Fam environment after Veh or Drug injection. Phase assignment is based on calculating the phase relative to the baseline trial, which is assigned a phase of 0°. Data from individual days (right) was in agreement with the spike ensemble phase data.

8.5.1.1 Mean phase of ensemble firing

I began by examining if there was any influence of the cannabinoid or environmental novelty on the mean theta phase of the spike ensembles across each of the four conditions. These analyses revealed that in Fam, the mean spike ensemble phases shifted by only a small amount after either Veh or Drug injection (Figure 8.13, left two columns; +4.8° and +3.0°, respectively). Analysing the distribution of mean ensemble spike phases from individual days yielded similar results (Figure 8.13, right column; Veh: +4.3 ± 6.9°; Drug: -2.9 ± 5.6°), suggesting that neither Veh nor Drug in the Fam environment affected the phase. In contrast, in the Nov environments there was a clear shift towards a later mean phase of place cell ensemble spiking after Veh injection (Figure 8.14, top row; +38.4° mean shift), but this shift was less pronounced after Drug injection (Figure 8.14, top row; +22.3°). The distribution of mean phases from individual days suggested that whilst Veh injection in novelty resulted in a consistent phase shift (Figure 8.14, top right; +36.9 ± 11.9°), those occurring after Drug injection were much more variable (Figure 8.14, top right; +42.1 ± 25.6°).

These data were analysed using a two-way repeated measures ANOVA to examine if cannabinoid or novelty reliably altered the phase across days. This revealed a marginally significant effect of novelty on theta firing phase ($F_{1,4}$=6.0, p=0.07), but no effect of the cannabinoid or any interaction of the two (Drug: $F_{1,4}$=0.2, p=0.67; Drug × Novelty: $F_{1,4}$=0.2, p=0.65). On the basis of the strong effect of novelty and prior work from our group showing a later phase of place cell firing in these conditions (Lever et al., 2010), I investigated the effects of Veh or Drug injection in the novel environments independently. Paired t-tests showed that whilst Veh injection lead to a consistently later phase in novelty (t_5=3.0, p=0.03), the greater variability after Drug injection disrupted this phase shift (t_4=1.7, p=0.17). This variability may arise from inter-subject differences in sensitivity to the Drug, as the rat with the largest phase increase also showed no Drug-mediated reduction in the intercept of the theta frequency-speed relationship (Figure 8.14, bottom right, blue arrow; phase increase of 138.8° accompanied by intercept change of 0.026 Hz). If this outlying data point is excluded, the increased phase accompanying Drug injection in Nov remains non-significant, although the magnitude of the shift is greatly reduced (paired t_3=1.7, p=0.18, mean shift +18.0 ± 10.4°).

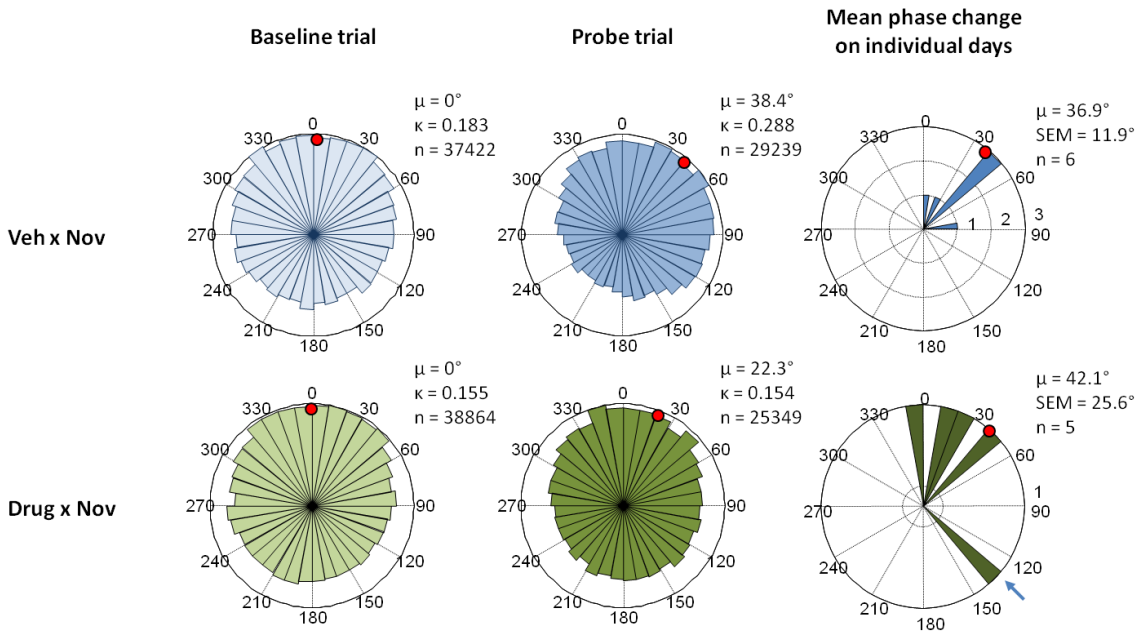

Figure 8.14. Environmental novelty elicited a later mean place cell spike ensemble phase (μ) in the probe trial (middle column) relative to baseline (left column) after Veh or Drug injection. The Veh injection was accompanied by an increase in the Von Mises' phase concentration (κ), where Drug injection was not. The mean phase shifts after Veh injection across individual days were consistent (top right), whereas those after Drug were much more variable (bottom right).

Thus, these findings suggest that Drug disrupts the coordinated phase shift of place cells in novelty, in agreement with previous reports of disrupted spike timing after cannabinoid administration (Hampson and Deadwyler, 2000; Robbe et al., 2006; Robbe and Buzsaki, 2009). In contrast, the consistently later phase of place cell firing observed after Veh injection in Nov replicates our previous findings of the effects of environmental novelty on the theta phase of CA1 ensembles (Lever et al., 2010). The disruption of this effect by cannabinoids suggests that the phase shift is a precisely coordinated event which involves, at least in part, a regulated contribution from the endogenous cannabinoid system.

8.5.1.2 Phase concentration

The influences of cannabinoid and novelty on the precision of ensemble spike timing were further investigated by calculating the Von Mises' phase concentration (κ) for pooled data in each of the four conditions. This is a measure of the phase

dispersion of the data that can be used to assess the depth of theta-modulation of cell firing (Cacucci et al., 2004). The phase concentration in Fam was similar in baseline and probe trials after either Veh or Drug injection (Figure 8.13, left two columns; Veh: κ=0.180 and 0.191 in baseline and probe trials respectively; Drug: κ=0.191 and 0.204), suggesting that neither affected the degree of theta-modulation of place cells. Likewise, the data from individual days showed no difference in phase concentration between the two trials, supporting this conclusion (Veh: mean κ=0.222 and 0.254 in baseline and probe trials, respectively; Drug: mean κ=0.217 and 0.226).

In contrast, there was a novelty-induced increase in the theta modulation of the place cell spike ensemble (Figure 8.14, top row, left two columns; Veh: κ=0.183 and 0.288 in baseline and probe trials, respectively) that was not observed after cannabinoid injection (Figure 8.14, bottom row, left two columns; Drug: κ=0.154 and 0.155, respectively). A two-way repeated measures ANOVA on data from individual days supported these findings, indicating that the cannabinoid alone did not affect the phase concentration ($F_{1,4}$=2.9, p=0.17); however, there was a significant effect of novelty and an interaction between the two factors (Novelty: $F_{1,4}$=24.5, p=0.008; Drug × Novelty: $F_{1,4}$=30.6, p=0.005). Paired t-tests on these data confirmed that the novelty-induced increase in phase concentration accompanying Veh injection was almost completely blocked by Drug injection (Veh: paired t_5=4.2, p=0.008, mean κ=0.223 and 0.373 in baseline and probe trials, respectively; Drug: paired t_4=0.8, p=0.49, mean κ=0.213 and 0.229, respectively).

8.5.1.3 Influence of running speed and firing rate on phase

This enhanced theta modulation during novelty may relate to the increase in average speed observed after vehicle, but not cannabinoid injection. This is because faster running speeds are associated with an increase in the number of spikes emitted by a place cell per theta cycle in its field (Geisler et al., 2007). In agreement with this, I found a significant positive correlation between the change in average speed and phase concentration from the baseline to probe trials (Figure 8.15, top panel; Pearson's r=0.868, p=0.0005). In contrast, there was no correlation between the change in speed and the extent of the novelty-induced phase shift (Figure 8.15, bottom panel; Pearson's r=0.021, p=0.95). This suggests that the more pronounced theta modulation observed in novelty is a result of higher running speeds, but that changes in speed do not account for the effects of novelty and cannabinoid on place cell theta phase tuning.

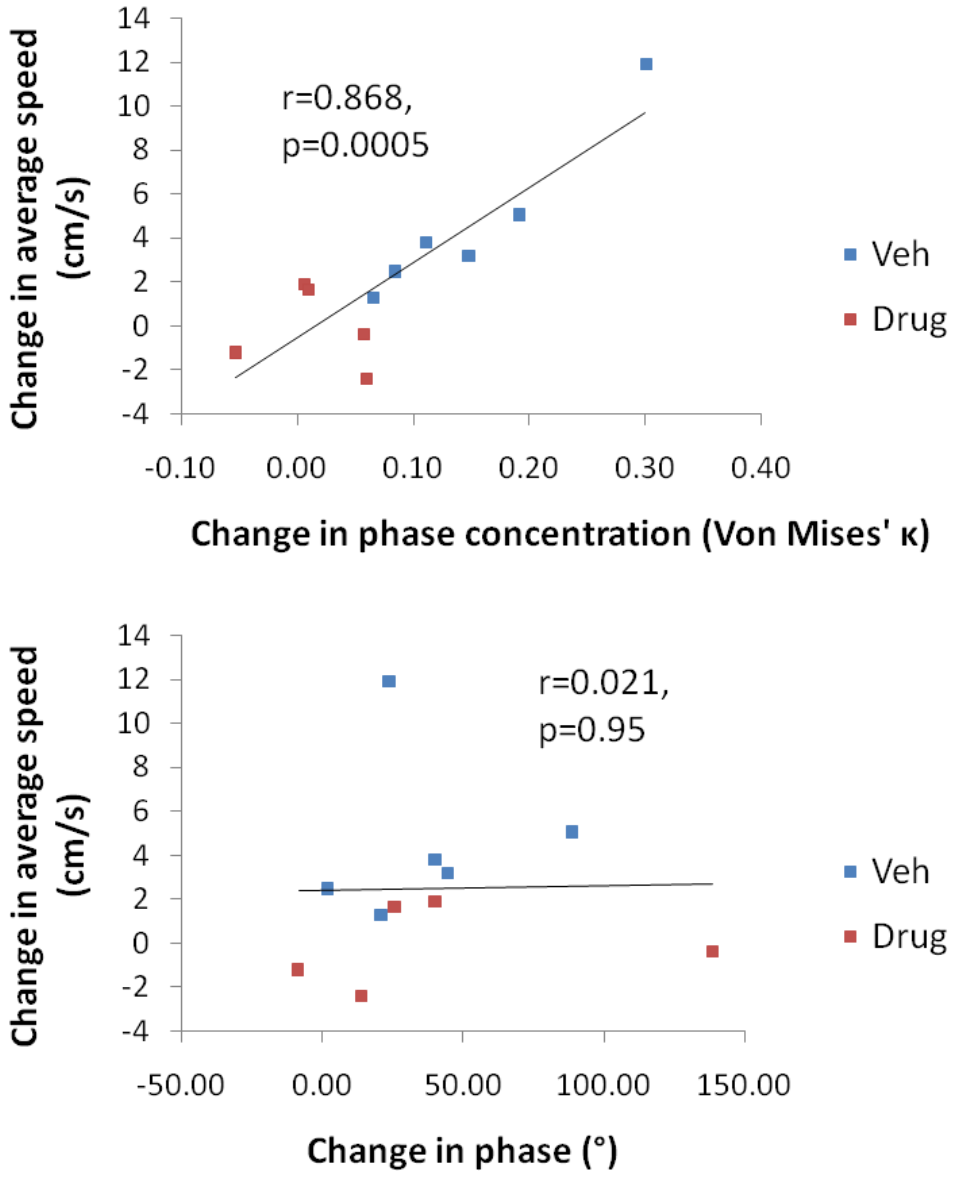

Figure 8.15. The change in average speed from the baseline to probe trial correlates positively with the change in phase concentration (top panel), but not with the change in mean place cell ensemble phase (bottom panel).

Next, I asked whether firing rate differences between the familiar and novel environments might account for the phase shift observed. It has been suggested that place cell phase precession is driven by an increase in the instantaneous firing rate of place cells, so that higher rates lead to an earlier phase of firing (Harris et al., 2002; Mizuseki et al., 2009). Conversely according to such a model, decreased firing rates are associated with a later phase of firing. In this study, there was a

(non-significant) trend towards lower peak firing rates in novelty (Figure 8.8), which may therefore explain the later phase in the novel environments (Figure 8.14). However, there was a clear difference in the peak rate change in the two novel environments, with peak rates decreasing in NovA but increasing in NovB (mean peak rate changes of -2.8 Hz and +1.9 Hz in NovA and NovB, respectively). Therefore, a firing rate-driven model of phase change would predict a later phase in NovA, but an earlier phase in NovB. In contrast, there was a consistently later phase observed with novelty in both of these environments (Figure 8.14, right; mean phase change on individual days is +35.5 ± 21.9° and +43.2 ± 12.1° in NovA and NovB, respectively). An unpaired t-test on data from individual days confirmed there was no difference in the mean phase change between the two environments (t_{10}=0.3, p=0.76). Therefore, this implies that the later phase observed in novelty cannot be accounted for by a change in firing rate.

8.5.1.4 Relationship of phase shift to slope reduction

Finally, I investigated whether the phase shift of place cell firing in novelty might share a common mechanism with the slope reduction concurrently observed. Contrary to this suggestion, I found that there was no correlation between the slope reduction and phase shift in Nov after Veh injection (Figure 8.16; Pearson's r=0.300, p=0.56) and likewise, no such effect after Drug injection (Pearson's r=-0.532, p=0.36). Combining all data following either injection also yielded a similar result (Pearson's r=-0.133, p=0.70). Therefore, the lack of a correlation between the slope reduction and phase shift indicates that these phenomena are likely mediated via distinct neural mechanisms.

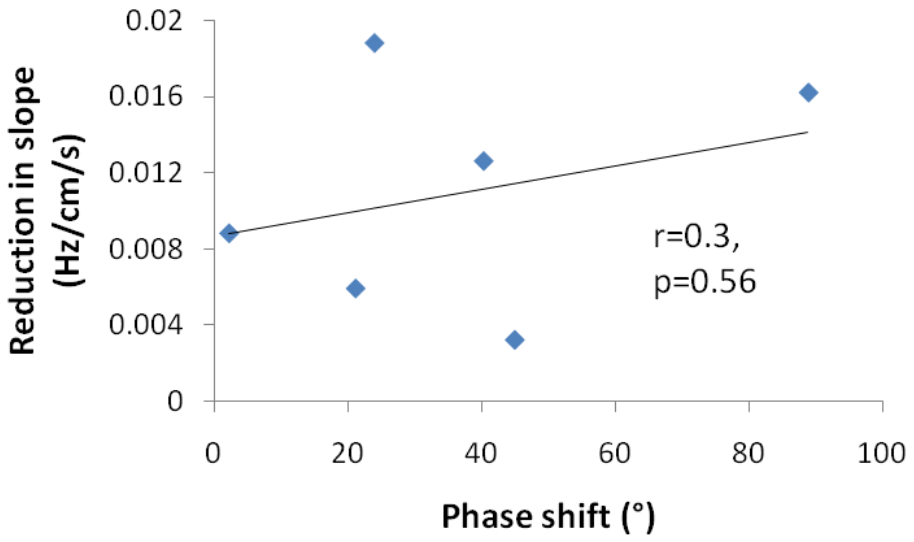

Figure 8.16. There is no correlation between the later phase of place cell firing in novelty after vehicle injection and the concurrent reduction in slope. This is also true following cannabinoid injection in novelty (r=-0.532, p=0.36) or if all novel data are correlated together (r=-0.133, p=0.70). This suggests that these two novelty-induced effects are mediated by distinct mechanisms.

8.5.2 Interneurons

8.5.2.1 Mean phase of ensemble firing

Interneuron spike ensemble phases were analysed in an identical fashion to the place cells by pooling data within the baseline and probe trials across all rats and days, assigning a phase of 0° to the baseline trial on each day.

First, phase changes in the Fam environment after either Veh or Drug injection were compared (Figure 8.17). The phase of interneuron firing was unaffected in either of these conditions, showing only a minor decrease in both cases (Figure 8.17; mean phase shifts of -1.8° and -4.8° in Veh and Drug, respectively). Data from individual days supported these data, showing no differences after either Veh or Drug injection in the mean phase (Veh: mean phase shift -4.7 ± 5.2°; Drug: mean phase shift +2.6 ± 5.9°). Therefore, the unaltered theta phase tuning of interneurons in the Fam environment was in line with the lack of phase shift observed in the place cell population under these conditions.

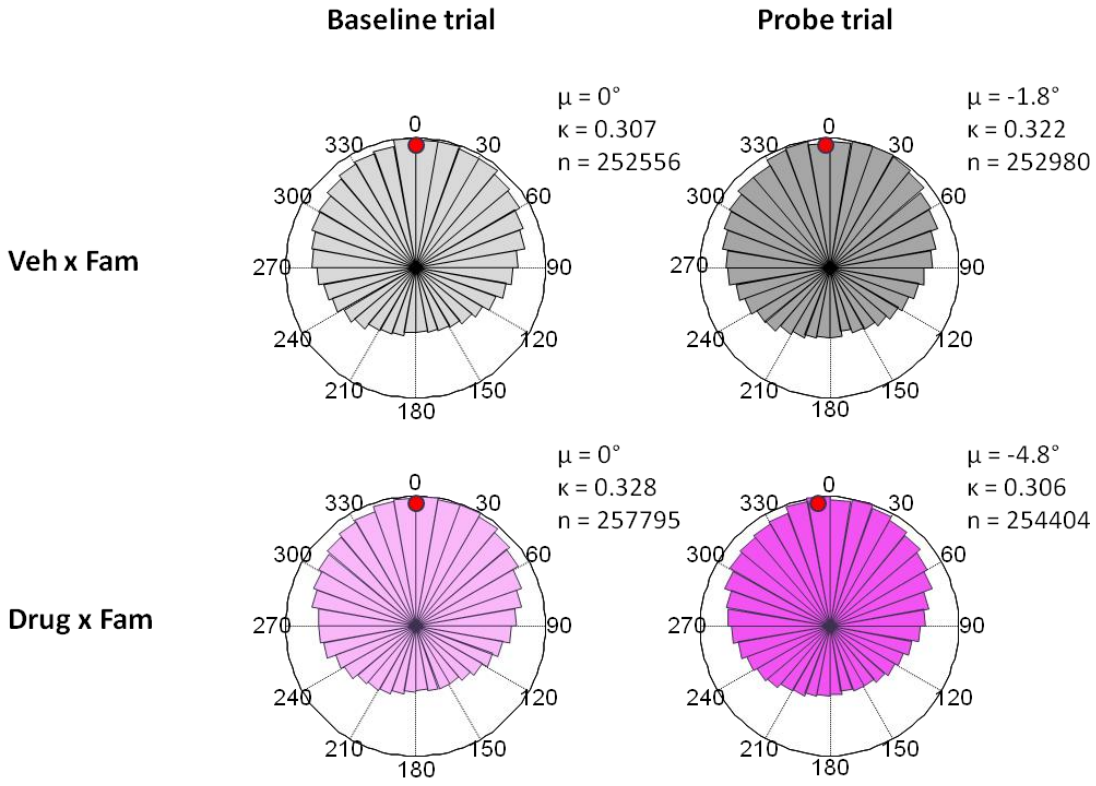

Figure 8.17. Interneuron mean spike ensemble phase was unaltered from the baseline (left column) to probe (right column) trials in the Fam environment after Veh or Drug injection. The phase concentration (κ) was also unaffected in both cases.

Next, I investigated whether the later theta phase of place cell firing in Nov was accompanied by an altered phase of interneuron firing. Surprisingly, there was no change in mean phase after either Veh or Drug injection (Figure 8.18; mean phase shifts of -5.8° and -0.9° in Veh and Drug, respectively), a result that was supported by the distribution of the data from individual days (Veh: mean phase shift +0.03 ± 13.8°; Drug: mean phase shift +4.2 ± 7.1°). A two-way repeated measures ANOVA confirmed that there were no effects of novelty or cannabinoid on the theta phase of interneuron firing, and no interaction between them (Novelty: $F_{1,4}$=0.5, p=0.53; Drug: $F_{1,4}$=0.2, p=0.69; Drug × Novelty: $F_{1,4}$=0.1, p=0.75). Therefore, these results show that the mean phase of firing of the interneuron population was stable across all four conditions

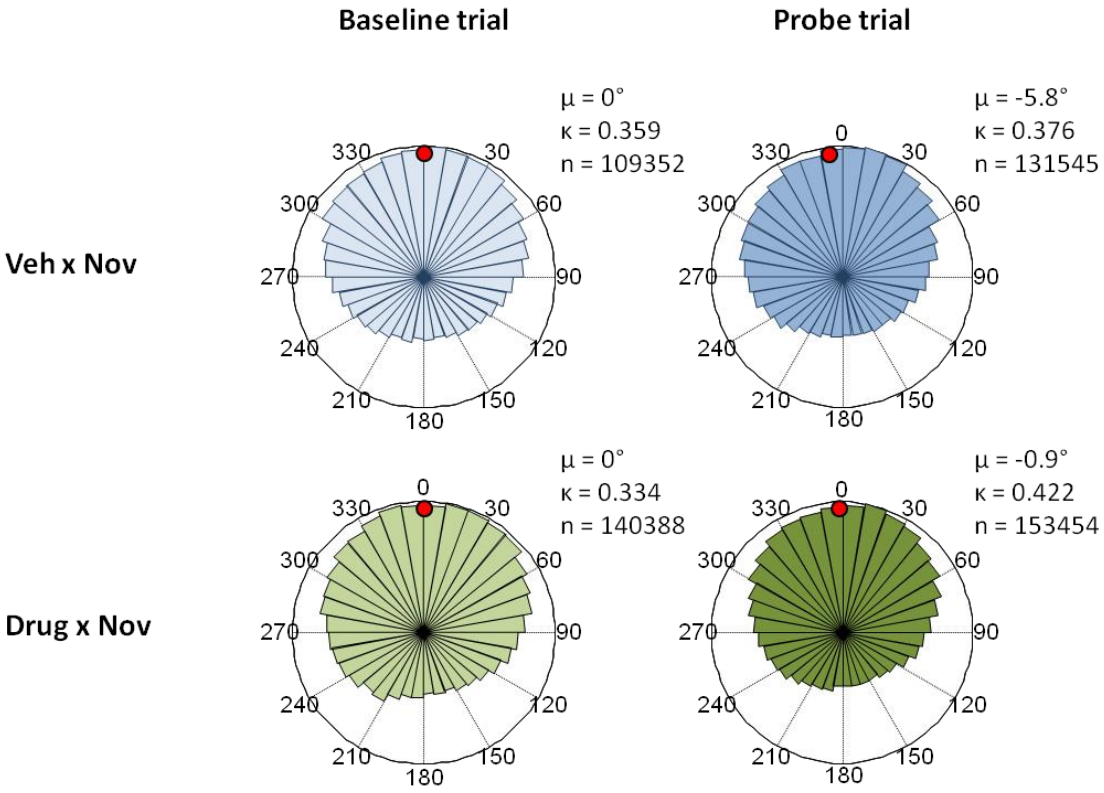

Figure 8.18. Interneuron mean spike ensemble phase did not change from the baseline (left column) to probe (right column) trials in the Nov environments after Veh or Drug injection. Although the overall ensembles above both show a phase concentration increase in the probe trial, a significant effect was not found across individual days. These data suggest that the later phase of place cell firing in novelty does not depend on a gross change in the firing phase of the interneuron population as a whole.

8.5.2.2 Phase concentration

Likewise, there was little change in the phase concentration of the pooled spike ensembles after either injection in the Fam environment (Figure 8.17; Veh: κ=0.307 and 0.322 in baseline and probe trials, respectively; Drug: κ=0.328 and 0.306), a finding that was supported by data from individual days (Veh: mean κ=0.331 and 0.314 in baseline and probe trials, respectively; Drug mean κ=0.309 and 0.314). Therefore, there was no sign of any Drug-mediated effect on the degree of theta-modulation of interneuron firing in the Fam environment.

In the Nov environments, the pooled spike ensembles showed some evidence of an increase in phase concentration during the probe trial (Figure 8.18; Veh: κ=0.359 and 0.376 in baseline and probe trials, respectively; Drug: κ=0.334 and 0.422), although these effects were not as pronounced in the mean data from individual days (Veh: κ=0.361 and 0.355 in baseline and probe trials, respectively; Drug: κ=0.367 and 0.415). Indeed, these data indicated that there were no effects of novelty or cannabinoid on the degree of interneuron theta-modulation, and no interaction between these factors (two-way repeated measures ANOVA; Novelty: F1,4=0.1, p=0.78; Drug: F1,4=1.1, p=0.35; Drug × Novelty: F1,4=0.02, p=0.91). Therefore, this shows that both the mean phase of firing and the phase concentration of the interneuron population were largely unaffected by either cannabinoid or novelty.

8.5.2.3 Mean phase of individual interneurons

The mean phase changes of individual theta-modulated interneurons (mean rate of at least 0.2 Hz, Rayleigh test on theta phase of cell spikes, $p < 0.05$) from the baseline to probe trial were examined to see if there were any differences in the phase tuning of individual cells that were not detected in the spike ensemble analyses (Figure 8.19). In agreement with the spike ensemble phase data, there was no effect of novelty on the mean theta phases of individual cells after either Veh or Drug injection (Figure 8.19, comparing left and right columns; Fam: mean phase shifts of -3.2° and +0.9° for Veh and Drug, respectively; Nov: mean phase shifts of -2.9° and +3.1°). A repeated measures ANOVA confirmed that there was no effect of either novelty or cannabinoid, nor any interaction of the two (Novelty: F1,3=0.1, p=0.80; Drug: F1,3=0.3, p=0.61; Drug × Novelty: F1,3=1.3, p=0.33).

However, there was evidence that the distribution of cell phases changed in the Nov environments relative to Fam, becoming much broader in response to novelty (Figure 8.19, comparing top and bottom rows). Levene's test of variance confirmed that the cell phases were significantly more varied in Nov than Fam environments (Veh: $F_{1,47}$=9.0, p=0.004, variances of 3.1° and 16.3° in Fam and Nov, respectively; Drug: $F_{1,51}$=11.5, p=0.001, variances of 2.4° and 9.9°). In contrast, there was no effect of Drug on the variability of preferred cell phases across the different environments (Fam: $F_{1,64}$=0.08, p=0.78; Nov: $F_{1,34}$=0.08, p=0.78). These results demonstrate that whilst novelty did not affect the overall mean phase of either the cell population or the group spike ensemble, it did affect the theta phase preferences of individual interneurons in a cell-specific manner.

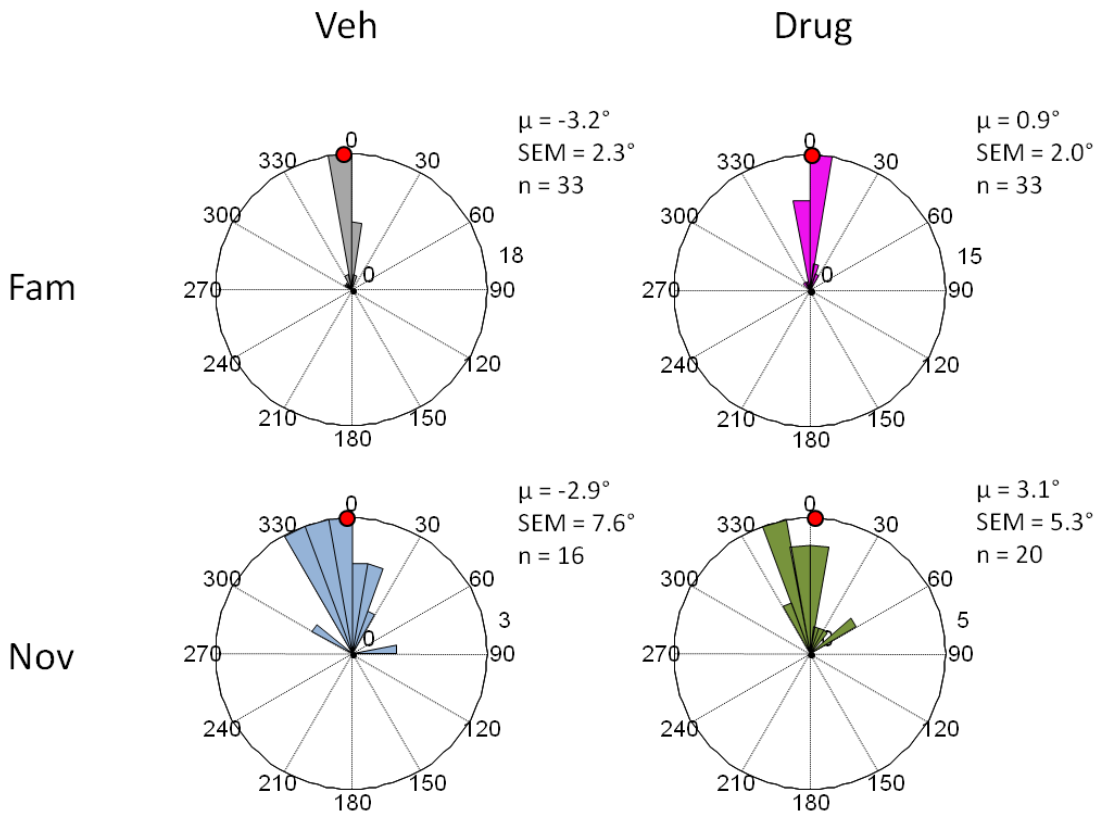

Figure 8.19. The mean and distribution of phase changes for individual interneurons after Veh (top) or Drug (bottom) injection were similar in both Fam and Nov environments. However, there was a novelty-induced increase in the variance of cell mean phases after either Veh or Drug. These data suggest that cell-specific changes in interneuron phase tuning may contribute to the later phase of place cell firing in novelty.

This cell-specific change suggests that the later phase of place cell firing elicited by novelty does not depend on a dramatic shift in the phase of the hippocampal interneuron population as a whole. Instead these results indicate that the change in place cell phase may be supported by cell-specific phase shifts in the interneuron population. Whether the interneurons exhibiting a particular phase shift in response to novelty belong to a common class or subclass cannot be determined at present. The lack of a clear cannabinoid-induced effect on the phase tuning of interneurons may be because an insufficient number of cannabinoid-sensitive interneurons were recorded or because cannabinoids do not alter interneuron phase *in vivo*. Based on the limited number of interneurons recorded (n=115), it is not possible to distinguish between these alternatives.

8.6 Place field properties

8.6.1 Field size

A previous study indicates that place field sizes are reduced by cannabinoid injection (Robbe and Buzsaki, 2009), but the interaction of this effect with novelty is not known. I therefore analysed place field sizes, using only place cells that fired at least 120 spikes with a peak rate of at least 1.0 Hz (n=360) to ensure accurate estimates could be made. As the sizes of both Nov environments were larger than the Fam environment (areas were 0.384m^2, 0.503m^2 and 1m^2 for Fam, NovA and NovB respectively), all comparisons were made by normalizing the field size to the total area of the relevant environments (Figure 8.20).

In contrast to the published data, I found that after either Veh or Drug injection, mean field sizes did not change in the Fam environment (Veh: mean decrease of 0.08%; Drug: mean decrease of 0.05%). However, a larger proportion of cells decreased their field size with Drug injection, suggesting that there was still a minor effect of Drug (Figure 8.20, top row; 49.6% vs. 59.8% of place cells for Veh and Drug, respectively). Therefore the differences between these results and the published data are likely a result of the much lower dose of cannabinoid used in the present study, which was chosen to avoid the strong behavioural effects observed in the prior study (Robbe et al., 2009; ref; see also Pilot study in the Methods chapter).

In contrast to the stable mean field sizes in the Fam environment, those in the Nov environments increased significantly with Veh injection, an effect which was completely blocked by Drug injection (Figure 8.20, bottom row; Veh: mean increase 3.2%; Drug: mean increase 0.2%). A repeated measures ANOVA revealed a main effect of Novelty on mean field size, but the effect of Drug or the interaction between the two factors did not reach the level of significance (Novelty: $F_{1,4}$=22.3, p=0.009, overall mean increases of 0.1% and 2.9% in Fam and Nov, respectively; Drug: $F_{1,4}$=3.1, p=0.15, overall mean increases of 1.1% and 0.4% in Veh and Drug, respectively; Drug × Novelty: $F_{1,4}$=3.5, p=0.13). Thus, environmental novelty increased field sizes relative to Fam, whilst there was a non-significant trend towards decreased field sizes with the cannabinoid.

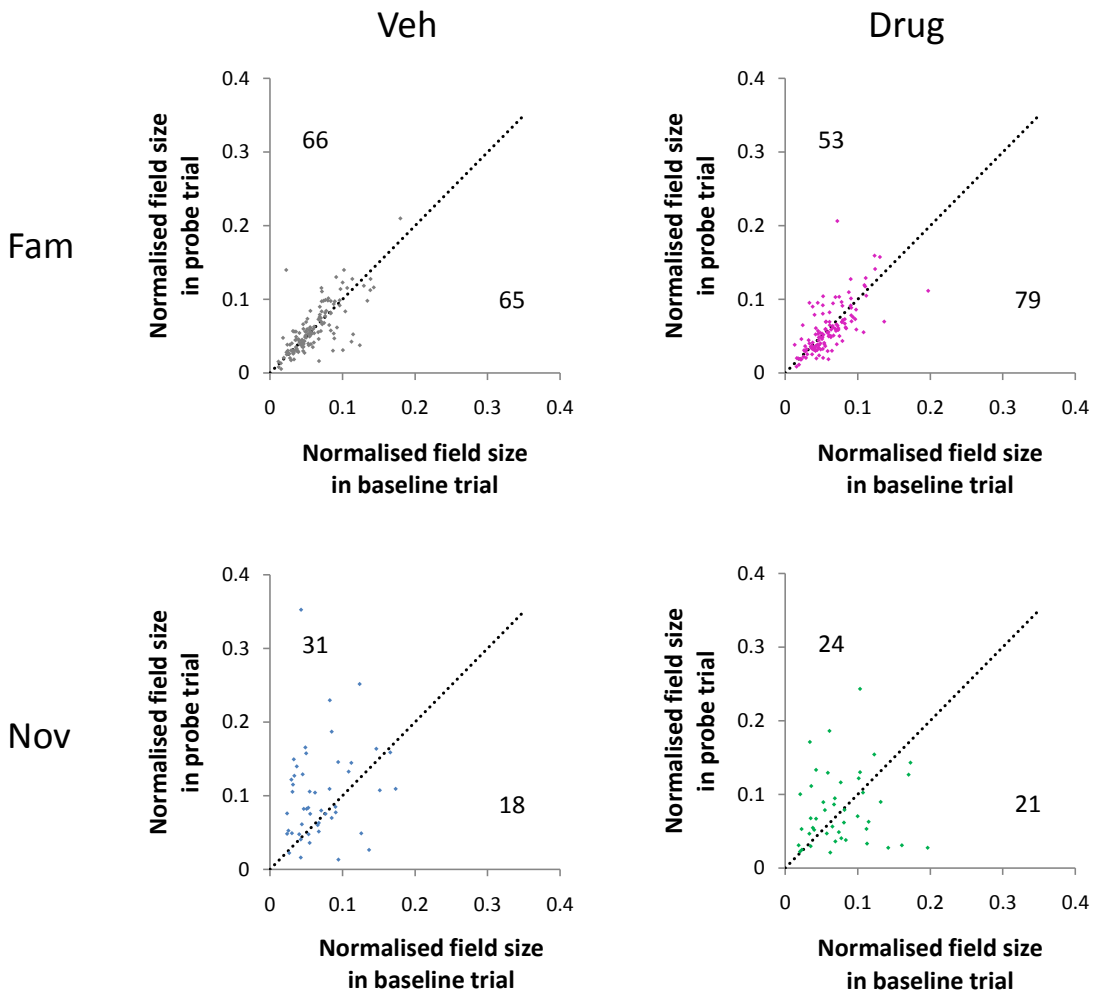

Figure 8.20. Normalized field sizes of place cells in each condition in the baseline and probe trials. Numbers on each side of the dotted equality line in each plot indicate the number of cells falling each side of the line (i.e. with greater field size in either the baseline or probe trial). (Top left) Field sizes are stable in Fam with Veh injection. (Top right) Drug causes the majority of cells to decrease their field sizes without affecting the overall group mean. (Bottom left) Veh injection in the Nov environment is associated with a robust increase in field size. (Bottom right) Drug prevents the increase in field size in Nov.

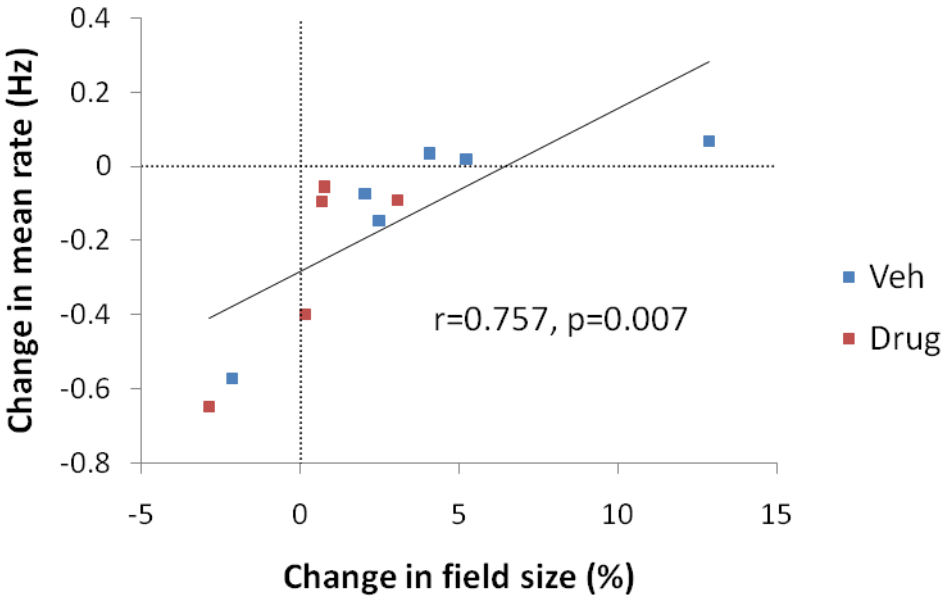

Figure 8.21. Change in field size from the baseline to probe trial in the Nov condition correlates positively with the change in the mean rate of the place cell population. In the absence of a change in mean rate, novelty alone is associated with a field size increase of 6.4% (x-axis intercept of regression line above).

As novelty was associated with lower mean place cell firing rates after Drug injection than Veh injection (Figure 8.5 and Figure 8.6), I examined whether this might account for the difference in field size between Veh and Drug in novelty. In agreement with this, I found a positive correlation between the change in mean rate and the change in field size on Nov days (Figure 8.21; Pearson's r=0.757, p=0.007). This regression suggested that the field size decrease by Drug in Nov was due to a reduction in mean rate. However, novelty alone elicited a 6.4% increase in field size if mean rate was constant between the baseline and probe trials (Figure 8.21, x-axis intercept of regression line). Therefore, this suggests that novelty causes an expansion of place fields, which may parallel the novelty-related expansion of grid cell fields (Fyhn et al., 2007; Barry et al., 2009, SFN Abstract 101.24).

According to several models of entorhino-hippocampal spatial firing, the localised firing fields of place cells are determined by convergent spatially-aligned inputs from subsets of grid cells (O'Keefe and Burgess, 2005; McNaughton et al., 2006a; Solstad et al., 2006; Burgess et al., 2007; Burgess, 2008). If there is a global

expansion of grid field scale, this might account for the increase in place field size observed. The oscillatory interference model links the grid field expansion to a reduction in the slope of the theta frequency-speed relationship (Burgess, 2008). Therefore, I examined whether the slope reduction might also predict the change in field size observed in novelty. In line with this, I found a positive correlation between the place cell field size change and the slope reduction on days when the vehicle was injected (Figure 8.22; Pearson's r=0.736, p=0.0007). However, this was not the case with the cannabinoid (Pearson's r=0.231, p=0.36), which might reflect the tendency of the Drug to independently affect field size, especially during novelty (effects of Drug and Drug × Novelty, p=0.15 and 0.13, as discussed above). There are insufficient data to come to a clear conclusion at present, but these findings are consistent with the field size expansion associated with novelty alone being driven by the concurrent slope reduction.

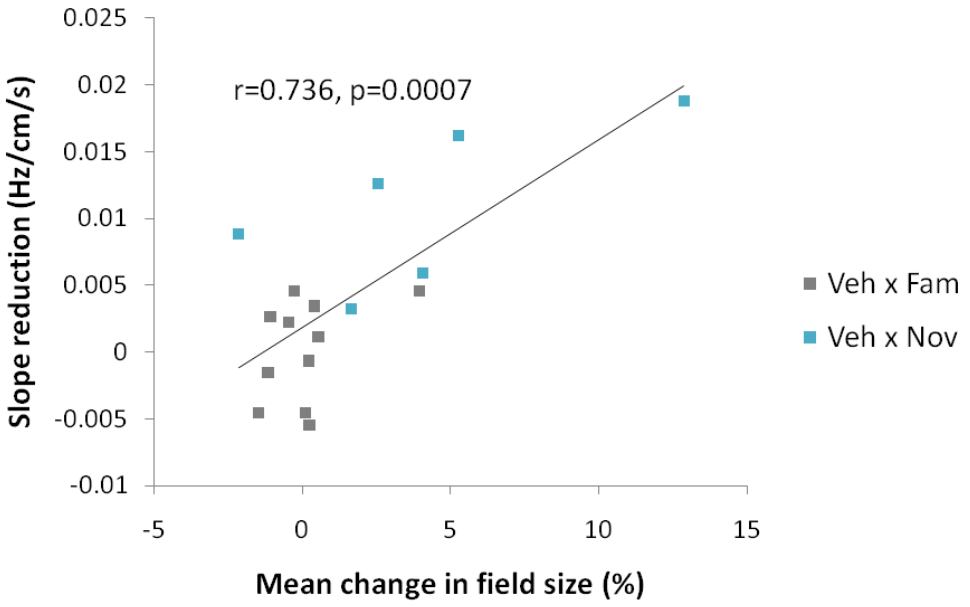

Figure 8.22. The change in place cell field size on days with novelty alone correlates positively with the reduction in slope. However, this correlation is abolished by the cannabinoid (r=0.231, p=0.36). This may be due to an interaction between the effects of the cannabinoid and novelty on place cell field size (two-way repeated measures ANOVA; Drug × Novelty, p=0.13).

8.6.2 Spatial information

As with field size, only the subset of cells firing with a mean rate of at least 0.2 Hz and a peak rate of at least 1.0 Hz (n=360) were analysed for spatial information, to exclude spurious estimates based on cells with a low number of spikes. Cannabinoid injection reduced the spatial information of place cell firing in the probe relative to baseline trial in both Fam (1.56 vs. 1.43 bits/spike in baseline and probe trials, respectively) and Nov environments (1.40 vs. 1.14 bits/spike, respectively). In contrast, with Veh injection there was no change in spatial information in either the Fam or Nov environments (Fam: 1.57 vs. 1.55 bits/spike in baseline vs. probe trials, respectively; Nov: 1.31 vs. 1.33 bits/spike, respectively). However, a repeated measures ANOVA showed the effect of the cannabinoid to be just below the level of significance ($F_{1,4}$=3.6, p=0.13), with no effect of novelty and no interaction of the two factors (Novelty: $F_{1,4}$=0.07, p=0.81; Drug × Novelty: $F_{1,4}$=0.37, p=0.57). Thus, there may be a trend towards decreased spatial information after cannabinoid injection, but additional data are needed to confirm this.

The only previous study to examine the spatial information content of place cell firing after cannabinoid injection found no indication of any effect of the drug (see Fig 2B, Robbe and Buzsaki, 2009). This discrepancy may result from the different types of environment and behaviour in each case: the previous study used maze environments that encouraged stereotyped behaviour, whereas this study employed open-field environments that encouraged free foraging behaviour. The sampling of the field is quite different in each case: in the former, there are quick, directionally-oriented runs through the field; whereas in the latter, movement through the field is at a range of speeds and from many directions. Therefore further studies using open field environments will be required to investigate these effects further.

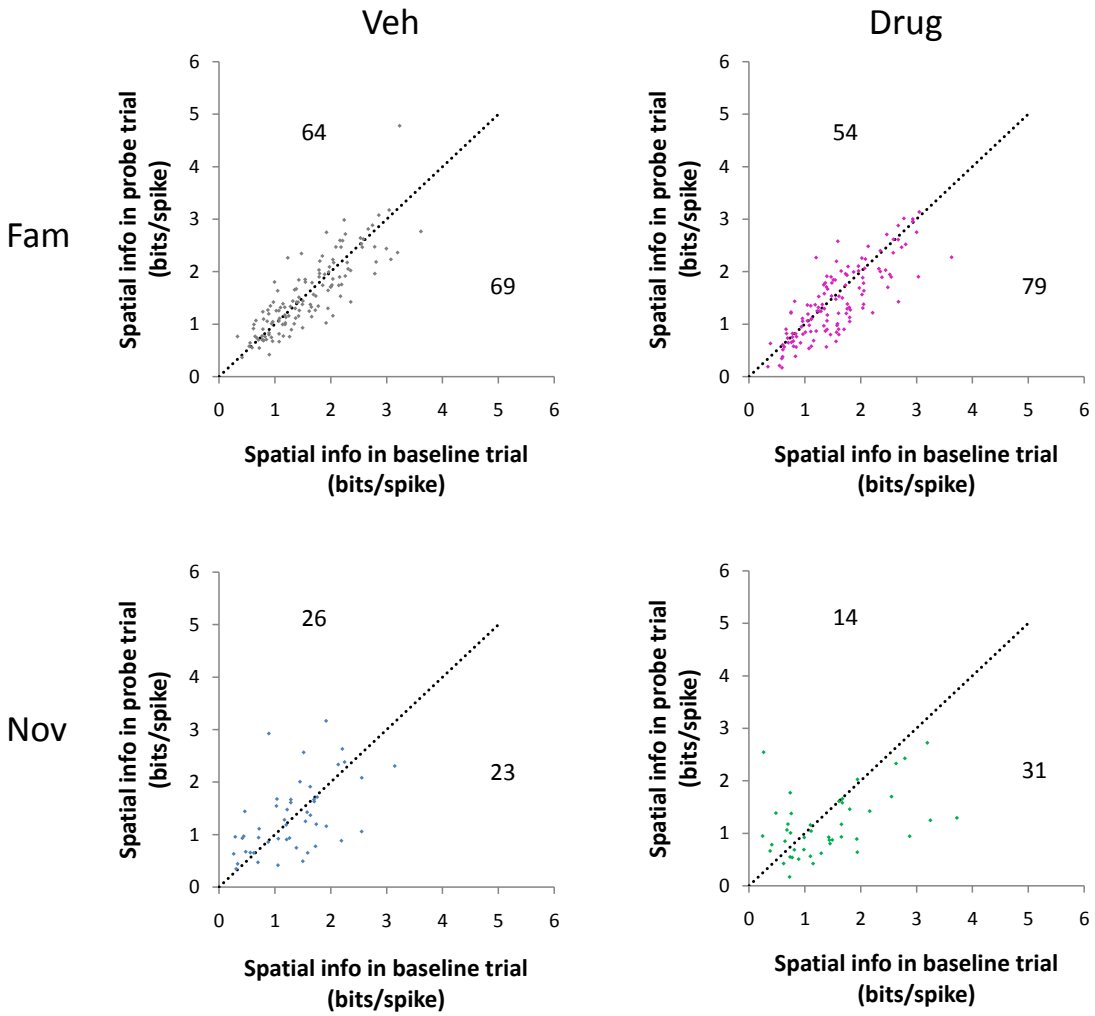

Figure 8.23. Spatial information of place cell firing in the baseline to probe trials in each of the four conditions. Numbers on each side of the dotted equality line indicate the number of cells on each side of the line (i.e. with greater spatial information in either the baseline or probe trial). (Top left) Spatial information does not change in Fam with Veh injection. (Top right) Drug tends to reduce spatial information in Fam. (Bottom left) As in Fam, spatial information is unaffected in Nov with Veh. (Bottom right) Drug also shows a trend towards reduced spatial information in Nov.

8.6.3 Remapping

The oscillatory interference model (Burgess, 2008) proposes that place cell remapping is driven by an expansion of grid cell fields in novelty (Fyhn et al., 2007; Barry et al., 2009, SFN Abstract 101.24) that is accompanied by a reduction in the slope of the theta frequency-speed relationship. The model predicts that a linear relationship exists between the reduction in slope associated with novelty (as

shown in the data presented in the previous chapter) and the extent of place cell remapping.

First, I assessed place cell remapping using a population activity measure that correlates the spatial firing of all place cells in each spatial bin (2.1 × 2.1 cm) of the ratemap between the baseline and probe trials (Leutgeb et al., 2005a). This "population ratemap correlation" (PRC) measures the similarity in the spatial firing of the place cell population as a whole, including cells that are silent in either the baseline or probe trial. As the Nov environments differed in size and shape to the Fam environment, place cell ratemaps were transformed to match the Fam environment using a commonly-used technique that preserves the similarity of un-remapped fields (Lever et al., 2002; Wills et al., 2005). For each experimental day, the distribution of correlations across all spatial bins was calculated and the mean of this value was taken as the measure of remapping for that day. Example ratemaps from days showing weak, moderate or strong remapping and their corresponding mean PRCs are shown in Figure 8.24.

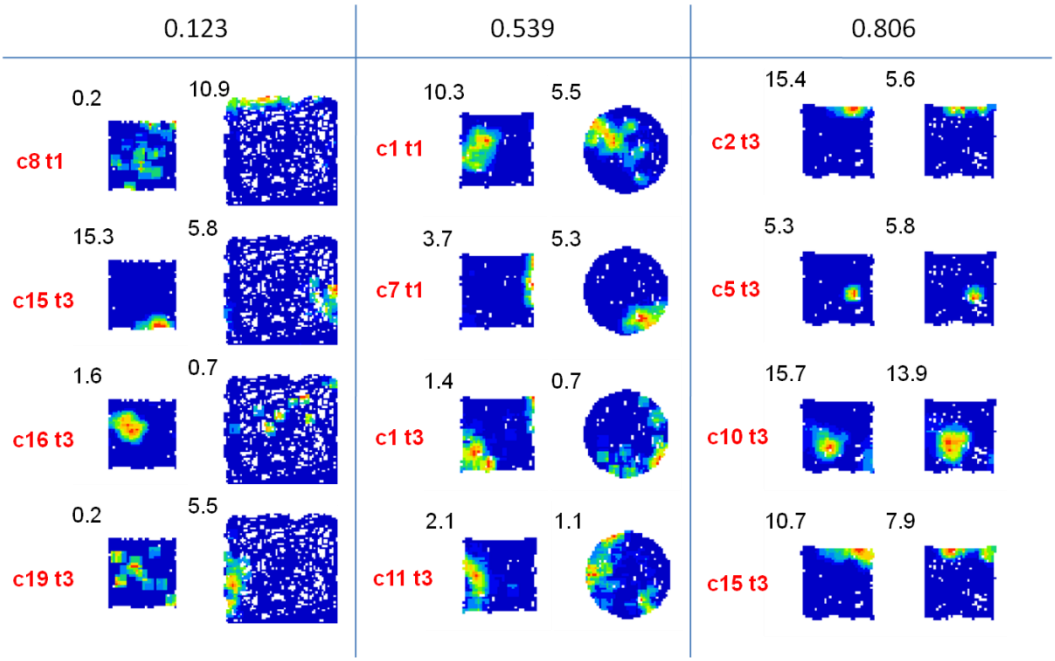

Figure 8.24. Example ratemaps taken from days where there was strong remapping (left), moderate remapping (middle) or weak/no remapping (right). Each column shows a sample of four place cells (named in red) recorded on each day, with the baseline trial on the left and probe trial on the right. The numbers at the top of each column indicate the mean population ratemap correlation (PRC) value for the day, whilst the numbers to the top left of each ratemap indicate the peak firing rate of the place cell in each trial.

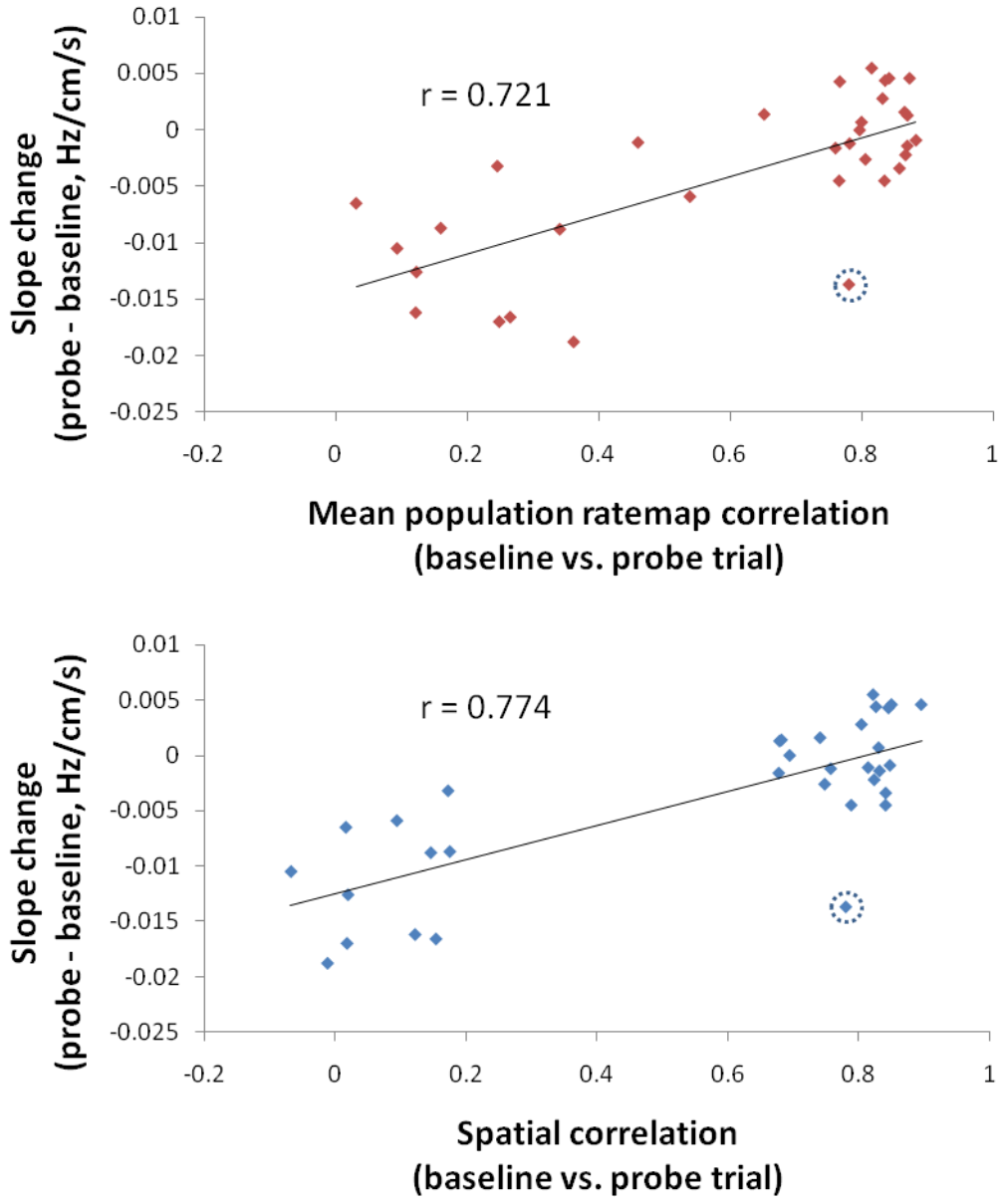

Figure 8.25. There is a significant positive correlation between the change in slope of the theta frequency-speed relationship and the extent of place cell remapping, measured either by spatial correlation (top panel) or by mean population ratemap correlation (bottom panel). These results corroborate the predictions of the oscillatory interference model (Burgess 2008). The circled outlier on each plot is from a day with noisy LFP data, where the slope reduction estimate is known to be poor. The Pearson's r values quoted are based on all data points, including the outlier.

A repeated measures ANOVA of the mean PRC for each condition showed strong remapping in the Nov environments, but no effect of Drug injection and no

interaction (Novelty: $F_{1,4}$=167.1, p=2×10^{-4}, mean PRCs of 0.82 and 0.22 in Fam and Nov, respectively; Drug: $F_{1,4}$=1.8, p=0.25, mean PRCs of 0.56 and 0.48 in Veh and Drug, respectively; Drug × Novelty: $F_{1,4}$=0.8, p=0.41). Therefore, data were pooled across the Veh and Drug conditions and the mean PRCs from each day were regressed against the change in slope measured on the corresponding day (Figure 8.25, top panel). In support of the prediction made by the model, there was a strong positive correlation between the two variables (Figure 8.25, top panel; Pearson's r=+0.721, p=2.2×10^{-6}).

In order to confirm this finding, the extent of remapping was also assessed using the spatial correlation of individual cells' ratemaps between the baseline and probe trial (Lever et al., 2002; Wills et al., 2005). This analysis compares the similarity of spatial firing in the two trials on a cell-by-cell basis and so is complementary to the PRC analysis performed above. As before, spatial correlations were calculated for each experimental day and the mean correlation across all cells was taken as the measure of remapping for that day.

In line with the results from the PRC analysis, a repeated measures ANOVA showed a main effect of novelty associated with remapping in the Nov environments, but no effect of the cannabinoid and no interaction between the two factors (Novelty: $F_{1,4}$=553.2, p=2×10^{-5}, mean correlations of 0.79 and 0.07 in Fam and Nov, respectively; Drug: $F_{1,4}$=0.9, p=0.39, mean correlations of 0.45 and 0.41 in Veh and Drug, respectively; Drug × Novelty: $F_{1,4}$=0.2, p=0.67). The data were therefore pooled as before across Veh and Drug conditions and the regression between the mean spatial correlation for each day and the slope change was plotted (Figure 8.25, bottom panel). In agreement with the PRC analysis and the prediction of the model, there was a strong positive correlation between the slope change and the degree of remapping (Figure 8.25, bottom panel; Pearson's r=+0.774, p=1.3×10^{-7}). However in contrast to the PRC analysis, the relationship was more bimodal, as there were no data with spatial correlation values in the range 0.2 – 0.6. The reason for this discrepancy is not clear, but it may be due to the inclusion of silent cells in the PRC but not the spatial correlation analysis.

Overall, the results of both the PRC and the spatial correlation analysis are consistent with the mechanism of remapping proposed in the oscillatory interference model (Burgess, 2008). These data demonstrate that the extent of place cell remapping in novel environments is proportional to the reduction in the slope of the theta frequency-speed relationship.

9 Discussion

9.1 Summary of main findings

9.1.1 Cannabinoid reduces the intercept and novelty reduces the slope

The LFP data presented in this thesis demonstrate specific effects of systemic cannabinoid injection and environmental novelty on the theta frequency-speed relationship. Cannabinoid injection selectively reduced the intercept, whilst novelty reduced the slope. When these two manipulations were combined, the effects were additive. Further analyses showed that these effects were not a result of changes in average speed or body temperature. Although the influence of temperature on intercept cannot be absolutely ruled out in the novelty condition, the data show that temperature accounts for only a small part of the cannabinoid-mediated intercept reduction.

9.1.2 Reduction in slope correlates with the extent of remapping

Using either a population or individual cell analysis of place cell remapping, there was a significant positive correlation between the slope reduction and the amount of remapping.

9.1.3 Place cell mean firing rates decrease in novelty, whereas interneuron firing rates tend to increase

Both place cells and interneurons showed speed-independent changes in mean firing rate in the novel, but not the familiar, condition. The changes observed were opposite and complementary, with place cell rates decreasing and interneuron rates increasing. The cannabinoid tended to diminish both interneuron and place cell mean firing rates.

9.1.4 Place cell field size increases in novelty

Novelty alone increased field size, whilst injection of cannabinoid tended to reduce it. Regression analyses suggest that the cannabinoid-mediated reduction in field size can be accounted for by differences in the mean firing rate of place cells.

9.1.5 Novelty elicits a later theta phase of place cell firing, cannabinoid disrupts this effect

Environmental novelty alone consistently induced a later phase of place cell firing. Firing phase was also later in novelty combined with cannabinoid, but the day-to-day effects were much more variable. The novelty-elicited phase shift did not correlate with the slope reduction, suggesting they are mediated by different neural mechanisms.

9.1.6 The later theta phase of place cell firing in novelty was not a result of changes in average speed or firing rate

Average speed correlated with the change in place cell ensemble phase concentration in novelty, but not the change in mean firing phase. Although there was a later phase of firing in both novel environments, the mean peak firing rate of the place cell population decreased in NovA, but increased in NovB. Therefore, the phase shift is not driven by changes in firing rate or average speed.

9.1.7 The overall theta phase tuning of the interneuron population is unaffected by novelty or cannabinoid

There were no effects on either the mean phase or phase concentration of interneuron ensembles with novelty or cannabinoid, either independently or in combination.

9.1.8 However, individual interneurons change their phase tuning in response to novelty

Whereas the phase tuning of interneurons was stable under familiar conditions, novelty caused individual cells to change their phase preferences without changing the population mean. The extent of the dispersion of phase preferences was not affected by cannabinoid in either the familiar or novel conditions.

9.1.9 Average speed increases with novelty alone, but not when combined with drug

Environmental novelty alone lead to an increased average speed, but this increased locomotion was prevented by concurrent cannabinoid administration. The cannabinoid showed a non-significant trend toward

increasing the amount of time spent in the centre of the enclosed novel environment (NovA), consistent with an anxiolytic effect.

9.2 Support for a two-component model of theta

The double dissociation demonstrated between the intercept and the slope of the theta frequency-speed relationship provides strong evidence in favour of a two-component model of theta generation (Burgess, 2008). The isolation of distinct components of theta has implications for the representation of space, the mechanisms of anxiolytic action and models of theta rhythm generation. I discuss these topics in detail below.

9.2.1 Slope reduction and spatial representation in novelty

During exposure to environmental novelty, there was a specific reduction of the slope of the theta frequency-speed relationship. This finding extends previous work from our group showing a novelty-induced theta frequency reduction (Jeewajee et al., 2008b) by clarifying its relation to movement speed. Since the theta rhythm reflects the concerted oscillatory activity of cells in the entorhino-hippocampal system (Buzsáki, 2002), a change to the slope implies a reduction of the speed-related gain in intrinsic cell oscillatory frequencies. The spatial scale of both place and grid cell fields have been found to correlate inversely to the frequency of cell oscillations (Maurer et al., 2005; Geisler et al., 2007; Jeewajee et al., 2008a). Therefore, this suggests that the slope reduction during novelty will be associated with an increased spatial scale of both place and grid cells.

9.2.1.1 Relationship to grid cell spatial scale and remapping

Indeed, such an expansion of spatial scale has been observed in grid cell fields in response to novelty (Fyhn et al., 2007; Barry et al., 2009, SFN Abstract 101.24). According to several models of hippocampal place cell activity, the spatially aligned inputs of a specific subset of grid cells determines the precise field location of each place cell (McNaughton et al., 2006a; Solstad et al., 2006; Blair et al., 2008; Burgess, 2008). The oscillatory interference model (Burgess, 2008) proposes that a global expansion in grid scale in response to novelty results in a misalignment of grid cell inputs to place cells, driving remapping. In agreement with this, I found a positive correlation between the extent of remapping in CA1 and the slope reduction elicited by novelty. This suggests that the reduction of the slope acts as a

signal or trigger for novelty-induced changes in the representation of space in the hippocampus (Burgess, 2008; Jeewajee et al., 2008b).

An important point to consider is whether CA1 place cell remapping can be accounted for by entorhinal-CA1 dynamics alone, since it involves a coordinated change throughout the entorhino-hippocampal system (Fyhn et al., 2007). The activities of principal cells in both CA3 and the DG change significantly during remapping, in fact generally much more so than CA1 place cells (Leutgeb et al., 2004, 2007). However, CA1 place cells display a faster timecourse of remapping during novelty than CA3 place cells, suggesting that direct entorhinal inputs, rather than intrinsic SC inputs, drive CA1 remapping (Brun et al., 2002; Leutgeb et al., 2004). In line with a dominant entorhinal influence, the elevation of hippocampal acetylcholine levels during novelty (Givens and Olton, 1995; Thiel et al., 1998; Giovannini et al., 2001) favours entorhinal inputs over intrinsic hippocampal activity (Hasselmo, 2006; Villarreal et al., 2007). These results suggest that, at least on the short timescales studied in this thesis, CA1 place cell remapping is likely to depend largely on entorhinal inputs. This would be consistent with the idea that the correlation between remapping and slope reduction observed in this thesis results directly from a novelty-elicited expansion of entorhinal grid cell fields. Further experiments are necessary to verify that the timecourse of the grid cell field expansion, CA1 place cell remapping and slope reduction are indeed in register with one another.

9.2.1.2 Place cells increase may also increase their spatial scale in novelty

Concurrent with the reduction in slope, I also found an expansion in the field size of place cells in novelty. If, as described above, overlapping grid cell inputs determine place cell fields, then the global increase in the spatial scale of grid fields should drive a corresponding increase in place cell field sizes (assuming grid cell firing rates and place cell firing thresholds remain relatively constant). The field size measure in the current study was somewhat confounded as the sizes of both novel environments were larger than the familiar environment. I attempted to account for this by measuring field sizes relative to the total area of each environment. In fact, this is likely to lead to an underestimate of field size change, since place cell field scaling in larger environments tends to be less than the environmental scaling itself (Muller and Kubie, 1987). Even using this conservative measure, I found that place cell field sizes were increased by novelty.

Comparisons with previous findings in the literature are complicated by the fact that novel field size measurements are often pooled over enclosures of different sizes and quoted in terms of absolute area, rather than relative to the size of the enclosure. Also the effects of novel experience on field size may differ depending on the type of environment used; for example on the linear track, field size has been reported to increase with experience (Mehta et al., 1997). Therefore, I focus on open field studies where place field and environment sizes have been described in detail.

In line with the findings of this thesis, Brun and colleagues (2008a) also reported a novelty-elicited field size increase (Fig 6 in Brun et al., 2008a). They found that CA1 place fields gradually diminish in size with continuing experience in the novel environment, a finding also reported by Leutgeb and colleagues (Table S2 in Leutgeb et al., 2004). This parallels both the gradual decrease in grid field scale with continuing novel experience (Barry et al., 2009, SFN Abstract 101.24) and the corresponding gradual increase of slope (Wells, Jeewajee, Burgess, Lever, unpub.). This corroborates the idea that changes in the slope occur in tandem with changes to place and grid field sizes. The fact that all these parameters gradually return to their "normal" familiar environment levels with experience is consistent with a habituation effect. Further work with familiar and novel enclosures of similar sizes is necessary to provide more reliable measures of place cell field sizes across environments. Concurrent CA1 place cell and entorhinal grid cell recordings in such environments would allow the correlation of slope with place and grid field sizes to be measured directly.

9.2.1.3 Functional role of the increase in spatial scale

The increase of grid cell spatial scale in novelty suggests that the entorhinal cortex does not provide a fixed, universal "spatial metric" (Moser and Moser, 2008), but one that can be modified by environmental influences. The function of such a plastic grid cell representation is not currently understood, but I propose that it may facilitate the encoding of information in novel environments. The expansion of grid fields, and putatively place fields, in novelty implies that each firing field covers a larger area, whilst the concurrent drop in theta frequency implies a longer duration for each theta cycle. This would provide longer spatial and temporal windows for the integration of novel sensory information into new place cell representations (Mizuseki et al., 2009; Jezek et al., 2010, FENS Abstract 087.29).

Anatomical data suggest that the LEA, rather than the MEA, is the predominant route for contextual and sensory information, but unlike the MEA its neurons are not spatially selective (Hargreaves et al., 2005; Yoganarasimha et al., 2010). This suggests that the inputs of the MEA and LEA, which converge on DG and CA3 principal cells, could work together, with the LEA providing the broad contextual information which is "spatially gated" by MEA grid cell activity. Similar to the iris of the eye widening to admit more light in the dark, the larger spatial and temporal integration windows might increase the quantity of multi-modal sensory and contextual information converging on each place cell. This could enable the hippocampus to form a new spatial representation rapidly in a novel environment, which is likely to be important ethologically. These claims are highly speculative at present, but a prediction arising from this proposal is that the degree of slope reduction (and putatively therefore, grid cell field expansion) would correlate inversely with the time taken for remapped place cell fields to stabilise. The trial duration used in this thesis (10 minutes) may be too short to study such effects, so this prediction awaits experimental verification.

9.2.2 Intercept reduction and anxiolytic action of cannabinoids

By using a low dose of cannabinoid as an anxiolytic agent (Haller et al., 2004; Moreira and Wotjak, 2010), I have shown a specific reduction of the intercept of the theta frequency-speed relationship. These results confirm and extend previous reports of a reduction in hippocampal theta frequency by cannabinoids (Gray et al., 1975; Robbe and Buzsaki, 2009) by demonstrating that this reduction is speed-independent and not accounted for by a change in body temperature or a gross change in locomotor activity. A similar selective reduction in the intercept has been found in parallel studies by our group using anxiolytics that target GABAergic and serotonergic systems (Wells, Jeewajee, Burgess, Lever, unpub.).

This suggests that anxiolytics affecting different neurotransmitter systems may share a common mechanism of action. Previous work has highlighted the midbrain reticular formation as an important central target (Gray and McNaughton, 2000; McNaughton et al., 2007). Hippocampal theta can be elicited by electrical stimulation of the reticular stimulation in anaesthetised, immobile and freely moving rats (Green and Arduini, 1954; Gray and McNaughton, 2000) and the frequency of reticular-elicited theta is reduced by a wide range of anxiolytics (reviewed in McNaughton et al., 2007). CB1 receptors are present at moderate levels in the reticular formation (Herkenham et al., 1991; Glass et al., 1997), so it is

possible cannabinoids exert a direct inhibitory effect on reticular neurons that causes the theta frequency reduction. There may alternatively or additionally be effects mediated by cannabinoid binding to CB1 receptors in other parts of the ascending theta-generating pathways, such as the septum or hypothalamus, which both project back to the reticular formation (Bland and Oddie, 1998).

The common action of so many classes of anxiolytics on reticular-elicited theta has lead to the proposal that it could be used to screen for anxiolytic drugs (McNaughton et al., 2007). However, stimulation of this region is likely to affect many brain areas and may therefore interfere with normal behaviours, preventing the concurrent use of behavioural anxiety tests. An alternative approach to studying the relationship of anxiety to theta is to isolate the "immobility-related" a-theta component using predator-elicited freezing or pharmacologically-induced immobility (Sainsbury et al., 1987; Seidenbecher et al., 2003). However, these conditions impose even stronger behavioural constraints, making such paradigms unsuitable for studying the full range of natural anxiety-related behaviours. In contrast, the novel analytical approach used in this thesis makes it possible to infer a specific effect of anxiolytics from movement-based theta without the need for artificial stimulation or behavioural constraints. This opens the door for anxiolytic drugs to be screened by measuring theta during normal movement and behaviour in classical anxiety tests.

9.2.3 Relationship of intercept and slope to the two types of theta

An important question is how the intercept and slope relate to the two types of theta, the cholinergic a-theta and non-cholinergic t-theta, which depend on projections to the HF from the MS/DBB and EC, respectively (Kramis et al., 1975; Vanderwolf et al., 1985). A-theta has typically been associated with immobile, aroused states that occur during freezing or motor preparation in the rat, but it also co-occurs with t-theta during voluntary movements. In rats in which the EC has been isolated from the rest of the cortex, movement elicits the normal range of theta frequencies but this theta can be abolished by the anti-cholinergic drug atropine (Vanderwolf et al., 1985). This implies that there is some contribution from the a-theta pathway during both immobility and movement.

It has been proposed that a-theta provides a "baseline frequency" that maintains a speed-independent arousal/anxiety-related drive, corresponding to the intercept, whilst t-theta provides a speed-dependent drive that corresponds to the slope

(Burgess, 2008). However, this is unlikely to be a complete description for a couple of reasons. Firstly, environmental novelty is associated with an increase in cholinergic signalling from the MS/DBB to the HF (Givens and Olton, 1995; Thiel et al., 1998; Giovannini et al., 2001), corresponding to the a-theta pathway. Thus, one might expect such novelty to affect the intercept, but in fact it selectively affects the slope. Secondly, increasing the rotational speed of immobilised rats results in an increase of theta frequency and power that is abolished by atropine or lesion of septal cholinergic afferents (Tai et al., 2011). This may reflect a cholinergic speed-dependent modulation of theta frequency, or might simply indicate that cholinergic stimulation is necessary to permit theta activity in the absence of translational movement (Vanderwolf et al., 1985; McNaughton et al., 2007). As cholinergic theta has typically been studied in immobilised or anaesthetised preparations, there is a sparsity of data on how the cholinergic and non-cholinergic pathways contribute to determining theta frequency during movement. The two component theta frequency-speed relationship demonstrated in this thesis offers a new paradigm for studying theta generation during both immobility and movement.

9.3 Theta phase of firing in novelty

9.3.1 Later phase of place cell firing

9.3.1.1 Function of phase shift

In agreement with a previous finding from our group (Lever et al., 2010), I found a later phase of place cell firing in the novel compared to the familiar environments. This specific shift of place cell activity during novelty may favour a theta phase of firing that facilitates encoding (Hasselmo et al., 2002). Previous work has shown that LTP occurs optimally in CA1 when spikes are emitted at the peak of the theta wave (generally recorded in SR), whereas activity at the trough has no effect or may even lead to LTD (Pavlides et al., 1988; Huerta and Lisman, 1993; Hölscher et al., 1997).

Therefore, to understand if the later phase observed promotes the encoding of novel information in the network, it is important to determine the absolute phase of place cell firing. This is greatly complicated by the theta phase reversal that occurs across SP (Winson, 1974), meaning that small changes to the recording depth

(layer) can change the absolute theta phase of place cell firing by 90° or more. Calculation of the absolute phase of place cell firing requires data to be combined across days, based on accurate estimates of the recording layer on each day. Although absolute phase analyses on the data in this thesis are ongoing, it has not been possible to produce a reliable estimate yet and so I continue the discussion by inferring the absolute phase from published data.

I found that environmental novelty elicited a 35-40° later phase of place cell firing than the familiar environment. Place cells fire at around 45° after the trough of SP theta (Csicsvari et al., 1999b; Mizuseki et al., 2009, 2011), which corresponds to approximately 115° after the trough in SR, depending on the precise depth (Bragin et al., 1995; Lubenov and Siapas, 2009). Therefore a 35-40° phase shift is estimated to bring the firing phase of place cells to around 160° after the trough, or equivalently 20° before the peak of SR theta. Therefore, this shift of firing towards the peak of theta could facilitate the encoding of novel environmental information in CA1 by favouring a theta phase of place cell firing at which LTP is optimal (Huerta and Lisman, 1993; Hasselmo et al., 2002; Lever et al., 2010).

9.3.1.2 Role of cholinergic system in the phase shift

The mechanisms driving the phase shift are unknown, but they could involve an increase in cholinergic stimulation from the MS/DBB during novelty (Givens and Olton, 1995; Thiel et al., 1998; Giovannini et al., 2001). Interestingly, preliminary evidence from our group (Douchamps, Jeewajee, Blundell, Burgess, Lever, unpub.) suggest that administration of the cholinergic blocker scopolamine causes a shift to an earlier phase of CA1 place cell firing. This is true whether the post-injection phase shift is measured in a familiar or a novel environment (relative to the familiar baseline trial). This suggests that cholinergic signaling could play an important role in determining the direction and extent of the phase shift.

This may also relate to the specific memory impairments associated with scopolamine administration. Local injection of scopolamine to either the hippocampus or MS/DBB has been shown to impair spatial encoding by blocking cholinergic signaling in the hippocampus (Blokland et al., 1992; Elvander et al., 2004). Studies in humans suggest that scopolamine interferes with the encoding, but not the retrieval of information (Atri et al., 2004; Hasselmo and McGaughy, 2004). Therefore, one contributing mechanism to this selective impairment of encoding might be that scopolamine shifts the phase of CA1 place cell firing

towards the trough of theta. In this case, the phase timing of the place cell population would be expected to have no effect on, or even depotentiate synaptic connections relevant for the encoding of novel information (Pavlides et al., 1988; Huerta and Lisman, 1993; Hölscher et al., 1997). However, such a simplistic model cannot account for all the effects of cholinergic modulation, since local injection of the cholinergic agonist carbachol to the MS/DBB (which increases hippocampal acetylcholine, putatively leading to a later phase) also impairs memory (Bunce et al., 2004; Elvander et al., 2004). This suggests that a balanced regulation of cholinergic inputs to the hippocampus may be important for encoding and perhaps for regulating the phase shift.

9.3.1.3 Influence of cannabinoids on phase shift

The combination of O-2545 with novelty lead to a much greater variability in the extent of the phase shift, although there was still a clear trend towards a later phase (that was not significant). This variability might reflect a dysregulation of place cell theta phase spike timing in novelty. This would be in line with published data showing the detrimental influence of cannabinoids on place cell spike timing (Hampson and Deadwyler, 2000; Robbe et al., 2006; Robbe and Buzsaki, 2009).

Alternatively, the variability might be due to a single outlying phase shift value from one rat (Rat 3), as described in the Single Units results (distribution shown in Figure 8.14, bottom right; Rat 3 mean shift 138.8° from baseline to probe trial, compared to a range of -8.4° to +40.3° for the other four rats in Drug × Nov). This outlier could have arisen due to error in the experimental measurement, but this seems unlikely given that the mean firing phase of two interneurons recorded in Rat 3 on the same day were stable from the baseline to probe trial (mean shift +4.2°). An better explanation might be that this unusual phase shift was the result of inter-animal differences in sensitivity to the cannabinoid. This contention is supported by the fact that the rat contributing the outlying data point showed the weakest cannabinoid-mediated intercept reduction of all the rats in both the familiar and novel environments.

Therefore, it might be easier to get a more accurate impression of the influence of cannabinoids on the phase shift if this outlying data point is excluded. Excluding this data reduces the variability of the grouped Drug × Nov data to a similar level as the Veh × Nov data (SEMs of 10.4° and 11.9°, respectively; SEM with Rat 3 included is 25.6°). Furthermore, excluding this data point reduces the magnitude of

the Drug × Nov phase shift to approximately half that observed in Veh × Nov (mean shifts of +18.0° and +36.9°, respectively; mean shift with Rat 3 included is +42.1°). Since there was no phase shift with the cannabinoid in the familiar environment, these calculations tentatively suggest that cannabinoids may reduce the degree of phase shift in novelty.

However, determining any firm conclusions rests on identifying the precise causes of the variability. Cannabinoids are known to exert complex modulatory effects on anxiety (Moreira and Wotjak, 2010) and hippocampal-dependent memory (Akirav, 2011) that depend on the precise dose administered (Ribeiro et al., 2009), the aversiveness of the environment (Haller et al., 2009) and many other factors. They have been shown to biphasically modulate both behavioural and pharmacological parameters (Tzavara et al., 2003; Haller et al., 2004; Hill et al., 2006; Rubino et al., 2008), so it is possible that they may display a bidirectional modulation of the phase shift. However, further data are needed to test these proposals. Nevertheless, the cannabinoid disrupted the well-coordinated phase shift seen in the Veh × Nov condition whether the Rat 3 data point is included or excluded: by increasing the variability in the former case, or reducing the phase shift in the latter case. The predominant cannabinoid effect observed in this study (in 4 out of 5 rats) was a reduction in the novelty-elicited phase shift relative to Veh × Nov.

9.3.1.4 Interactions between cannabinoids and cholinergic system

The cannabinoid effect on phase shift may be mediated partly or fully through modulation of cholinergic signaling. There is significant overlap between the functioning of the cannabinoid and cholinergic systems, as virtually all cholinergic neurons in the rodent basal forebrain express the enzymes necessary for cannabinoid synthesis (Harkany et al., 2003). Interestingly, cannabinoids have been shown to biphasically modulate acetylcholine release in the hippocampus (Gifford and Ashby, 1996; Carta et al., 1998; Gessa et al., 1998; Acquas et al., 2000, 2000, 2001). Tzavara and colleagues (2003) showed that a low dose of the CB1 agonist WIN 55,212-2 (0.5 mg/kg, i.p.) caused a transient increase in hippocampal acetylcholine, whereas a high dose (5.0 mg/kg, i.p.) caused a prolonged decrease. For comparison, in the present study the i.p. dose of O-2545 was ten times lower (0.05 mg/kg), but O-2545 is more than 3 times as potent at binding the CB1 receptor as WIN 55,212-2 (K_i=1.5 and 5.05 nM for O-2545 and WIN 55,212-2, respectively; Griffin et al., 1998; Martin et al., 2006). Therefore, the level of CB1

receptor activation is estimated to be approximately 3 times lower in this study, well within the range expected to increase hippocampal acetylcholine.

However it must be remembered that during novelty, septal release of acetylcholine to the hippocampus is already increased (Givens and Olton, 1995; Thiel et al., 1998; Giovannini et al., 2001). The Tzavara study was carried out in familiar environmental conditions and therefore it is not clear whether the cannabinoid modulation of cholinergic release would function similarly in a novel environment. Interestingly, Tzavara and colleagues (2003) also showed using specific dopaminergic antagonists that the CB1-mediated ACh increase depended on D1 receptors in the MS/DBB, whereas the CB1-mediated ACh decrease depended on hippocampal D2 receptors. It may therefore be possible in future studies to use D1 and D2 antagonists to dissect the role of cannabinoids in modulating hippocampal cholinergic levels during novelty, particularly in relation to the dynamics of the phase shift.

9.3.2 Interneuron firing phase

Surprisingly, despite the later phase of place cell firing in novelty observed either with or without cannabinoid injection, there was no change in the mean firing phase of the interneuron population. However, when the preferred firing phases of individual cells were examined, these showed a greater variation during novelty. The remarkable stability of the population mean phase throughout all the conditions suggests that regulatory mechanisms exist to maintain the overall interneuron phase tuning, even when the relative phase of place cells or individual interneurons changes. This may be achieved by setting a “master rhythm” that is paced by inputs from the MS/DBB in conjunction with reciprocal projections from the HF. Having this master rhythm may allow the interneuron population as a whole to provide a reliable “clockwork” against which place cell activity is timed, whilst allowing flexibility in the timing of individual cell firing (Freund, 2003; Klausberger and Somogyi, 2008).

The fact that the place cell phase shift is so well-coordinated in novelty (at least with the vehicle injection) suggests that the variation in interneuron phases is unlikely to simply result from a general disorganisation of interneuron firing. Rather, it might reflect the specific phase changes of individual functionally-relevant interneurons, for example interneurons that are monosynaptically connected to remapped or newly active place cells. Alternatively, it might correlate

to whole classes of interneuron that alter their phase to fulfil a particular role in hippocampal network activity during novelty. In order to distinguish between these possibilities it will be necessary to identify the classes to which each interneuron belongs. This classification is still ongoing with the current data, but I describe the relevant analytical approaches below.

One way in which the interneuron classes can be separated is on the basis of their firing phases. Different classes of interneuron have been shown to display specific theta phase tunings in anaesthetised preparations (Klausberger et al., 2003, 2004, 2005; Tukker et al., 2007; Klausberger, 2009). For example, CCK-expressing interneurons fire at the phase at which place cells fire as the rat enters the place field (Klausberger et al., 2005) and therefore could putatively delay place cell activity to produce a later phase of firing. In contrast, PV-expressing basket cells fire on the descending phase of theta oscillations, roughly anti-phase to the time of maximal place cell activity, and provide a "clockwork" theta-rhythmic inhibitory drive (Ylinen et al., 1995; Freund, 2003). A variety of other interneuron types including axo-axonic cells, bistratified cells and O-LM cells each display characteristic spiking activity during hippocampal network oscillations (reviewed in Klausberger and Somogyi, 2008). However, identifying these classes *in vivo* this is a challenging task due to the difficulties in estimating the recording depth and therefore determining the absolute firing phases of the cells. Nevertheless, Czurko and colleagues (2011) recently distinguished four interneuron classes in freely moving animals on the basis of their phase tunings, demonstrating that this is indeed possible. Classification of the interneurons recorded in this study by absolute phase is ongoing. Isolation of distinct interneuron classes will help to elucidate the mechanisms underlying the place cell phase shift and the roles of different interneuron classes in novelty processing.

9.4 Firing rate changes in novelty

Interestingly, the peak rates of place cells decreased in the walled circle (NovA), but increased in the unenclosed square (NovB). In line with previous findings (Huxter et al., 2003; Geisler et al., 2007), I found that the peak rate correlated with running speed. Since the average speed was higher in NovB than in NovA both after vehicle (mean change from baseline to probe trial: 6.9 vs. 2.3 cm/s, respectively) and cannabinoid (2.7 vs. -1.3 cm/s, respectively), then this is likely to

account for the peak firing rate difference (see Figure 8.10). Since the peak firing rate approximates the instantaneous firing frequency of the place cell, these results show that the later phase shifts in novelty (mean phase shifts of +35.5° and +43.2° in NovA and NovB, respectively) are not due to changes in peak firing rates, as suggested by some studies (Harris et al., 2002; Mizuseki et al., 2009).

Both place cell and interneuron mean firing rates were stable in the familiar environment (with either cannabinoid or vehicle injection), but in the novel environments, the mean rate of place cells decreased, whilst that of interneurons showed a non-significant increase. Therefore, the changes found were opposite and complementary, suggesting that enhanced inhibitory interneuron activity in novelty suppressed place cell activity. Unlike the peak firing rates, the mean firing rates were reduced in both NovA and NovB after either vehicle (-0.19 vs. -0.06 Hz, respectively, relative to pre-injection baseline) or cannabinoid injection (-0.32 vs. -0.1 Hz, respectively). As with the peak firing rates, the mean firing rate changes of place cells reliably reflected changes in running speed. However in addition to this speed-related modulation of firing, there was a speed-independent reduction of both mean and peak place cell firing rates observed in novelty (i.e. the rate decreased even if there was no change in speed between the baseline and probe trials).

Previous studies of CA1 place cell activity in novelty have generally found little change in firing rate between familiar and novel environments (Wilson and McNaughton, 1993; Frank et al., 2004), although one study found elevated rates (Nitz and McNaughton, 2004). Additionally, interneuron rates are generally reported to be reduced by novelty (Wilson and McNaughton, 1993; Frank et al., 2004; Nitz and McNaughton, 2004). Nevertheless, the specific changes reported in each case are quite different. Whilst the McNaughton studies found a decrease in interneuron rates across 10 minute blocks of novel exploration, in the study of Frank and colleagues, this reduction was only apparent during the first minute of novel exploration and not during the rest of the 20-25 minute trial. This suggests that there was no significant change in interneuron firing rate across the whole trial, in line with the findings of this thesis. Frank and colleagues also found that place cells did not generally become active until around 1-2 minutes after the beginning of novel exploration. Thus, unless the firing rate was greatly elevated for the remainder of the trial then the overall mean rate would be lower (no place cell mean rate data were reported). Further analyses of the timecourse of place cell and

interneuron activity in the current study are required to examine if the duration of novel experience affected firing rate in a similar fashion. Overall, the variation in place cell and interneuron firing changes observed in the different studies suggest that the experimental setup employed may be critical to determining the precise outcome in each case.

9.5 Behavioural effects of cannabinoids and novelty

This study employed a low dose of cannabinoid to minimise the behavioural differences between drug and vehicle injections, in addition to ensuring it had an anxiolytic and not anxiogenic action. In the familiar environment, behaviour was very similar after either injection, with only a small, non-significant decrease in average speed due to the cannabinoid. The environmental coverage was also similar (data not shown), suggesting that this dose did not exert any major effects on motor or anxiety-related behaviours.

However, in the novel environment the behavioural differences were much more apparent, with the large increase in locomotor activity elicited by novelty alone substantially reduced by cannabinoid injection. Thigmotaxic behaviour in the enclosed novel environment (NovA) was actually non-significantly reduced by the cannabinoid, consistent with an anxiolytic action of the drug (Haller et al., 2004; Moreira and Wotjak, 2010). Therefore, this suggests that anxiety-related behavioural inhibition is unlikely to account for the speed decrease. Instead, the attenuation of locomotor activity may instead be due to changes in motivation or novelty-seeking behaviour.

Previous studies using a hole-board paradigm have found evidence of a cannabinoid-mediated impairment of novel hole exploration (Hernández-Tristán et al., 2000; Fox et al., 2009). However, these studies are confounded by the concurrent effects of the drug on memory and anxiety, so it is unclear whether cannabinoids do indeed inhibit novelty-seeking. An alternative explanation is that the decreased speed is the result of a general sedative effect on motor activity that only becomes apparent during excited behavioural states. As the highest densities of CB1 receptor expression are found in the basal ganglia (Herkenham et al., 1991), this seems a plausible explanation given the very low dose of cannabinoid employed in this study. However further behavioural and pharmacological work,

for example combining cannabinoids with dopaminergic or noradrenergic agents, is necessary to distinguish between these possible explanations.

9.6 Other topics for further investigation

9.6.1 Effects of novelty and cannabinoids on other frequency bands

In this thesis, I have focused on the effect of cannabinoids on theta-band activity in the hippocampus. However, there is ample evidence that they affect other frequency bands, decreasing the power of slow and fast gamma, and ripples (Robbe et al., 2006; Hajós et al., 2008; Holderith et al., 2011; Maier et al., 2011). The disruption of these oscillations may contribute to the spatial memory impairments elicited by cannabinoids, since they have been implicated in coordinating hippocampal encoding and retrieval (Colgin et al., 2009; Ego-Stengel and Wilson, 2010; O'Neill et al., 2010). Although there were no immediate effects on CA1 place cell remapping with the low dose of cannabinoid used, if there is reduced ripple activity during the post-trial consolidation period then the stability of the new place cell representations may be affected. Further studies are required to test if cannabinoids do indeed affect the long-term dynamics of newly-formed place cell representations.

Environmental novelty by itself has been found to modulate activity in a couple of other frequency bands, although the functions of these oscillations are not clear. Nerad and Bilkey (2005) reported a 10-12 Hz "flutter" oscillation that occurred during exploration of familiar but not novel environments in the rat. Interestingly, I also observed activity in this frequency band in 2 out of 6 rats. However, it occurred rarely and the conditions under which it was produced were not clear, making it difficult to study systematically. Berke and colleagues (2008) found 23-30 Hz oscillations during novel exploration in the mouse that were dependent on NMDA receptors in CA3. It is not known currently whether such oscillations also occur in the rat.

9.6.2 Relationship between intrinsic cell and theta frequencies in novelty

An important question to address is whether the relationship between instrinsic cell and LFP theta oscillations is maintained after changes to the theta frequency-speed relationship. According to the oscillatory interference model, the spatial scale of grid cells is determined by the interference of the cell oscillatory frequency with

the theta frequency. In order for the grid cell to maintain spatially stable firing fields regardless of the speed of the animal, the intrinsic oscillatory frequency must increase linearly above the theta frequency with speed. Novelty elicits a marked reduction in the slope of the theta frequency-speed relationship and an expansion of grid fields (Barry et al., 2009, SFN Abstract 101.24). This therefore offers an excellent opportunity to test whether the observed frequencies of grid cells and theta at different speeds in novelty match the grid scale predictions of the model.

9.7 Conclusions

The hippocampus has been implicated in the processing of novelty, anxiety and in spatial cognition. The experimental paradigm used in this thesis links these aspects of hippocampal functioning together based on the theta frequency-running speed relationship. I have demonstrated that this relationship has two dissociable components that are selectively affected by environmental novelty or a low dose of cannabinoid, used as an anxiolytic agent. The theta frequency-speed relationship may have important implications for how space is represented at different scales, how anxiety is integrated into cognition and how novelty drives the formation of new memories. Efficient memory encoding may also depend on a coordinated shift in the firing of hippocampal place cell ensembles relative to theta, which is disrupted by the cannabinoid. These findings help to elucidate the mechanisms of novelty processing in the hippocampus and extend our understanding of the roles of the theta oscillation in cognition and emotion.

10 References

Acquas E, Pisanu A, Marrocu P, Di Chiara G (2000) Cannabinoid CB(1) receptor agonists increase rat cortical and hippocampal acetylcholine release in vivo. Eur J Pharmacol 401:179–185.

Acquas E, Pisanu A, Marrocu P, Goldberg SR, Di Chiara G (2001) Delta9-tetrahydrocannabinol enhances cortical and hippocampal acetylcholine release in vivo: a microdialysis study. Eur J Pharmacol 419:155–161.

Adhikari A, Topiwala MA, Gordon JA (2010) Synchronized activity between the ventral hippocampus and the medial prefrontal cortex during anxiety. Neuron 65:257–269.

Ainge JA, Tamosiunaite M, Woergoetter F, Dudchenko PA (2007) Hippocampal CA1 place cells encode intended destination on a maze with multiple choice points. J Neurosci 27:9769–9779.

Akirav I (2011) The Role of Cannabinoids in Modulating Emotional and Non-Emotional Memory Processes in the Hippocampus. Front Behav Neurosci 5.

Ali AB (2007) Presynaptic Inhibition of GABAA receptor-mediated unitary IPSPs by cannabinoid receptors at synapses between CCK-positive interneurons in rat hippocampus. J Neurophysiol 98:861–869.

Amaral D, Lavenex P (2007) Hippocampal Neuroanatomy. In: The Hippocampus Book, pp.37–114. Oxford: Oxford University Press.

Amit DJ (1989) Modelling Brain Function: The World of Attractor Networks. New York: Cambridge University Press.

Anderson MI, O'Mara SM (2003) Analysis of recordings of single-unit firing and population activity in the dorsal subiculum of unrestrained, freely moving rats. J Neurophysiol 90:655–665.

Atri A, Sherman S, Norman KA, Kirchhoff BA, Nicolas MM, Greicius MD, Cramer SC, Breiter HC, Hasselmo ME, Stern CE (2004) Blockade of central cholinergic receptors impairs new learning and increases proactive interference in a word paired-associate memory task. Behav Neurosci 118:223–236.

Barnes CA, McNaughton BL, Mizumori SJ, Leonard BW, Lin LH (1990) Comparison of spatial and temporal characteristics of neuronal activity in sequential stages of hippocampal processing. Prog Brain Res 83:287–300.

Barry C, Hayman R, Burgess N, Jeffery KJ (2007) Experience-dependent rescaling of entorhinal grids. Nat Neurosci 10:682–684.

Barry C, O'Keefe J, Burgess N (2009) Effect of novelty on grid cell firing. Presented at the Society for Neuroscience Annual Meeting, Abstract 101.24.

Bast T, Wilson IA, Witter MP, Morris RGM (2009) From rapid place learning to behavioral performance: a key role for the intermediate hippocampus. PLoS Biol 7:e1000089.

Berke JD, Hetrick V, Breck J, Greene RW (2008) Transient 23-30 Hz oscillations in mouse hippocampus during exploration of novel environments. Hippocampus 18:519–529.

Bisogno T, Di Marzo V (2007) Short- and long-term plasticity of the endocannabinoid system in neuropsychiatric and neurological disorders. Pharmacol Res 56:428–442.

Black SC (2004) Cannabinoid receptor antagonists and obesity. Curr Opin Investig Drugs 5:389–394.

Blair HT, Cho J, Sharp PE (1998) Role of the lateral mammillary nucleus in the rat head direction circuit: a combined single unit recording and lesion study. Neuron 21:1387–1397.

Blair HT, Gupta K, Zhang K (2008) Conversion of a phase- to a rate-coded position signal by a three-stage model of theta cells, grid cells, and place cells. Hippocampus 18:1239–1255.

Blair HT, Welday AC, Zhang K (2007) Scale-invariant memory representations emerge from moiré interference between grid fields that produce theta oscillations: a computational model. J Neurosci 27:3211–3229.

Bland BH, Colom LV, Konopacki J, Roth SH (1988) Intracellular records of carbachol-induced theta rhythm in hippocampal slices. Brain Res 447:364–368.

Bland BH, Declerck S, Jackson J, Glasgow S, Oddie S (2007) Septohippocampal properties of N-methyl-D-aspartate-induced theta-band oscillation and synchrony. Synapse 61:185–197.

Bland BH, Oddie SD (1998) Anatomical, Electrophysiological and Pharmacological Studies of Ascending Brainstem Hippocampal Synchronizing Pathways. Neuroscience & Biobehavioral Reviews 22:259–273.

Bliss TV, Lomo T (1973) Long-lasting potentiation of synaptic transmission in the dentate area of the anaesthetized rabbit following stimulation of the perforant path. J Physiol (Lond) 232:331–356.

Blokland A, Honig W, Raaijmakers WG (1992) Effects of intra-hippocampal scopolamine injections in a repeated spatial acquisition task in the rat. Psychopharmacology (Berl) 109:373–376.

Boccara CN, Sargolini F, Thoresen VH, Solstad T, Witter MP, Moser EI, Moser M-B (2010) Grid cells in pre- and parasubiculum. Nat Neurosci 13:987–994.

Bostock E, Muller RU, Kubie JL (1991) Experience-dependent modifications of hippocampal place cell firing. Hippocampus 1:193–205.

Bragin A, Jandó G, Nádasdy Z, Hetke J, Wise K, Buzsáki G (1995) Gamma (40-100 Hz) oscillation in the hippocampus of the behaving rat. J Neurosci 15:47–60.

Brankack J, Stewart M, Fox SE (1993) Current source density analysis of the hippocampal theta rhythm: associated sustained potentials and candidate synaptic generators. Brain Res 615:310–327.

Brun VH, Leutgeb S, Wu H-Q, Schwarcz R, Witter MP, Moser EI, Moser M-B (2008a) Impaired spatial representation in CA1 after lesion of direct input from entorhinal cortex. Neuron 57:290–302.

Brun VH, Otnass MK, Molden S, Steffenach H-A, Witter MP, Moser M-B, Moser EI (2002) Place cells and place recognition maintained by direct entorhinal-hippocampal circuitry. Science 296:2243–2246.

Brun VH, Solstad T, Kjelstrup KB, Fyhn M, Witter MP, Moser EI, Moser M-B (2008b) Progressive increase in grid scale from dorsal to ventral medial entorhinal cortex. Hippocampus 18:1200–1212.

Bullock TH, Buzsáki G, McClune MC (1990) Coherence of compound field potentials reveals discontinuities in the CA1-subiculum of the hippocampus in freely-moving rats. Neuroscience 38:609–619.

Bunce JG, Sabolek HR, Chrobak JJ (2004) Intraseptal infusion of the cholinergic agonist carbachol impairs delayed-non-match-to-sample radial arm maze performance in the rat. Hippocampus 14:450–459.

Buonamici M, Young GA, Khazan N (1982) Effects of acute delta 9-THC administration on EEG and EEG power spectra in the rat. Neuropharmacology 21:825–829.

Burgalossi A, Herfst L, von Heimendahl M, Förste H, Haskic K, Schmidt M, Brecht M (2011) Microcircuits of functionally identified neurons in the rat medial entorhinal cortex. Neuron 70:773–786.

Burgess N (2008) Grid cells and theta as oscillatory interference: theory and predictions. Hippocampus 18:1157–1174.

Burgess N, Barry C, O'Keefe J (2007) An oscillatory interference model of grid cell firing. Hippocampus 17:801–812.

Burwell RD, Amaral DG (1998) Perirhinal and postrhinal cortices of the rat: interconnectivity and connections with the entorhinal cortex. J Comp Neurol 391:293–321.

Burwell RD, Witter MP, Amaral DG (1995) Perirhinal and postrhinal cortices of the rat: a review of the neuroanatomical literature and comparison with findings from the monkey brain. Hippocampus 5:390–408.

Buzsáki G (1986) Hippocampal sharp waves: their origin and significance. Brain Res 398:242–252.

Buzsáki G (2002) Theta Oscillations in the Hippocampus. Neuron 33:325–340.

Buzsáki G, Gage FH, Czopf J, Björklund A (1987) Restoration of rhythmic slow activity (theta) in the subcortically denervated hippocampus by fetal CNS transplants. Brain Res 400:334–347.

Buzsáki G, Grastyán E, Tveritskaya IN, Czopf J (1979) Hippocampal evoked potentials and EEG changes during classical conditioning in the rat. Electroencephalogr Clin Neurophysiol 47:64–74.

Buzsáki G, Leung LW, Vanderwolf CH (1983) Cellular bases of hippocampal EEG in the behaving rat. Brain Res 287:139–171.

Böcker KBE, Hunault CC, Gerritsen J, Kruidenier M, Mensinga TT, Kenemans JL (2010) Cannabinoid modulations of resting state EEG θ power and working memory are correlated in humans. J Cogn Neurosci 22:1906–1916.

Cabral GA, Raborn ES, Griffin L, Dennis J, Marciano-Cabral F (2008) CB2 receptors in the brain: role in central immune function. Br J Pharmacol 153:240–251.

Cacucci F, Lever C, Wills TJ, Burgess N, O'Keefe J (2004) Theta-modulated place-by-direction cells in the hippocampal formation in the rat. J Neurosci 24:8265–8277.

Carta G, Nava F, Gessa GL (1998) Inhibition of hippocampal acetylcholine release after acute and repeated Delta9-tetrahydrocannabinol in rats. Brain Res 809:1–4.

Cea-del Rio CA, Lawrence JJ, Tricoire L, Erdelyi F, Szabo G, McBain CJ (2010) M3 Muscarinic Acetylcholine Receptor Expression Confers Differential Cholinergic Modulation to Neurochemically Distinct Hippocampal Basket Cell Subtypes. The Journal of Neuroscience 30:6011–6024.

Chaperon F, Thiébot MH (1999) Behavioral effects of cannabinoid agents in animals. Crit Rev Neurobiol 13:243–281.

Chiang PH, Yeh WC, Lee CT, Weng JY, Huang YY, Lien CC (2010) M(1)-like muscarinic acetylcholine receptors regulate fast-spiking interneuron excitability in rat dentate gyrus. Neuroscience 169:39–51.

Chiu CQ, Castillo PE (2008) Input-specific plasticity at excitatory synapses mediated by endocannabinoids in the dentate gyrus. Neuropharmacology 54:68–78.

Cho J, Sharp PE (2001) Head direction, place, and movement correlates for cells in the rat retrosplenial cortex. Behav Neurosci 115:3–25.

Chrobak JJ, Buzsáki G (1998) Gamma oscillations in the entorhinal cortex of the freely behaving rat. J Neurosci 18:388–398.

Chávez AE, Chiu CQ, Castillo PE (2010) TRPV1 activation by endogenous anandamide triggers postsynaptic long-term depression in dentate gyrus. Nat Neurosci 13:1511–1518.

Clark BD, Goldberg EM, Rudy B (2009) Electrogenic tuning of the axon initial segment. Neuroscientist 15:651–668.

Cobb SR, Buhl EH, Halasy K, Paulsen O, Somogyi P (1995) Synchronization of neuronal activity in hippocampus by individual GABAergic interneurons. Nature 378:75–78.

Colgin LL, Denninger T, Fyhn M, Hafting T, Bonnevie T, Jensen O, Moser M-B, Moser EI (2009) Frequency of gamma oscillations routes flow of information in the hippocampus. Nature 462:353–357.

Colgin LL, Kramár EA, Gall CM, Lynch G (2003) Septal modulation of excitatory transmission in hippocampus. J Neurophysiol 90:2358–2366.

Colgin LL, Moser EI (2010) Gamma oscillations in the hippocampus. Physiology (Bethesda) 25:319–329.

Colom LV, Castaneda MT, Reyna T, Hernandez S, Garrido-Sanabria E (2005) Characterization of medial septal glutamatergic neurons and their projection to the hippocampus. Synapse 58:151–164.

Colom LV, Nassif-Caudarella S, Dickson CT, Smythe JW, Bland BH (1991) In vivo intrahippocampal microinfusion of carbachol and bicuculline induces theta-like oscillations in the septally deafferented hippocampus. Hippocampus 1:381–390.

Costall B, Naylor RJ, Tyers MB (1990) The psychopharmacology of 5-HT3 receptors. Pharmacol Ther 47:181–202.

Cota D (2008) The role of the endocannabinoid system in the regulation of hypothalamic-pituitary-adrenal axis activity. J Neuroendocrinol 20 Suppl 1:35–38.

Crawley JN, Corwin RL, Robinson JK, Felder CC, Devane WA, Axelrod J (1993) Anandamide, an endogenous ligand of the cannabinoid receptor, induces hypomotility and hypothermia in vivo in rodents. Pharmacol Biochem Behav 46:967–972.

Cressant A, Muller RU, Poucet B (1997) Failure of centrally placed objects to control the firing fields of hippocampal place cells. J Neurosci 17:2531–2542.

Csicsvari J, Hirase H, Czurko A, Buzsáki G (1998) Reliability and state dependence of pyramidal cell-interneuron synapses in the hippocampus: an ensemble approach in the behaving rat. Neuron 21:179–189.

Csicsvari J, Hirase H, Czurkó A, Mamiya A, Buzsáki G (1999a) Fast network oscillations in the hippocampal CA1 region of the behaving rat. J Neurosci 19:RC20.

Csicsvari J, Hirase H, Czurkó A, Mamiya A, Buzsáki G (1999b) Oscillatory Coupling of Hippocampal Pyramidal Cells and Interneurons in the Behaving Rat. The Journal of Neuroscience 19:274–287.

Csicsvari J, Jamieson B, Wise KD, Buzsáki G (2003) Mechanisms of gamma oscillations in the hippocampus of the behaving rat. Neuron 37:311–322.

Czurkó A, Hirase H, Csicsvari J, Buzsáki G (1999) Sustained activation of hippocampal pyramidal cells by “space clamping” in a running wheel. Eur J Neurosci 11:344–352.

Czurkó A, Huxter J, Li Y, Hangya B, Muller RU (2011) Theta phase classification of interneurons in the hippocampal formation of freely moving rats. J Neurosci 31:2938–2947.

Daw MI, Tricoire L, Erdelyi F, Szabo G, McBain CJ (2009) Asynchronous transmitter release from cholecystokinin-containing inhibitory interneurons is widespread and target-cell independent. J Neurosci 29:11112–11122.

Day JC, Fibiger HC (1994) Dopaminergic regulation of septohippocampal cholinergic neurons. J Neurochem 63:2086–2092.

Deboer T (2002) Electroencephalogram theta frequency changes in parallel with euthermic brain temperature. Brain Res 930:212–215.

Diana MA, Marty A (2004) Endocannabinoid-mediated short-term synaptic plasticity: depolarization-induced suppression of inhibition (DSI) and depolarization-induced suppression of excitation (DSE). Br J Pharmacol 142:9–19.

Diekelmann S, Born J (2010) The memory function of sleep. Nat Rev Neurosci 11:114–126.

Dolleman-van der Weel MJ, Morris RGM, Witter MP (2009) Neurotoxic lesions of the thalamic reuniens or mediodorsal nucleus in rats affect non-mnemonic aspects of watermaze learning. Brain Struct Funct 213:329–342.

Dong H-W, Swanson LW, Chen L, Fanselow MS, Toga AW (2009) Genomic-anatomic evidence for distinct functional domains in hippocampal field CA1. Proc Natl Acad Sci USA 106:11794–11799.

Düzel E, Bunzeck N, Guitart-Masip M, Düzel S (2010) NOvelty-related motivation of anticipation and exploration by dopamine (NOMAD): implications for healthy aging. Neurosci Biobehav Rev 34:660–669.

Ego-Stengel V, Wilson MA (2010) Disruption of ripple-associated hippocampal activity during rest impairs spatial learning in the rat. Hippocampus 20:1–10.

Elvander E, Schött PA, Sandin J, Bjelke B, Kehr J, Yoshitake T, Ogren SO (2004) Intraseptal muscarinic ligands and galanin: influence on hippocampal acetylcholine and cognition. Neuroscience 126:541–557.

Etienne AS, Jeffery KJ (2004) Path integration in mammals. Hippocampus 14:180–192.

Fanselow MS, Dong H-W (2010) Are the dorsal and ventral hippocampus functionally distinct structures? Neuron 65:7–19.

Fellous JM, Sejnowski TJ (2000) Cholinergic induction of oscillations in the hippocampal slice in the slow (0.5-2 Hz), theta (5-12 Hz), and gamma (35-70 Hz) bands. Hippocampus 10:187–197.

Fenton AA, Kao H-Y, Neymotin SA, Olypher A, Vayntrub Y, Lytton WW, Ludvig N (2008) Unmasking the CA1 ensemble place code by exposures to small and large environments: more place cells and multiple, irregularly arranged, and expanded place fields in the larger space. J Neurosci 28:11250–11262.

Fenton AA, Muller RU (1998) Place cell discharge is extremely variable during individual passes of the rat through the firing field. Proc Natl Acad Sci USA 95:3182–3187.

Fernández de Sevilla D, Cabezas C, de Prada ANO, Sánchez-Jiménez A, Buño W (2002) Selective muscarinic regulation of functional glutamatergic Schaffer collateral synapses in rat CA1 pyramidal neurons. J Physiol (Lond) 545:51–63.

Fernández-Ruiz J (2009) The endocannabinoid system as a target for the treatment of motor dysfunction. Br J Pharmacol 156:1029–1040.

Fernández-Ruiz J, Gonzáles S (2005) Cannabinoid control of motor function at the basal ganglia. Handb Exp Pharmacol:479–507.

Ferrari F, Ottani A, Vivoli R, Giuliani D (1999) Learning impairment produced in rats by the cannabinoid agonist HU 210 in a water-maze task. Pharmacol Biochem Behav 64:555–561.

Fox KM, Sterling RC, Van Bockstaele EJ (2009) Cannabinoids and novelty investigation: Influence of age and duration of exposure. Behavioural Brain Research 196:248–253.

Frank LM, Stanley GB, Brown EN (2004) Hippocampal plasticity across multiple days of exposure to novel environments. J Neurosci 24:7681–7689.

Frazier CJ, Rollins YD, Breese CR, Leonard S, Freedman R, Dunwiddie TV (1998) Acetylcholine activates an alpha-bungarotoxin-sensitive nicotinic current in rat hippocampal interneurons, but not pyramidal cells. J Neurosci 18:1187–1195.

Freedman R, Wetmore C, Strömberg I, Leonard S, Olson L (1993) Alpha-bungarotoxin binding to hippocampal interneurons: immunocytochemical characterization and effects on growth factor expression. J Neurosci 13:1965–1975.

Freund TF (1992) GABAergic septal and serotonergic median raphe afferents preferentially innervate inhibitory interneurons in the hippocampus and dentate gyrus. Epilepsy Res Suppl 7:79–91.

Freund TF (2003) Interneuron Diversity series: Rhythm and mood in perisomatic inhibition. Trends Neurosci 26:489–495.

Freund TF, Buzsáki G (1996) Interneurons of the hippocampus. Hippocampus 6:347–470.

Freund TF, Gulyás AI, Acsády L, Görcs T, Tóth K (1990) Serotonergic control of the hippocampus via local inhibitory interneurons. Proc Natl Acad Sci USA 87:8501–8505.

Freund TF, Katona I (2007) Perisomatic Inhibition. Neuron 56:33–42.

Freund TF, Katona I, Piomelli D (2003) Role of Endogenous Cannabinoids in Synaptic Signaling. Physiol Rev 83:1017–1066.

Fricker D, Miles R (2000) EPSP amplification and the precision of spike timing in hippocampal neurons. Neuron 28:559–569.

Fride E, Mechoulam R (1993) Pharmacological activity of the cannabinoid receptor agonist, anandamide, a brain constituent. Eur J Pharmacol 231:313–314.

Fride E, Perchuk A, Hall FS, Uhl GR, Onaivi ES (2006) Behavioral methods in cannabinoid research. Methods Mol Med 123:269–290.

Fuhs MC, Touretzky DS (2006) A spin glass model of path integration in rat medial entorhinal cortex. J Neurosci 26:4266–4276.

Fukudome Y, Ohno-Shosaku T, Matsui M, Omori Y, Fukaya M, Tsubokawa H, Taketo MM, Watanabe M, Manabe T, Kano M (2004) Two distinct classes of muscarinic action on hippocampal inhibitory synapses: M2-mediated direct suppression and M1/M3-mediated indirect suppression through endocannabinoid signalling. Eur J Neurosci 19:2682–2692.

Furtak SC, Wei S-M, Agster KL, Burwell RD (2007) Functional neuroanatomy of the parahippocampal region in the rat: the perirhinal and postrhinal cortices. Hippocampus 17:709–722.

Fyhn M, Hafting T, Treves A, Moser M-B, Moser EI (2007) Hippocampal remapping and grid realignment in entorhinal cortex. Nature 446:190–194.

Fyhn M, Molden S, Witter MP, Moser EI, Moser M-B (2004) Spatial representation in the entorhinal cortex. Science 305:1258–1264.

Férézou I, Cauli B, Hill EL, Rossier J, Hamel E, Lambolez B (2002) 5-HT3 receptors mediate serotonergic fast synaptic excitation of neocortical vasoactive intestinal peptide/cholecystokinin interneurons. J Neurosci 22:7389–7397.

Földy C, Lee SY, Szabadics J, Neu A, Soltesz I (2007) Cell type-specific gating of perisomatic inhibition by cholecystokinin. Nat Neurosci 10:1128–1130.

Gardner EL (2005) Endocannabinoid signaling system and brain reward: emphasis on dopamine. Pharmacol Biochem Behav 81:263–284.

Gaztelu JM, Buño W Jr (1982) Septo-hippocampal relationships during EEG theta rhythm. Electroencephalogr Clin Neurophysiol 54:375–387.

Geisler C, Robbe D, Zugaro M, Sirota A, Buzsáki G (2007) Hippocampal place cell assemblies are speed-controlled oscillators. Proc Natl Acad Sci USA 104:8149–8154.

Gemma C, Imeri L, Mancia M (1999) Hippocampal type 1 (movement-related) theta rhythm positively correlates with serotonergic activity. Arch Ital Biol 137:151–160.

Gessa GL, Casu MA, Carta G, Mascia MS (1998) Cannabinoids decrease acetylcholine release in the medial-prefrontal cortex and hippocampus, reversal by SR 141716A. Eur J Pharmacol 355:119–124.

Gibson HE, Edwards JG, Page RS, Van Hook MJ, Kauer JA (2008) TRPV1 channels mediate long-term depression at synapses on hippocampal interneurons. Neuron 57:746–759.

Gifford AN, Ashby CR Jr (1996) Electrically evoked acetylcholine release from hippocampal slices is inhibited by the cannabinoid receptor agonist, WIN 55212-2, and is potentiated by the cannabinoid antagonist, SR 141716A. J Pharmacol Exp Ther 277:1431–1436.

Giocomo LM, Zilli EA, Fransén E, Hasselmo ME (2007) Temporal frequency of subthreshold oscillations scales with entorhinal grid cell field spacing. Science 315:1719–1722.

Giovannini MG, Rakovska A, Benton RS, Pazzagli M, Bianchi L, Pepeu G (2001) Effects of novelty and habituation on acetylcholine, GABA, and glutamate release from the frontal cortex and hippocampus of freely moving rats. Neuroscience 106:43–53.

Girardeau G, Benchenane K, Wiener SI, Buzsáki G, Zugaro MB (2009) Selective suppression of hippocampal ripples impairs spatial memory. Nat Neurosci 12:1222–1223.

Givens B, Olton DS (1995) Bidirectional modulation of scopolamine-induced working memory impairments by muscarinic activation of the medial septal area. Neurobiol Learn Mem 63:269–276.

Glass M, Dragunow M, Faull RL (1997) Cannabinoid receptors in the human brain: a detailed anatomical and quantitative autoradiographic study in the fetal, neonatal and adult human brain. Neuroscience 77:299–318.

Glickfeld LL, Scanziani M (2006) Distinct timing in the activity of cannabinoid-sensitive and cannabinoid-insensitive basket cells. Nat Neurosci 9:807–815.

Gordon JA, Lacefield CO, Kentros CG, Hen R (2005) State-dependent alterations in hippocampal oscillations in serotonin 1A receptor-deficient mice. J Neurosci 25:6509–6519.

Gothard KM, Skaggs WE, Moore KM, McNaughton BL (1996) Binding of hippocampal CA1 neural activity to multiple reference frames in a landmark-based navigation task. J Neurosci 16:823–835.

Gray JA, McNaughton N (2000) The neuropsychology of anxiety. Oxford: Oxford University Press.

Gray JA, McNaughton N, James DT, Kelly PH (1975) Effect of minor tranquillisers on hippocampal theta rhythm mimicked by depletion of forebrain noradrenaline. Nature 258:424–425.

Green JD, Arduini AA (1954) Hippocampal electrical activity in arousal. J Neurophysiol 17:533–557.

Griffin G, Atkinson PJ, Showalter VM, Martin BR, Abood ME (1998) Evaluation of cannabinoid receptor agonists and antagonists using the guanosine-5'-O-(3-[35S]thio)-triphosphate binding assay in rat cerebellar membranes. J Pharmacol Exp Ther 285:553–560.

Gulyás AI, Hájos N, Freund TF (1996) Interneurons containing calretinin are specialized to control other interneurons in the rat hippocampus. J Neurosci 16:3397–3411.

Gulyás AI, Megías M, Emri Z, Freund TF (1999) Total number and ratio of excitatory and inhibitory synapses converging onto single interneurons of different types in the CA1 area of the rat hippocampus. J Neurosci 19:10082–10097.

Hafting T, Fyhn M, Bonnevie T, Moser M-B, Moser EI (2008) Hippocampus-independent phase precession in entorhinal grid cells. Nature 453:1248–1252.

Hafting T, Fyhn M, Molden S, Moser M-B, Moser EI (2005) Microstructure of a spatial map in the entorhinal cortex. Nature 436:801–806.

Hajós M, Hoffmann WE, Kocsis B (2008) Activation of Cannabinoid-1 Receptors Disrupts Sensory Gating and Neuronal Oscillation: Relevance to Schizophrenia. Biological Psychiatry 63:1075–1083.

Haller J, Barna I, Barsvari B, Gyimesi Pelczer K, Yasar S, Panlilio LV, Goldberg S (2009) Interactions between environmental aversiveness and the anxiolytic effects of enhanced cannabinoid signaling by FAAH inhibition in rats. Psychopharmacology (Berl) 204:607–616.

Haller J, Varga B, Ledent C, Freund TF (2004) CB1 cannabinoid receptors mediate anxiolytic effects: convergent genetic and pharmacological evidence with CB1-specific agents. Behav Pharmacol 15:299–304.

Hampson RE, Deadwyler SA (2000) Cannabinoids reveal the necessity of hippocampal neural encoding for short-term memory in rats. J Neurosci 20:8932–8942.

Hangya B, Borhegyi Z, Szilagyi N, Freund TF, Varga V (2009) GABAergic Neurons of the Medial Septum Lead the Hippocampal Network during Theta Activity. J Neurosci 29:8094–8102.

Hangya B, Li Y, Muller RU, Czurkó A (2010) Complementary spatial firing in place cell-interneuron pairs. J Physiol (Lond) 588:4165–4175.

Hargreaves EL, Rao G, Lee I, Knierim JJ (2005) Major dissociation between medial and lateral entorhinal input to dorsal hippocampus. Science 308:1792–1794.

Harkany T, Härtig W, Berghuis P, Dobszay MB, Zilberter Y, Edwards RH, Mackie K, Ernfors P (2003) Complementary distribution of type 1 cannabinoid receptors and vesicular glutamate transporter 3 in basal forebrain suggests input-specific retrograde signalling by cholinergic neurons. Eur J Neurosci 18:1979–1992.

Harris KD, Henze DA, Hirase H, Leinekugel X, Dragoi G, Czurko A, Buzsaki G (2002) Spike train dynamics predicts theta-related phase precession in hippocampal pyramidal cells. Nature 417:738–741.

Harris KD, Hirase H, Leinekugel X, Henze DA, Buzsáki G (2001) Temporal interaction between single spikes and complex spike bursts in hippocampal pyramidal cells. Neuron 32:141–149.

Harro J, Vasar E, Bradwejn J (1993) CCK in animal and human research on anxiety. Trends Pharmacol Sci 14:244–249.

Hasselmo ME (2006) The Role of Acetylcholine in Learning and Memory. Curr Opin Neurobiol 16:710–715.

Hasselmo ME (2008) Grid cell mechanisms and function: contributions of entorhinal persistent spiking and phase resetting. Hippocampus 18:1213–1229.

Hasselmo ME, Bodelón C, Wyble BP (2002) A proposed function for hippocampal theta rhythm: separate phases of encoding and retrieval enhance reversal of prior learning. Neural Comput 14:793–817.

Hasselmo ME, McGaughy J (2004) High acetylcholine levels set circuit dynamics for attention and encoding and low acetylcholine levels set dynamics for consolidation. Prog Brain Res 145:207–231.

Hasselmo ME, Sarter M (2011) Modes and models of forebrain cholinergic neuromodulation of cognition. Neuropsychopharmacology 36:52–73.

Hasselmo ME, Schnell E (1994) Laminar selectivity of the cholinergic suppression of synaptic transmission in rat hippocampal region CA1: computational modeling and brain slice physiology. J Neurosci 14:3898–3914.

Hasselmo ME, Stern CE (2006) Mechanisms underlying working memory for novel information. Trends Cogn Sci (Regul Ed) 10:487–493.

Hefft S, Jonas P (2005) Asynchronous GABA release generates long-lasting inhibition at a hippocampal interneuron-principal neuron synapse. Nat Neurosci 8:1319–1328.

Henriksen EJ, Colgin LL, Barnes CA, Witter MP, Moser M-B, Moser EI (2010) Spatial representation along the proximodistal axis of CA1. Neuron 68:127–137.

Henze DA, Borhegyi Z, Csicsvari J, Mamiya A, Harris KD, Buzsáki G (2000) Intracellular features predicted by extracellular recordings in the hippocampus in vivo. J Neurophysiol 84:390–400.

Herkenham M, Lynn AB, Johnson MR, Melvin LS, de Costa BR, Rice KC (1991) Characterization and localization of cannabinoid receptors in rat brain: a quantitative in vitro autoradiographic study. J Neurosci 11:563–583.

Hernández-Tristán R, Arévalo C, Canals S, Leret ML (2000) The effects of acute treatment with delta9-THC on exploratory behaviour and memory in the rat. J Physiol Biochem 56:17–24.

Hetherington PA, Shapiro ML (1997) Hippocampal place fields are altered by the removal of single visual cues in a distance-dependent manner. Behav Neurosci 111:20–34.

Heyser CJ, Hampson RE, Deadwyler SA (1993) Effects of delta-9-tetrahydrocannabinol on delayed match to sample performance in rats: alterations in short-term memory associated with changes in task specific firing of hippocampal cells. J Pharmacol Exp Ther 264:294–307.

Hill MN, Froese LM, Morrish AC, Sun JC, Floresco SB (2006) Alterations in behavioral flexibility by cannabinoid CB1 receptor agonists and antagonists. Psychopharmacology (Berl) 187:245–259.

Hirase H, Czurkó A, Csicsvari J, Buzsaki G (1999) Firing rate and theta-phase coding by hippocampal pyramidal neurons during “space clamping.” Eur J Neurosci 11:4373–4380.

Hok V, Lenck-Santini P-P, Roux S, Save E, Muller RU, Poucet B (2007) Goal-related activity in hippocampal place cells. J Neurosci 27:472–482.

Holderith N, Nemeth B, Papp OI, Veres JM, Nagy GA, Hajos N (2011) Cannabinoids attenuate hippocampal gamma oscillations by suppressing excitatory synaptic input onto CA3 pyramidal neurons and fast spiking basket cells. The Journal of Physiology Available at: http://www.ncbi.nlm.nih.gov/pubmed/21859823 [Accessed September 11, 2011].

Hollup SA, Molden S, Donnett JG, Moser MB, Moser EI (2001) Accumulation of hippocampal place fields at the goal location in an annular watermaze task. J Neurosci 21:1635–1644.

Hopfield JJ (1982) Neural networks and physical systems with emergent collective computational abilities. Proc Natl Acad Sci USA 79:2554–2558.

Horvath Z, Kamondi A, Czopf J, Bliss T, Buzsaki G (1988) NMDA receptors may be involved in generation of hippocampal theta rhythm. In: Synaptic Plasticity in the Hippocampus (Haas H, Buzsaki G, eds), pp.45. Berlin: Springer-Verlag.

Hounsgaard J (1978) Presynaptic inhibitory action of acetylcholine in area CA1 of the hippocampus. Exp Neurol 62:787–797.

Howlett AC (2002) The cannabinoid receptors. Prostaglandins & Other Lipid Mediators 68-69:619–631.

Howlett AC, Breivogel CS, Childers SR, Deadwyler SA, Hampson RE, Porrino LJ (2004) Cannabinoid physiology and pharmacology: 30 years of progress. Neuropharmacology 47:345–358.

Huerta PT, Lisman JE (1993) Heightened synaptic plasticity of hippocampal CA1 neurons during a cholinergically induced rhythmic state. Nature 364:723–725.

Huxter J, Burgess N, O'Keefe J (2003) Independent rate and temporal coding in hippocampal pyramidal cells. Nature 425:828–832.

Huxter JR, Senior TJ, Allen K, Csicsvari J (2008) Theta phase-specific codes for two-dimensional position, trajectory and heading in the hippocampus. Nat Neurosci 11:587–594.

Hájos N, Papp EC, Acsády L, Levey AI, Freund TF (1998) Distinct interneuron types express m2 muscarinic receptor immunoreactivity on their dendrites or axon terminals in the hippocampus. Neuroscience 82:355–376.

Hölscher C, Anwyl R, Rowan MJ (1997) Stimulation on the positive phase of hippocampal theta rhythm induces long-term potentiation that can Be depotentiated by stimulation on the negative phase in area CA1 in vivo. J Neurosci 17:6470–6477.

Jackson J, Bland BH (2006) Medial septal modulation of the ascending brainstem hippocampal synchronizing pathways in the anesthetized rat. Hippocampus 16:1–10.

Jeewajee A, Barry C, O'Keefe J, Burgess N (2008a) Grid cells and theta as oscillatory interference: electrophysiological data from freely moving rats. Hippocampus 18:1175–1185.

Jeewajee A, Lever C, Burton S, O'Keefe J, Burgess N (2008b) Environmental novelty is signaled by reduction of the hippocampal theta frequency. Hippocampus 18:340–348.

Jensen O, Lisman JE (2000) Position reconstruction from an ensemble of hippocampal place cells: contribution of theta phase coding. J Neurophysiol 83:2602–2609.

Jentsch JD, Andrusiak E, Tran A, Bowers MB, Roth RH (1997) Delta 9-tetrahydrocannabinol increases prefrontal cortical catecholaminergic utilization and impairs spatial working memory in the rat: blockade of dopaminergic effects with HA966. Neuropsychopharmacology 16:426–432.

Jezek K, Treves A, Moser M-B, Moser EI (2010) Theta oscillation control for segregation of spatial memories. Presented at the Federation for European Neuroscience Symposium, Abstract 087.29.

Jones BJ, Costall B, Domeney AM, Kelly ME, Naylor RJ, Oakley NR, Tyers MB (1988) The potential anxiolytic activity of GR38032F, a 5-HT3-receptor antagonist. Br J Pharmacol 93:985–993.

Järbe TU, Hiltunen AJ (1987) Cannabimimetic activity of cannabinol in rats and pigeons. Neuropharmacology 26:219–228.

Järbe TU, Sheppard R, Lamb RJ, Makriyannis A, Lin S, Goutopoulos A (1998) Effects of delta-9-tetrahydrocannabinol and (R)-methanandamide on open-field behavior in rats. Behav Pharmacol 9:169–174.

Kamondi A, Acsády L, Wang XJ, Buzsáki G (1998) Theta oscillations in somata and dendrites of hippocampal pyramidal cells in vivo: activity-dependent phase-precession of action potentials. Hippocampus 8:244–261.

Katona I, Sperlágh B, Sík A, Käfalvi A, Vizi ES, Mackie K, Freund TF (1999) Presynaptically located CB1 cannabinoid receptors regulate GABA release from axon terminals of specific hippocampal interneurons. J Neurosci 19:4544–4558.

Kawaguchi Y, Katsumaru H, Kosaka T, Heizmann CW, Hama K (1987) Fast spiking cells in rat hippocampus (CA1 region) contain the calcium-binding protein parvalbumin. Brain Res 416:369–374.

Kawamura Y, Fukaya M, Maejima T, Yoshida T, Miura E, Watanabe M, Ohno-Shosaku T, Kano M (2006) The CB1 cannabinoid receptor is the major cannabinoid receptor at excitatory presynaptic sites in the hippocampus and cerebellum. J Neurosci 26:2991–3001.

King C, Recce M, O'Keefe J (1998) The rhythmicity of cells of the medial septum/diagonal band of Broca in the awake freely moving rat: relationships with behaviour and hippocampal theta. Eur J Neurosci 10:464–477.

Kirk IJ (1998) Frequency modulation of hippocampal theta by the supramammillary nucleus, and other hypothalamo-hippocampal interactions: mechanisms and functional implications. Neurosci Biobehav Rev 22:291–302.

Kirk IJ, McNaughton N (1991) Supramammillary cell firing and hippocampal rhythmical slow activity. Neuroreport 2:723–725.

Kjelstrup KB, Solstad T, Brun VH, Hafting T, Leutgeb S, Witter MP, Moser EI, Moser M-B (2008) Finite scale of spatial representation in the hippocampus. Science 321:140–143.

Klausberger T (2009) GABAergic interneurons targeting dendrites of pyramidal cells in the CA1 area of the hippocampus. Eur J Neurosci 30:947–957.

Klausberger T, Magill PJ, Márton LF, Roberts JDB, Cobden PM, Buzsáki G, Somogyi P (2003) Brain-state- and cell-type-specific firing of hippocampal interneurons in vivo. Nature 421:844–848.

Klausberger T, Marton LF, O'Neill J, Huck JHJ, Dalezios Y, Fuentealba P, Suen WY, Papp E, Kaneko T, Watanabe M, Csicsvari J, Somogyi P (2005) Complementary roles of cholecystokinin- and parvalbumin-expressing GABAergic neurons in hippocampal network oscillations. J Neurosci 25:9782–9793.

Klausberger T, Márton LF, Baude A, Roberts JDB, Magill PJ, Somogyi P (2004) Spike timing of dendrite-targeting bistratified cells during hippocampal network oscillations in vivo. Nat Neurosci 7:41–47.

Klausberger T, Roberts JDB, Somogyi P (2002) Cell type- and input-specific differences in the number and subtypes of synaptic GABA(A) receptors in the hippocampus. J Neurosci 22:2513–2521.

Klausberger T, Somogyi P (2008) Neuronal diversity and temporal dynamics: the unity of hippocampal circuit operations. Science 321:53–57.

Kloosterman F, van Haeften T, Lopes da Silva FH (2004) Two reentrant pathways in the hippocampal-entorhinal system. Hippocampus 14:1026–1039.

Kocsis B, Bragin A, Buzsáki G (1999) Interdependence of multiple theta generators in the hippocampus: a partial coherence analysis. J Neurosci 19:6200–6212.

Konopacki J, Bland BH, MacIver MB, Roth SH (1987) Cholinergic theta rhythm in transected hippocampal slices: independent CA1 and dentate generators. Brain Res 436:217–222.

Kosaka T, Katsumaru H, Hama K, Wu JY, Heizmann CW (1987) GABAergic neurons containing the Ca2+-binding protein parvalbumin in the rat hippocampus and dentate gyrus. Brain Res 419:119–130.

Kramis R, Vanderwolf CH, Bland BH (1975) Two types of hippocampal rhythmical slow activity in both the rabbit and the rat: relations to behavior and effects of atropine, diethyl ether, urethane, and pentobarbital. Exp Neurol 49:58–85.

Krout KE, Belzer RE, Loewy AD (2002) Brainstem projections to midline and intralaminar thalamic nuclei of the rat. J Comp Neurol 448:53–101.

Kumaran D, Maguire EA (2006) An Unexpected Sequence of Events: Mismatch Detection in the Human Hippocampus. PLoS Biol 4.

Lafenêtre P, Chaouloff F, Marsicano G (2007) The endocannabinoid system in the processing of anxiety and fear and how CB1 receptors may modulate fear extinction. Pharmacol Res 56:367–381.

Lee I, Hunsaker MR, Kesner RP (2005) The role of hippocampal subregions in detecting spatial novelty. Behav Neurosci 119:145–153.

Lee I, Yoganarasimha D, Rao G, Knierim JJ (2004) Comparison of population coherence of place cells in hippocampal subfields CA1 and CA3. Nature 430:456–459.

Lee S-H, Földy C, Soltesz I (2010) Distinct endocannabinoid control of GABA release at perisomatic and dendritic synapses in the hippocampus. J Neurosci 30:7993–8000.

Lenck-Santini P-P, Rivard B, Muller RU, Poucet B (2005) Study of CA1 place cell activity and exploratory behavior following spatial and nonspatial changes in the environment. Hippocampus 15:356–369.

Leung LW, Yim CY (1991) Intrinsic membrane potential oscillations in hippocampal neurons in vitro. Brain Res 553:261–274.

Leutgeb JK, Leutgeb S, Moser M-B, Moser EI (2007) Pattern separation in the dentate gyrus and CA3 of the hippocampus. Science 315:961–966.

Leutgeb JK, Leutgeb S, Treves A, Meyer R, Barnes CA, McNaughton BL, Moser M-B, Moser EI (2005a) Progressive transformation of hippocampal neuronal representations in "morphed" environments. Neuron 48:345–358.

Leutgeb JK, Moser EI (2007) Enigmas of the dentate gyrus. Neuron 55:176–178.

Leutgeb S, Leutgeb JK, Barnes CA, Moser EI, McNaughton BL, Moser M-B (2005b) Independent codes for spatial and episodic memory in hippocampal neuronal ensembles. Science 309:619–623.

Leutgeb S, Leutgeb JK, Treves A, Moser M-B, Moser EI (2004) Distinct ensemble codes in hippocampal areas CA3 and CA1. Science 305:1295–1298.

Lever C, Burton S, Jeewajee A, O'Keefe J, Burgess N (2009) Boundary vector cells in the subiculum of the hippocampal formation. J Neurosci 29:9771–9777.

Lever C, Burton S, Jeewajee A, Wills TJ, Cacucci F, Burgess N, O'Keefe J (2010) Environmental novelty elicits a later theta phase of firing in CA1 but not subiculum. Hippocampus 20:229–234.

Lever C, Burton S, O'Keefe J (2006) Rearing on hind legs, environmental novelty, and the hippocampal formation. Rev Neurosci 17:111–133.

Lever C, Wills T, Cacucci F, Burgess N, O'Keefe J (2002) Long-term plasticity in hippocampal place-cell representation of environmental geometry. Nature 416:90–94.

Li XG, Somogyi P, Ylinen A, Buzsáki G (1994) The hippocampal CA3 network: an in vivo intracellular labeling study. J Comp Neurol 339:181–208.

Lichtman A, Dimen K, Martin B (1995) Systemic or intrahippocampal cannabinoid administration impairs spatial memory in rats. Psychopharmacology 119:282–290.

Lindvall O, Stenevi U (1978) Dopamine and noradrenaline neurons projecting to the septal area in the rat. Cell Tissue Res 190:383–407.

Lisman J (2005) The theta/gamma discrete phase code occuring during the hippocampal phase precession may be a more general brain coding scheme. Hippocampus 15:913–922.

Llano I, Leresche N, Marty A (1991) Calcium entry increases the sensitivity of cerebellar Purkinje cells to applied GABA and decreases inhibitory synaptic currents. Neuron 6:565–574.

Lubenov EV, Siapas AG (2009) Hippocampal theta oscillations are travelling waves. Nature 459:534–539.

Léránth C, Frotscher M (1987) Cholinergic innervation of hippocampal GAD- and somatostatin-immunoreactive commissural neurons. J Comp Neurol 261:33–47.

Löw K, Crestani F, Keist R, Benke D, Brünig I, Benson JA, Fritschy JM, Rülicke T, Bluethmann H, Möhler H, Rudolph U (2000) Molecular and neuronal substrate for the selective attenuation of anxiety. Science 290:131–134.

Maejima T, Hashimoto K, Yoshida T, Aiba A, Kano M (2001) Presynaptic inhibition caused by retrograde signal from metabotropic glutamate to cannabinoid receptors. Neuron 31:463–475.

Maier N, Morris G, Schuchmann S, Korotkova T, Ponomarenko A, Böhm C, Wozny C, Schmitz D (2011) Cannabinoids disrupt hippocampal sharp wave-ripples via inhibition of glutamate release. Hippocampus Available at: http://www.ncbi.nlm.nih.gov/pubmed/21853502 [Accessed September 13, 2011].

Mailleux P, Vanderhaeghen JJ (1992) Distribution of neuronal cannabinoid receptor in the adult rat brain: a comparative receptor binding radioautography and in situ hybridization histochemistry. Neuroscience 48:655–668.

Manns JR, Zilli EA, Ong KC, Hasselmo ME, Eichenbaum H (2007) Hippocampal CA1 spiking during encoding and retrieval: relation to theta phase. Neurobiol Learn Mem 87:9–20.

Manseau F, Goutagny R, Danik M, Williams S (2008) The hippocamposeptal pathway generates rhythmic firing of GABAergic neurons in the medial septum and diagonal bands: an investigation using a complete septohippocampal preparation in vitro. J Neurosci 28:4096–4107.

Mansour AAH, Babstock DM, Penney JH, Martin GM, McLean JH, Harley CW (2003) Novel objects in a holeboard probe the role of the locus coeruleus in curiosity: support for two modes of attention in the rat. Behav Neurosci 117:621–631.

Markus EJ, Qin YL, Leonard B, Skaggs WE, McNaughton BL, Barnes CA (1995) Interactions between location and task affect the spatial and directional firing of hippocampal neurons. J Neurosci 15:7079–7094.

Marr D (1971) Simple memory: a theory for archicortex. Philos Trans R Soc Lond, B, Biol Sci 262:23–81.

Marsicano G, Lutz B (1999) Expression of the cannabinoid receptor CB1 in distinct neuronal subpopulations in the adult mouse forebrain. Eur J Neurosci 11:4213–4225.

Martin BR, Wiley JL, Beletskaya I, Sim-Selley LJ, Smith FL, Dewey WL, Cottney J, Adams J, Baker J, Hill D, Saha B, Zerkowski J, Mahadevan A, Razdan RK (2006) Pharmacological Characterization of Novel Water-Soluble Cannabinoids. Journal of Pharmacology and Experimental Therapeutics 318:1230–1239.

Martin LA, Alger BE (1999) Muscarinic facilitation of the occurrence of depolarization-induced suppression of inhibition in rat hippocampus. Neuroscience 92:61–71.

Maru E, Takahashi LK, Iwahara S (1979) Effects of median raphe nucleus lesions on hippocampal EEG in the freely moving rat. Brain Res 163:223–234.

Di Marzo V, Fontana A, Cadas H, Schinelli S, Cimino G, Schwartz JC, Piomelli D (1994) Formation and inactivation of endogenous cannabinoid anandamide in central neurons. Nature 372:686–691.

Di Marzo V, Lastres-Becker I, Bisogno T, De Petrocellis L, Milone A, Davis JB, Fernandez-Ruiz JJ (2001) Hypolocomotor effects in rats of capsaicin and two long chain capsaicin homologues. Eur J Pharmacol 420:123–131.

Matsuda LA, Bonner TI, Lolait SJ (1993) Localization of cannabinoid receptor mRNA in rat brain. The Journal of Comparative Neurology 327:535–550.

Maurer AP, Vanrhoads SR, Sutherland GR, Lipa P, McNaughton BL (2005) Self-motion and the origin of differential spatial scaling along the septo-temporal axis of the hippocampus. Hippocampus 15:841–852.

McFarland WL, Teitelbaum H, Hedges EK (1975) Relationship between hippocampal theta activity and running speed in the rat. Journal of Comparative and Physiological Psychology 88:324–328.

McNaughton BL, Barnes CA, O'Keefe J (1983) The contributions of position, direction, and velocity to single unit activity in the hippocampus of freely-moving rats. Exp Brain Res 52:41–49.

McNaughton BL, Battaglia FP, Jensen O, Moser EI, Moser M-B (2006a) Path integration and the neural basis of the "cognitive map." Nat Rev Neurosci 7:663–678.

McNaughton N, Kocsis B, Hajós M (2007) Elicited hippocampal theta rhythm: a screen for anxiolytic and procognitive drugs through changes in hippocampal function? Behav Pharmacol 18:329–346.

McNaughton N, Ruan M, Woodnorth M-A (2006b) Restoring theta-like rhythmicity in rats restores initial learning in the Morris water maze. Hippocampus 16:1102–1110.

Mechoulam R (1986) The pharmacohistory of Cannabis sativa. In: Cannabinoids as Therapeutic Agents, pp.1–19. Boca Raton, FL: CRC Press.

Mechoulam R, Braun P, Gaoni Y (1967) A stereospecific synthesis of (-)-delta 1- and (-)-delta 1(6)-tetrahydrocannabinols. J Am Chem Soc 89:4552–4554.

Mechoulam R, Gaoni Y (1967) The absolute configuration of delta-1-tetrahydrocannabinol, the major active constituent of hashish. Tetrahedron Lett 12:1109–1111.

Megías M, Emri Z, Freund TF, Gulyás AI (2001) Total number and distribution of inhibitory and excitatory synapses on hippocampal CA1 pyramidal cells. Neuroscience 102:527–540.

Mehta MR, Barnes CA, McNaughton BL (1997) Experience-dependent, asymmetric expansion of hippocampal place fields. Proc Natl Acad Sci USA 94:8918–8921.

Mendiguren A, Pineda J (2006) Systemic effect of cannabinoids on the spontaneous firing rate of locus coeruleus neurons in rats. Eur J Pharmacol 534:83–88.

Mitzdorf U (1985) Current source-density method and application in cat cerebral cortex: investigation of evoked potentials and EEG phenomena. Physiol Rev 65:37–100.

Mizuseki K, Diba K, Pastalkova E, Buzsáki G (2011) Hippocampal CA1 pyramidal cells form functionally distinct sublayers. Nat Neurosci 14:1174–1181.

Mizuseki K, Sirota A, Pastalkova E, Buzsáki G (2009) Theta oscillations provide temporal windows for local circuit computation in the entorhinal-hippocampal loop. Neuron 64:267–280.

Molina-Holgado F, González MI, Leret ML (1995) Effect of delta 9-tetrahydrocannabinol on short-term memory in the rat. Physiol Behav 57:177–179.

Monmaur P, Breton P (1991) Elicitation of hippocampal theta by intraseptal carbachol injection in freely moving rats. Brain Res 544:150–155.

Morales M, Bloom FE (1997) The 5-HT3 receptor is present in different subpopulations of GABAergic neurons in the rat telencephalon. J Neurosci 17:3157–3167.

Morales M, Hein K, Vogel Z (2008) Hippocampal interneurons co-express transcripts encoding the [alpha]7 nicotinic receptor subunit and the cannabinoid receptor 1. Neuroscience 152:70–81.

Moreira FA, Lutz B (2008) The endocannabinoid system: emotion, learning and addiction. Addict Biol 13:196–212.

Moreira FA, Wotjak CT (2010) Cannabinoids and anxiety. Curr Top Behav Neurosci 2:429–450.

Morgan NH, Stanford IM, Woodhall GL (2008) Modulation of network oscillatory activity and GABAergic synaptic transmission by CB1 cannabinoid receptors in the rat medial entorhinal cortex. Neural Plast 2008:808564.

Moriconi A, Cerbara I, Maccarrone M, Topai A (2010) GPR55: Current knowledge and future perspectives of a purported "Type-3" cannabinoid receptor. Curr Med Chem 17:1411–1429.

Moser EI, Kropff E, Moser M-B (2008) Place cells, grid cells, and the brain's spatial representation system. Annu Rev Neurosci 31:69–89.

Moser EI, Moser M-B (2008) A metric for space. Hippocampus 18:1142–1156.

Moser MB, Moser EI (1998) Functional differentiation in the hippocampus. Hippocampus 8:608–619.

Muller R (1996) A quarter of a century of place cells. Neuron 17:813–822.

Muller RU, Bostock E, Taube JS, Kubie JL (1994) On the directional firing properties of hippocampal place cells. J Neurosci 14:7235–7251.

Muller RU, Kubie JL (1987) The effects of changes in the environment on the spatial firing of hippocampal complex-spike cells. J Neurosci 7:1951–1968.

Muller RU, Kubie JL, Ranck JB Jr (1987) Spatial firing patterns of hippocampal complex-spike cells in a fixed environment. J Neurosci 7:1935–1950.

Muller RU, Ranck JB Jr, Taube JS (1996) Head direction cells: properties and functional significance. Curr Opin Neurobiol 6:196–206.

Mátyás F, Freund TF, Gulyás AI (2004) Convergence of excitatory and inhibitory inputs onto CCK-containing basket cells in the CA1 area of the rat hippocampus. Eur J Neurosci 19:1243–1256.

Nakamura T, Barbara JG, Nakamura K, Ross WN (1999) Synergistic release of Ca2+ from IP3-sensitive stores evoked by synaptic activation of mGluRs paired with backpropagating action potentials. Neuron 24:727–737.

Nava F, Carta G, Battasi AM, Gessa GL (2000) D(2) dopamine receptors enable delta(9)-tetrahydrocannabinol induced memory impairment and reduction of hippocampal extracellular acetylcholine concentration. Br J Pharmacol 130:1201–1210.

Nerad L, Bilkey DK (2005) Ten- to 12-Hz EEG oscillation in the rat hippocampus and rhinal cortex that is modulated by environmental familiarity. J Neurophysiol 93:1246–1254.

Neu A, Földy C, Soltesz I (2007) Postsynaptic origin of CB1-dependent tonic inhibition of GABA release at cholecystokinin-positive basket cell to pyramidal cell synapses in the CA1 region of the rat hippocampus. J Physiol (Lond) 578:233–247.

Nitz D, McNaughton B (2004) Differential modulation of CA1 and dentate gyrus interneurons during exploration of novel environments. J Neurophysiol 91:863–872.

Nunzi MG, Gorio A, Milan F, Freund TF, Somogyi P, Smith AD (1985) Cholecystokinin-immunoreactive cells form symmetrical synaptic contacts with pyramidal and nonpyramidal neurons in the hippocampus. J Comp Neurol 237:485–505.

Nyberg L (2005) Any novelty in hippocampal formation and memory? Curr Opin Neurol 18:424–428.

Nyíri G, Freund TF, Somogyi P (2001) Input-dependent synaptic targeting of alpha(2)-subunit-containing GABA(A) receptors in synapses of hippocampal pyramidal cells of the rat. Eur J Neurosci 13:428–442.

Nyíri G, Stephenson FA, Freund TF, Somogyi P (2003) Large variability in synaptic N-methyl-D-aspartate receptor density on interneurons and a comparison with pyramidal-cell spines in the rat hippocampus. Neuroscience 119:347–363.

Nyíri G, Szabadits E, Cserép C, Mackie K, Shigemoto R, Freund TF (2005) GABAB and CB1 cannabinoid receptor expression identifies two types of septal cholinergic neurons. Eur J Neurosci 21:3034–3042.

Oades RD, Sadile AG, Sagvolden T, Viggiano D, Zuddas A, Devoto P, Aase H, Johansen EB, Ruocco LA, Russell VA (2005) The control of responsiveness in ADHD by catecholamines: evidence for dopaminergic, noradrenergic and interactive roles. Dev Sci 8:122–131.

Olton DS, Branch M, Best PJ (1978) Spatial correlates of hippocampal unit activity. Exp Neurol 58:387–409.

Olypher AV, Lánský P, Fenton AA (2002) On the location-specific positional and extra-positional information in the discharge of rat hippocampal cells. BioSystems 67:167–175.

Onaivi ES, Green MR, Martin BR (1990) Pharmacological characterization of cannabinoids in the elevated plus maze. Journal of Pharmacology and Experimental Therapeutics 253:1002–1009.

Oropeza VC, Page ME, Van Bockstaele EJ (2005) Systemic administration of WIN 55,212-2 increases norepinephrine release in the rat frontal cortex. Brain Res 1046:45–54.

O'Keefe J (1976) Place units in the hippocampus of the freely moving rat. Exp Neurol 51:78–109.

O'Keefe J (2007) Hippocampal Neurophysiology in the Behaving Animal. In: The Hippocampus Book, pp.475–548. Oxford: Oxford University Press.

O'Keefe J, Burgess N (1996) Geometric determinants of the place fields of hippocampal neurons. Nature 381:425–428.

O'Keefe J, Burgess N (2005) Dual phase and rate coding in hippocampal place cells: theoretical significance and relationship to entorhinal grid cells. Hippocampus 15:853–866.

O'Keefe J, Conway DH (1978) Hippocampal place units in the freely moving rat: why they fire where they fire. Exp Brain Res 31:573–590.

O'Keefe J, Dostrovsky J (1971) The hippocampus as a spatial map. Preliminary evidence from unit activity in the freely-moving rat. Brain Research 34:171–175.

O'Keefe J, Nadel L (1978) The hippocampus as a cognitive map. Oxford: Oxford University Press.

O'Keefe J, Recce ML (1993) Phase relationship between hippocampal place units and the EEG theta rhythm. Hippocampus 3:317–330.

O'Keefe J, Speakman A (1987) Single unit activity in the rat hippocampus during a spatial memory task. Exp Brain Res 68:1–27.

O'Neill J, Pleydell-Bouverie B, Dupret D, Csicsvari J (2010) Play it again: reactivation of waking experience and memory. Trends Neurosci 33:220–229.

Page ME, Oropeza VC, Van Bockstaele EJ (2008) Local administration of a cannabinoid agonist alters norepinephrine efflux in the rat frontal cortex. Neurosci Lett 431:1–5.

Papp E, Leinekugel X, Henze DA, Lee J, Buzsáki G (2001) The apical shaft of CA1 pyramidal cells is under GABAergic interneuronal control. Neuroscience 102:715–721.

Pavlides C, Greenstein YJ, Grudman M, Winson J (1988) Long-term potentiation in the dentate gyrus is induced preferentially on the positive phase of theta-rhythm. Brain Res 439:383–387.

Pawelzik H, Hughes DI, Thomson AM (2002) Physiological and morphological diversity of immunocytochemically defined parvalbumin- and cholecystokinin-positive interneurones in CA1 of the adult rat hippocampus. J Comp Neurol 443:346–367.

Peck BK, Vanderwolf CH (1991) Effects of raphe stimulation on hippocampal and neocortical activity and behaviour. Brain Res 568:244–252.

Pertwee RG (2000) Neuropharmacology and therapeutic potential of cannabinoids. Addict Biol 5:37–46.

Pertwee RG (2006) The pharmacology of cannabinoid receptors and their ligands: an overview. Int J Obes (Lond) 30 Suppl 1:S13–S18.

Pertwee RG (2008) The diverse CB1 and CB2 receptor pharmacology of three plant cannabinoids: delta9-tetrahydrocannabinol, cannabidiol and delta9-tetrahydrocannabivarin. Br J Pharmacol 153:199–215.

De Petrocellis L, Di Marzo V (2009) Role of endocannabinoids and endovanilloids in Ca2+ signalling. Cell Calcium 45:611–624.

Petsche H, Stumpf C, Gogolak G (1962) The significance of the rabbit's septum as a relay station between the midbrain and the hippocampus. I. The control of hippocampus arousal activity by the septum cells. Electroencephalogr Clin Neurophysiol 14:202–211.

Pikkarainen M, Rönkkö S, Savander V, Insausti R, Pitkänen A (1999) Projections from the lateral, basal, and accessory basal nuclei of the amygdala to the hippocampal formation in rat. J Comp Neurol 403:229–260.

Pitkänen A, Pikkarainen M, Nurminen N, Ylinen A (2000) Reciprocal connections between the amygdala and the hippocampal formation, perirhinal cortex, and postrhinal cortex in rat. A review. Ann N Y Acad Sci 911:369–391.

Pop E (1999) Cannabinoids, endogenous ligands and synthetic analogs. Curr Opin Chem Biol 3:418–425.

Posner MI, Petersen SE (1990) The attention system of the human brain. Annu Rev Neurosci 13:25–42.

Poucet B, Lenck-Santini PP, Hok V, Save E, Banquet JP, Gaussier P, Muller RU (2004) Spatial navigation and hippocampal place cell firing: the problem of goal encoding. Rev Neurosci 15:89–107.

Quirk GJ, Muller RU, Kubie JL (1990) The firing of hippocampal place cells in the dark depends on the rat's recent experience. J Neurosci 10:2008–2017.

Ranck JB Jr (1973) Studies on single neurons in dorsal hippocampal formation and septum in unrestrained rats. I. Behavioral correlates and firing repertoires. Exp Neurol 41:461–531.

Ravard S, Dourish CT (1990) Cholecystokinin and anxiety. Trends Pharmacol Sci 11:271–273.

Rawls SM, Cabassa J, Geller EB, Adler MW (2002) CB1 receptors in the preoptic anterior hypothalamus regulate WIN 55212-2 [(4,5-dihydro-2-methyl-4(4-morpholinylmethyl)-1-(1-naphthalenyl-carbonyl)-6H-pyrrolo[3,2,1ij]quinolin-6-one]-induced hypothermia. J Pharmacol Exp Ther 301:963–968.

Rawls SM, Ding Z, Cowan A (2006a) Role of TRPV1 and cannabinoid CB1 receptors in AM 404-evoked hypothermia in rats. Pharmacol Biochem Behav 83:508–516.

Rawls SM, Schroeder JA, Ding Z, Rodriguez T, Zaveri N (2007) NOP receptor antagonist, JTC-801, blocks cannabinoid-evoked hypothermia in rats. Neuropeptides 41:239–247.

Rawls SM, Tallarida RJ, Zisk J (2006b) Agmatine and a cannabinoid agonist, WIN 55212-2, interact to produce a hypothermic synergy. Eur J Pharmacol 553:89–98.

Recce M, O'Keefe J (1989) The tetrode: an improved technique for multi-unit extracellular recording. In: Society for Neuroscience Abstracts, pp.1250.

Redish AD, Battaglia FP, Chawla MK, Ekstrom AD, Gerrard JL, Lipa P, Rosenzweig ES, Worley PF, Guzowski JF, McNaughton BL, Barnes CA (2001) Independence of firing correlates of anatomically proximate hippocampal pyramidal cells. J Neurosci 21:RC134.

Redish AD, Rosenzweig ES, Bohanick JD, McNaughton BL, Barnes CA (2000) Dynamics of hippocampal ensemble activity realignment: time versus space. J Neurosci 20:9298–9309.

Rennó-Costa C, Lisman JE, Verschure PFMJ (2010) The mechanism of rate remapping in the dentate gyrus. Neuron 68:1051–1058.

Ribeiro A, Ferraz-de-Paula V, Pinheiro ML, Palermo-Neto J (2009) Dose-response effects of systemic anandamide administration in mice sequentially submitted to the open field and elevated plus-maze tests. Braz J Med Biol Res 42:556–560.

Rivas J, Gaztelu JM, García-Austt E (1996) Changes in hippocampal cell discharge patterns and theta rhythm spectral properties as a function of walking velocity in the guinea pig. Exp Brain Res 108:113–118.

Robbe D, Buzsaki G (2009) Alteration of Theta Timescale Dynamics of Hippocampal Place Cells by a Cannabinoid Is Associated with Memory Impairment. J Neurosci 29:12597–12605.

Robbe D, Montgomery SM, Thome A, Rueda-Orozco PE, McNaughton BL, Buzsaki G (2006) Cannabinoids reveal importance of spike timing coordination in hippocampal function. Nat Neurosci 9:1526–1533.

Robertson B, Baker GB, Vanderwolf CH (1991) The effects of serotonergic stimulation on hippocampal and neocortical slow waves and behavior. Brain Res 555:265–275.

Rolls ET, Treves A, Robertson RG, Georges-François P, Panzeri S (1998) Information about spatial view in an ensemble of primate hippocampal cells. J Neurophysiol 79:1797–1813.

Roohbakhsh A, Moghaddam AH, Massoudi R, Zarrindast M-R (2007) Role of dorsal hippocampal cannabinoid receptors and nitric oxide in anxiety like behaviours in rats using the elevated plus-maze test. Clin Exp Pharmacol Physiol 34:223–229.

Rose GM, Dunwiddie TV (1986) Induction of hippocampal long-term potentiation using physiologically patterned stimulation. Neurosci Lett 69:244–248.

Ross RA (2003) Anandamide and vanilloid TRPV1 receptors. Br J Pharmacol 140:790–801.

Rowntree CI, Bland BH (1986) An analysis of cholinoceptive neurons in the hippocampal formation by direct microinfusion. Brain Res 362:98–113.

Rubino T, Guidali C, Vigano D, Realini N, Valenti M, Massi P, Parolaro D (2008) CB1 receptor stimulation in specific brain areas differently modulate anxiety-related behaviour. Neuropharmacology 54:151–160.

Rubino T, Sala M, Viganò D, Braida D, Castiglioni C, Limonta V, Guidali C, Realini N, Parolaro D (2007) Cellular mechanisms underlying the anxiolytic effect of low doses of peripheral Delta9-tetrahydrocannabinol in rats. Neuropsychopharmacology 32:2036–2045.

Ryberg E, Larsson N, Sjögren S, Hjorth S, Hermansson N-O, Leonova J, Elebring T, Nilsson K, Drmota T, Greasley PJ (2007) The orphan receptor GPR55 is a novel cannabinoid receptor. Br J Pharmacol 152:1092–1101.

Sainsbury RS, Heynen A, Montoya CP (1987) Behavioral correlates of hippocampal type 2 theta in the rat. Physiol Behav 39:513–519.

Sara SJ, Dyon-Laurent C, Hervé A (1995) Novelty seeking behavior in the rat is dependent upon the integrity of the noradrenergic system. Brain Res Cogn Brain Res 2:181–187.

Sargolini F, Fyhn M, Hafting T, McNaughton BL, Witter MP, Moser M-B, Moser EI (2006) Conjunctive representation of position, direction, and velocity in entorhinal cortex. Science 312:758–762.

Sañudo-Peña MC, Tsou K, Walker JM (1999) Motor actions of cannabinoids in the basal ganglia output nuclei. Life Sci 65:703–713.

Seidenbecher T, Laxmi TR, Stork O, Pape H-C (2003) Amygdalar and hippocampal theta rhythm synchronization during fear memory retrieval. Science 301:846–850.

Senior TJ, Huxter JR, Allen K, O'Neill J, Csicsvari J (2008) Gamma oscillatory firing reveals distinct populations of pyramidal cells in the CA1 region of the hippocampus. J Neurosci 28:2274–2286.

Shapiro ML, Tanila H, Eichenbaum H (1997) Cues that hippocampal place cells encode: dynamic and hierarchical representation of local and distal stimuli. Hippocampus 7:624–642.

Sharp PE, Turner-Williams S, Tuttle S (2006) Movement-related correlates of single cell activity in the interpeduncular nucleus and habenula of the rat during a pellet-chasing task. Behav Brain Res 166:55–70.

Shiroyama T, Kayahara T, Yasui Y, Nomura J, Nakano K (1999) Projections of the vestibular nuclei to the thalamus in the rat: a Phaseolus vulgaris leucoagglutinin study. J Comp Neurol 407:318–332.

Sirota A, Csicsvari J, Buhl D, Buzsáki G (2003) Communication between neocortex and hippocampus during sleep in rodents. Proc Natl Acad Sci USA 100:2065–2069.

Skaggs WE, McNaughton BL (1998) Spatial firing properties of hippocampal CA1 populations in an environment containing two visually identical regions. J Neurosci 18:8455–8466.

Skaggs WE, McNaughton BL, Gothard KM, Markus EJ (1993) An Information-Theoretic Approach to Deciphering the Hippocampal Code. IN 5:1030--1037.

Slawinska U, Kasicki S (1998) The frequency of rat's hippocampal theta rhythm is related to the speed of locomotion. Brain Research 796:327–331.

Sloviter RS, Ali-Akbarian L, Elliott RC, Bowery BJ, Bowery NG (1999) Localization of GABA(B) (R1) receptors in the rat hippocampus by immunocytochemistry and high resolution autoradiography, with specific reference to its localization in identified hippocampal interneuron subpopulations. Neuropharmacology 38:1707–1721.

Smirnov MS, Kiyatkin EA (2008) Behavioral and temperature effects of delta 9-tetrahydrocannabinol in human-relevant doses in rats. Brain Res 1228:145–160.

Smith PF (1997) Vestibular-hippocampal interactions. Hippocampus 7:465–471.

Smith PF, Darlington CL, Zheng Y (2010) Move it or lose it--is stimulation of the vestibular system necessary for normal spatial memory? Hippocampus 20:36–43.

Smythe JW, Colom LV, Bland BH (1992) The extrinsic modulation of hippocampal theta depends on the coactivation of cholinergic and GABA-ergic medial septal inputs. Neurosci Biobehav Rev 16:289–308.

Sokolov (1963) Perception and the conditioned reflex. London: Pergamon Press.

Solstad T, Boccara CN, Kropff E, Moser M-B, Moser EI (2008) Representation of geometric borders in the entorhinal cortex. Science 322:1865–1868.

Solstad T, Moser EI, Einevoll GT (2006) From grid cells to place cells: a mathematical model. Hippocampus 16:1026–1031.

Souilhac J, Poncelet M, Rinaldi-Carmona M, Le Fur G, Soubrié P (1995) Intrastriatal injection of cannabinoid receptor agonists induced turning behavior in mice. Pharmacol Biochem Behav 51:3–7.

Stackman RW, Taube JS (1998) Firing properties of rat lateral mammillary single units: head direction, head pitch, and angular head velocity. J Neurosci 18:9020–9037.

Stensland H, Kirkesola T, Moser MB, Moser EI (2010) Orientational geometry of entorhinal grid cells.

Stewart M, Fox SE (1990) Do septal neurons pace the hippocampal theta rhythm? Trends in Neurosciences 13:163–169.

Strata F (1998) Intrinsic oscillations in CA3 hippocampal pyramids: physiological relevance to theta rhythm generation. Hippocampus 8:666–679.

van Strien NM, Cappaert NLM, Witter MP (2009) The anatomy of memory: an interactive overview of the parahippocampal-hippocampal network. Nat Rev Neurosci 10:272–282.

Swanson LW, Cowan WM (1979) The connections of the septal region in the rat. J Comp Neurol 186:621–655.

Szabadics J, Varga C, Molnár G, Oláh S, Barzó P, Tamás G (2006) Excitatory effect of GABAergic axo-axonic cells in cortical microcircuits. Science 311:233–235.

Szabó GG, Holderith N, Gulyás AI, Freund TF, Hájos N (2010) Distinct synaptic properties of perisomatic inhibitory cell types and their different modulation by cholinergic receptor activation in the CA3 region of the mouse hippocampus. Eur J Neurosci 31:2234–2246.

Szabó I, Czurkó A, Csicsvari J, Hirase H, Leinekugel X, Buzsáki G (2001) The application of printed circuit board technology for fabrication of multi-channel micro-drives. J Neurosci Methods 105:105–110.

Tai SK, Ma J, Ossenkopp K-P, Leung LS (2011) Activation of immobility-related hippocampal theta by cholinergic septohippocampal neurons during vestibular stimulation. Hippocampus Available at: http://www.ncbi.nlm.nih.gov/pubmed/21542057 [Accessed September 13, 2011].

Tamamaki N, Abe K, Nojyo Y (1987) Columnar organization in the subiculum formed by axon branches originating from single CA1 pyramidal neurons in the rat hippocampus. Brain Res 412:156–160.

Taube J (1995) Head direction cells recorded in the anterior thalamic nuclei of freely moving rats. The Journal of Neuroscience 15:70–86.

Terrazas A, Krause M, Lipa P, Gothard KM, Barnes CA, McNaughton BL (2005) Self-motion and the hippocampal spatial metric. J Neurosci 25:8085–8096.

Teruel-Martí V, Cervera-Ferri A, Nuñez A, Valverde-Navarro AA, Olucha-Bordonau FE, Ruiz-Torner A (2008) Anatomical evidence for a ponto-septal pathway via the nucleus incertus in the rat. Brain Res 1218:87–96.

Thiel CM, Huston JP, Schwarting RK (1998) Hippocampal acetylcholine and habituation learning. Neuroscience 85:1253–1262.

Thinschmidt JS, Kinney GG, Kocsis B (1995) The supramammillary nucleus: is it necessary for the mediation of hippocampal theta rhythm? Neuroscience 67:301–312.

Thompson LT, Best PJ (1989) Place cells and silent cells in the hippocampus of freely-behaving rats. J Neurosci 9:2382–2390.

Thompson LT, Best PJ (1990) Long-term stability of the place-field activity of single units recorded from the dorsal hippocampus of freely behaving rats. Brain Res 509:299–308.

Thomson AM, Bannister AP, Hughes DI, Pawelzik H (2000) Differential sensitivity to Zolpidem of IPSPs activated by morphologically identified CA1 interneurons in slices of rat hippocampus. Eur J Neurosci 12:425–436.

Tomida I, Pertwee RG, Azuara-Blanco A (2004) Cannabinoids and glaucoma. British Journal of Ophthalmology 88::708–713.

Tsou K, Mackie K, Sañudo-Peña MC, Walker JM (1999) Cannabinoid CB1 receptors are localized primarily on cholecystokinin-containing GABAergic interneurons in the rat hippocampal formation. Neuroscience 93:969–975.

Tukker JJ, Fuentealba P, Hartwich K, Somogyi P, Klausberger T (2007) Cell type-specific tuning of hippocampal interneuron firing during gamma oscillations in vivo. J Neurosci 27:8184–8189.

Tzavara ET, Wade M, Nomikos GG (2003) Biphasic Effects of Cannabinoids on Acetylcholine Release in the Hippocampus: Site and Mechanism of Action. J Neurosci 23:9374–9384.

Vallebuona F, Paudice P, Raiteri M (1993) Release of cholecystokinin-like immunoreactivity in the frontal cortex of conscious rats as assessed by transcerebral microdialysis: effects of different depolarizing stimuli. J Neurochem 61:490–495.

Le Van Quyen M, Bragin A, Staba R, Crépon B, Wilson CL, Engel J Jr (2008) Cell type-specific firing during ripple oscillations in the hippocampal formation of humans. J Neurosci 28:6104–6110.

Vanderwolf CH (1969) Hippocampal electrical activity and voluntary movement in the rat. Electroencephalogr Clin Neurophysiol 26:407–418.

Vanderwolf CH, Baker GB (1986) Evidence that serotonin mediates non-cholinergic neocortical low voltage fast activity, non-cholinergic hippocampal rhythmical slow activity and contributes to intelligent behavior. Brain Res 374:342–356.

Vanderwolf CH, Leung LW, Cooley RK (1985) Pathways through cingulate, neo- and entorhinal cortices mediate atropine-resistant hippocampal rhythmical slow activity. Brain Res 347:58–73.

Varga C, Lee SY, Soltesz I (2010) Target-selective GABAergic control of entorhinal cortex output. Nat Neurosci 13:822–824.

Vertes RP, Crane AM, Colom LV, Bland BH (1995) Ascending projections of the posterior nucleus of the hypothalamus: PHA-L analysis in the rat. J Comp Neurol 359:90–116.

Vertes RP, Fortin WJ, Crane AM (1999) Projections of the median raphe nucleus in the rat. J Comp Neurol 407:555–582.

Vertes RP, Kocsis B (1997) Brainstem-diencephalo-septohippocampal systems controlling the theta rhythm of the hippocampus. Neuroscience 81:893–926.

Villarreal DM, Gross AL, Derrick BE (2007) Modulation of CA3 afferent inputs by novelty and theta rhythm. J Neurosci 27:13457–13467.

Viveros M-P, Marco E-M, Llorente R, Lamota L (2007) The role of the hippocampus in mediating emotional responses to nicotine and cannabinoids: a possible neural substrate for functional interactions. Behav Pharmacol 18:375–389.

Viveros MP, Marco EM, File SE (2005) Endocannabinoid system and stress and anxiety responses. Pharmacol Biochem Behav 81:331–342.

Welday AC, Shlifer IG, Bloom ML, Blair HT, Zhang K (2010) Cosine directional tuning of theta cell burst frequencies in anterior thalamus: Evidence for an oscillatory path integration circuit in the rat brain. Presented at the Society for Neuroscience Annual Meeting, Abstract 203.20.

West MJ, Slomianka L, Gundersen HJ (1991) Unbiased stereological estimation of the total number of neurons in thesubdivisions of the rat hippocampus using the optical fractionator. Anat Rec 231:482–497.

Whishaw IQ, Vanderwolf CH (1971) Hippocampal EEG and behavior: effects of variation in body temperature and relation of EEG to vibrissae movement, swimming and shivering. Physiology & Behavior 6:391–392, IN2, 393–397.

Whishaw IQ, Vanderwolf CH (1973) Hippocampal EEG and behavior: Change in amplitude and frequency of RSA (Theta rhythm) associated with spontaneous and learned movement patterns in rats and cats. Behavioral Biology 8:461–484.

Wickens AP, Pertwee RG (1993) delta 9-Tetrahydrocannabinol and anandamide enhance the ability of muscimol to induce catalepsy in the globus pallidus of rats. Eur J Pharmacol 250:205–208.

Wiebe SP, Stäubli UV (1999) Dynamic filtering of recognition memory codes in the hippocampus. J Neurosci 19:10562–10574.

Wiener SI, Paul CA, Eichenbaum H (1989) Spatial and behavioral correlates of hippocampal neuronal activity. J Neurosci 9:2737–2763.

Williams JM, Givens B (2003) Stimulation-induced reset of hippocampal theta in the freely performing rat. Hippocampus 13:109–116.

Wills TJ, Cacucci F, Burgess N, O'Keefe J (2010) Development of the hippocampal cognitive map in preweanling rats. Science 328:1573–1576.

Wills TJ, Lever C, Cacucci F, Burgess N, O'Keefe J (2005) Attractor dynamics in the hippocampal representation of the local environment. Science 308:873–876.

Wilson MA, McNaughton BL (1993) Dynamics of the hippocampal ensemble code for space. Science 261:1055–1058.

Wilson RI, Nicoll RA (2001) Endogenous cannabinoids mediate retrograde signalling at hippocampal synapses. Nature 410:588–592.

Winson J (1974) Patterns of hippocampal theta rhythm in the freely moving rat. Electroencephalogr Clin Neurophysiol 36:291–301.

Winson J (1978) Loss of hippocampal theta rhythm results in spatial memory deficit in the rat. Science 201:160–163.

Wise LE, Thorpe AJ, Lichtman AH (2009) Hippocampal CB1 Receptors Mediate the Memory Impairing Effects of [Delta]9-Tetrahydrocannabinol. Neuropsychopharmacology 34:2072–2080.

Witter MP (2006) Connections of the subiculum of the rat: topography in relation to columnar and laminar organization. Behav Brain Res 174:251–264.

Witter MP, Moser EI (2006) Spatial representation and the architecture of the entorhinal cortex. Trends Neurosci 29:671–678.

Wood ER, Dudchenko PA, Eichenbaum H (1999) The global record of memory in hippocampal neuronal activity. Nature 397:613–616.

Xu J-Y, Chen R, Zhang J, Chen C (2010) Endocannabinoids differentially modulate synaptic plasticity in rat hippocampal CA1 pyramidal neurons. PLoS ONE 5:e10306.

Ylinen A, Soltész I, Bragin A, Penttonen M, Sik A, Buzsáki G (1995) Intracellular correlates of hippocampal theta rhythm in identified pyramidal cells, granule cells, and basket cells. Hippocampus 5:78–90.

Yoganarasimha D, Rao G, Knierim JJ (2010) Lateral entorhinal neurons are not spatially selective in cue-rich environments. Hippocampus Available at: http://www.ncbi.nlm.nih.gov/pubmed/20857485 [Accessed September 11, 2011].

Zinyuk L, Kubik S, Kaminsky Y, Fenton AA, Bures J (2000) Understanding hippocampal activity by using purposeful behavior: place navigation induces place cell discharge in both task-relevant and task-irrelevant spatial reference frames. Proc Natl Acad Sci USA 97:3771–3776.

11 Appendix: List of Abbrieviations

BC	Basket cell
CA	*Cornu ammonis*
CB1	Cannabinoid receptor 1
CB2	Cannabinoid receptor 2
CCK	Cholecystokinin
CCK-BC	Cholecystokinin-expressing basket cell
CPG	Central pattern generator
DA	Dopamine
DG	Dentate gyrus
DSE	Depolarisation-induced suppression of excitation
DSI	Depolarisation-induced suppression of inhibition
EC	Entorhinal cortex
EEG	Electroencephalogram
EPSC	Excitatory post-synaptic current
EPSP	Excitatory post-synaptic potential
GABA	Gamma aminobutyric acid
GCL	Granule cell layer
HF	Hippocampal formation
HPA	Hypothalamic-pituitary-adrenal (axis)
IPN	Interpeduncular nucleus
IPSC	Inhibitory post-synaptic current
IPSP	Inhibitory post-synaptic potential
LC	Locus coeruleus

LEA	Lateral entorhinal area
LFP	Local field potential
LIA	Large amplitude irregular activity
LS	Lateral septum
LTD	Long-term depression
LTP	Long-term potentiation
MEA	Medial entorhinal area
MPO	Membrane potential oscillation
MR	Median raphe nucleus
mRNA	Messenger ribonucleic acid
MS	Medial septum
MS/DBB	Medial septum/diagonal Band of Broca
NA	Noradrenaline
NAcc	Nucleus accumbens
NMDA	N-methyl D-aspartate
PER	Perirhinal cortex
PFC	Prefrontal cortex
PH	Posterior hypothalamus
PHR	Parahippocampal region
PL	Polymorphic layer
POAH	Postoptic anterior hypothalamus
POR	Postrhinal cortex
PP	Perforant path
PRE	Presubiculum

PV	Parvalbumin
PV-BC	Parvalbumin-expressing basket cell
RPO	Reticularis pontis oralis
RSC	Retrosplenial cortex
SC	Schaffer collateral
SIA	Small amplitude irregular activity
SL	Stratum lucidum
SLM	Stratum lacunosum-moleculare
SO	Stratum oriens
SP	Stratum pyramidale
SR	Stratum radiatum
SUB	Subiculum
SuM	Supramammillary nucleus
SWR	Sharp-wave ripple
THC	Tetrahydrocannabinol
VCO	Velocity-controlled oscillator
VTA	Ventral tegmental area
VTN	Ventral tegmental nucleus